



# Interactions entre organo-silanes et client : conséquences sur l'hydratation et les propriétés mécaniques

Anca Itul

## ► To cite this version:

Anca Itul. Interactions entre organo-silanes et client : conséquences sur l'hydratation et les propriétés mécaniques. Autre. Université de Bourgogne, 2010. Français. NNT : 2010DIJOS061 . tel-00656843

**HAL Id: tel-00656843**

**<https://theses.hal.science/tel-00656843>**

Submitted on 5 Jan 2012

**HAL** is a multi-disciplinary open access archive for the deposit and dissemination of scientific research documents, whether they are published or not. The documents may come from teaching and research institutions in France or abroad, or from public or private research centers.

L'archive ouverte pluridisciplinaire **HAL**, est destinée au dépôt et à la diffusion de documents scientifiques de niveau recherche, publiés ou non, émanant des établissements d'enseignement et de recherche français ou étrangers, des laboratoires publics ou privés.

UNIVERSITE DE BOURGOGNE  
Laboratoire Interdisciplinaire Carnot de Bourgogne

THÈSE  
Pour obtenir le grade de  
Docteur de l'Université de Bourgogne  
Discipline: Chimie Physique

par  
Anca Itul

Le 20 Mai 2010

Interactions entre organo-silanes et ciment.  
Conséquences sur l'hydratation et les propriétés mécanique

Directeur de thèse  
André Nonat

#### Jury

Mme. Bourgeois Sylvie	Directrice de Recherche, CNRS, Président
M. Macphee Donald	Professeur, University of Aberdeen, Rapporteur
Mme. Geiker Mette	Professeur, Norwegian University of Science and Technology, Rapporteur
M. Legat Andraž	Docteur, ZAG Ljubljana, Rapporteur
M. Nonat André	Directeur de Recherches, CNRS, Directeur de thèse
M.Flatt Robert	Docteur, Sika Technology AG, Responsable industriel



## Acknowledgements

Herewith I would like to thank all the people who contributed and who have helped me in completing this work.

First of all I would like to thank Professor André Nonat, my thesis supervisor, for his scientific guidance and for his overall support throughout my entire work (and living in France), particularly in the end. Nevertheless, I greatly appreciated all his non-scientific advices and the help I received throughout the years.

Equally, thanks to Dr. Robert Flatt, my industrial advisor for his constant encouragement during some less challenging times of my PhD and for never losing patience. Also, I want to express my gratitude for all his constructive critical comments and opinions.

Also, I would like to thank Dr. Franc Švegl and Jerneja Šuput Strupi from ZAG Ljubljana and to all the people from the Laboratory for Mineral Binders and Mortars for technical support during the early stages of my work. Special thanks go to Prof. Andraž Legat and to my best roommate ever, Andrej Kranjc, for all their generosity and for helping me to adapt in a country which language I still don't speak nor understand.

A further special thanks goes to all the staff members from the department “Interface et Réactivité dans les Matériaux” from University of Bourgogne. In particular, I am grateful to Sandrine Garrault for advice on rheological aspects, Danièle Perrey for Atomic Emission Spectroscopy measurements and Agnes Birot for handling all the administrative details of my work. Also, many thanks to my fellow PhD students, postdoctoral researchers, and interns for assistance in the lab and for improving my French language skills.

Thanks to my co-workers during my secondment at Sika Technology A.G. for their enthusiasm towards my work and for valuable scientific inputs.

Thanks to Nanocem consortium for acquiring research funds from the European Commission for funding this work. Tremendous thanks to my fellow Nanocem Marie Curie students for the awesome times we spent together.

Thanks to Alex who constantly encouraged me to pursue my dreams and thanks to the acquaintances whose infinite wisdom and eye-opening discussion during the last and most difficult part meant the world to me.

And of course, a huge thanks to my parents Liliana and Franți, and my brother, Tudor.

Last but not least, I would like to thank the members of my Jury for reviewing this work: Professor Donald Macphee from University of Aberdeen (Aberdeen, UK), Professor Mette Geiker from Norwegian University of Science and Technology (Trondheim, Norway), Dr. Andraž Legat from ZAG Ljubljana (Ljubljana, Slovenia), Prof. Nonat André from University of Bourgogne (Dijon, France), Flatt Robert from Sika Technology AG (Zürich, Switzerland). A special thank to Professor Sylvie Bourgeois for accepting the president position of this Jury.

## Abstract

Nowadays concrete is the most attractive option for the construction sector. This is because concrete itself is a low cost, low energy and low environmental impact material. Moreover, concrete structures are very durable and high load bearing. This is achieved by incorporating steel, because concrete itself is a very low tensile strength material.

Chemically, the weakness originates in the cohesive nature of cement used for concrete making. Nanoscale experimental investigations and numerical simulations showed that cohesion of cement paste is caused by short range surface forces acting between calcium silicate hydrates (C-S-H) in the interstitial solution.

This thesis addresses the possibility of engineering the bonding between hydrates in order to tune the mechanical properties of cementitious materials. We aim at introducing long range cohesion forces between hydrates in addition to the existing ones. This should potentially lead to an increase in strength and toughness. The strategy chosen was to hybridize the cement prior to hydration with organofunctional silanes. Two possible methods of silanization were investigated and the modified products have been characterized.

The first method consisted in dry blending cement powder to silanes. It is shown that by doing so, cement pastes and mortars exhibit improved workability. In addition, we have observed that silane agents strongly affect the hydration kinetics, mainly by retarding the hydration of silicates and reducing their degree of hydration. As a consequence, severe strength loss was evidenced in all standard mechanical tests. This was related to excessive dosage of silane to cement imposed to reach good mix homogeneity during hybridization.

A second silanization methodology was developed in order to allow diminishing the dosage of silane without facing inhomogeneity mix issues. It is shown that by adsorbing silane from organic solvents we gain a better understanding of silane-cement interactions. In addition, the adsorption data provide indirect means to help

characterize the modified substrates. It was found that silane-cement interactions strongly depend on the type of the solvent used as vehicle media. The surface coverage has also been calculated and is far from being monolayer because both chemically bonded and physically adsorbed species are assumed to be present. This further influences the properties of the modified cements.

In terms of hydration kinetics, stronger retarding effects of silicates hydration are always associated to silanes displaying lower surface affinity, but stronger surface bonding. In terms of rheology, all silanes greatly improved the ability of pastes to withstand load above the critical deformation. This results in increased bending strength by up to 35% compared to neat cement.

Keywords: cement, organofunctional silanes, hydration, rheology, strength.

## Résumé

Aujourd'hui le béton est l'option la plus attrayante pour le secteur de la construction. Ceci est dû au fait que le béton est un matériau peu coûteux et que sa fabrication nécessite peu d'énergie et a un faible impact environnemental. En outre, les structures en béton sont durables et performantes mais le béton nécessite d'être associé à des armatures d'acier, car il présente une faible résistance à la traction.

Du point de vue de la chimie, le point faible provient de l'origine de la cohésion du ciment utilisé pour la fabrication du béton. Des expériences à l'échelle nanométrique et des simulations numériques ont montré que la cohésion de la pâte de ciment résulte de forces de courte portée qui s'exercent entre les surfaces de silicates de calcium hydratés (C-S-H) dans la solution interstitielle.

Cette thèse explore l'ingénierie de la liaison entre les grains de ciment en vue d'améliorer les propriétés mécaniques des matériaux cimentaires. Nous visons à introduire en plus de celles déjà existantes, des forces de cohésion à longue portée entre les grains à l'aide de liaisons chimiques pour conduire à une augmentation de la résistance à la traction et de la ténacité. La stratégie choisie a été de greffer différents silanes organo-fonctionnels sur le ciment anhydre. Deux méthodes possibles de silanisation ont été étudiées et les produits modifiés ont été caractérisés.

La première méthode a consisté à mélanger directement la poudre de ciment avec les silanes. Il a été montré que, ce faisant, pâtes de ciment et de mortiers présentent une maniabilité améliorée. En outre, il a été observé que les silanes influent fortement l'hydratation, principalement en retardant l'hydratation des silicates et en réduisant leur degré d'hydratation. En conséquence, une perte sévère de résistance a été constatée dans tous les tests mécaniques standards effectués. Ceci est lié à la dose excessive de silane incorporée au ciment pour atteindre l'homogénéité du mélange au cours de l'hydratation.

Une deuxième méthode de silanisation a été développée afin de permettre la diminution du dosage des silanes en gagnant en homogénéité. Elle consiste à mélanger le ciment dans une solution de silane dans un solvant non aqueux. Cette



méthode à permis en outre d'obtenir des données quantitatives relatives à l'adsorption des silanes utiles à une meilleure compréhension des interactions silane-ciment. Elles constituent en effet des moyens indirects aidant à caractériser les substrats modifiés. Il a été constaté que les interactions silane-ciment dépendent fortement du type de solvant utilisé. La couverture de la surface a également été calculée et est loin d'être une monocouche. Elle est constituée d'espèces chimiquement et physiquement adsorbées qui influencent les propriétés des ciments modifiés.

En termes de vitesse d'hydratation, les plus forts effets de ralentissement sur l'hydratation des silicates sont toujours associés aux silanes affichant une plus faible affinité avec la surface, mais fortes de liaisons avec cette dernière. En termes de rhéologie, tous les silanes améliorent grandement la capacité des pâtes à résister à une charge au-dessus de la limite élastique. Il en résulte une augmentation de résistance à la flexion jusqu'à 35% par rapport au ciment pur.

Mots-clés : ciment, silanes organofonctionnels, hydratation, rhéologie, résistance.

# Table of contents

<b>ACKNOWLEDGEMENTS .....</b>	<b>III</b>
<b>ABSTRACT .....</b>	<b>V</b>
<b>RESUME .....</b>	<b>VII</b>
<b>TABLE OF CONTENTS .....</b>	<b>IX</b>
<b>LIST OF TABLES.....</b>	<b>XIII</b>
<b>LIST OF FIGURES.....</b>	<b>XV</b>
<b>LIST OF ANNEXES .....</b>	<b>XXIII</b>
<b>1 INTRODUCTION.....</b>	<b>1</b>
<b>2 GENERAL CONSIDERATIONS. CEMENT AND SILANE AGENTS .....</b>	<b>9</b>
2.1 CEMENT .....	10
2.1.1 <i>Anhydrous cement</i> .....	10
2.1.2 <i>Hydrated cement</i> .....	11
2.1.2.1 Time dependent chemical changes.....	11
2.1.2.2 Time dependent physical changes.....	14
2.1.3 <i>Cohesion of cement pastes</i> .....	16
2.1.3.1 C-S-H.....	16
2.1.3.2 Origin of cohesion.....	19
2.1.3.3 Interparticle forces .....	20
Van der Waals forces .....	21
Electric double layer forces .....	23
Capillarity forces .....	27
Summary on the forces controlling the cohesion .....	28
2.2 SILANES .....	29
2.2.1 <i>Basics chemistry</i> .....	29
2.2.2 <i>Silanes at interfaces</i> .....	32
2.2.3 <i>General applications of organofunctional alkoxysilane</i> .....	34
2.2.4 <i>Silanes applications related to cementitious materials</i> .....	38
2.2.4.1 Silane silica fume cement.....	38
2.2.4.2 Silane steel fibres reinforced cement.....	39
2.2.4.3 Silane carbon fibres and silane silica fume cement.....	39
2.2.4.4 Silane polymer modified mortar .....	40
2.2.4.5 Silane cement pastes .....	41
<b>3 MATERIALS .....</b>	<b>43</b>
3.1 CEMENT AND TRICALCIUM SILICATE .....	45
3.2 SILANES .....	46
<b>4 SILANE MODIFIED CEMENT OBTAINED BY DRY BLENDING OF CONSTITUENTS</b>	<b>49</b>
4.1 METHODOLOGY .....	51
4.1.1 <i>In principle</i> .....	51
4.1.2 <i>In practice</i> .....	51
4.2 CHARACTERIZATION OF MODIFIED PRODUCTS.....	52
4.2.1 <i>Techniques used for investigating the properties of modified products</i> .....	52
4.2.1.1 Standard consistency water .....	52
4.2.1.2 Setting time .....	52
4.2.1.3 Workability .....	53
4.2.1.4 Strength.....	53
A. Experimental procedure for mixing, curing and strength testing for paste.....	53
B. Experimental procedure for mixing, curing and strength testing for mortar.....	54
4.2.1.5 Calorimetry .....	54
General considerations.....	54
Isothermal calorimetry .....	55
4.2.2 <i>Results</i> .....	57

4.2.2.1	Standard consistency water .....	57
4.2.2.2	Workability .....	59
	A. Pastes .....	59
	B. Mortars .....	60
4.2.2.3	Setting time .....	61
4.2.2.4	Bending and compressive strength tests .....	63
	A. Paste .....	63
	B. Mortars .....	65
4.2.2.5	Heat development .....	67
	Effect of silane nature .....	67
	Effect of silane dosage .....	71
4.2.3	<i>Discussion</i> .....	74
4.3	CONCLUSIONS .....	77
<b>5</b>	<b>SILANE MODIFIED CEMENT OBTAINED BY LIQUID PHASE DEPOSITION AND EXCESS SOLVENT REMOVAL .....</b>	<b>79</b>
5.1	METHODOLOGY .....	82
5.1.1	<i>In principle</i> .....	82
5.1.2	<i>In practice</i> .....	83
5.2	ADSORPTION .....	85
5.2.1	<i>Techniques used for investigating the adsorption</i> .....	85
5.2.1.1	Inductively Coupled Plasma-Atomic Emission Spectroscopy (ICP-AES) .....	85
5.2.1.2	Transmission Electron Microscopy (TEM) .....	86
5.2.1.3	Other investigation methods .....	86
5.2.2	<i>Results</i> .....	87
5.2.2.1	Effect of silane dosage .....	87
5.2.2.2	Effect of solvent .....	91
	Nature of solvent .....	91
	Solvent to cement ratio .....	93
5.2.2.3	Effect of silane nature .....	95
5.2.2.4	Effect of adsorbate .....	96
5.2.3	<i>Conclusions on adsorption</i> .....	98
5.3	CHARACTERIZATION OF MODIFIED PRODUCTS .....	98
5.3.1	<i>Techniques used for investigating the properties</i> .....	99
5.3.1.1	Techniques used for investigating the hydration kinetics .....	99
	Semi-adiabatic calorimetry .....	99
	Electrical conductivity .....	100
	A. General considerations .....	100
	B. Experimental set-up .....	103
	ICP-AES spectrometry .....	104
5.3.1.2	Techniques used to investigate viscoelastic properties .....	104
	Basics of rheology .....	104
	Rheology of viscoelastic fluids – cement based systems .....	108
	Rheological measurements .....	110
	A. Rheometer .....	110
	B. Tests performed in oscillatory mode .....	112
	C. Simultaneous calorimetric and rheological measurements .....	113
5.3.2	<i>Results</i> .....	113
5.3.2.1	Effect of silanes on the hydration kinetics of cement paste .....	114
	Effect of dosage .....	114
	Effect of solvent nature .....	116
	Is the solvent used as dispersion media retarding the hydration of cement? .....	122
	Could the ethanol released during the hydrolysis of silane be responsible and/or contributing to the retardation of cement hydration? .....	123
	Effect of silane nature .....	125
	A. Individually silane modified cement .....	125
	B. Effects of blends of individually modified cements .....	128
	Effect of substrate .....	132
	Effects of the silanization methodology .....	135
	Investigations on the retarding mechanism .....	139
5.3.2.2	Conclusions .....	144
5.3.2.3	Effect of silanes on the viscoelastic properties of cement paste at early age .....	145
	Individually silane modified cement .....	145
	A. Linear viscoelastic domain (LVD) .....	145
	A.1. Neat cement paste .....	146

A.2. Silane modified cement pastes .....	147
Discussion .....	147
B. Structure stiffening.....	149
B.1. Neat cement paste .....	149
B.2. Silane modified cement pastes .....	151
Discussion .....	154
Silane modified tricalciumsilicate.....	156
A. Linear viscoelastic domain (LVD).....	156
B. Structure stiffening.....	158
B.1. Neat tricalciumsilicate paste .....	159
B.2. APTES modified tricalcium silicate .....	160
Discussion.....	160
Blends of individually silane modified cement.....	162
A. Linear viscoelastic domain (LVD).....	163
B. Structure stiffening.....	166
Conclusions .....	169
<b>6 SILANE MODIFIED CEMENT OBTAINED BY LIQUID PHASE DEPOSITION WITH SOLVENT EVAPORATION .....</b>	<b>171</b>
6.1 METHODOLOGY .....	174
6.1.1 <i>In principle</i> .....	174
6.1.2 <i>In practice</i> .....	174
6.2 CHARACTERIZATION OF MODIFIED PRODUCTS.....	175
6.2.1 <i>Techniques used for investigating the properties</i> .....	175
6.2.1.1 Semi-adiabatic calorimetry .....	175
6.2.1.2 Penetrometry.....	175
6.2.1.3 Three point bending test.....	176
6.2.1.4 Scanning electron microscopy (SEM).....	177
6.2.1.5 X-Ray diffraction (XRD).....	177
6.2.2 <i>Results and discussion</i> .....	178
6.2.2.1 Method validation .....	178
6.2.2.2 Simultaneous hydration rate and rheology measurements .....	179
6.2.2.3 Three point bending tests .....	184
6.2.2.4 SEM.....	186
6.2.2.5 XRD-Rietveld .....	190
6.3 CONCLUSIONS .....	192
<b>7 CONCLUSIONS AND PERSPECTIVES.....</b>	<b>195</b>
7.1 GENERAL OVERVIEW .....	197
7.2 CONCLUSIONS ON THE SILANE MODIFIED CEMENTS OBTAINED BY DRY BLENDING OF CONSTITUENTS .....	199
7.3 CONCLUSIONS ON THE SILANE MODIFIED CEMENTS OBTAINED BY LIQUID PHASE ADSORPTION OF SILANES TO CEMENT .....	200
7.4 PERSPECTIVES .....	202
<b>REFERENCES.....</b>	<b>205</b>
<b>ANNEXES.....</b>	<b>219</b>
ANNEX I GLOSSARY .....	221
ANNEX II PATTERNS FROM TEM/EDS AND SEM/EDS INVESTIGATIONS.....	223
ANNEX III DATA FROM INVESTIGATIONS ON THE HYDRATION KINETICS OF SILANE MODIFIED CEMENT AND TRICALCIUMSILICATE MODIFIED CEMENT .....	225
ANNEX IV DATA FROM INVESTIGATIONS ON VISCOELASTIC PROPERTIES OF SILANE MODIFIED CEMENTS AND SILANE MODIFIED TRICALCIUM SILICATES. ....	231



## List of Tables

<i>Table 2-1. Simplified writing of the major crystalline phases found in Portland cement. ....</i>	<i>11</i>
<i>Table 3-1. Physical characteristics of cement and tricalcium silicate. ....</i>	<i>45</i>
<i>Table 3-2. Chemical characteristics of cement. ....</i>	<i>46</i>
<i>Table 3-3. Characteristics of the silanes used. ....</i>	<i>47</i>
<i>Table 5-1. Effect of substrate on the adsorption of silanes from ethanol and toluene suspensions. ....</i>	<i>96</i>
<i>Table 5-2. Adsorption of silanes from ethanol and toluene suspensions to silicate phases. Comparison between the calculated dosages as resulted from experiments carried out for cement to measured fractions from experiments carried out for tricalcium silicate. ....</i>	<i>97</i>
<i>Table 6-1. Phase composition of cement paste with and without APTES from XRD-Rietveld analysis ....</i>	<i>191</i>



## List of Figures

<i>Figure 2-1. Schematic cement hydration thermogram showing five distinct stages in the hydration process (reproduced from [16]).</i>	12
<i>Figure 2-2. Nomenclature of pores (reproduced from [5]).</i>	15
<i>Figure 2-3. (a) TEM micrograph of C-S-H prepared by pozzolanic reaction of calcium oxide with silica (reproduced from [6]); (b) C-S-H schematic representation (reproduced from [18]).</i>	17
<i>Figure 2-4 Several C-S-H layered structure configurations illustrating the progressive loss of bridging tetrahedral and the localisation of the surface charge (reproduced from [31]).</i>	18
<i>Figure 2-5. Previous concept of hydrated cement (adapted from [25]).</i>	20
<i>Figure 2-6. Polarisability of the electronic cloud. Inducing dipoles.</i>	21
<i>Figure 2-7. Schematic illustration of the electrical double layer developed when a surface which is negatively charged and immersed in an aqueous solution is attracting (positive) counterions and creates a depletion zone of the (negative) co-ions. (reproduced from [38]).</i>	24
<i>Figure 2-8. (a) Two negatively charged surfaces of surface charge density <math>\sigma</math> separated by a distance <math>D</math>; (b) the counterions density profile <math>\rho_x</math> and electrostatic potential <math>\psi_x</math>.</i>	25
<i>Figure 2-9. Example of meniscus formed on the top water surface in a tube.</i>	27
<i>Figure 2-10. Alkoxysilane hydrolysis and condensation (reproduced from [50]).</i>	31
<i>Figure 2-11. Hydrolysis and condensation rate of a typical silane (adapted from [51]).</i>	31
<i>Figure 2-12. The silane coupling mechanism (reproduced from [48]).</i>	32
<i>Figure 2-13. Schematic representation of conceptual bonding of trialkoxysilane to the inorganic surface (reproduced from [48]).</i>	33
<i>Figure 2-14. Bonding siloxane to polymer through diffusion (reproduced from [48]).</i>	34
<i>Figure 2-15. Structure of sulfidosilanes used in rubber compounds. X ranges from 2 to 10 (reproduced from [48]).</i>	36
<i>Figure 2-16. Bonding organic rubber to silica with sulphur silanes (reproduced from [48]).</i>	36



Figure 2-17. (a) Structure of polyethylene crosslinked through C-to-C bond (by peroxidation or radiation). The bond appears rigid; (b) Structure of polyethylene crosslinked through Si-O-Si bond by silane agent. The bond provides flexibility. (reproduced from [72]) .....	37
Figure 3-1. Molecular structure of APTES (a), GTO (b), AEAPTMS (c) and TEOS (d). .....	47
Figure 4-1. Schematic representation of heat evolution during hydration of cement (reproduced from [86]) .....	55
Figure 4-2. Graphic determination for the onset of acceleration period for cement hydration from a heat evolution rate curve. ....	56
Figure 4-3. Standard consistency water for silane modified cement pastes determined according to EN 196-3:2005. Dosage of silane by weight of cement is (a) 1 % and (b) 10%. ....	58
Figure 4-4. Standard consistency water variation for different silanes and different addition levels. ....	59
Figure 4-5. Comparison of values for flow table spread of neat and 10 % silane modified cement paste at constant w/c = 0.25. ....	60
Figure 4-6. Water demands for silane mortars needed for constant 200 mm flow table spread at constant silane to cement concentration. ....	61
Figure 4-7. Setting time values measured for high silane modified cement on standard consistency pastes using Vicat penetration method. ....	62
Figure 4-8. Setting time values measured for low silane modified cement on standard consistency pastes using Vicat penetration method. ....	63
Figure 4-9. Bending strength for neat and 10% APTES silane modified pastes prepared at constant w/c= 0.25. Percentage of silane by weight of cement. ....	64
Figure 4-10. Compressive strength for neat and 10% APTES silane modified pastes prepared at constant w/c=0.25. Percentage of silane by weight of cement. ....	64
Figure 4-11. Bending strength of silane modified mortars and reference ones prepared with constant w/c =0.5. ....	66
Figure 4-12. Compressive strength of silane modified mortars and reference ones prepared with constant w/c =0.5. ....	67
Figure 4-13. Heat evolution curves for high addition levels of silane modified cement pastes (10% wt silane to cement) prepared with constant w/c=0.3. ....	68

<i>Figure 4-14. Cumulative heat evolution curves for high addition levels of silane modified cement pastes (10% wt silane to cement) prepared with constant <math>w/c=0.3</math>.</i>	68
<i>Figure 4-15. Heat flow curves (a) and cumulative heat flow curves (b) for low addition levels of silane modified cement pastes (1% wt silane to cement) prepared with constant <math>w/c=0.3</math>.</i>	70
<i>Figure 4-16. Effect of different dosages of APTES on the heat flow (a) and cumulative heat flow (b) of cement pastes prepared with constant <math>w/c=0.3</math>. Percentage of silane by weight of cement.</i>	71
<i>Figure 4-17. Effect of different dosages of GTO on the heat flow (a) and cumulative heat flow (b) of cement pastes prepared with constant <math>w/c=0.3</math>. Percentage of silane by weight of cement.</i>	72
<i>Figure 4-18. Effect of different dosages of AEAPTMS on the heat flow (a) and cumulative heat flow (b) of cement pastes prepared with constant <math>w/c=0.3</math>. Percentage of silane by weight of cement.</i>	73
<i>Figure 5-1. Schematic illustration of various aminosilanes interaction types in the reaction phase (a) hydrogen bonding (b) proton transfer (c) condensation to siloxane (reproduced from [88]).</i>	83
<i>Figure 5-2. Schematic representation of the flip mechanism for APTES reaction with silica surface under dry conditions (a) physisorption (b) condensation (c) structure after curing ( reproduced from [88]).</i>	83
<i>Figure 5-3. Adsorption data for APTES to cement from ethanol suspensions.</i>	88
<i>Figure 5-4. TEM micrographs of APTES adsorbed to tricalcium silicate. The darker region defines the inorganic substrate (tricalcium silicate), while the clusters exemplify APTES's presence.</i>	91
<i>Figure 5-5. Adsorption data for APTES on cement from ethanol suspensions (upper curve) and toluene suspensions (lower one).</i>	92
<i>Figure 5-6. Effect of solid (cement) to liquid (solvent) ratio on the adsorption of APTES. 1% APTES to cement by weight was used in all cases.</i>	94
<i>Figure 5-7. Adsorption data for APTES, GTO and AEAPTMS to cement from ethanol suspensions.</i>	95
<i>Figure 5-8. Schematic representation of a semi -adiabatic calorimeter cell: insulated vessel containing the sample under measurement and the temperature sensor.</i>	100

<i>Figure 5-9. Evolution of electrical conductivity over time for cement in diluted suspensions (L/S=250). Lime saturated solution <math>[Ca^{2+}]=22</math> mmol/L) was chosen as dissolution media .</i>	102
<i>Figure 5-10. Schematic illustration of a thermostated cell used in electrical conductivity measurements (reproduced from [105]).</i>	103
<i>Figure 5-11. Schematic representation of two parallel planes of equal areas A, moving parallel to each other but at different velocities.</i>	105
<i>Figure 5-12. Evolution versus time of the viscoelastic properties of cement paste by viscoelastimetry ( reproduced from [112]).</i>	110
<i>Figure 5-13. Schematic representation of the parallel plate geometry used in this study and its operational principle: the bottom plate submits the sample to a strain (angular displacement) with the result that the top one tends also to turn because of the viscous drag exerted by the sample. The torque to prevent it from turning is measured and converted into stress.</i>	111
<i>Figure 5-14. Heat evolution curves for different APTES modified cement pastes prepared with a constant w/c=0.3. APTES was deposited from ethanol. Percentage of silane by weight of cement.</i>	115
<i>Figure 5-15. Total heat flow curves for different APTES modified cement pastes prepared with a w/c of 0.3. APTES was deposited from ethanol. Percentage of silane by weight of cement.</i>	115
<i>Figure 5-16. Effect of solvent nature used as vehicle media on the hydration of APTES modified cement pastes. Similar concentrations of silane induce different retardation levels on cement hydration.</i>	117
<i>Figure 5-17. Heat evolution curves for APTES modified cement pastes prepared with a constant w/c = 0.3. APTES was deposited from 100 % ethanol, 100 % toluene and 96 % ethanol. Different dosages of APTES lead to similar retardation levels depending on the solvent's nature used as dispersive media. Percentage of silane by weight of cement.</i>	118
<i>Figure 5-18. Schematic representation of hypothetical configuration of APTES adsorbed to cement from toluene (a) and ethanol 96% (b). It is suggested that in both cases equal number of covalent bonding to substrate occurs leading to similar retardation levels, despite the fact that different APTES to cement ratios were found to be adsorbed.</i>	120

<i>Figure 5-19. Total heat flow curves for different APTES modified cement pastes prepared with a constant w/c=0.3. Different APTES to cement concentrations lead to similar retardation levels depending on the solvent's nature. However, the overall values for heat release are different depending on the solvent's nature. Percentage of silane by weight of cement. ....</i>	<i>121</i>
<i>Figure 5-20. Heat evolution curves for plain cement, ethanol pre-treated cement and toluene pre-treated cement prepared with a constant w/c of 0.3. Initially, the solvents were removed by centrifugation. Additional oven curing was applied for entire solvent removal. ....</i>	<i>122</i>
<i>Figure 5-21. Effect of ethanol on hydration of cement. The ethanol was added to water before beginning of mixing. ....</i>	<i>124</i>
<i>Figure 5-22. Effect of direct addition of ethanol (lower curve) and of the quantity of ethanol assumed to be released from the hydrolysis of APTES (upper curve) on the cement hydration.....</i>	<i>125</i>
<i>Figure 5-23. Effect of silane nature on the hydration kinetics of cement. The induction period was determined graphically, as described in Section 5-23. ....</i>	<i>126</i>
<i>Figure 5-24. Heat evolution curves for GTO modified cement paste, AEAPTMS modified cement paste and their 1:1 by weight blend. All samples were prepared with a constant w/c =0.3. Percentage of silane by weight of cement. ....</i>	<i>129</i>
<i>Figure 5-25. Heat evolution curves for GTO modified cement paste, APTES modified cement paste and their mix 1:1 by weight. All samples were prepared with a constant w/c of 0.3. Percentage of silane by weight of cement. ....</i>	<i>129</i>
<i>Figure 5-26. Total heat flow curves for GTO modified cement paste, AEAPTMS modified cement paste and their mix 1:1 by weight. Percentage of silane by weight of cement. ....</i>	<i>131</i>
<i>Figure 5-27. Total heat flow curves for GTO modified cement paste, AEAPTMS modified cement paste and their mix 1:1 by weight. Percentage of silane by weight of cement. ....</i>	<i>132</i>
<i>Figure 5-28. Heat evolution curves for tricalcium silicate and APTES modified tricalcium silicate. Percentage of silane by weight of cement.....</i>	<i>133</i>
<i>Figure 5-29. Heat evolution curves for cement and APTES modified cement. Percentage of silane by weight of cement.....</i>	<i>133</i>
<i>Figure 5-30. Effect of different methodology used for silanization on cement hydration kinetics. Percentage of silane by weight of cement.....</i>	<i>136</i>

Figure 5-31. GTO dosage effect on the hydration kinetics; (a) silanization obtained by dry blending of constituents (b) silanization obtained from ethanol adsorption. ....	138
Figure 5-32. AEAPTMS dosage effect on the hydration kinetics; (a) silanization obtained by dry blending of constituents (b) silanization obtained from ethanol adsorption. ....	138
Figure 5-33. Evolution of calcium ions concentration during the first 30 minutes of hydration for cement and APTES modified cement, in pure water, L/S = 50 000. ....	140
Figure 5-34. Evolution of silicon ions concentration during the first 30 minutes of hydration for cement and APTES modified cement, in pure water, L/S = 50 000. ....	140
Figure 5-35. Evolution over time of the electrical conductivity during the hydration of cement and APTES modified cement in pure water, L/S=250. ....	141
Figure 5-36. Evolution over time of the electrical conductivity during the hydration of cement and APTES modified cement in lime saturated solution, L/S=250. ....	142
Figure 5-37. Evolution of the storage modulus as a function of the strain applied for plain and silane-containing cement pastes prepared with constant w/c = 0.25. For convenience, all measurements have been performed for equal storage modulus values of $3 \cdot 10^8$ Pa. All silanes have been adsorbed from ethanol and the results are reported in percentage of silane by weight of cement. ....	146
Figure 5-38. Evolution of storage modulus and evolution of total heat output for plain cement paste with w/c=0.25 during the first 800 min of hydration. Measurements have been performed under constant strain of $10^{-5}$ and constant frequency of 1 rad/s. ....	150
Figure 5-39. Evolution of storage modulus and evolution of total heat output for plain cement paste with w/c=0.25 during the first 400 min of hydration (enlarged from Figure 5-38). This is in line to what has been previously reported. ....	150
Figure 5-40. Storage modulus and cumulative heat flow for silane modified cement pastes with w/c=0.25 during the first 2000 min. Measurements have been performed under constant strain of $10^{-5}$ and constant frequency of 1 rad/s. All silanes have been adsorbed from ethanol and the results are reported in percentage of silane by weight of cement. ....	152
Figure 5-41. Storage modulus and cumulative heat flow for silane modified cement pastes with w/c=0.25 during the first 1100 min (enlarged from Figure 5-40). All silanes have been adsorbed from ethanol and the results are reported in percentage of silane by weight of cement. ....	153

Figure 5-42. Strain sweep tests for plain tricalciumsilicate ( $w/c = 0.3$ ) and APTES-containing tricalciumsilicate pastes ( $w/c = 0.25$ ). The measurements were performed for storage modulus in the same range of values ( $10^8$ Pa). APTES has been adsorbed from ethanol and the results are reported in percentage by weight of cement.....	157
Figure 5-43. Evolution of storage modulus and cumulative heat flow for tricalcium silicate ( $w/c=0.3$ ) and APTES modified tricalciumsilicate pastes ( $w/c=0.25$ ). Measurements have been performed under constant strain of $10^{-5}$ and constant frequency of 1 rad/s. ....	158
Figure 5-44. Evolution storage modulus and cumulative heat flow for tricalcium silicate ( $w/c=0.3$ ) and APTES modified tricalcium silicate pastes ( $w/c=0.25$ ), during the first 1500 min (enlarged from Figure 5-43).....	159
Figure 5-45. Consolidation of structure over time for neat & APTES modified cement pastes and neat & APTES modified tricalciumsilicate at constant APTES/solid ratio. ....	161
Figure 5-46. Evolution of the storage modulus as a function of the strain applied for individual and blended silane modified cement pastes prepared with constant $w/c = 0.25$ . The measurements have been performed for equal storage modulus values ( $3 \cdot 10^8$ Pa). Percentage of silane by weight of cement. ....	164
Figure 5-47. Evolution of the storage modulus as a function of the strain applied for blended silane modified cement pastes prepared with constant $w/c = 0.25$ . The measurements have been performed for equal storage modulus values ( $3 \cdot 10^8$ Pa). Percentage of silane by weight of cement. ....	165
Figure 5-48. Evolution of storage modulus blended and individually silane modified cement pastes prepared with $w/c=0.25$ . Measurements have been performed under constant strain of $10^{-5}$ and constant frequency of 1 rad/s. Percentage of silane by weight of cement. ....	167
Figure 5-49. Evolution of storage modulus for blended silane modified cement pastes prepared with $w/c=0.25$ . Measurements have been performed under constant strain of $10^{-5}$ and constant frequency of 1 rad/s. Percentage of silane by weight of cement. ..	168
Figure 6-1. Time dependant temperature curves for two silane modified cement pastes. The good signal superposition indicates that 'one pot' approach can be successfully used for surface modification. Percentage of silane by weight of cement. ....	179

<i>Figure 6-2. Needle penetration and cumulative heat release as a function of time for cement pastes with and without APTES. Percentage of silane by weight of cement.</i>	180
<i>Figure 6-3. Schematic illustration of penetrometer needle geometry (reproduced from [122]).</i>	181
<i>Figure 6-4. Storage modulus and cumulative heat flow for 0.7% APTES modified cement pastes measured by low amplitude oscillatory shear test and isothermal calorimetry versus penetration tests and semi-adiabatic calorimetry.</i>	183
<i>Figure 6-5. Comparison between heat flow curves obtained for cement and 0.7% APTES modified cement. The dashed lines indicate that strength tests have been carried out for equivalent amounts of heat release. The values on the curves represent the flexural strength test values measured.</i>	184
<i>Figure 6-6. Comparison between bending strength values for cement pastes with and without admixture prepared with constant w/c =0.3. Percentage of APTES by weight of cement.</i>	185
<i>Figure 6-7. Evolution over time of the heat outputs obtained for plain and 0.5% APTES modified cement pastes. ESEM investigations have been carried out on samples displaying similar amount of heat outs as indicated by the dashed lines.</i>	187
<i>Figure 6-8. ESEM images of cement paste and 0.5%APTES cement pastes. The samples imaged displayed similar amount of heat outputs.</i>	188
<i>Figure 6-9. ESEM images of cement paste and 0.5%APTES cement pastes. The samples imaged displayed similar amount of heat outputs.</i>	189

## List of annexes

<i>ANNEX I GLOSSARY .....</i>	<i>221</i>
<i>ANNEX II PATTERNS FROM TEM/EDS AND SEM/EDS INVESTIGATIONS.....</i>	<i>223</i>
<i>ANNEX III DATA FROM INVESTIGATIONS ON THE HYDRATION KINETICS OF SILANE MODIFIED CEMENT AND TRICALCIUMSILICATE MODIFIED CEMENT .....</i>	<i>225</i>
<i>ANNEX IV DATA FROM INVESTIGATIONS ON VISCOELASTIC PROPERTIES OF SILANE MODIFIED CEMENTS AND SILANE MODIFIED TRICALCIUM SILICATES.....</i>	<i>231</i>





# **1 Introduction**



## Introduction

This work has been carried out within the framework of the Nanocem Marie Curie Research and Training Network ‘Fundamental understanding of cementitious materials for improved chemical, physical, and aesthetic performance’ program funded by the European Community with an emphasis on mobility. The program supported nine PhD students and six post doctoral fellows working on a set of interrelated research projects aiming to promote intersectorial exchange between academia and industry. The present work was part an innovative focused research towards exploring the next generation of multifunctional cementitious materials, aiming in particular for increased ductility, flexibility and adhesion in cement based materials. The research work has been carried out at University of Bourgogne (France), ZAG Ljubljana (Slovenia) and Sika Technology (Switzerland).

Concrete is an essential product, providing society with what it needs in terms of safe, comfortable housing and reliable infrastructure [1]. Besides water, it is the most used material on the planet. This success stems from the ease with which a mixture of grey powder and water can be transformed into a highly functional solid of readily manipulated shapes at room temperature. Furthermore it is a low cost, low energy material made from the most widely available elements on earth [2].

Concrete is defined as a mixture of cement, sand, gravel and water, where cement acts as the binding phase. Huge amounts of cement (140 million t reported for 2006) are annually produced worldwide to satisfy the needs of an ever increasing population and strong urbanisation. Despite the worldwide recession, economic growth remains relatively high. This is not extremely encouraging in regards to the most demanding challenges that confront mankind today, climate change and abrupt global warming. Cement production accounts for some 5–8% of manmade CO<sub>2</sub> emissions [2]. Therefore, there is a continuous pressure to improve the environmental footprint and drive towards sustainability.

During the last years, the cement industry has been answering this tough challenge by increasing energy efficiency (reducing the fossil fuel dependency, fuel optimization, energy recovering) and by efficient use of resources (alternative raw materials). However, the extremely inconvenient reality is that almost 50% of the total CO<sub>2</sub>

## Introduction

emissions originate in the cement production. They come from the decarbonation of the calcium carbonate ( $\text{CaCO}_3$ ) and there isn't even the minor sign suggesting that something is going to change. Therefore, the construction sector must focus on building sustainable housing, roads, schools and other structures that would result in real progress in reducing the overall  $\text{CO}_2$  emission associated with concrete and thus controlling the climate change.

It is known that concrete structures are highly durable and can withstand remarkable compressive loads. However, concrete is extremely weak in tension. In practice, this inconvenience was overcome starting in the mid 1800's when it was found that one could greatly increase concrete tensile strength by embedding steel. Constant progress has ever since been reported in regard to higher strength, better ductility, improved durability and reduced ecological impact.

For example, admixtures have become nowadays an essential component in concrete making. In particular, superplasticizers bring exceptional advantages. On the one hand, they enable to reduce the cement content in a mix, while maintaining normal strength and workability. On the other hand, they give high strength concrete for low the water to cement ratios. This is an extremely important aspect, because the w/c ratio is a key parameter in tailoring the porosity concrete. A low w/c ratio leads to reduced porosity, which results in higher strength, less permeable material that is less prone to damage and ultimately more durable.

Other aspects that makes admixture such an attractive choice for concrete making are the significant economy in manpower and the reduction of construction time as concrete can be pumped straight into the forms, eliminating the need for vibrations and hoisting. As a result there is an important reduction in noise on the job site [2].

Furthermore, superplasticizers allow incorporation of industrial by-products such as coal combustion fly ash, blastfurnace slag, silica fume or other local or market niche products in concrete mix. Apart from good industrial waste management there is also a benefit in strength and durability gain. Nonetheless, the use of supplementary cementitious materials (SCM) reduces the ecological impact of concrete by clinker substitutions. However, the combined availability and reactivity of SCMs is too

## Introduction

limited to match the challenges faced by the cement industry. Therefore, SCMs cannot be regarded as the unique long-term solution.

Technically, nowadays it is possible to obtain cementitious materials with high compressive and tensile strength which are also ductile. Macro defect free cement (MDF), dense silica particle cement (DSP) and compact reinforced composite (CRC) can provide matrix strengths of nearly 200 MPa in tension (MDF) and 400 MPa in compression (CRC) [3]. Strengths up to 800 MPa in compression and 50 MPa in tension can be achieved by sand replacement with metallic powder [4]. Their features are very low water/binder ratios, organic admixtures, improved packing density, high contents of fibres, limitations on the maximum aggregate size and careful control of the particle size distribution. Equally, they appear prohibitively expensive and the applications of such systems need serious incentives on the changes in the societal values towards sustainability [3].

Meanwhile, countries such as Japan or Korea report annual outlay for infrastructure maintenance surpassing that of a new construction [3]. In Europe, nearly 50% of the budget is spent on overall maintenance and repair [5]. This happens because the vast majority of the structures are built using a relatively cheap and low quality concrete that faces durability issues.

The present work subscribes to the efforts towards building performant concrete structures with high flexural strength and toughness. So far, improving the concrete properties addressed physical (improved packing density, low porosity, and low permeability) or chemical (improved ITZ bonding between organic admixtures and inorganic aggregates) aspects related to concrete. The focus here is exclusively on cement and on drastically improving the properties within the cement matrix by tackling chemical aspects.

As said, cement is extremely weak in tension. When subject to tensile loads, it displays a short linear elastic behaviour followed by softening and no ‘hardening’ region. On nanoscale shot, the short elastic domain is the consequence of weak physical surface forces existing between particles in the hardened cement paste. Three types of forces have been identified so far, namely electrostatic, Van der Waals and

## Introduction

capillarity forces [6-11] to be responsible for cohesion in cement stone (mainly in between C-S-H). Also, it has been shown that hydration leads to an increase in the number of contact points among hydrated phases, but does not changes the nature of those forces [12].

This work targets a disruptive innovation which is systematically addressed in this thesis along its seven chapters. Chapter 1 sets the context of the research and defines the objective and the strategy. Our objective is to investigate the possibility of modifying the bonding scheme for cohesion in cement pastes. The concept that we are approaching here is to introduce additional chemical bonding between hydrates that will lead to dramatic changes in the linear elastic domain and as a result in the overall material's performance.

In this task, we will use organofunctional silanes that have been previously reported and extensively used to bond inorganic to organic materials in various industries. Because initially, we aim to graft different silanes to anhydrous cement particles a brief overview of cement as a material and basics of silane chemistry and applicability are discussed (Chapter 2). The grafting implies the formation of covalent siloxane bonds, among cement surface hydroxyls and silanes' hydrolysable groups. To our knowledge no work has been published up to now dealing with chemically bonding silanes to cement, except for [13].

Chapter 3 presents the materials used in the experimental work.

First, we will investigate this hypothesis (grafting) by direct mixing of the two components. Although easy to use, the method proves to lack scientifically and provides highly insufficient control of the grafting process. Moreover, the modified cement substrates appear to exhibit significant loss in mechanical properties. This will be pointed out in Chapter 4.

A second grafting technique, previously reported in literature as an efficient for grafting silanes to inorganic substrates, will be investigated. This will enable better control of the grafting process and of the parameters influencing it by working on

## Introduction

very small sample size (Chapter 5). At a later time, the study will focus on the properties of the modified substrate: hydration and viscoelastic properties.

Additionally, a complementary method will be looked at (Chapter 6). The objective here will be to efficiently upscale the grafting methodology for producing sufficient material for macroscopic tests. Thus, several mechanical tests and rheological experiments will be carried out on large scale samples. The macroscopical data tests results will be linked to the rheological properties.

In a second step, the work will investigate rather briefly, the possibility of another chemical bonding assumed to be taking place among reactively compatible end groups of species that have been already attached to cement while still in anhydrous state (amine and epoxy). This will be done by looking on how blends of two individually silane modified cements perform in terms of rheology and hydration kinetics (Chapter 5).

Finally, the most important findings and their implications in regard to future work will be presented (Chapter 7).





## **2 General considerations. Cement and silane agents**

General considerations. Cement and silane agents.

The present chapter deals with general aspects of cement and silanes.

The first section gives a brief overview on cement by focusing on the transformations of anhydrous cement to a hard solid material. Physical and chemical changes will be highlighted. Then we will address the cohesion of cement. This will be done by investigating the characteristics of main phase responsible for cohesion in cement (C-S-H) and of hypotheses made throughout the manuscript concerning the forces controlling the hardened material's integrity.

The second section deals with basics of silanes chemistry. The concept of coupling two dissimilar materials with organofunctional silanes will be addressed by considering some of the existing applications. In addition, other key roles played by silane agents will be presented and their applications will be shortly reviewed. Finally, the work involving the use of silanes in cementitious materials area is briefly reviewed and the most important changes in properties are discussed.

## **2.1 Cement**

### **2.1.1 Anhydrous cement**

Portland cement is the most common type of cement used around the world. In principle, it is made by heating a mixture of limestone and clay, or other materials of similar bulk composition and sufficient reactive, ultimately to a temperature of about 1450<sup>0</sup>C when clinker nodules are produced [14]. Once cooled these are finely ground (fineness characterized by particles with diameter below 150 µm) and mixed with some form of calcium sulphate to delay the setting. Thus ordinary Portland cement (OPC) is produced. The dry cement powder contains four major phases but several other phases as alkali sulphate and calcium oxide are normally present in minor amounts (Table 2-1).

General considerations. Cement and silane agents.

*Table 2-1. Simplified writing of the major crystalline phases found in Portland cement.*

Pure phase	Name	Simplified notation	Impure phase	Proportion by weight
$3\text{CaOSiO}_2$	Tricalcium silicate	$\text{C}_3\text{S}$	alite	60-65%
$2\text{CaOSiO}_2$	Dicalcium silicate	$\text{C}_2\text{S}$	belite	10-20%
$3\text{CaOAl}_2\text{O}_3$	Tricalcium aluminate	$\text{C}_3\text{A}$	celite	8-12%
$4\text{CaOAl}_2\text{O}_3\text{Fe}_2\text{O}_3$	Tetracalcium ferroaluminate	$\text{C}_4\text{AF}$		8-10%

Partial replacement of clinker with limestone, pozzolana or industrial by-products such as coal combustion fly ash, blast furnace slag, silica fume is today a common standardized practice (EN 197-1:2000). These materials are generically termed supplementary cementitious materials (SCM). Apart from bringing additional benefits (better space filling) to cement-based systems, they also respond to the increasing trends in social attitudes towards global warming issues. This is because producing 1kg of cement accounts roughly for 1kg of  $\text{CO}_2$  being released in the atmosphere (summing up the  $\text{CO}_2$  from limestone decarbonation and from fuel combustion). In order to limit the detrimental impact on the environment, the clinker is being partially substituted by SCM's. Thus, the nominal emissions corresponding to 1kg of binder are lowered.

## 2.1.2 Hydrated cement

### 2.1.2.1 Time dependent chemical changes

In contact with water cement hydrates. Cement hydration is not a single reaction but a sequence of overlapping reactions leading to setting and hardening [15]. It is now generally agreed that hydration takes place due to a difference of solubility between the anhydrous cement phases and the hydrates: hydrates solubility is lower than the

General considerations. Cement and silane agents.

one of cement phases and they are thermodynamically more stable in presence of water (a thermodynamically stable system aims for its lowest energy state).

Cement hydration involves a time dependent heat release. This (cement hydration) can be oversimplified but conveniently and continuously monitored by calorimetric measurements. Overall, the hydration reaction of Portland cement is identified as exothermic as it sums up the heat evolved by all the reactions occurring at any time. Although the associated thermal effects vary depending on the cement particle size, the reactivity and w/c ratio, similar stages of cement hydration can be identified as characteristic for all Portland cements. A typical heat evolution curve is presented in Figure 2-1.

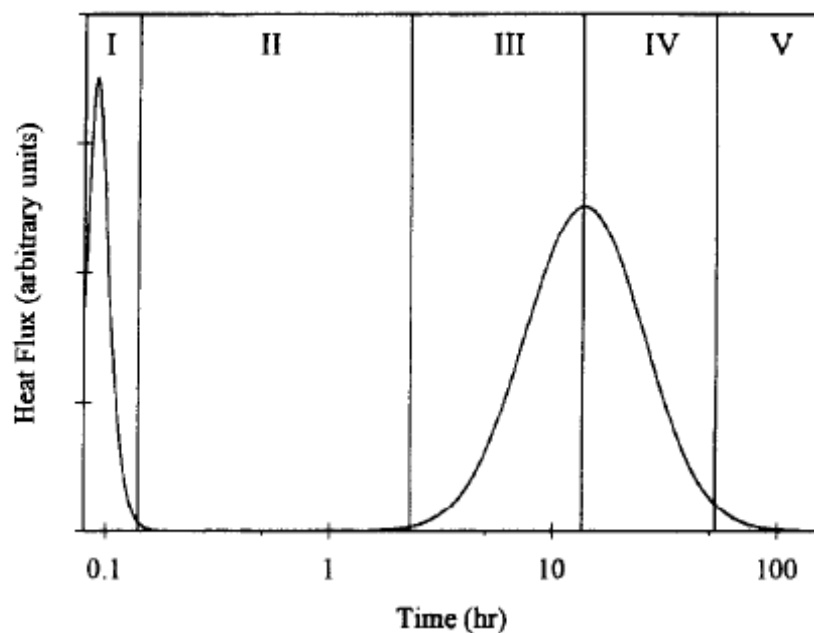


Figure 2-1. Schematic cement hydration thermogram showing five distinct stages in the hydration process (reproduced from [16]).

- I. Initial period.
- II. Induction (or dormant ) period.
- III. Acceleration period.
- IV. Deceleration period.
- V. Slow reaction period.

During the **initial period**, corresponding to first instants of cement-water mixing, a series of rapid dissolutions take place leading to the first exothermic peak on the heat evolution curves. Aluminate phases (exothermic), alkali sulphates (although endothermic), free lime and calcium sulphate (weakly exothermic) dissolve and ions are released into the interstitial solution where the pH increases rapidly. The silicate phases are superficially hydroxylated and they start releasing calcium and silicate ions into solution but their contribution is much lower to the initial heat release compared to the aluminates. Following the dissolution processes, rapid precipitation of aluminate hydrates occurs. In addition precipitation of hydrated sulphate phases often takes place [15].

After several minutes the reaction slows down significantly, enters into what is referred in the literature as **induction or dormant period** characterised mainly by a high rate of heat release. Reaction of aluminates continues and may lead to two undesired chemical phenomena depending on the sulphate availability. Insufficient sulphate levels triggers a 'flash set' (excessive nucleation and growth of hexagonal C-A-H) while too high additional levels of calcium sulphate hemihydrate may result in 'false set' (massive nucleation and growth of gypsum). Nucleation of early C-S-H and of portlandite takes place as the interstitial solution becomes saturated first with respect to C-S-H and afterwards to Portlandite.

A second exothermic heat peak defines the **acceleration period** which produces a sharp increase in the rate of cement hydration. Simultaneous dissolution of silicate phase and precipitation of both C-S-H and portlandite are the main chemical processes within this period. As the concentrated suspension of flocculated particles changes to a viscoelastic skeleton capable of supporting an applied stress [17], setting takes place. The process is assumed to be related to the physical evolution of the system and will be discussed in the next section. As a result, the structure develops early strength and gains consistency.

A continuous development of the solid skeleton takes place during the **deceleration and the slow reaction periods** leading to the ultimate development of mechanical properties. Formation of C-S-H and portlandite rate decelerates but continues slowly

General considerations. Cement and silane agents.

over time (years if water is available). Additional calcium monosulphoaluminate hydrate is formed as ettringite reacts with the remaining tricalcium aluminate, provided that all the sulphate has been already consumed.

### 2.1.2.2 Time dependent physical changes

As mentioned above, when mixed with water anhydrous cement phases hydrate over time forming a hard solid body able to sustain loads. Along with the chemical transformations and strongly dependent on them, the system passes through several stages as it develops strength.

Hydration comes along with **volume changes**. As hydration advances, anhydrous phases and water are consumed and hydrates and pores are created. The process is associated with volume changes because the specific volume of the products is lower than that of the reactants. This can come mainly from the fact that water is more densely packed when bound (in hydrates) than in free state [18]. Equation (2-1) provides a simplified look this phenomenon simply considering the case of  $C_3S$ .

$$V_{C_3S} + 1.318V_{H_2O} \Rightarrow 1.57V_{C-S-H} + 0.597V_{CH} \quad (2-1)$$

The overall volume balance indicates:

$$\sim 2.318 \quad \Rightarrow \quad \sim 2.157 \quad (2-2)$$

This suggests that there is an overall total decrease in system's volume ( $\sim 7\%$ ). This is referred to as chemical shrinkage, well known and documented subject since 1904 [19]. However, practically the decrease in volume is much less ( $\sim 1\%$ ) because the structure is rigid and optimum packing can never be achieved. On the other hand, the volume of solids almost doubles. This means that as hydration advances porosity decreases as space is filled with hydrates [20].

In addition, water dosage with respect to cement is a key factor until the paste becomes a hard solid body. Generally considered as weight ratio, it influences a lot the other physical sequences that the system is passing through. The amount of added

General considerations. Cement and silane agents.

water controls the spacing between the cement grains. The minimum water/cement ratio necessary to reach full hydration in a closed system is 0.42 [19]. When the water/cement ratio is greater than this value, the hydrated cement paste will still contain some free water after its full hydration leading to additional porosity which will negatively impact the system's properties.

Generally, hydrated cement pastes display a wide variety of pores ranging from nm to  $\mu\text{m}$ , varying in amount, size, distribution and origins. A schematic representation is given in Figure 2-2.

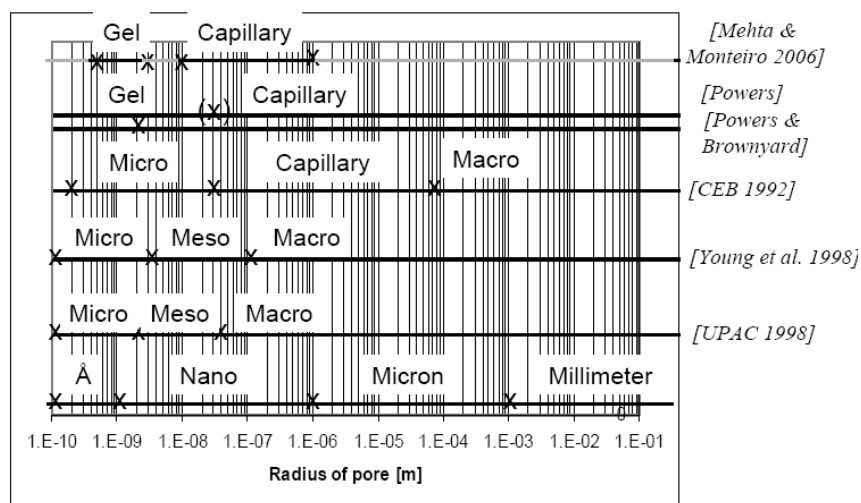


Figure 2-2. Nomenclature of pores (reproduced from [5])

Many studies can be found pointing out the fact that porosity is a key factor in hardened cement pastes because it influences the material's strength [20, 21]. In addition, pores (mainly capillary pores) are responsible for the transport phenomena, making possible penetration of hazardous ions (sulphates, chlorides, carbonates) which results in reduced performances. Ultimately, materials' durability is negatively affected.

The transition from the soft state of a paste to the hardened state is defined as **setting**. It involves two fundamental processes namely coagulation and rigidification. The first one, results from the attractive forces between particles and leads to the formation of a mechanically reversible connected network. During the second one, hydrates, mainly



General considerations. Cement and silane agents.

C-S-H, precipitate near the contact zones increasing the number of contact points. Thus, C-S-H strengthens the structure resulting from coagulation leading to a mechanically irreversible network of particles [22]. Over time, **hardening** leads to an increase in material strength by a continuously filling up the pore space.

### **2.1.3 Cohesion of cement pastes**

Among the precipitated hydrated phases, C-S-H is the main component (at least 60 % in a fully hydrated cement paste) responsible for setting and hardening of cement [9] and also for its subsequent mechanical performances. It is known that cement paste can exhibit a high compressive strength ( $>100$  MPa), whereas its tensile strength is extremely low ( $<2$  MPa) [9]. It was suggested that this is because the cohesion of the network is due to short range surface forces between C-S-H particle and cement grains and C-S-H particles themselves [23].

In this context it appears logical to take a closer look at this main phase (C-S-H) and at the interparticle forces controlling the cohesion in cement pastes.

#### **2.1.3.1 C-S-H**

Over the years, several models for C-S-H have been proposed [20, 24-26], but debates are still ongoing. Apart from providing a clear conceptual understanding of cement paste structure, C-S-H models also help to understand the nature of cohesion.

Nowadays, it is generally accepted that C-S-H is a nanostructured compound extremely variable in stoichiometry and poorly ordered. Therefore, it is referred to as ‘C-S-H gel’ in cement paste [21].

Compositionally, C-S-H gel in cement paste is generally characterized by a mean Ca/Si ratio of about 1.75, with a range of values within a given paste from around 1.2 to 2.1 [27]. Locally values were found to decrease down to 0.6.

Morphologically, it is generally admitted to be made of ordered stacks of up to several tens or even hundreds of nm-thick lamellae. The stacks are negatively charged

General considerations. Cement and silane agents.

lamellae separated by hydrated calcium ions. An ordered stack containing, on the average 4 silicate layers and 3 interlayer spaces giving a thickness of 5 nm, is usually referred to as a particle. A TEM observation on the ordered stacks and a schematic representation of a ‘particle’ is presented in Figure 2-3.

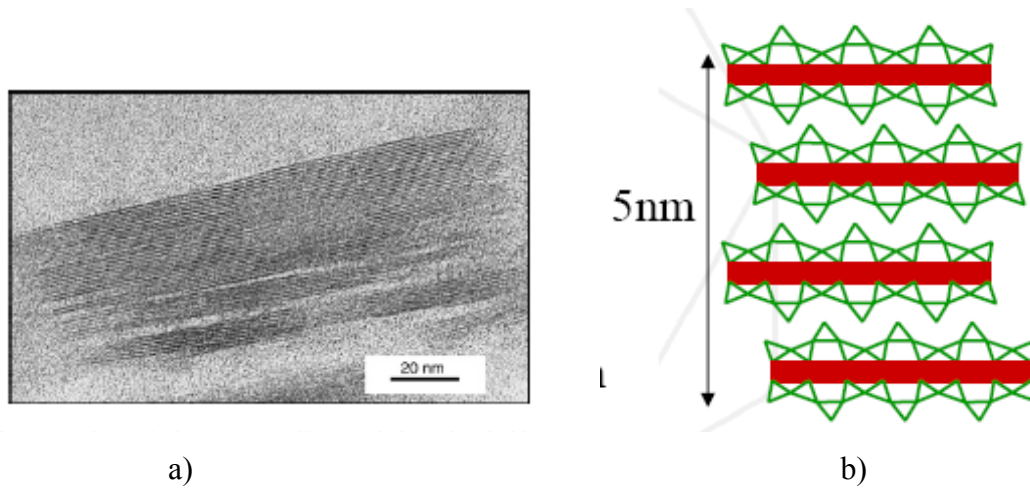


Figure 2-3. (a) TEM micrograph of C-S-H prepared by pozzolanic reaction of calcium oxide with silica (reproduced from [6]); (b) C-S-H schematic representation (reproduced from [18])

Advancement of hydration does not proceed by particle growth, but by their multiplication and aggregation often along a preferred orientation. Lateral growth is always faster, but the ratio of axial over lateral growth appears to depend on the lime concentration in the solution, high lime concentration favouring the axial growth of high Ca:Si ratio C-S-H [28]. As structure develops, it loses order. [6]

A large number of models have been proposed for C-S-H nanostructure mainly by drawing structural analogies to the crystalline calcium silicate hydrate minerals tobermorite and jennite. Richardson recently published an exhaustive and well documented review [29]. The difference from the reference mineral tobermorite with Ca:Si=0.66 where the chains are infinite and run parallel to the b axis, is that C-S-H consists of disordered silica chains.  $^{29}\text{Si}$  NMR experiments have revealed that only finite silicate chain lengths are known to exist in C-S-H [30]. The repeating units along the chains are called dreierketten and consist of tetrahedral silica edge grafted on each side of two parallel  $\text{Ca}^{2+}$  ions multi coordinated planes (coordination higher

General considerations. Cement and silane agents.

than 6) (Figure 2-4). The higher the Ca:Si ratio the larger the number of missing bridging tetrahedra and the shorter the average chain length [31].

So far, bonding discontinuity marked by defects and disorders can be considered as a hypothesis for system's failure.

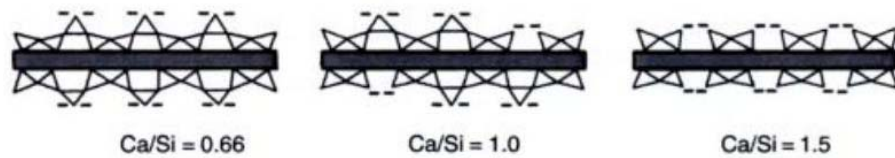


*Figure 2-4 Several C-S-H layered structure configurations illustrating the progressive loss of bridging tetrahedral and the localisation of the surface charge (reproduced from [31])*

Similar structural arrangements can be found in smectite clays. A well documented example is montmorillonite [32]. Both smectite clays and C-S-H have individual negatively charged nm thick layers that can accommodate hydrated cations to compensate the deficit in charge in the interlayer space. It must be noted that dissimilarities exist as well. Larger lateral extension of the layers up to  $\mu\text{m}$  range and negatively charged surfaces originating from isomorphous substitutions in the tetrahedral and octahedral layers are typically characteristics for smectite clays. Also the surface charge for montmorillonite is 2 up to 5 times (depending on the Ca:Si ratio considered) less significant in comparison to tobermorite [33]. Therefore a less cohesive behaviour is expected for clays.

Surprisingly, when immersed in water clays are far from exhibiting the cohesion of cement hydrates. On the contrary, their most characteristic behaviour is swelling [32]. However, it is interesting that Ca-smectite clays exhibit restricted swelling, while Na or Li-smectite clays exhibit a quasi unlimited increase of the interlamellae distance [31]. Therefore lots of parallel comparative studies between smectite clays and C-S-H clays have been carried out, aiming to shed some light on their different behaviour and provide a clue for understanding the latter.

### 2.1.3.2 Origin of cohesion

Seeking for an explanation on the source of strength of the gel itself Powers was questioning the cohesive nature of C-S-H. He made a fair speculative assumption that: “strength arises from two general kind of cohesive forces: (1) physical attraction between solid surfaces and (2) chemical bonds. Since gel pores are only about 15 a.u. ( $\sim 8 \text{ \AA}$  nm) wide on the average, it seems that van der Waals forces ought to tend to draw particles in positions of least potential energy. In either case, those forces give rise to cohesion. Since water cannot disperse gel particles, i.e. since cement belongs in the limited-swelling category, it seems that the particles are chemically bonded to each other (cross- linked) [20]. Such bonds, much stronger than van der Waals, add significantly to overall strength.”

Power’s assumptions regarding cohesion were based on assemblage of spheres  $100 \text{ \AA}$  in diameter, separated by films of water  $6 \text{ \AA}$  thick. To provide this body with strength and keep it together the existence of solid bonds between the spheres was postulated (Figure 2-5 A and B). Water–vapour can penetrate all the spaces between particles and can move reversibly in and out of the spaces. When the hydrated cement is dried, the spheres are said to come together. (Figure 2-5 C). Later the findings through electron microscopy revealing that C-S-H was composed of thin sheets and foils changed the model accordingly (Figure 2-5 D)

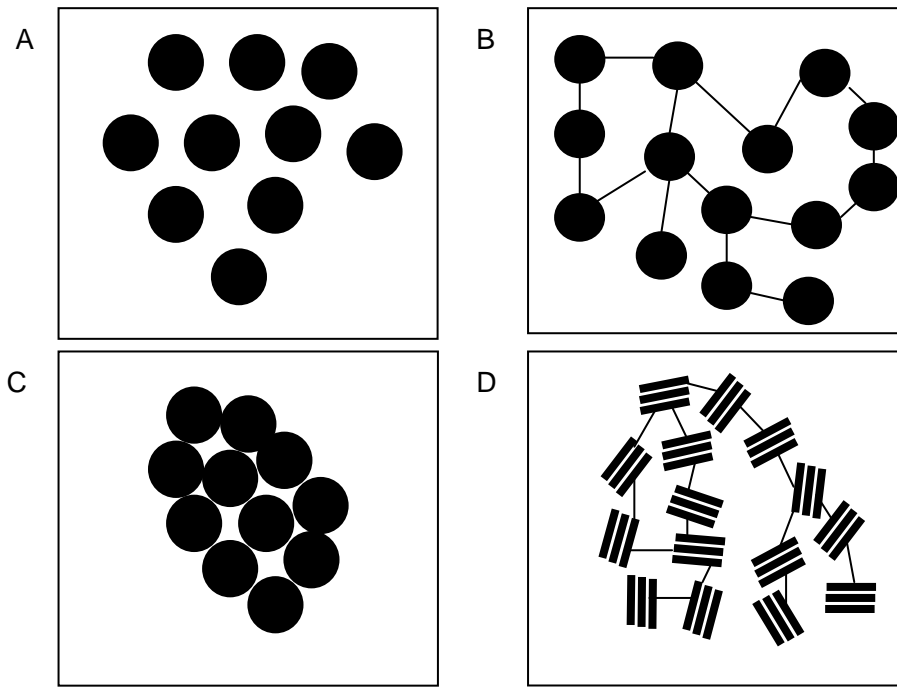


*Figure 2-5. Previous concept of hydrated cement (adapted from [25])*

The possibility of covalent bonds between layers via bridging tetrahedras was soon unconceivable and contradicted by several experimental observations.

Sereda and Soroka [34] showed that one gets the same hardness and the same elastic modulus for a pellet obtained from compacting a cement powder hydrated in a large volume of water and filtered afterwards as for a cement paste hydrated in normal conditions at equivalent porosity. Sereda, Feldman, and Ramachandran [35] confirmed previous findings by compacting a crushed and ground hydrated cement sample into a pellet and compare it to a piece of hardened cement paste prepared in normal conditions. Remarkably, the strength was the same for both specimens. Consequently, the covalent bonding concept was no longer valid and surface forces were considered responsible for interparticle cohesion.

### **2.1.3.3 Interparticle forces**

In what follows we will present several theoretical considerations regarding interparticle surface forces that are believed to be responsible for holding the C-S-H lamellas together. The purpose of the next paragraph is not to give a full analytical

General considerations. Cement and silane agents.

description of surface forces, but rather to introduce the strictly necessary aspects to understand the cohesion of cement paste by taking a microscopic snapshot.

The simplest framework in which this subject will be discussed is by considering the DLVO theory [36]. This theory originated in colloidal science and proved to be a valuable tool in gaining understanding of C-S-H cohesion at microscopic scale. DLVO theory describes the forces between charged surfaces interacting through a liquid medium. It combines the effects of the van der Waals attraction and the electrostatic repulsion originating in the electrical double layer. However, DLVO is not totally efficient in describing the cohesion phenomena in cement paste. These aspects will be discussed below.

### Van der Waals forces

Van der Waals forces in between two identical particles are always attractive.

Microscopically, van der Waals forces originate in rapidly fluctuating dipoles caused by the polarizability of the electronic cloud. This dipole interacts with other nearby molecules and induces similar temporary polarity (Figure 2-6).

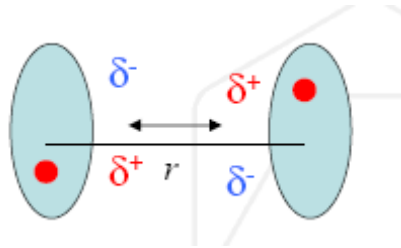


*Figure 2-6. Polarisability of the electronic cloud. Inducing dipoles.*

The energy of attractive interactions between the two dipoles is:

$$w(r) = -\frac{\alpha_0 a_0^2 e^2}{(4\pi\epsilon_0)^2 r^6} = -\frac{C_6}{r^6} \quad (2-3)$$

General considerations. Cement and silane agents.

Where:

$\alpha_0$  is the polarisability

$a_0$  is the first Bohr radius

$e$  is the electron unit charge

$\epsilon_0$  is the permittivity of free space

$r$  is the separation

$C_6$  is a constant

The force is extremely weak ( $\sim 1\text{kJ/mol}$ ) compared to ionic-covalent ( $\sim 500\text{kJ/mol}$ ) or to hydrogen bonds ( $20\text{ kJ/mol}$ ) [37]

If we now integrate this energy of interaction between of all the atoms in one body with all the atoms in the other body we obtain the ‘two-body’ potential energy. This procedure can be carried out for all geometries. For example, the interaction energy for two identical spheres is given by:

$$W = -\frac{AR}{12D} \quad (2-4)$$

Where:

$A$  is the Hamaker constant

$R$  is the radius of the sphere

$D$  is the separation distance calculated between the centres of the two spheres

The main difference compared to atomic scale is that the range of the force is greater. The Hamaker constant is given by the equation (2-5):

$$A = \pi^2 C \rho_1 \rho_2 \quad (2-5)$$

General considerations. Cement and silane agents.

Where:

C is the interatomic pair potential coefficient

$\rho_1$  and  $\rho_2$  are the number of atoms per unit volume in the two bodies (density)

Typical values for Hamaker constants are in the range of  $10^{-19}$  J for air or vacuum and in the range of  $10^{-20}$  J for water [38]. As for our case, given the separation distance between the C-S-H lamellas, it is immediately noticeable that the force is extremely low in intensity can not provide the full explanation for cement paste cohesion. Moreover, experimental evidence [22] suggests that other types of forces than van der Waals need to be considered for explaining the cohesion in cement pastes.

### **Electric double layer forces**

Most solids bare electrical charges on their surfaces. In contact with a liquid usually of high dielectric constant, surface groups dissociate and ions are released into solution. This results in the development of a wall surface potential which will attract counterions from the surrounding solution and exclude co-ions. In equilibrium, the wall surface charge is balanced by an equal but oppositely charge of counterions. The region of counterions is called the electrical double layer (EDL). A schematic representation is illustrated in Figure 2-7.



General considerations. Cement and silane agents.

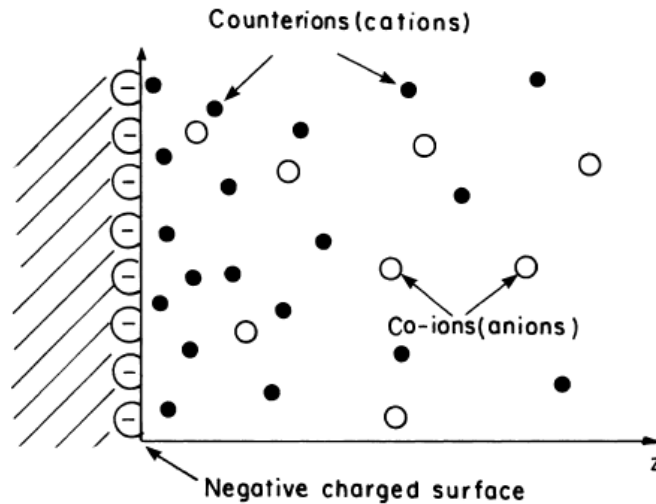


*Figure 2-7. Schematic illustration of the electrical double layer developed when a surface which is negatively charged and immersed in an aqueous solution is attracting (positive) counterions and creates a depletion zone of the (negative) co-ions. (reproduced from [38]).*

The properties of the EDL have been extensively studied [38, 39]. It is relevant for the purpose of this work to consider two situations (i) low surface charge density and high surface charge density and divalent counterions.

In case of low surface charge density, the distribution of the counterions is described using a primitive model where ions are treated as charged hard spheres that cannot overlap and interactions between them are neglected. The solvent is regarded as a dielectric continuum.

Consider now two charged flat surfaces, in a symmetrical electrolyte facing each other. The separation distance in between plate is  $D$  and the mid-plane separation is  $x=D/2$  (Figure 2-8 a)

General considerations. Cement and silane agents.

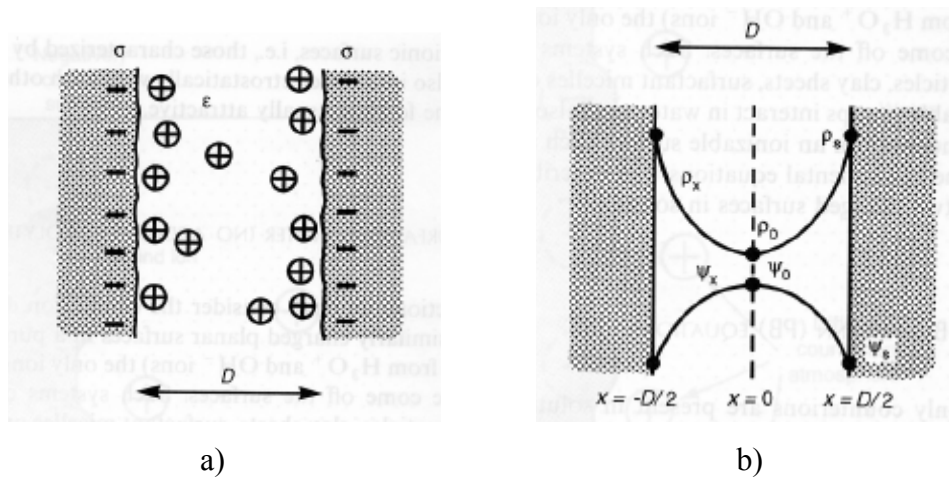


Figure 2-8. (a) Two negatively charged surfaces of surface charge density  $\sigma$  separated by a distance  $D$ ; (b) the counterions density profile  $\rho_x$  and electrostatic potential  $\psi_x$ .

The concentration of the counterions is described by a Boltzman distribution (2-6)

$$\rho = \rho_0 e^{\frac{-ze\psi}{kT}} \quad (2-6)$$

Where:

$\rho$  is the counter ions density

$\rho_0$  is the counter ions density at mid-plane

$z$  is the valence

$e$  is the electron unit charge (magnitude of the electron charge)

$\psi$  is the electrostatic potential

$k$  is Boltzmann's constant

$T$  is the temperature

The equation (2-6) combined with the Poisson law (which describes the relation between the electric potential  $\psi$  and the charge density  $\rho$  at any point) gives the Poisson- Boltzmann equation (2-7):

General considerations. Cement and silane agents.

$$\frac{d^2\psi}{dx^2} = -\left(\frac{ze\rho_0}{\varepsilon\varepsilon_0}\right)e^{-\frac{ze\psi}{kT}} \quad (2-7)$$

Where:

$\varepsilon$  and  $\varepsilon_0$  are the dielectric permittivity and the vacuum permittivity

At equilibrium the confinement of the cations in the diffuse double layers generates an osmotic pressure, known as the osmotic pressure, leading to repulsion. The pressure at any point  $x$  in the gap is:

$$P_x(D) = kT\rho_0(D) = -\frac{\varepsilon_r\varepsilon_0}{2}\left(\frac{d\psi}{dx}\right)_{x(D)}^2 + kT\rho_x(D) \quad (2-8)$$

We note that the above equation sums up two terms: a first one negative, the attractive electrostatic term and a second one positive, the osmotic term. Surprisingly, the electrostatic contribution is actually attractive, but the latter dominates and the net result is repulsive [38]. Consequently, we can consider that the ionic double layer forces in the case of low surface charge density are always repulsive.

In this case (low surface charge density and low salt concentration) by summing up the repulsive double layer and the attractive van der Waals forces the DLVO theory predicts repulsion between C-S-H lamella behaviour. This is where the DLVO theory fails to explain cement paste cohesion because of the reasons which will be described below.

Hydrated cement pore solution is far from being a monovalent symmetric electrolyte where ions size and interaction can be neglected. The ionic conditions in paste are of extreme high concentration of hydroxyl ions. These ions react with the surface groups of C-S-H particles inducing a high surface charge density. In addition, there is high concentrations of calcium ions to balance the charge from hydroxyl ions [40]. Therefore, it is clear that in order to correctly account for the conditions existing in

General considerations. Cement and silane agents.

cement pastes one has to take into account the size of the ions, the interactions between, their divalent nature and the high surface charge density of the walls.

By doing so, there is no analytical solution, but Monte Carlo (MC) and hypernetted chain (HNC) numerical simulations evidenced the existence of an attractive component at short ranges that gives a total osmotic pressure that is in fact attractive [6, 28, 39, 41-44]. This has been possible by taking into account the so called ion-ion correlation forces and the local fluctuations of the potential whereas in the mean field treatment only the average potential and a smoothed ionic distribution are considered.

Moreover, the fact that those interactions between C-S-H particles become attractive at high surface charge density and in the presence of divalent calcium ions have been experimentally evidenced by atomic force microscopy (AFM ) [9, 10, 45, 46].

### **Capillarity forces**

Another type of attractive forces, that contributes to cement paste cohesion is the capillarity force. In general we become aware of the existence of capillarity phenomenon by looking of the surface of a liquid, for example water, in a small cylinder as shown in Figure 2-9.

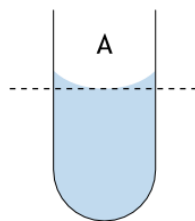


*Figure 2-9. Example of meniscus formed on the top water surface in a tube.*

As a consequence of surface energy minimization, the water top surface curves, generating a meniscus (concave for water) while the surface tension tends to straighten it, putting water in the vessel under tension. This results in a lower vapour pressure of the water in the tube than normal for the existing temperature, which

General considerations. Cement and silane agents.

accounts to saying that there is an attractive force between the walls of the tube. The narrower the tube, the more significant is the difference to the atmospheric pressure and the attraction among the walls gets important.

This pressure drop across the curved surface is given by the Young Laplace equation:

$$P_{cap} = 2\gamma\kappa \quad (2-9)$$

Where:

$\gamma$  is the surface tension, and

$\kappa$  is the curvature radius for a spherical meniscus.

Having in mind these assumptions and considering now the water in between the C-S-H lamella, at a spacing of 1.5 nm the pressure becomes considerable (-100 MPa) [31].

In saturated materials capillary forces are however not present. Because hardened cement keeps its strength quasi-indefinitely in water, capillary forces are unable to provide the general explanation for the cohesion of cement hydrates. However, some contribution of capillary forces to the overall cohesive behaviour may be assumed.

### **Summary on the forces controlling the cohesion**

Having highlighted all these aspects, it is now clear that cohesion in cement paste is controlled by purely physical surface forces acting on a short range. Moreover, the overall attractive behaviour is the sum of the van der Waals forces, electrical double layer forces and capillary forces. Despite the fact that, the first and the last are always attractive none of them can individually provide a reasonable explanation for cement paste cohesion.

In conditions representative of the pore solution in cement paste (very high negative charge density and presence of the divalent counterions) the electrical double layer forces are overall attractive. This is the consequence of ion-ion correlation forces. The

General considerations. Cement and silane agents.

fact that DLVO theory fails to explain the cohesion in cement paste is because the Poisson Boltzmann equation does not take into account the ion-ion correlation forces.

Even earlier Powers did not reject the existence of physical bonding: ‘there is a good reason to believe, that only a small fraction of the boundary of the gel particle is chemically bonded to neighbouring particles and that physical bonds are perhaps the more important’[20]. The assumption was based on the fact that steam curing at 204°C destroys cohesion and turns the gel into well organized crystals.

## **2.2 Silanes**

This section will provide a general overview on the key ‘ingredient’ used in this work: organofunctional silanes. Aspects concerning their chemistry and ability to react with both organic and inorganic materials will be shortly outlined. In what follows, we will present several applications pointing their significant role in the adhesion processes. Also, examples where silanes have already been used in cementitious materials will be reviewed and the observed change in properties will be pointed out.

### **2.2.1 Basics chemistry**

In principle, silanes are compounds of silicon and hydrogen, of the formula  $\text{Si}_n\text{H}_{2n+2}$  analogues of alkanes [47]. Silanes tend to be less stable than their carbon analogues because Si-Si bond has slightly lower strength than C-C bond.

In practice, terminology has been extended and it includes also compounds in which any or all of the hydrogen have been replaced. A silane that contains at least one carbon-silicon bond structure is known as an organosilane. Carbon-silicon bond is very stable, very non-polar and gives rise to low surface energy and hydrophobic effects as a consequence of silicon’s more electropositive nature when compared to carbon [48]. Therefore, bond strengths, bond angles, and bond lengths are quite different from most organic compounds, especially those including electronegative elements, such as oxygen, fluorine, and chlorine.

General considerations. Cement and silane agents.

Organofunctional silanes are hybrid compounds that combine the functionality of a reactive organic group and the inorganic functionality in a single molecule. A typical general formula of an organofunctional silane is:



Where:

R is a nonhydrolyzable organic head group moiety that can be either alkyl, aryl, organofunctional, or a combination of any of these groups

X represents the hydrolysable group, alkoxy moieties, such as methoxy, ethoxy, acetoxy.

Given the wide variety of possible substitutions one can easily imagine the amount of resulting combinations. However, most of the widely used organosilanes have one organic substituent. For the purpose of the present study, we will focus our attention on the alkoxysilanes, in particular on the trialkoxysilanes. However, for convenience and to avoid repeating the long terminology defining the compound it will be simply referred to as silane agent or silane.

Trialkoxysilanes,  $RSi(OR^I)_3$  are water miscible. In water they hydrolyze stepwise to give the corresponding silanols, which ultimately condense to siloxane. The reactions are well documented in the literature [49]. The hydrolysis is relatively fast (minutes), while the condensation reaction is much slower (hours) [49]. Both reactions (hydrolysis and condensation) can be acid or base catalyzed. Thus, the pH is a major factor governing the stability of silanes in aqueous solution. A schematic illustration is given in Figure 2-10.

General considerations. Cement and silane agents.

#### ALKOXYSIANE HYDROLYSIS & CONDENSATION

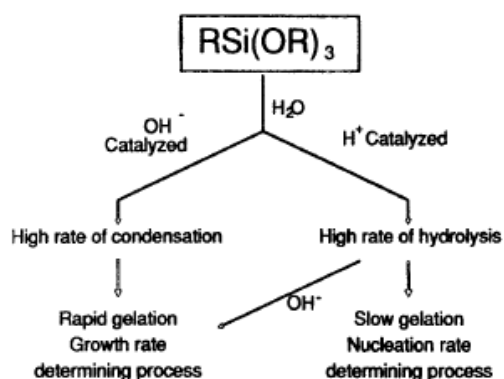


Figure 2-10. Alkoxysilane hydrolysis and condensation (reproduced from [50])

Among other factors influencing the kinetics and the equilibrium of hydrolysis and condensation reactions are the nature of the organofunctional group and its spacing compared to silicon atom, the concentration of silanes in water and the temperature. For example, it is generally reported that higher alkoxysilanes hydrolyze more slowly than lower alkoxysilanes. Figure 2-11 illustrates the pH dependency of the hydrolysis and condensation reaction of a typical silane.

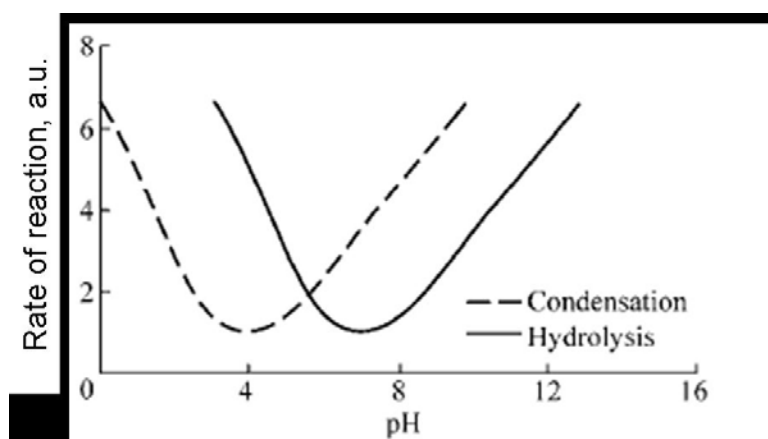


Figure 2-11. Hydrolysis and condensation rate of a typical silane (adapted from [51])

Also, the distance of the organofunctional group from the silicon atom plays a significant role in the compound's reactivity. The shorter the spacer group, the more reactive the silane agent [52].



## 2.2.2 Silanes at interfaces

As said, organofunctional silanes are very valuable molecules containing both organic and inorganic reactivity in the same molecule. This makes them extremely attractive for their capacity to bond two otherwise dissimilar materials.

Their value has been first discovered in the mid 30's in conjunction with the development of fibreglass-reinforced polyester composites [53]. When initially fabricated, these new composites were very strong, but their strength declined rapidly during aging. This weakening was caused by a loss of bond strength between the glass and resin[48]. Silanes were found to provide stable bonds between these otherwise poorly bonding surface. An oversimplified picture of the coupling mechanism is shown in Figure 2-12. [48].



*Figure 2-12. The silane coupling mechanism (reproduced from [48])*

The inorganic reactivity represents the capacity to form bonds with inorganic surfaces. The inorganic surface hydroxyl groups coordinate with the silanols resulting from silanes' hydrolysis to form siloxane type bonds. This happens either through the addition of water or from residual water on the inorganic substrate. Additionally, silane molecules also react with each other (crosslink) to give a Si-O-Si network. This results in a tight siloxane network close to the inorganic surface that becomes more diffuse away from the surface [48]. A schematic representation is given in Figure 2-13.

General considerations. Cement and silane agents.

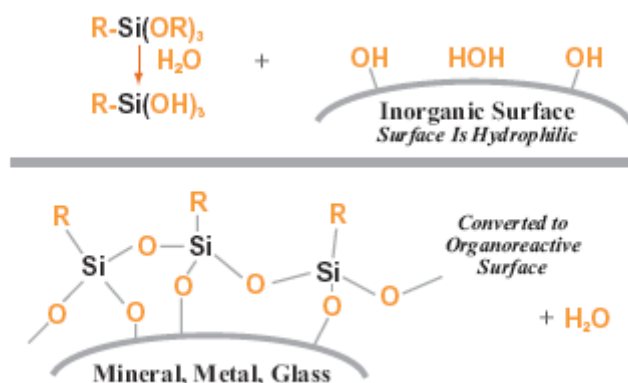


Figure 2-13. Schematic representation of conceptual bonding of trialkoxysilane to the inorganic surface (reproduced from [48])

The chemical bonding theory has been a long debated subject and it is still a controversial topic. There are however some basic mechanism which are well established and agreed upon. Hydrolysis of silane agents drives their attachment to the substrate resulting initially in hydrogen bonds formed with hydroxyl groups or with water layers from the mineral surface. The question arose whether those silanols groups ever condense to oxane bonds with the surface.

With the development of Fourier transform infrared (FT-IR) spectroscopy it has been possible to observe the covalent bonds between silane agent and inorganic surfaces [49, 54, 55]. Also, high resolution X-ray Photoelectron spectroscopy (XPS) has evidenced the formation of chemical bonding among various silanes and E-glass surfaces [56] silica, glass, metals . Furthermore, solid state NMR, using labelled  $^{13}C$  has shown the direct link between the silane agent and the inorganic substrate [57, 58]. Nevertheless, Raman scattering spectra have proved the existence of chemically bound aminosilanes on silica gel [59].

Because silane hydrolysis is a hard to control process, surface depositions of monolayer are hardly achieved. Some of the studies surveyed claimed both excessive aggregations leading to thick silanes layers (overabundance of water) as well as incomplete monolayer formation (deficiency of water) [60]. Even if monolayer coverage is achieved, films are subject to disorder because adsorbed molecules may

General considerations. Cement and silane agents.

bend [61, 62]. However, some authors report the possibility of obtaining flat and homogenous silane monolayer [63].

The organic reactivity defines the ability of the organofunctional silane to react with organics. It involves the organic portion of the molecule and it does not directly involve the silicon atom.

The organic functional part can polymerize with an organic matrix provided that it contains the appropriate functional groups [47]. Exhaustive studies can be found in the literature dealing with silane to organics compatibility in terms of chemical reactivity, solubility and structural characteristics [48, 49]. In case of thermoplastic polymers, bonding through a silane can be explained by interdiffusion and interpenetrating interphase region. An illustrative situation is presented in Figure 2-14 [50].

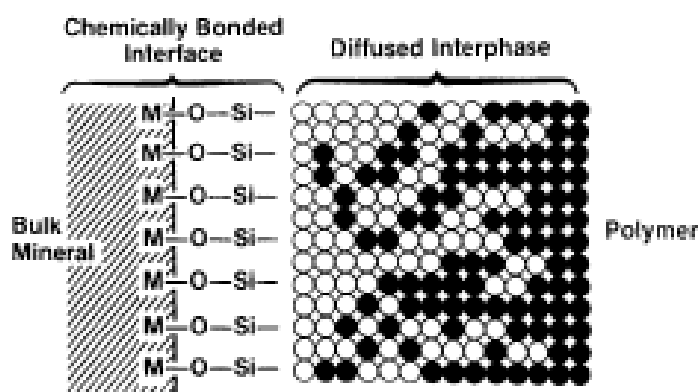


Figure 2-14. Bonding siloxane to polymer through diffusion (reproduced from [48])

In case of thermosetting polymers the organofunctional group of silane agent is selected for chemical reactivity.

### 2.2.3 General applications of organofunctional alkoxysilane

Organofunctional alkoxysilane have widespread applications in lots of industrial domains including adhesion promoters, coupling agents, crosslinking agents, moisture scavenger and hydrophobic and dispersing agents.

General considerations. Cement and silane agents.

When used in paints, inks, coatings, adhesives and sealants as integral additives or primers, alkoxysilanes provide dramatic improvement in **adhesion**. The mechanism is similar to that described earlier for bonding an inorganic to an organic substrate. When blended as integral additives they migrate to the interface between the adherent product and the substrate. As primers, they are applied from diluted solution of 0.5 -5 % silane in alcohol or water/alcohol to the inorganic substrate before the product to be adhered is applied. They are wiped or sprayed on the substrate, after which the solvent is allowed to evaporate. A remarkable improvement is often realized because the bonds show greater temperature, chemical and moisture resistance to attacks on the interface.

Applications of organofunctional alkoxysilane employed as **coupling agents** target reinforcements such as fibreglass and mineral fillers incorporated into plastics and rubbers. Without silane treatment on the hygroscopic glass surface, the bond between the glass fibre and the resin would weaken and eventually fail. Silane agents are used on fibreglass for general-purpose reinforced plastic applications because they improve the interfacial adhesion. Application range from automotive, marine, sporting goods to high-performance applications in printed circuit boards and aerospace composites.

Alkoxysilanes are a natural fit to treat the hydrophilic filler surface of the mineral to make it more compatible and dispersible in the polymer. Minerals with silicon and aluminum hydroxyl groups on their surfaces are generally very receptive to bonding with alkoxysilanes. Silica (both fumed and precipitated), glass beads [64], quartz [65], sand, talc, mica, clay and wollastonite [66] have all been effectively used in filler polymer systems after they had been treated with silane agents [67]. Other metal hydroxyl groups, such as magnesium hydroxide [68], iron oxide [69], copper oxide [70], and tin oxide [71], may be reactive to a lesser extent, but often benefit from silane treatment. Corrosion protection properties of organosilanes on metals is an intensively investigated research topic due to the significant need for ‘green’ technology in metal-finishing. This is because the traditional chromate passivation has been reported to be toxic and carcinogenic and that organic coatings give hazardous air pollutants. Thus, silanes are definitely a viable alternative.

General considerations. Cement and silane agents.

Another specific example of a 'green' application is the silane coupled mineral-filled rubber products used for automotive industry, shoe soles, belts and hoses. Tires are known to be 'green' because they provide improved fuel economy while improving other properties like abrasion and rolling, grip on wet and snow/ice surface resistance. This is done by using mineral derived filler rather than one derived from fossil fuel (carbon black). But in order to be efficient non-black reinforcing fillers need to undergo surface treatment with silane coupling agents. Silane coupling agents typically used for this kind of applications have trialkoxy groups at both ends of a polysulfido organic moiety. An example of the structure of a sulfidosilane is given in Figure 2-15. Also the bonding mechanism to silica on the one hand and to rubber on the other hand is shown in Figure 2-16.

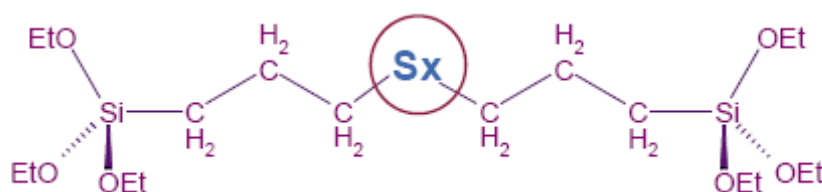


Figure 2-15. Structure of sulfidosilanes used in rubber compounds. X ranges from 2 to 10 (reproduced from [48]).

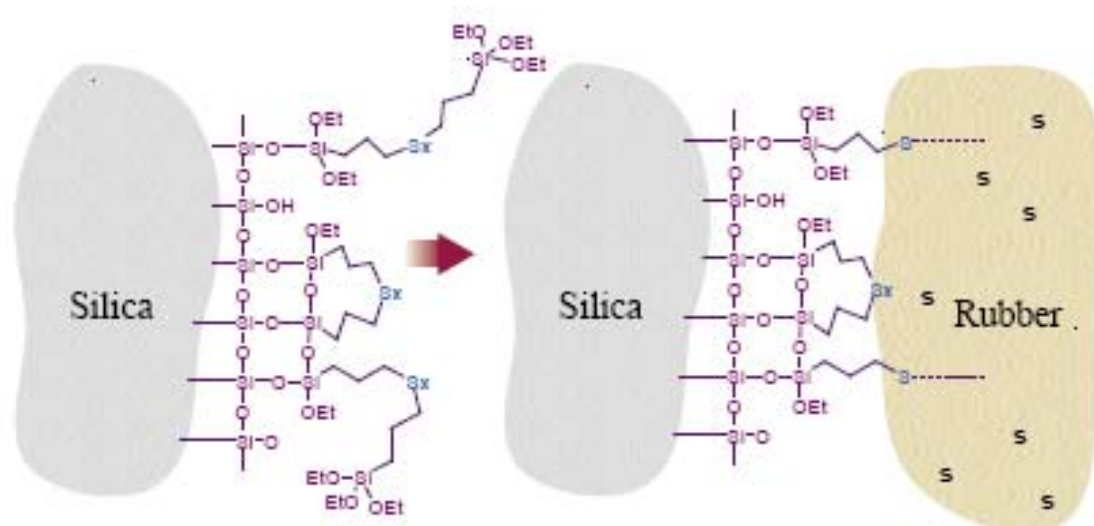
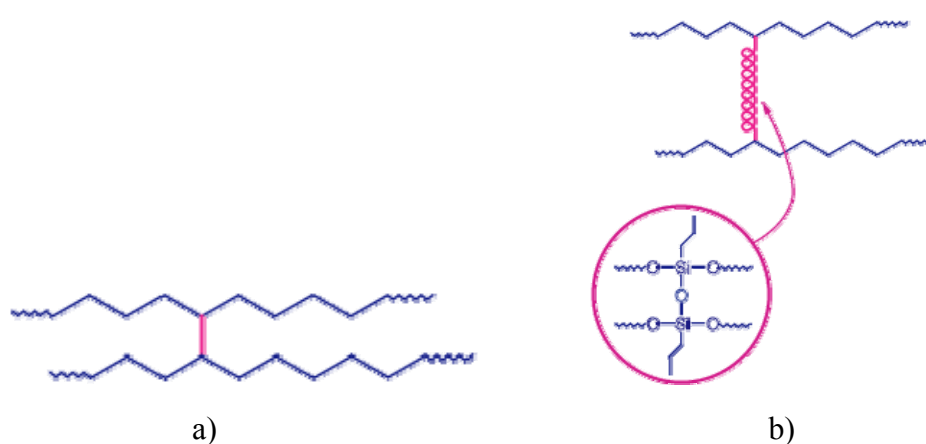


Figure 2-16. Bonding organic rubber to silica with sulphur silanes (reproduced from [48])

General considerations. Cement and silane agents.

Silanes can be used also to **crosslink** polymers such as acrylates, polyethers, polyurethanes and polyesters. In a first step, the organofunctional portion of the silane can react, and bond to the polymer backbone in a sealant or adhesive followed by a step two, when under the influence of moisture and tin compounds or other suitable catalysts the alkoxysilyl groups undergo hydrolysis and condensation. A silane-crosslinked sealant or adhesive can show enhanced properties, such as tear resistance, elongation at break, abrasion resistance, thermal stability, moisture resistance due to the less rigid siloxane bridges formed that give flexibility to the crosslinked polymer in comparison to the C-C bonds. A typical example is shown in Figure 2-17.



*Figure 2-17. (a) Structure of polyethylene crosslinked through C-to-C bond (by peroxidation or radiation). The bond appears rigid; (b) Structure of polyethylene crosslinked through Si-O-Si bond by silane agent. The bond provides flexibility. (reproduced from [72])*

Their ability to react very rapidly with water makes them useful in sealant and adhesive formulations to capture excess moisture coming from fillers or the surrounding environment. As a result silane **water scavengers** in a formulation can prevent premature cure during compounding, enhance uniform curing and improve in-package stability.

Their unique **hydrophobic** or oleophobic properties allow them to be used in durable formulating solutions for protection against harmful water and oil-borne elements. The main application, in this case lie in the construction (concrete, sandstone, granite,

General considerations. Cement and silane agents.

brick, tile, grout, wood, gypsum, perlite, limestone, marble) where lots of water repellent and surface protection formulations are successfully used and provide major benefits including reduced efflorescence, reduced freeze-thaw damage, chloride ion resistance to deter corrosion of reinforcing steel in concrete structures, preservation of aesthetics [48].

#### **2.2.4 Silanes applications related to cementitious materials**

So far, we have seen that organofunctional silanes can be successfully employed in a wide range of industrial applications from automotive to marine and to aerospace bringing major benefits. Some of the applications mentioned previously included also the construction field where silanes are used in surface protection formulations. This means that silane agents are applied on the hardened concrete structures. In what follows we will present an overview of the work done that addresses the use of silanes in cement pastes and mortars making processes.

##### **2.2.4.1 Silane silica fume cement**

The addition of silica fume to concrete is a common practice in civil structures because of its positive effects on the mechanical properties. It mainly adds strength and decreases the permeability of concrete. However, some unfavourable properties are associated with the addition of silica fume to concrete such as workability loss and ductility reduction [73].

Xu Y. et al investigated the use of silane on silica fume cement in several parallel studies [74, 75] The surface of silica particles have been treated with aqueous solution of N-2-aminoethyl-3-aminopropyltrimethoxy silane and 3 glycidoxypropyltrimethoxy silane) filtrated, dried and oven cured. The silane used as an admixture (amino vinyl silane) has been added directly into the cement mix from an aqueous solution.

The silane surface treatment of silica prior to incorporation has been found to greatly enhance workability, increase both the tensile and the compressive strength by 31% and 27%, relative to the values obtained without treatment. The use of silane in the

General considerations. Cement and silane agents.

form of an admixture gave similar results. However, the latter method gives silica fume cement paste of lower compressive ductility, lower damping capacity, more drying shrinkage, lower air void content, higher density, higher specific heat, and greater thermal conductivity [76].

The results show some improved performance when silanes are used. The increase in workability can be attributed either to better wettability of the silica particles after the silane treatment which comes from its hydrophilic nature or to an improved dispersion with silanes acting as steric dispersion on the silica. The improvement in strength is most likely associate with the crosslinked network (based on siloxane bonds) resulting from silane hydrolysis and polymerisation during the hydration of cement. This causes also the ductility to increase. The increase in thermal conductivity was obtained by increasing the specific heat.

#### **2.2.4.2 Silane steel fibres reinforced cement**

Similar tests have been performed with steel fibres reinforced mortar where similar silanes have been used as admixture and as steel fibres surface treatments prior to incorporation [77]. Improved steel fibre dispersion has been observed for both cases, but silane fibre surface treatment has been found less effective. Differences in compressive and tensile ductility are consistent with the reported effect of silane as admixture on silica fume cement paste without fibres [76].

#### **2.2.4.3 Silane carbon fibres and silane silica fume cement**

Investigations carried out by Xu Y and Chung D on silane-treated carbon fibres and silane-treated silica fume, using similar silanes as mentioned above, indicate significant decrease of the drying shrinkage of cement paste by 32% at 28 days [78], increase in tensile strength, modulus, ductility and reduce air voids content [79]. Once more these effects of silane treatment are attributed to their hydrophilic nature. Furthermore, increase of specific heat of cement paste (desired ability for temperature stability in structures) by 12% and decrease in thermal conductivity (desired ability



General considerations. Cement and silane agents.

for energy conservation in buildings) by 40 % was achieved [80]. The specific heat increase due to the silane treatment of the fibres is attributed to the movement of the silane molecules while decreased thermal conductivity is attributed to the thermal resistance of the silane at the fibre-matrix interface.

#### **2.2.4.4 Silane polymer modified mortar**

Chmielewska et al. investigated the influence of vinyl trimethoxy silane in vinylester resin mortars [81]. Significant changes in mortars properties and performances were observed but the effects are strongly dependent on how the modification is performed. Two methods have been considered here: direct silane addition to the resin binder and silane pre-treated silica flour.

Both showed spectacular changes in fracture surfaces (polygons structures similar to the ones observed during unstable equilibrium of volcanic lava consolidation) and increased the fracture energy, most effective for silane pre-treated silica. The biggest improvement on addition of silane directly to resin was in the tensile strength (30%), while the highest compressive strength (28%) has been observed for silane-treated silica surface. Surprisingly, an increase in brittleness and shrinkage of the mortar was noticed when silane direct addition to the resin binder was considered. The opposite has been found for silane pre-treated silica. In addition, 70% decrease in viscosity has been observed in the case of direct silane addition to the resin mix, whereas there has been no change in viscosity for the silane pre-treated silica.

These results clearly showed that silane addition improves adhesion between mineral grains and resin binder, but silane particles deposited on the surface of silica modify the whole matrix more uniformly as compared to the composite with silane added to the resin. The effects are mainly associated with the improved crosslinking of polymer and higher structure flexibility provided by the use of the silane agent.

Improved adhesion properties have also been reported by Svegl [82, 83] for the case of ethylene-vinyl-acetate based polymer with the addition of silane agents and silica fume. Results indicated over 90 % better adhesion in pull-off tests, reduced drying

General considerations. Cement and silane agents.

shrinkage, reduced air voids content up to 55 % and increased flexural strength by 60% compared to reference mortar. The explanation for these effects has been the formation of chemical bonds between mineral-mineral and mineral-polymer evidenced by in-situ ATR FT-IR spectroscopy.

#### **2.2.4.5 Silane cement pastes**

Svegl et al [84] investigated also the influence of aminosilanes on macroscopic properties of cement pastes. The silane agents have been added as an admixture to the cement system. They reported that aminosilanes (N-2-aminoethyl-3-aminopropyltrimethoxy silane and aminopropyltrimethoxy silane) improve the workability of cement paste and reduce the water demand. Flexural and compressive strength has been found to increase by 20% and 5%, but only after 28 days of curing (from 7 days onward in air). However, Vicat set time measurement indicated strongly retarding effect on the cement hydration.



### **3 Materials**



### 3.1 Cement and tricalcium silicate

A normal hardening sulphate resistant Portland cement (CEM I 42.5 N) obtained from Salanit Anhovo (Slovenia) was used in all experiments.

A pure tricalcium silicate ( $C_3S$ ) obtained from Lafarge with a Blaine specific surface of  $0.370 \text{ m}^2 \text{ g}^{-1}$  was used in a limited number of experiments for comparison purposes.

Several physical characteristics and bulk chemical compositions of the cement powder are given in Table 3-1 and Table 3-2. The chemical composition was determined by Salanit Anhovo Gradbeni Materiali d.d. using XRF. The BET specific surface area of the powder was determined by the Chemical Institute of Ljubljana using  $N_2$  adsorption.

*Table 3-1. Physical characteristics of cement and tricalcium silicate.*

Parameter	Cement	Tricalcium silicate
LOI ( EN 196-2), %	0.8	
Specific surface Blaine, $\text{m}^2 \text{ g}^{-1}$	0.305	0.370
Specific surface BET, $\text{m}^2 \text{ g}^{-1}$	1.0014	
Density, $\text{kg/m}^3$	3190	

*Table 3-2. Chemical characteristics of cement.*

Oxide, mass %	Cement
SiO <sub>2</sub>	21.7
Al <sub>3</sub> O <sub>3</sub>	3.93
Fe <sub>2</sub> O <sub>3</sub>	4.94
CaO	63.34
MgO	1.68
SO <sub>3</sub>	2.22
Na <sub>2</sub> O	0.27
K <sub>2</sub> O	0.73

### 3.2 Silanes

Three silanes among, today's most examined ones were used for this study. All three of them are organofunctional trialkoxy silanes bearing trimethoxy or triethoxy groups and one non hydrolysable organic function, amine and epoxy. A fourth organofunctional silane agent (TEOS – tetraethoxyorthosilane) was chosen and used in a limited number of experiments for comparison purposes only. This is because all of its four substituents are hydrolysable organic functions.

They are listed in Table 3-3 together with some of their characteristics. All products are commercially available ones and were purchased from Merck (APTES - 3 aminopropyltriethoxysilane, AEAPTMS - N-2-aminoethyl-3-aminopropyltrimethoxysilane, TEOS) and Prolabo (GTO - 3 glycidoxypropyltrimethoxy). They were supplied as 97% alcoholic solution for GTO and 100% pure component for APTES and AEAPTMS. They were all used as received. Their corresponding molecular structures are given in Figure 3-1.

Table 3-3. Characteristics of the silanes used.

Designation	Chemical type	Molecular weight, g mol <sup>-1</sup>	Water miscibility
APTES	Amino functional triethoxysilane	221.37	total miscible
GTO	Epoxy functional trimethoxysilane	236.34	total miscible
AEAPTMS	Primary and secondary amine functional trimethoxysilane	222.36	total miscible
TEOS	Tetra ethoxy substituted silicon hydride	209	immiscible

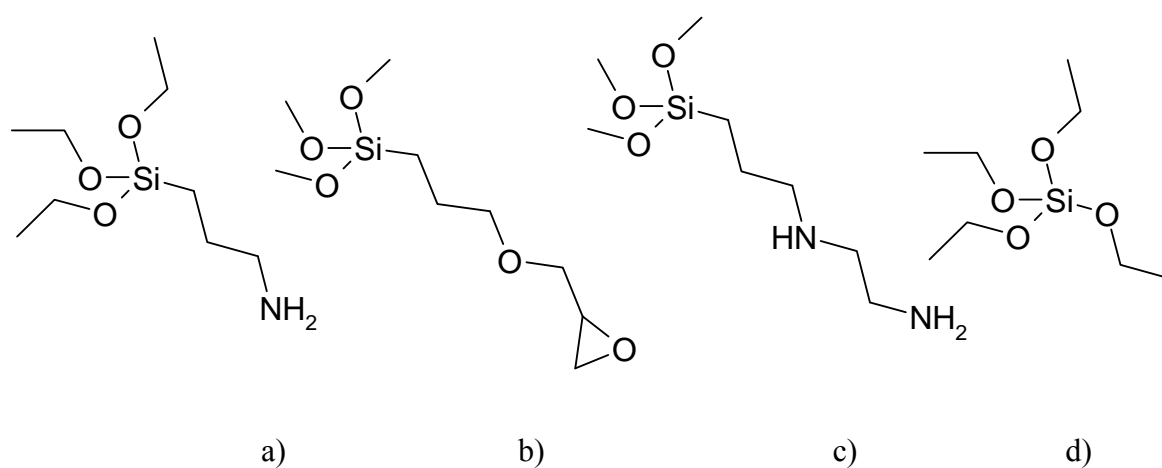


Figure 3-1. Molecular structure of APTES (a), GTO (b), AEAPTMS (c) and TEOS (d).





#### **4 Silane modified cement obtained by dry blending of constituents**



The aim of the work presented in this chapter is to modify the anhydrous cement powder with organofunctional silanes and to investigate the properties of the hybrid system. Surface modification was performed by the adding a silane agent through dry blending of constituents. The properties of the hybrid material have been explored using physical, mechanical and heat development techniques.

## **4.1 Methodology**

### **4.1.1 In principle**

The method consists in dry blending of the constituents at room temperature. The technique has been reported to be used for treatment of fillers used in polymer mixes [49]. The ease and simplicity in preparation are however not always leading to the best results because of two conflicting requirements: dispersion and condensation. Small amounts of silane disperse badly and as a consequence the extent of condensation with the substrate is sometimes insufficient. Addition of a catalyst, such as an amine or a silane incorporating amine function or use of elevated temperature was found to aid in surface treatment and to overcome the difficulties reported.

### **4.1.2 In practice**

The anhydrous cement powder was dry-blended with the silane using a stainless steel mixer at a speed of  $140 \pm 5 \text{ min}^{-1}$  for 10 min, followed by a period of 24h treatment at ambient atmosphere and temperature conditions (at about RH ~30 and  $22 \pm 2 \text{ }^{\circ}\text{C}$ ), which allowed further silane diffusion and thus better dispersion. Concentrations of silane ranging from 1% to 10% by weight of cement were prepared. In all cases oven curing at  $80^{\circ}\text{C}$  for 4 hours was carried out to enhance dispersion and condensation for all silanes considered (including APTES, which is an aminosilanes and is expected to perform as self-catalyst). Silane modified cements were prepared in 1 kg batches.

Silane modified cement obtained by dry blending of constituents

Alternatively, hand mixing was employed when small quantities of silane modified cement were prepared.

## **4.2 Characterization of modified products**

### **4.2.1 Techniques used for investigating the properties of modified products**

#### **4.2.1.1 Standard consistency water**

The standard consistency water represents the quantity of water required for a paste to reach standard consistency. The latter is usually defined by a specific resistance to penetration by a standard plunger and is expressed in percentage of water with respect to cement.

In this work standard consistency water tests were carried out according to European standard EN 196-3:2005, using a manual Vicat apparatus at room temperature. A Toni Technik mixer was used for mixing the water with the cement powder. Standardized Vicat moulds containing the pastes to be tested were replaced by plastic cylindrical containers 43 mm deep and with an internal diameter of 30 mm. The plunger was gently lowered until it was in contact with the paste and was then released. The standard consistency is said to have been reached when the distance between the plunger and the base-mould is  $6 \pm 2$  mm.

In our case, standard consistency water measurements were carried out for three silanes modified cements and two references: a plain cement containing no admixtures and a TEOS modified cement.

#### **4.2.1.2 Setting time**

The setting time of pastes is determined by observing the penetration of a Vicat needle into a cement paste of a standard consistency until it reaches a specific value [85]. The values defined by European standard EN 196-3:2005 are  $6 \pm 3$  mm measured between the needle and the base-plate for the initial setting time and less than 0.5 mm penetration into the specimen for the final setting time. The release of the needle and

penetration into the paste was started 4 min after the time zero (the point in time marked by the addition of water from which the initial and the final setting time were calculated). Modified Vicat measuring moulds have been used similarly to the case of standard consistency water tests.

#### **4.2.1.3 Workability**

A simple way of assessing differences in rheological behaviour among controlled cement pastes and silane modified ones, was possible by testing differences in workability. One measures the spread of a fresh prepared paste or mortar sample on a flow table by 15 consecutive jolts after having removed the flow mould.

For mortar samples, testing was performed according to the European Standard 13395-1:2002. For cement paste samples, small adjustments have been made regarding the flow mould (an adapted truncated conical mould with an upper diameter of 40 mm and lower diameter of 45 mm was used instead of the standard prescribed one

The workability was assessed with respect to spread. The diameter of the flattened sample was measured on the platen in two directions at right angles to one another. Each type of specimen was tested twice by preparing different batches. The flow value is equivalent to the mean value result. All cement paste samples were prepared with same w/c (0.25).

For pastes, tests were carried out for high silane addition levels (10% silane to cement by weight), whereas for mortars low silane addition levels were considered (1% silane to cement by weight).

#### **4.2.1.4 Strength**

##### **A. Experimental procedure for mixing, curing and strength testing for paste**

The pastes were prepared by mixing water and cement powder using a rotary (stationary turbine) mixer (Toni Technik) with a typical shape, size and tolerance, revolving around its own axis, driving planetary movement according to the European

Silane modified cement obtained by dry blending of constituents

standard EN 196-1:2005. All samples were prepared at room temperature using a water-to-cement ratio 0.25.

Specimens were prepared and were cast into 10 x 10 x 60 mm moulds. At least two specimens were cast for each individual silane and for each curing age. After 24 h curing at 20° C and RH of not less than 90 %, the samples were de-moulded if their mechanical strength allowed it and immediately submerged horizontally under water in plastic containers. The temperature of the water was maintained at  $21 \pm 2$  ° C during the curing period.

Measurements of compressive and three point bending strengths were carried out at the ages of 1, 7, 28 days according to the European standard EN 196-1:2005 with the necessary adjustments made for testing small specimens. The loading rates of flexural and compressive tests were 0.020 kN/s and 0.4 kN/s, respectively.

## **B. Experimental procedure for mixing, curing and strength testing for mortar**

All the procedures and equipments used for mixing, curing and strength testing for mortars were carried out closely following the European Standard EN 196-1:2005. The silane modified mortars were prepared using silane modified cement prepared according to the direct mix, as described in Section 4.1.

### **4.2.1.5 Calorimetry**

#### **General considerations**

Calorimetry is a technique that measures heat differences over time. Bearing in mind that the hydration of cement based systems is strongly time dependent [21] and moreover exothermic, this technique is suitable, although oversimplified, to follow the progress of cement hydration by using the heat evolution curves [86] (Figure 4-1).

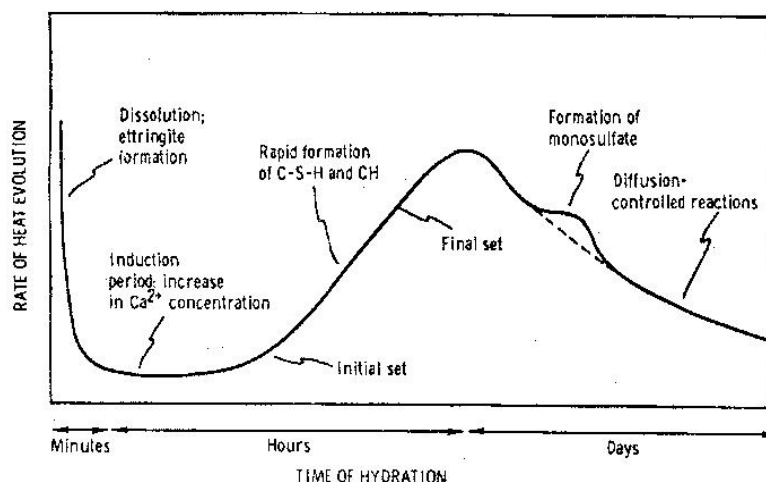


Figure 4-1. Schematic representation of heat evolution during hydration of cement (reproduced from [86]).

### Isothermal calorimetry

A TAM Air multichannel twin type isothermal calorimeter from Thermometric was used for the investigations carried out in this work. Heat exchange measurements were recorded between the sample under investigation and the thermostat. Each sample under investigation has a corresponding reference, usually a cell filled with the right amount of water corresponding to the same heat capacity as the sample. The reference vessel is used to reduce the signal to noise ratio and to correct measurement and temperature artefacts. Each vessel is connected to the surrounding heat sink by a Pelletier module. When heat is produced as a consequence of the hydration reaction, the temperature in the vessel changes and a temperature gradient across the Pelletier module is developed. It generates a voltage that is measured and that is proportional to the rate of the process taking place in the sample vessel.

10 ml plastic ampoules were used for both sample and reference cell. Ultra pure 25 °C tempered water was used for both sample preparation and served as reference material. All measurements were performed at 25 °C.

For each sample 1.000 g of cement was directly weighed (Precisa, Switzerland) into the measuring ampoule and 0.300 ml of water were added. All specimens were prepared by ex situ mixing using a small high speed uniaxial mixer at a mixing speed



of 2700 rpm for 30 sec. Afterwards the ampoule was capped and immediately placed inside the calorimeter. Due to the external mixing the initial heat release peak could not be measured.

It must be noted that this preparation procedure brings some additional initial heat due to the friction between the sample's cell and the measuring channel's chamber when placing. However, since all the samples were prepared in the same way and moreover, the technique was used mainly to assess the onset of the acceleration period, inaccuracy can be kept to a minimum. For reproducibility reasons each measurement was performed at least twice.

From the calorimetric curve the onset of the acceleration period was obtained graphically. A schematic representation is given in Figure 4-2.

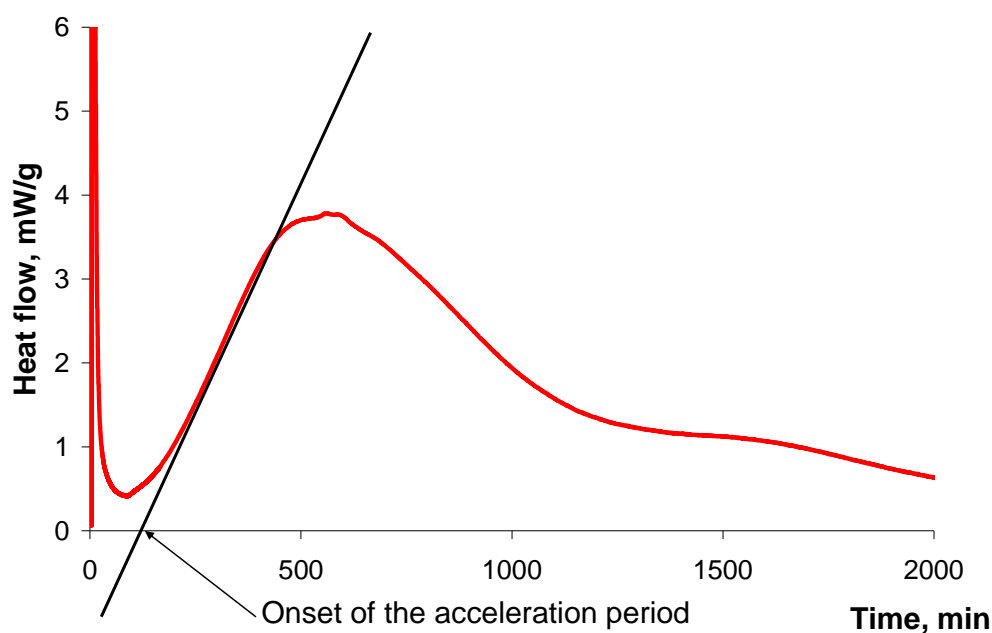


*Figure 4-2. Graphic determination for the onset of acceleration period for cement hydration from a heat evolution rate curve.*

## **4.2.2 Results**

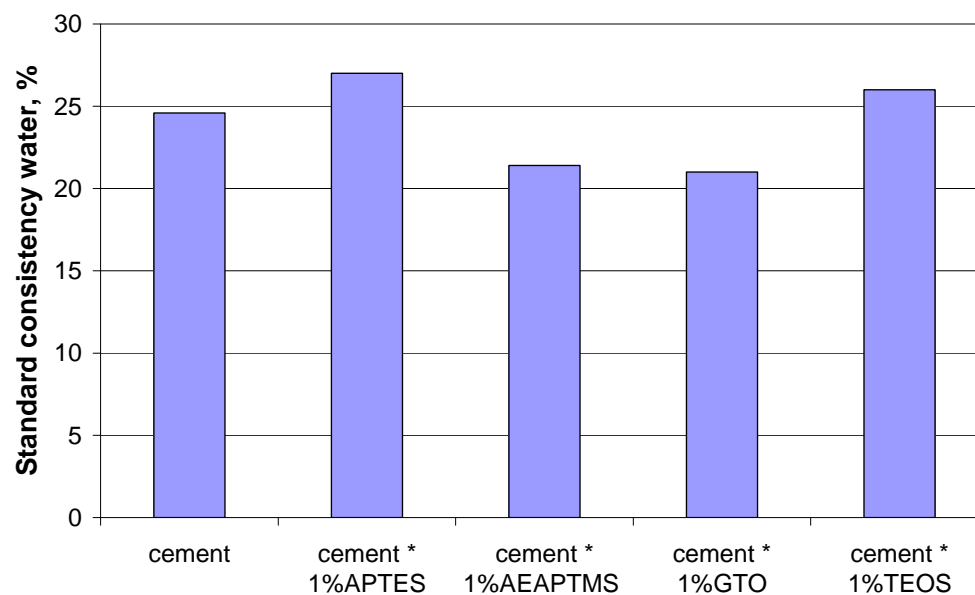
### **4.2.2.1 Standard consistency water**

Standard consistency water was determined for all three silane modified cement pastes. The dosages of silane to cement by weight were 1 % (Figure 4-3 a) and 10 % (Figure 4-3 b). Neat cement paste and TEOS modified cement paste values are presented for comparison. It must be noted that TEOS is another silane agent, but its structure is significantly different compared to the three admixtures considered in our investigations. It has been considered for comparison purposes only. Its molecular structure has been reported in Chapter 3.

The values of standard consistency water for 10 % silane modified pastes were in the range of 11.5% to 17.3%, while for 1% silane modified pastes were in the range of 21% to 27%. Paste prepared with TEOS had water demands for standard consistency pastes ranging between 26% and 29.7% for addition levels of 1% and 10 %, respectively. Standard consistency water for plain cement paste was 24.5%. All the reported results were the average of two measurements.

Generally, the results point out towards reduced standard consistency water for silane modified cement pastes. Furthermore, increasing the silane addition level results in decreased water demands to reach standard consistency. AEATMS and GTO show linear dependency between the addition level and the water demand (Figure 4-4). However, an exception must be noted. This concerns the case of 1% APTES silane modified cement paste, which showed slightly increased values for standard consistency water with respect to the plain paste.

**a) 1% silane to cement**



**b) 10% silane to cement**

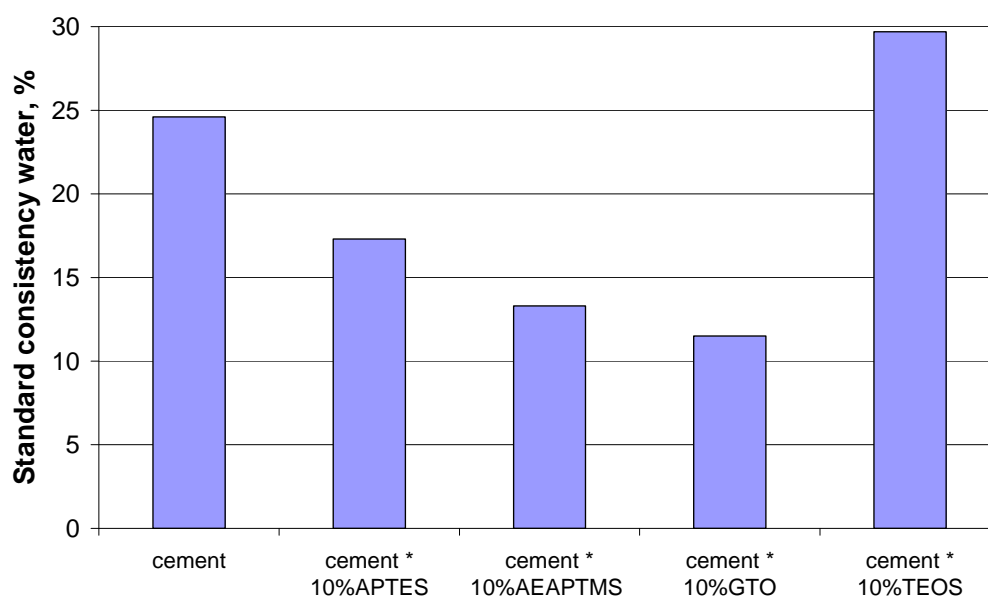


*Figure 4-3. Standard consistency water for silane modified cement pastes determined according to EN 196-3:2005. Dosage of silane by weight of cement is (a) 1 % and (b) 10%.*

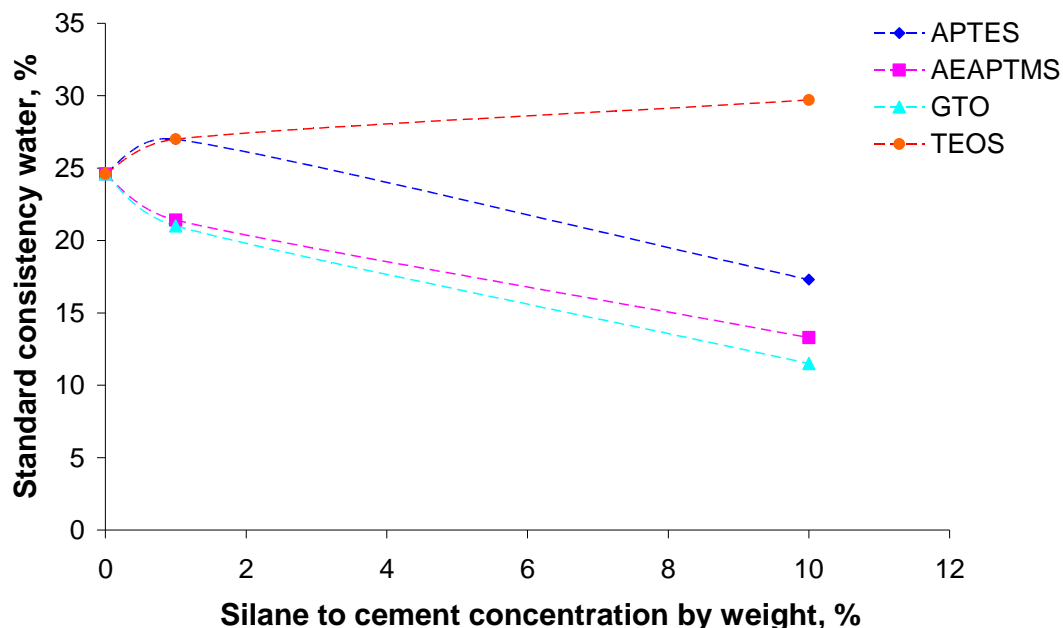


Figure 4-4. Standard consistency water variation for different silanes and different addition levels.

#### 4.2.2.2 Workability

##### A. Pastes

Figure 4-5 gives the spreading on a flow table for 10 % silane modified cement pastes prepared at constant  $w/c = 0.25$  and compares them with the values obtained for plain and TEOS modified pastes. The pastes were tested immediately after mixing.

Considerable differences in flow values were measured despite the fact that the silanes to cement ratios were kept constant. The flow table spread values for the three silane modified cement paste that we investigated were found to be 123, 160 and 168 mm. Neat cement paste gave a flow table value of 102 mm, while TEOS modified paste 80 mm.

The highest value for the flow table spread was measured for GTO paste, while the smallest was recorded in the case of TEOS modified pastes. AEAPTMS and APTES pastes gave lower flow values with respect to the GTO, but superior compared to neat

cement paste. The results indicate similar tendency in behaviour of modified cement pastes as for the case of standard consistency water investigations.

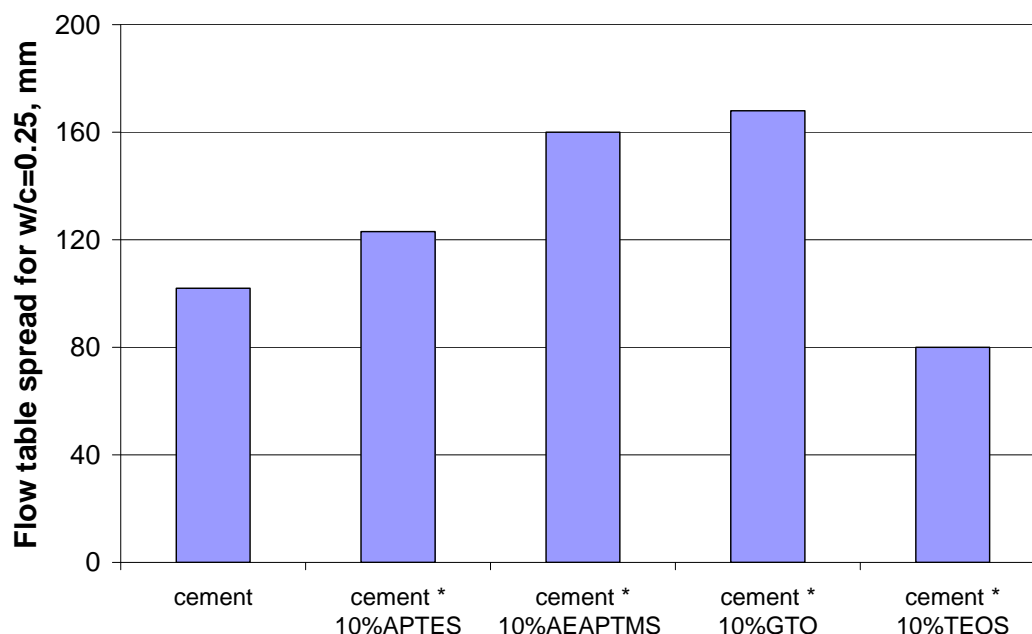


Figure 4-5. Comparison of values for flow table spread of neat and 10 % silane modified cement paste at constant  $w/c = 0.25$ .

## B. Mortars

Investigations on workability of silane modified mortars were carried out for mortar prepared with 1 % silane modified cement. Unlike the case of the modified paste, where a fixed  $w/c$  ratio was considered and the flow table spread values were measured, the tests performed on mortars aimed to determine the  $w/c$  ratios giving a constant 200 mm value for the flow table spread. The value represents the flow table spread of a standard mortar prepared with  $w/c = 0.5$ . The results are plotted in Figure 4-6.

The  $w/c$  values found were 0.48, 0.45 and 0.41 for APTES-, AEAPTMS- and GTO modified mortar. The increase in mortar workability is dependent on the nature of the silane, as similarly observed for the tests carried out on pastes. GTO was found to have the strongest effect, while among the two aminosilanes investigated, AEAPTMS performed better in terms of enhancing the workability.

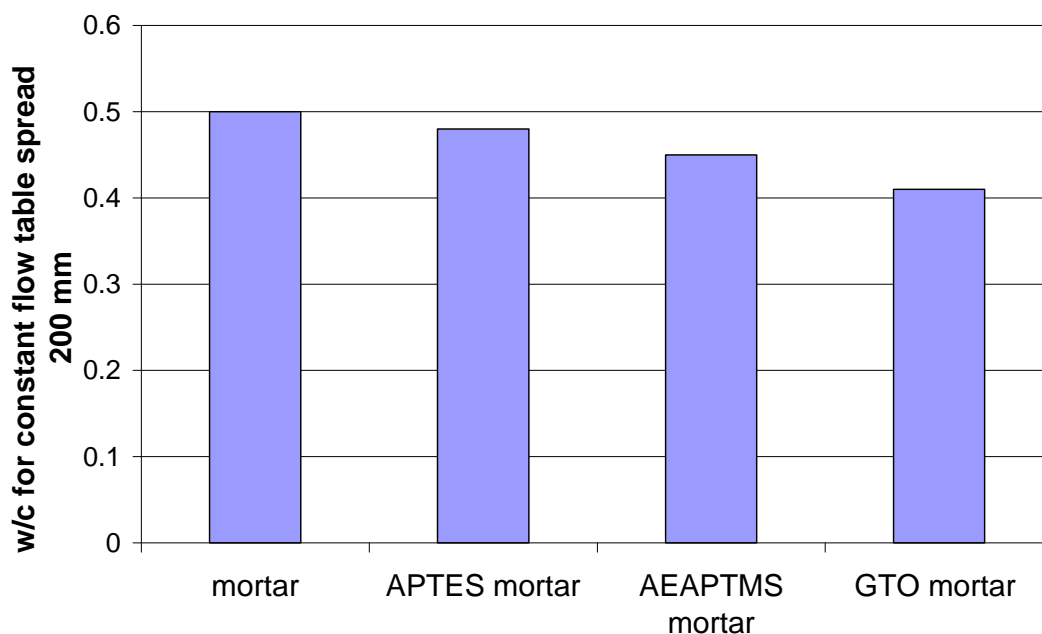


Figure 4-6. Water demands for silane mortars needed for constant 200 mm flow table spread at constant silane to cement concentration.

#### 4.2.2.3 Setting time

Figure 4-7 and Figure 4-8 show the setting time values measured by sample penetration using a Vicat needle on standard consistency pastes. Initial and final setting time values were recorded for high (10%) and low (1%) silane to cement concentrations.

On the one hand, for high silane concentrations (Figure 4-7) the results point out always towards higher setting time values for modified cement pastes with respect to the neat ones. The setting time of GTO modified cement paste was more than ten times longer in comparison to the neat paste.

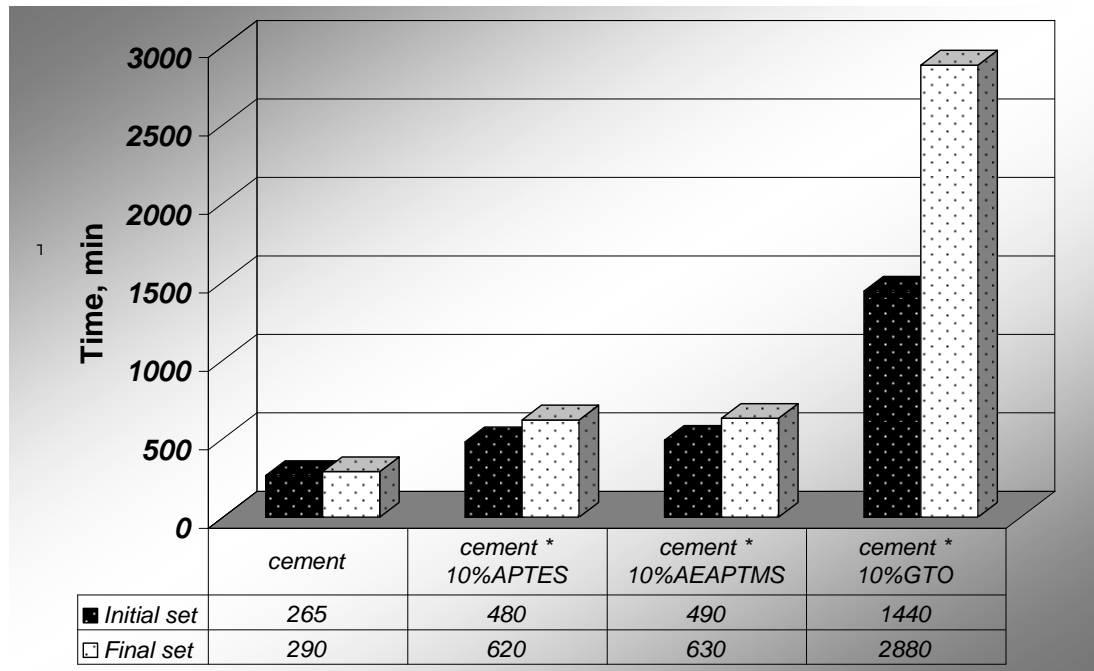


Figure 4-7. Setting time values measured for high silane modified cement on standard consistency pastes using Vicat penetration method.

On the other hand, for low silane concentrations (Figure 4-8), no correspondence among set values and the nature of silane could be found. The set values are spread over a long period of time. Both shorter and longer setting times were found with respect to the neat paste. For example, APTES strongly delays both the initial and the final set, while AEAPTMS and GTO strongly accelerates both of them.

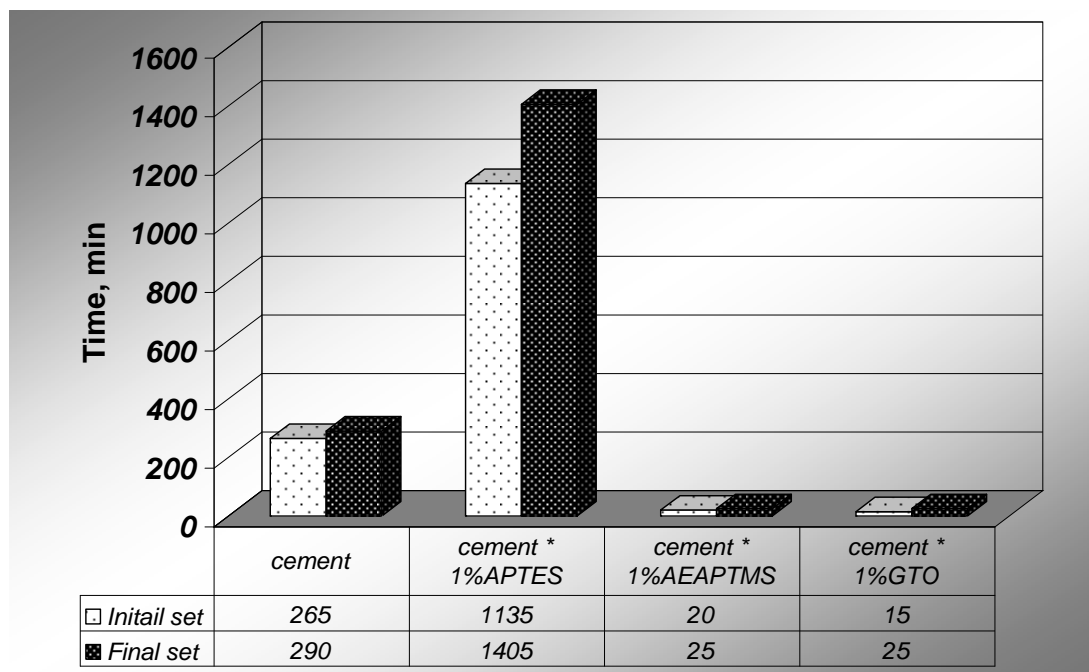


Figure 4-8. Setting time values measured for low silane modified cement on standard consistency pastes using Vicat penetration method.

#### 4.2.2.4 Bending and compressive strength tests

##### A. Paste

Bending and compressive strength tests were considered for modified pastes at constant w/c ratios of 0.25. However, due to the fact that several problems regarding experimental aspects have been encountered, the amount of the tests and therefore results was reduced considerably with respect to the initial plan.

On the one hand, fresh pastes containing 10% AEAPTMS and 10 % GTO were highly fluid and therefore impossible to be cast. On the other hand, no such problematic situation was found for the pastes containing 10% APTES, but demoulding was not possible to be performed before 48h. Furthermore, upon placing under water in the curing tank, the modified specimens immediately disintegrated. For this reason, the curing of silane modified cement paste specimens had to be carried out in air.

Figure 4-9 and Figure 4-10 give the results from bending and compressive tests for neat and 10% APTES modified cement pastes.



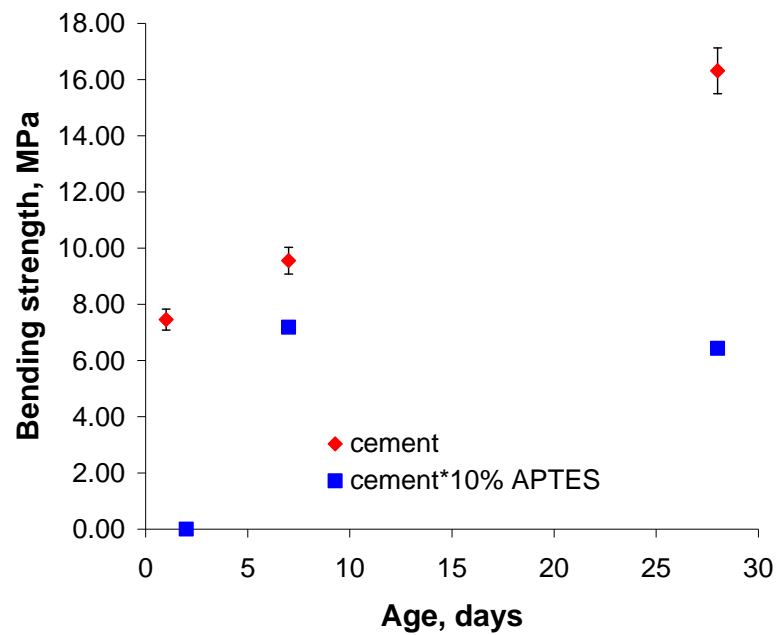


Figure 4-9. Bending strength for neat and 10% APTES silane modified pastes prepared at constant  $w/c = 0.25$ . Percentage of silane by weight of cement.

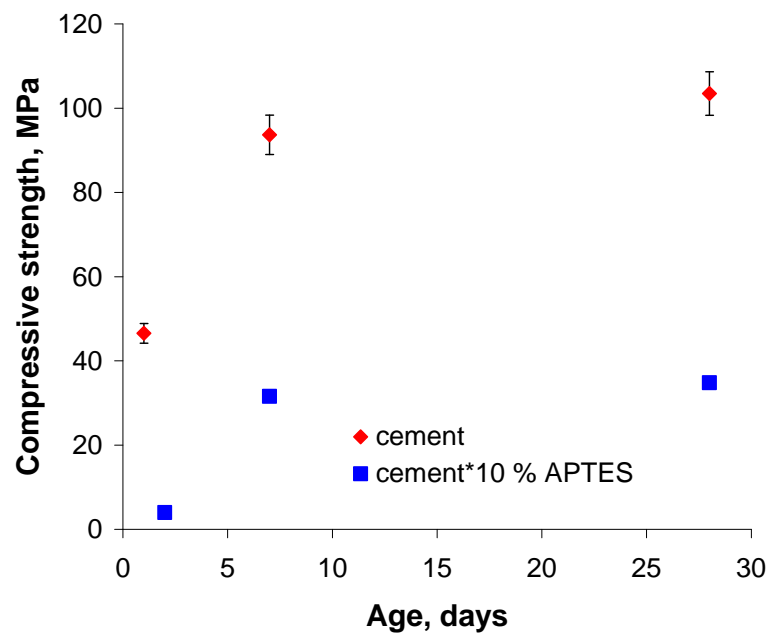


Figure 4-10. Compressive strength for neat and 10% APTES silane modified pastes prepared at constant  $w/c=0.25$ . Percentage of silane by weight of cement.

The presence of APTES in the system negatively affected both bending and compressive strength, regardless of the curing age. The modified specimens exhibited significantly lower strengths in comparison to the reference.

The 28 days measured bending strength value for silane modified cement represents less than 40 % of the one measured for the reference, while compressive strength is less than 33% from the references. Moreover, strength reduction in bending is observed at 28 days for APTES modified cement pastes. Compressive strength is not affected by this problem, but does not show any improvement after 7 days.

## **B. Mortars**

For each different silane, mortar modified specimens have been prepared using one part by weight of a cement modified with, one half part water ( $w/c=0.5$ ) and three parts by weight CEN standard sand. As a result, the final concentration of silane with respect to the solid (by weight) is reduced four times in mortar. We recall that modified mortars specimens were cured in air, due to the fact that under water curing would have led to their disintegration.

Bending strength of modified mortar specimens is plotted in Figure 4-11 and compared to the one measured for the reference specimens. Considerable strength reduction was noticed at all ages and for all of the silanes used. Among the different silanes used, AEAPTMS seems to have less negative effects on bending strength development. However, values remain always inferior to the ones measured for the reference.

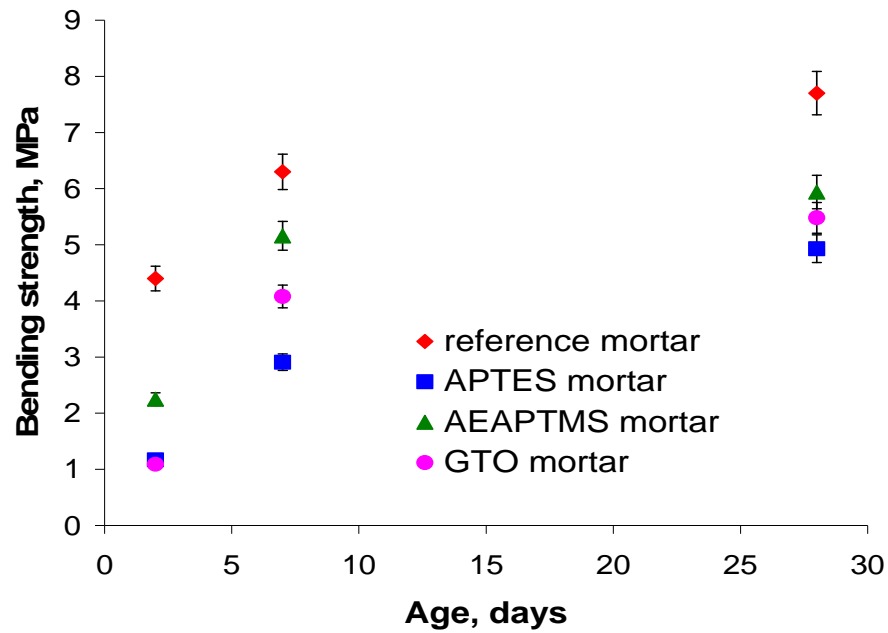


Figure 4-11. Bending strength of silane modified mortars and reference ones prepared with constant  $w/c = 0.5$ .

Compressive strength of modified mortar specimens shows fairly similar trends (Figure 4-12). The reference mortar always performed better. Surprisingly, AEAPTMS modified mortar gave equal values for strength measured at 7 days, but showed strength reduction afterwards.

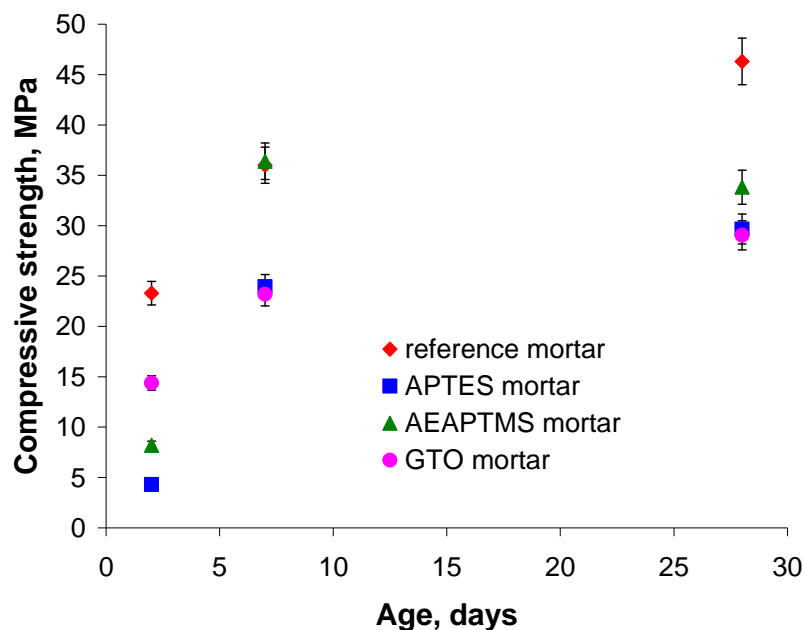


Figure 4-12. Compressive strength of silane modified mortars and reference ones prepared with constant  $w/c = 0.5$ .

#### 4.2.2.5 Heat development

The present section provides information on how different silanes and different silane dosages affect cement hydration. We recall that silanes are surface deposited on the cement by dry blending.

##### Effect of silane nature

Figure 4-13 and Figure 4-14 show the heat evolution and cumulative heat evolution curves for **high addition levels** of silane modified cement pastes. Heat flow for the neat cement paste was recorded and is given for comparison in both figures.

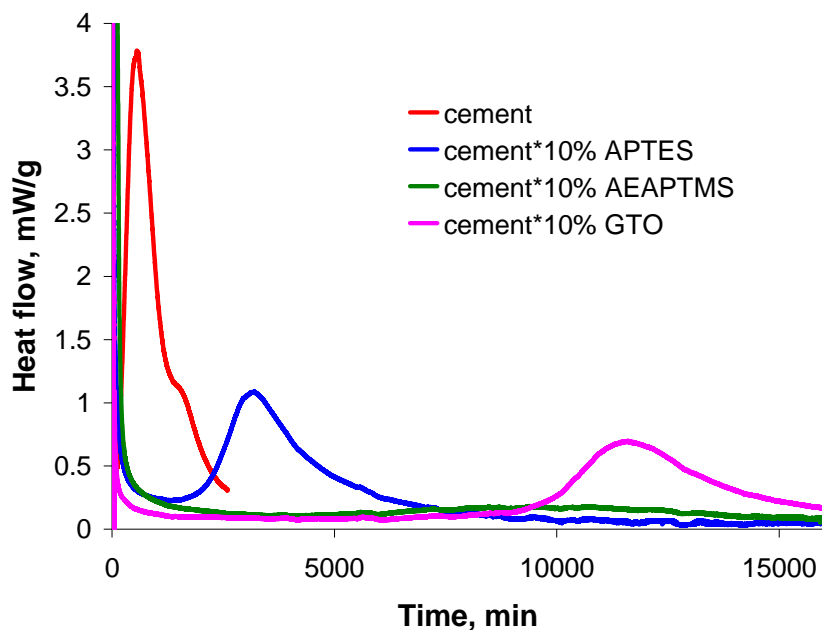


Figure 4-13. Heat evolution curves for high addition levels of silane modified cement pastes (10% wt silane to cement) prepared with constant  $w/c=0.3$ .

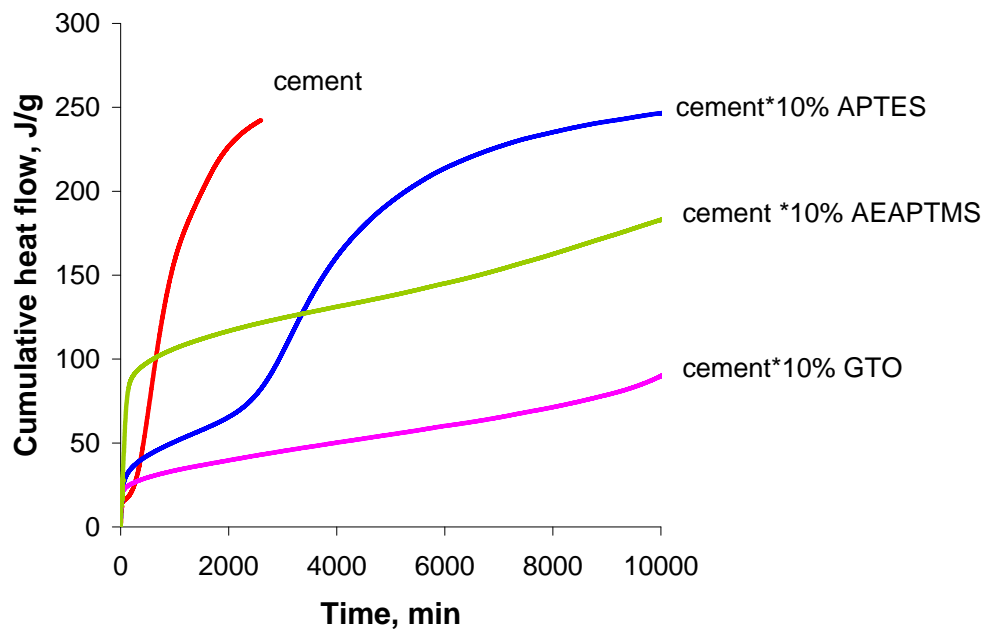


Figure 4-14. Cumulative heat evolution curves for high addition levels of silane modified cement pastes (10% wt silane to cement) prepared with constant  $w/c=0.3$ .

The addition of high levels of silanes (10% wt) led to major changes in the hydration process of the modified products. The curves (Figure 4-13) differ visibly from each other. First, the presence of silanes decreased considerably the maximum rate of heat output to 1.08 mW/g (APTES), 0.69 mW/g (GTO) and 0.29 mW/g (AEAPTMS), respectively, in comparison to the reference paste which had a maximum heat peak release corresponding to 3.77 mW/g. Second, the induction period was extended up to 2000 min for APTES modified paste and up to 10000 min for the one containing GTO. No clear delimitation between the induction period and the onset of hydration could be established for the paste containing AEAPTMS due to the very small value of maximum heat output.

In addition, there is a clear decrease in the heat of hydration, in particular concerning in the silicate hydration as the area under the main heat peak release decreases significantly compared to plain paste. For example, after 24 h of reaction the total heat output corresponding to the silane modified cement pastes was reduced by up to 43% (AEAPTMS), 71% (APTES) and 82% (GTO) (Figure 4-14). At that time, there is no the hydration of silicates. The contribution to the total heat release stems exclusively in the initial heat release. It is important to note that all modified cements samples display a higher initial heat release than the plain cement sample. In particular, AEAPTMS modified paste had up to 360% more initial heat release than the reference paste. Heat of hydrolysis of the silane is not expected to have a significant effect on calorimetric data.

A second series of experiments has been carried out for **low level addition** of silanes (1% wt). In this case, the changes in cement hydration were less significant. The results are reported in Figure 4-15 (a and b).

## Silane modified cement obtained by dry blending of constituents

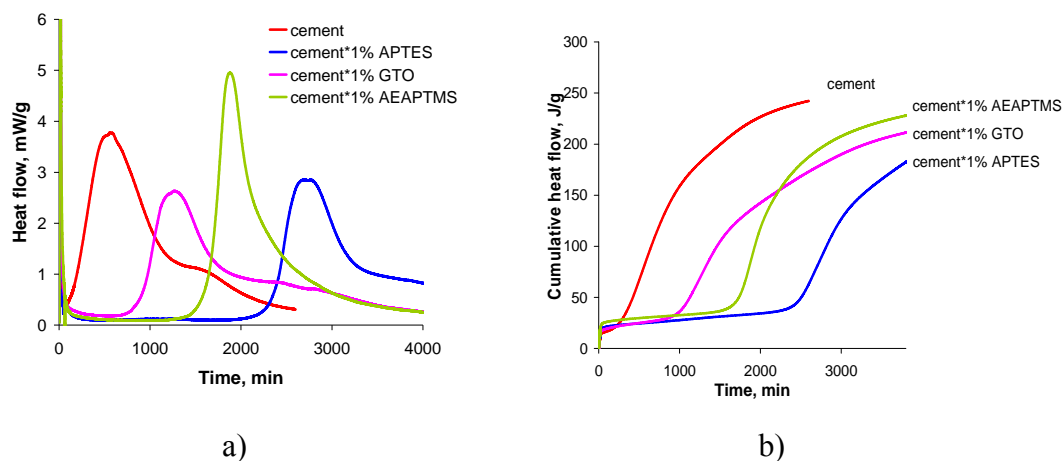


Figure 4-15. Heat flow curves (a) and cumulative heat flow curves (b) for low addition levels of silane modified cement pastes (1% wt silane to cement) prepared with constant  $w/c=0.3$ .

In this particular concentration range, all silanes displayed a retarding effect on cement hydration. The onset of the acceleration period was found to be dependent on their nature. Thus, the length of the induction period increased from the 100 min (plain paste) up to 800 min (GTO), up to 1500 min (AEAPTMS) and up to 2200 min (APTES).

In addition, APTES and GTO modified pastes displayed a reduced maximum rate of heat output against time (Figure 4-15 a) up to 2.6 mW/g and 2.85 mW/g, respectively. On the other hand, AEAPTMS presence was found to increase the maximum peak of heat release up to 5 J/g compared to plain cement paste (3.75 mW/g). The silanes did not change the typical shape of the main heat peak release, but the peak profiles differ from each other, especially in broadness. In particular, the sharp main peak in the case of AEAPTMS modified cement must be noted.

With respect to the total heat output, the low level addition of silanes reduced the overall heat released (Figure 4-15 b) except for the initial period, when the neat cement paste gave the smallest cumulative heat release.

### Effect of silane dosage

Next, we have chosen to evaluate the effect of different silane dosages, on the hydration of cement. Therefore we compare the data obtained previously in such a way that it can provide information on how different dosages influence the cement hydration. Figure 4-16 to Figure 4-18 show the incremental and cumulative heat evolution curves obtained for APTES, GTO and AEAPTMS modified cement pastes containing low (1%) and high (10%) silane addition levels by weight of cement.

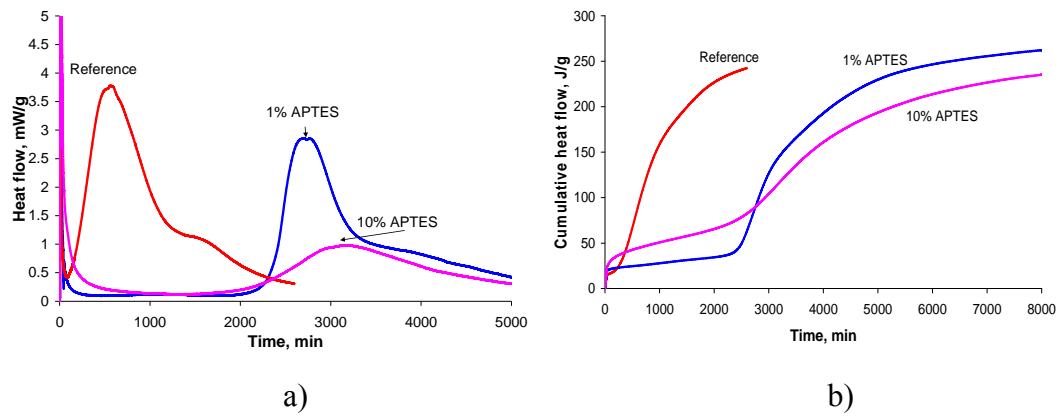


Figure 4-16. Effect of different dosages of APTES on the heat flow (a) and cumulative heat flow (b) of cement pastes prepared with constant  $w/c=0.3$ . Percentage of silane by weight of cement.

Both low and high addition levels of APTES induced a retardation effect on cement hydration by similarly extending the induction period with respect to the cement paste (Figure 4-16).

In addition, a high dosage of APTES resulted in significantly decreased maximum heat output up to 1 mW/g, while the low dosage of APTES only slightly reduced it to 2.85 J/g. As a result, the total heat flow corresponding to the high level addition of APTES after 8000 min was reduced up to 10% with respect to the low level additions. However, a higher initial total heat flow was recorded for paste with high APTES content due to a higher rate of heat released in the early ages of the hydration.



The heat evolution curves for GTO modified cement pastes are illustrated in Figure 4-17.

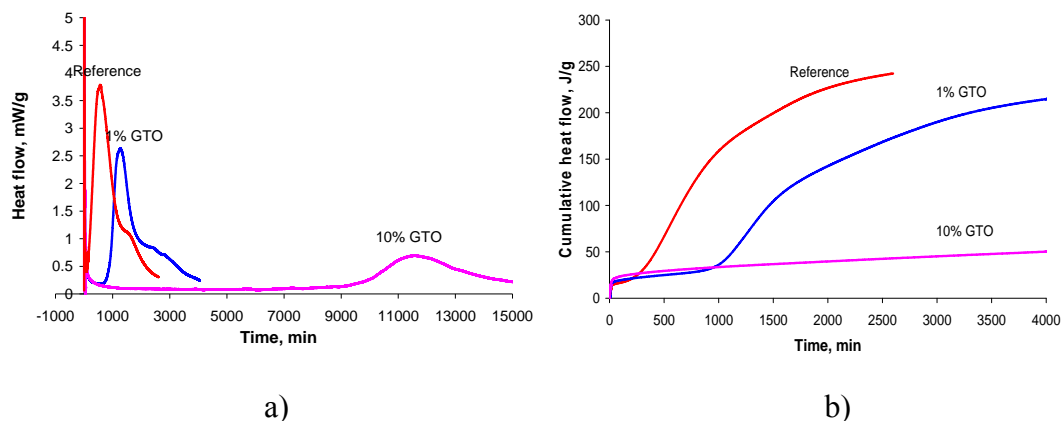


Figure 4-17. Effect of different dosages of GTO on the heat flow (a) and cumulative heat flow (b) of cement pastes prepared with constant  $w/c=0.3$ . Percentage of silane by weight of cement.

Both concentrations tested acted as retarders on the cement hydration, but there were major differences observed depending on the dosage used.

First, there is a significant decrease in the maximum rate of heat output down to 0.7 mW/g for high GTO addition level, while low GTO dosages reduced the heat value to 2.6 mW/g. Second, the length of the induction period was extended up to 10' 000 min for high GTO concentrations compared to 800 min for low GTO concentration. Plain cement paste had an induction period of 100 min. As a consequence, the total heat output for low GTO dosage is always lowered by up to 50 % when compared to reference cement paste after 24 h of hydration. High GTO level addition reduced the total heat output by up to 81.5 % after the same period. In addition, for the cases investigated, the presence of GTO did not affect the initial heat release in modified pastes compared to neat pastes.

Figure 4-18 gives the heat evolution curves for AEAPTMS modified cement pastes.

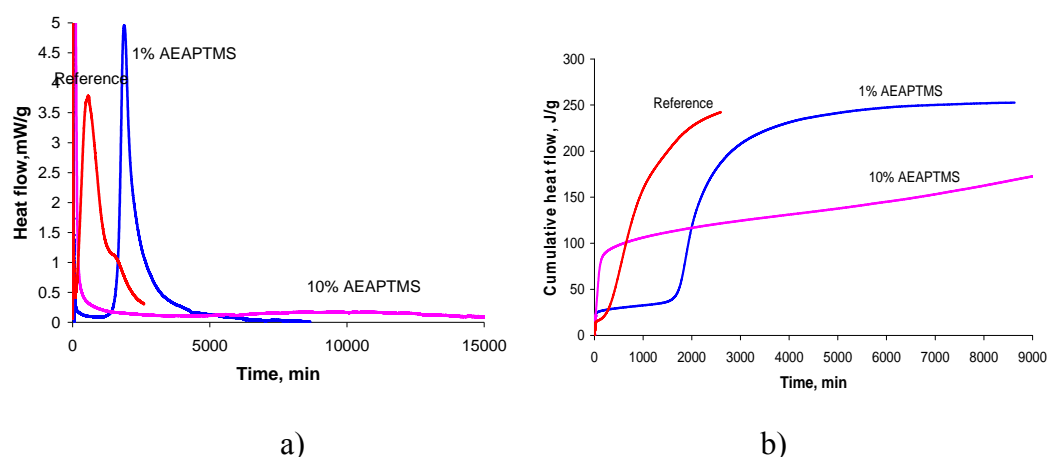


Figure 4-18. Effect of different dosages of AEAPTMS on the heat flow (a) and cumulative heat flow (b) of cement pastes prepared with constant  $w/c=0.3$  Percentage of silane by weight of cement.

Also in the case of AEAPTMS major changes in the cement hydration are visible depending on the dosage employed.

For the low addition level, an increased maximum rate of heat output of up to 33 % and a 15 times longer induction period were observed compared to the reference cement paste. In addition, a very sharp peak marks the hydration of the silicate phase.

On the contrary, for the high addition level, a major decrease in the maximum rate of heat output of up to 92.5% was found compared to the reference cement paste. Furthermore, a very broad main heat release peak was observed. Because of that the length of the induction period could not be clearly defined. However, we estimated it roughly at about 5000 min.

In terms of total heat output, AEAPTMS modified cement pastes gave initially higher values compared to reference paste, in particular for higher addition levels of AEAPTMS. After that, the reference cement paste showed constantly higher total heat outputs as silicates hydration contributed substantially to the total heat release.

### 4.2.3 Discussion

The effects of silane addition to anhydrous cement by dry blending were explored by investigating some of the properties of modified cement pastes and mortars. Physico-mechanical tests have been carried out for two different concentrations of silane by weight of cement: low addition levels (1% wt) and high addition levels (10% wt). In addition, isothermal calorimetry measurements provided information on the hydration. The discussion below aims to correlate some aspects of the results obtained above.

The standard consistency water and workability data obtained for the silanes modified cement investigated have been analysed by comparing them to a plain cement paste and to other pastes modified with different types of silanes. The results indicated that the presence of silanes results in a reduction of the amount of water needed for pastes to reach standard consistency and to an enhanced workability compared to plain cement paste. As a result, the modified cement systems exhibit fluidifying effects. The results are in good agreement with the data published in the literature which reported silanes as water reducing and workability enhancement agents [84].

The effect was found to increase with the dosage and to depend on the nature of silanes used. GTO was found to be the best dispersing agent among the silanes investigated. AEAPTMS has shown stronger dispersive effects on than APTES. It was suggested [84] that the longer organic chain length associated with two amine functional groups prevails against the shorter chain molecule carrying only one amine group (amine groups are inherently hydrophilic). The fact that AEAPTMS appears to be a better dispersant agent correlates well with the shape of the main peak from calorimetric measurements for low level additions. The relationship between the dispersing effect of superplasticizers and its consequences on hydration kinetics has been previously investigated by Jiang. It has been shown that sharper peak indicates better dispersive characteristics [87]. This is because superplasticizers cause dispersion of agglomerated cement particles into smaller grains, which provide an increased number of nucleation sites, thus C-S-H formation are reached more quickly.

By comparing the test results for the three silanes investigated to the ones obtained for the other silane agent considered (TEOS) (Figure 4-4), we found that there is no dispersive effect present in the latter. This implies that the effect is clearly connected to the non-hydrolysable organic chain present in all of the structures of silanes we investigated. Similar correlations relating the molecular structure of the admixture to the dispersive effects were reported by others [88-90], but only limited data in silane-cement systems are available.

As discussed in Chapter 2, the case of neat cement pastes can be very well assimilated to surfaces with high charge densities and multivalent counterions environments. Attractive electrostatic interactions promoted by ion-ion correlation forces between particles of same charges are responsible for cohesion between C-S-H, along with van der Waals forces. Consider now the case of silanes modified cement pastes. By grafting silane onto the surface we alter the surface properties of the cement particles and thus its interactions with the solution and as well as with other cement particles. This will result in reduced ion-ion correlation forces because the surface charge is screened. Hence, the decrease in attractiveness among surfaces, which explains the increased dispersion. However, it must be pointed out that dispersive effects could be associated with physical interference (steric hindrances). Each three silanes carry one relatively large side chain that could prevent particles to agglomerate as they normally do in the case of unmodified cement system. This results in additional repulsion between neighbouring particles and thus the fluidification. Up to now, it was difficult to detect or attribute the dispersive effects to either electric double layer or steric force, therefore both types are to be considered in explaining the fluidification of cement pastes.

Vicat set-time tests indicated that silanes act both as set retarders and set accelerators on cement hydration. For high addition levels, all silanes were found to retard the set. The increase was depending on their nature and was found to be inversely proportionally with the standard consistency water demands. For low addition levels both reduced (AEAPTMS and GTO) and increased (APTES) set values were measured. The results are in good agreement with the literature data [84], which report shorter setting time values for cement pastes containing AEAPMTS than for

cement pastes containing APTES for silane to cement concentrations up to 1% by weight.

The heat development measurements can offer some additional information regarding setting since one generally associates the initial and final set to certain positions on the calorimetric curve. The correlation has been described in Section 4.2.1.5. The heat development measurements showed clearly that all the silanes investigated in this study retard the hydration of normal Portland cement. The induction period was prolonged with increasing the silane fraction. No accelerating effect was observed on calorimetric measurements contrary to what was found by Vicat set-time tests. This indicates stiffening of pastes prior to the time when hydration of silicates started. The stiffening is detected for both high and low silane addition levels. The phenomenon can be explained by flash and/or or false set that prevents the needle to penetrate the sample and inaccurately indicating the setting. This is due to the fact that silanes participated in, or interfered with several process associated to the aluminates and/or sulphate phases from cement. This is furthermore confirmed by higher total heat outputs recorded initially for silane modified cement pastes compared to reference. Aminosilanes appear to have a stronger effect on the initial heat release compared to GTO. Nevertheless, the experiments confirmed the overly simplistic approach and arbitrary interpretation of the results of this conventional method (Vicat set-time) that has been previously brought up by Sant [91].

The results obtained from mechanical tests indicate that silanes affect drastically the development of mechanical properties. Moreover, they were found to induce some loss of hydraulic behaviour in some cases. It is known that development of mechanical properties of cement based systems is highly linked to the hydration reaction of cement, therefore the heat development can provide valuable information. The low early strength observed in all modified specimens can be attributed to the retarding effect observed on hydration. The problematic specimens demoulding issues encountered after 24 h and the necessity to air cure samples are explained by the fact that at the demoulding time selected the hydration reaction was still in the induction period. Thus highly insufficient hydration products were generated for paste cohesion

The overall reduced performances of the silane modified systems are due to the largely reduced degree of cement hydration. Calorimetric measurements confirmed that there is a significant decrease in the height of the main heat peak release and of area beneath. Hence, a considerable decreased in hydration degree for silane modified systems takes place and this badly affected the mechanical performances regardless of the specimens' age.

In contrast, Svegl et al.[84] report a turning point in strength development of the silane modified mortars in between 14 and 24 days and, as a result, the 28 days tests reported show better strength values for modified specimens. In this case mortars specimens have been prepared using APTES and AEAPTMS added as admixture. Both aminosilanes dosages ranged from 0.3 to 1.2% by weight of cement.

Considerations upon the mechanisms of the retardation could not be established up to this point in time. However, based on the observed facts it is reasonable to assume that silanes retard mainly the hydration of alite subsequently to their grafting on this phase.

We can conclude that the silanes we investigated bring fluidifying effects on cement pastes, retard the set and affect drastically the kinetics of silicate phase hydration. This results in decreased mechanical performances, regardless of the testing age.

### **4.3 Conclusions**

It has been shown in this chapter that by dry blending silane and cement powder changes significantly the properties of the modified products. Different silane to cement addition levels has been investigated: low addition level (1%) and high addition level (10%).

The first investigations showed that trialkoxysilanes carrying a non-hydrolysable organic chain induce a fluidifying effect on cement pastes and mortars. This has been concluded after analysing the standard consistency water and flow table tests. Higher addition levels of silane result in lower water demands for standard consistency pastes and enhance workability. Moreover, it was found that the dispersive effect increases

with the dosage. The dispersive effect is very likely associated to the non-hydrolysable organic chain present on all the silanes investigated. This was inferred after comparing the results to the data acquired for a silane carrying four hydrolysable groups.

The effect of silanes on setting time has been investigated by using Vicat set-time tests. In the case of high addition levels the set times were found to always increase compared to neat cement., while as the standard consistency water decreased. For low silane dosages both accelerating and retarding set effects have been found. The accelerating effect was proved to be a stiffening not involving silicate hydration as is usually the case. This was possible comparing Vicat time set values to the heat development curves. The Vicat needle measurement is correct, but the interpretation made of it is no more valid in this case.

Mechanical tests performed on pastes and mortars revealed significant decrease in performances for all silane modified cements. This fact has been carefully correlated to calorimetric measurements. The results showed that silanes affect significantly cement hydration, particularly silicate phase hydration. It was found that depending on the nature and on the dosage, the length of the dormant period is significantly extended and the maximum rate of heat output is drastically reduced. Consequently, the modified specimens displayed reduced degree of hydration which explains fairly well the loss in mechanical performances.

The attempt to improve mechanical properties by dry blending silane with cement has therefore not been successful. Most probably because the dosages used were too high. Nonetheless, this approach does not provide clear information concerning the grafting process. Based on these hypotheses, a new methodological approach has been developed and applied for grafting silanes to cement. This will be presented and discussed in what follows

## **5 Silane modified cement obtained by liquid phase deposition and excess solvent removal**





So far, we have seen that adding silanes to cement powder by direct blending of the two constituents prior to hydration results in significant strength loss for both modified pastes and modified mortars. Most likely, the dosages of silanes employed were too high resulting in strong delays of cement hydration. Nevertheless, the method employed lacked a scientific approach and it was doubtfully addressing the nature and the magnitude of silane to cement interactions, despite its ease in sample preparation.

Consequently, it appeared logical to start by reducing the dosage of silane with respect to cement. But, by drastically reducing the dosage of silane and maintaining the direct blending as deposition method, we would not have obtained a homogeneous mix, because of two conflicting phenomena: dispersion and condensation. Small amount of silanes disperse badly in the powder and as a result condensation with the surface is highly insufficient both quantitatively and in terms of space distribution [49]. Therefore, another deposition methodology was chosen namely, the liquid phase deposition method. This allowed a drastic reduction of the dosage, while maintaining a good dispersion of silanes throughout the cement powder. In addition, it provided accurate control on the amount of silanes adsorbed on the surface by quantifying the unabsorbed amount left in solution.

In this chapter, development of a new method for silane cement surface functionalisation will be presented. By carefully studying the adsorption process of silane toward the cement surface from an inert liquid phase, more understanding on the cement-silane interactions will be gained.

Then, we will present principles, experimental set-ups and operational modes for several techniques used to study the properties of the modified products. The work will focus on two directions: investigation of the hydration kinetics and of the viscoelastic properties of the modified products. Isothermal calorimetry and dynamic mode rheometry will be the main techniques used to examine the changes in properties related to the presence of silanes.

## 5.1 Methodology

### 5.1.1 In principle

The liquid phase deposition and solvent excess removal uses a liquid as transport medium to aid dispersion of silane throughout the substrate. Once equilibrium is reached, the supernatant containing the unabsorbed silane fraction is removed and the silane modified substrate is further oven cured for complete solvent removal and condensation enhancement.

Extensive studies have been carried out investigating bonding of different silanes to mineral substrates [49, 54, 92, 93]. As explained in Chapter 2, bonding occurs between silanols of the targeted surface and alkoxy or silanols groups of the silane agent. As a result siloxane bonds (Si-O-Si) are formed. Water or organic solvents are employed as vehicle media depending on the working conditions.

The method developed below was similar to the one used for silane silica surface modification [88]. This approach served as starting point for silane cement surface modification given the similarities among silica and silicates from cement.

In the case of silane modified silica surfaces, there is a debate in the literature as whether chemical bonding to substrate results from direct condensation between alkoxy groups and surface silanols. From experiments, Blitz [94] concluded that direct condensation does not take place and even that post curing treatment results in evaporation of the adsorbed molecules. Alkoxysilanes may only chemically bond to the surface provided that there is water on it or a catalyst as ammonia is used [95]. The pivotal role of water from the targeted surface in the chemical bonding has been also brought up by others [57, 96-98].

Investigating the interaction of aminoethyltriethoxy silane and silica surface Caravajal [99] and Kelly [100] proposed a two step reaction mechanism distinguishing between a reaction step and a post-reaction curing step. They reported hydrogen bonding (10%), proton transfer (22%) and condensation reactions (68%) taking place in the reaction phase, while upon curing the aminosilanes molecules turn from the original

Silane modified cement obtained by liquid phase deposition and excess solvent removal

amine-down position towards an amine-up position through a flip mechanism (Figure 5-1) [88]. Figure 5-2 outlines the basic mechanism proposed.

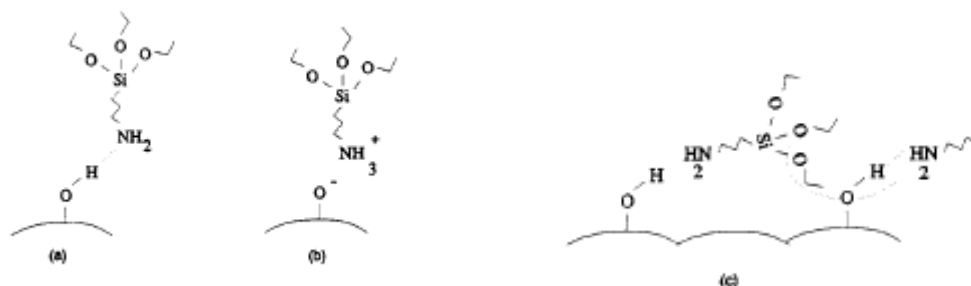


Figure 5-1. Schematic illustration of various aminosilanes interaction types in the reaction phase (a) hydrogen bonding (b) proton transfer (c) condensation to siloxane (reproduced from [88])

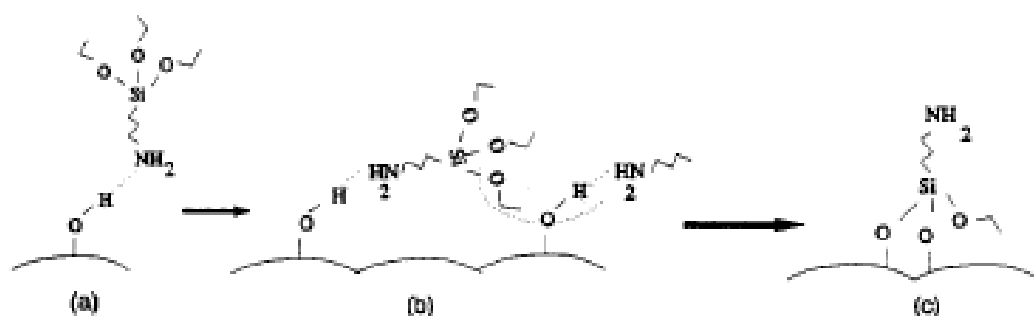


Figure 5-2. Schematic representation of the flip mechanism for APTES reaction with silica surface under dry conditions (a) physisorption (b) condensation (c) structure after curing (reproduced from [88])

### 5.1.2 In practice

Two full dried organic solvents, namely ethanol and toluene were chosen and used for this study. The solvents were inert with respect to the cement. 99.96% pure ethanol was purchased by Prolabo and used as received. Toluene (Sigma-Aldrich) was

Silane modified cement obtained by liquid phase deposition and excess solvent removal

distilled at reduced pressure before use and was stored on a molecular sieve (5 Å) to assure complete dryness. 4.000 g of cement were placed in a diluted silane solution of i) ethanol and ii) toluene. The mixture was stirred on a vibrating table (GFL, Germany) for 24 h in sealed 12 ml polypropylene tubes at a temperature of 23°C. Mixing enables silanes to diffuse easily in solution and interact with cement surface.

In a first set of experiments **the liquid to solid ratio was kept constant** ( $l/s=1.37$ ) while varying the silane to cement concentration from 0.1% to 5% by weight. After 24 h stirring, the mixes were centrifuged 10 min at 9000 rpm (Universal 32, Hettich, Germany). This led to phase separation. The modified solid substrate (cement or tricalcium silicate) was oven cured for 4 hours at 80 ° C and stored in sealed plastic containers. After the heat treatment, an unusual separation of a white phase was noticed within the modified substrate. The distinct phase was analyzed. SEM/EDX analysis confirmed the presence of a species containing calcium, sulphur and oxygen ions. This implies that subsequently to cement dispersion in solvent, gypsum separates. Therefore, after cooling, the samples were homogenized for 24 h using a heavy-duty shaker mixer (Turbula, Wab, Switzerland).

An alternative phase separation technique investigated, but used only to a limited extent and just for comparison purposes, considered filtration phase separation using a fritted filter funnel (borosilicate glass based) under vacuum. The modified substrate was similarly treated as described above and identical problems of gypsum separation were encountered.

The supernatant was collected in 100 ml polypropylene bottles. In the case of grafting carried out in ethanol, the liquid phase was heated at 80°C for complete ethanol evaporation. After cooling 80 ml of NaOH 0.01M (prepared from a 1M NaOH purchased by Prolabo and diluted with ultra pure water obtained from a Milli-Q2, Millipore) were added to each vessel. The new obtained solution was analysed for silicon content by Inductively Coupled Plasma Atomic Emission Spectrometry (ICP-AES Vista, Varian). The amount of silane remained in solution was determined by the measured amount of silicon. By difference the adsorbed fraction was calculated.

Silane modified cement obtained by liquid phase deposition and excess solvent removal

In the case of grafting carried out in toluene, the supernatant was phase-exchanged in a NaOH 0.01 M solution using a separatory tap funnel. The aqueous phase was collected and the silicon content was analysed by ICP-AES. Similar correlations led to quantify the fraction of adsorbed silanes.

In a second set of experiments **the silane to cement ratio was kept constant** (1% APTES by weight of cement) while varying the liquid (solvent) to solid (cement) ratio from 1.37 to 9.5. Similar procedures were employed for all steps.

## 5.2 Adsorption

In this section we present data on how silanes adsorb onto a chosen solid (cement and tricalcium silicate) subsequent to a liquid phase grafting method following excess of solvent removal as described above. Several parameters like the nature and dosage of silane, the nature and dosage of the solvent, the nature of the adsorbent will be systematically examined in order to obtain more information concerning the reactivity of silanes versus the considered adsorbent.

It must be noted that the terminology **adsorption** is used to define here the collection of silane molecules on the surface of the adsorbent solid (cement or C<sub>3</sub>S). Since during the reaction phase the extent of each possible bonding type (hydrogen bonding, proton transfer or covalent bonding) is unclear, the adsorption defines here both physisorbed species and chemically bonded ones.

### 5.2.1 Techniques used for investigating the adsorption

#### 5.2.1.1 Inductively Coupled Plasma-Atomic Emission Spectroscopy (ICP-AES)

In order to evaluate the fraction of silanes adsorbed, the unabsorbed fraction remained in solution was measured by an Inductively Coupled Plasma-Atomic Emission Spectroscopy (ICP – AES) Vista Pro spectrometer from Varian.

Silane modified cement obtained by liquid phase deposition and excess solvent removal

The analysis consisted in determining the content of silicon from the collected supernatant solution and treated according to the procedures described above. From the measured silicon values the unadsorbed fraction of silane has been determined. This was subtracted from the initial dosage and thus, the adsorbed silane fraction has been calculated.

#### **5.2.1.2 Transmission Electron Microscopy (TEM)**

A transmission electron microscope (TEM) was used to investigate the presence and the conformation of silanes at the interface with the adsorbent. Only examinations on tricalcium silicate as adsorbent have been carried out, because it was more convenient. The microscope used was a JEOL 2100 LaB<sub>6</sub> having a field emission gun, operating at 200 KV. High resolution images were recorded using a Gatan Ultrascan camera. Preparation of the samples involved dispersing the solid substrate into anhydrous ethanol. From the dispersion a small amount has been collected and placed on the measuring grid.

#### **5.2.1.3 Other investigation methods**

Two additional investigation techniques namely Infra Red Attenuated Total Reflexion (IR – ATR) and X-Ray Photoelectron Spectroscopy (XPS) have been used to identify the character of the bonding solid-adsorbate. The methods have been reported successfully used in analyzing the nature of the bonds between adsorbents and adsorbates [49, 54, 93]. Moreover, using these techniques covalent bonding of silanes to silicate based substrates, like glass or silica have been confirmed [55, 56, 59, 65, 101]. One usually measures the disappearance/diminishing of a certain peaks (corresponding to the available bonding sites) and the appearance of new ones (corresponding to the new formed chemical bond).

In our case, by IR-ATR investigations, we examined the decrease in intensity or/and final disappearance of intensity lines corresponding to surface silanols and appearance of the ones defining siloxane bonds. However, due to the low sensitivity of the measuring tool along with the low dosage of adsorbent with respect to adsorbate, the

Silane modified cement obtained by liquid phase deposition and excess solvent removal

small changes in peak heights could not provide enough information to conclude that silanol groups disappeared and siloxane bonds were formed. Moreover, the complex nature of cement compared to silica complicated the band assignments from the recorded spectrum and it was not possible to clearly identify the changes.

XPS has been used to investigate any possible changes in intensity of the binding energy for the oxygen (1s), nitrogen (1s), silicon (2p) and carbon (1s) by comparing the control to silane modified sample. Once more, given the low percentage of the silane with respect to the substrate and the limitation due to the detection limit, a straight forward conclusion regarding chemical bonding of silane to cement could not be formulated at this point in time.

None of the results obtained using the last two techniques will be reported within this work.

## **5.2.2 Results**

### **5.2.2.1 Effect of silane dosage**

A first series of experiments were performed for a constant solvent to cement ratio and variable concentrations of silane to cement by weight. The adsorbed silane fractions have been calculated subtracting from the initial dosage the unadsorbed one that has been measured by ICP-AES from the separated liquid phase.

The adsorption curve of APTES to cement from ethanol is illustrated in Figure 5-3. It was plotted using the mean values obtained from a minimum of two measurements performed for each case and it give the dependence of adsorbed fraction versus unabsorbed one. Initial concentration of APTES to cement by weight ranged from 3.6 to 181  $\mu\text{mol/g}$  of cement, which converted to percentage units leads to values in the range of 0.1% to 5%. All experiments have been carried out at 23 °C.



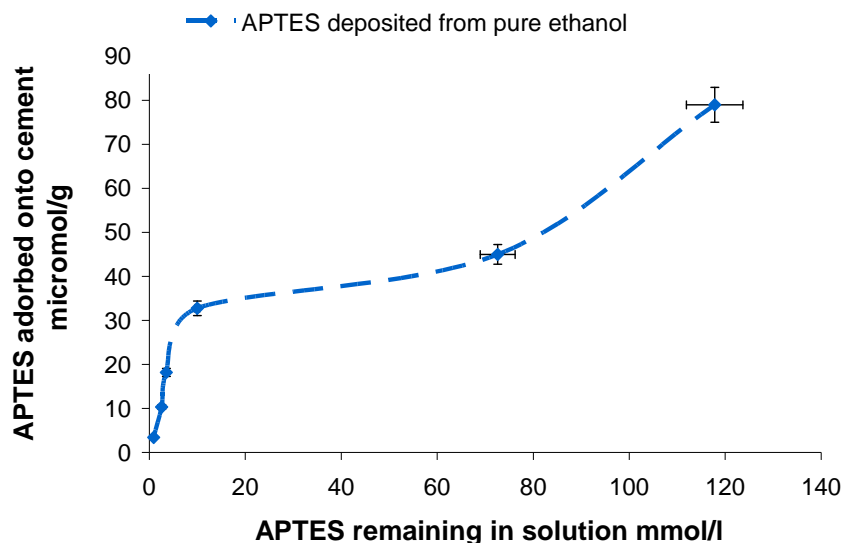


Figure 5-3. Adsorption data for APTES to cement from ethanol suspensions.

Converted to percentage units, the results from above indicate, higher APTES dosages adsorb to cement for low initial addition levels (about 75% adsorbed and 25 % in solution) compared to high initial addition levels (about 35% adsorbed and 65% in solution).

Also, the adsorption profile shows a step-like behaviour defined by three different domains. The first one, linear, corresponding to the initial vertical rise, defines the situation when the quantity of adsorbed silane varies proportionally to the introduced one. The slope, always characteristic of the adsorbate shows here a strong affinity adsorbate-adsorbent. This region usually corresponds to incomplete monolayer coverage of the surface.

The second step corresponds to a plateau region. This usually accounts for saturated surface coverage. Once the plateau region has been attained, one does not see significant variations in APTES adsorption. This means that even when increasing the APTES concentration in the initial solution no further adsorption on the cement is being noticed and the excess remains in solution. For this case, the plateau value for APTES adsorbed to cement from ethanol suspensions was identified to be 32.75  $\mu\text{mol}$

Silane modified cement obtained by liquid phase deposition and excess solvent removal

APTES/g cement. The plateau value depends both on the adsorbate and on the type of the vehicle media as will be later discussed in Section 5.2.2.2.

Above the plateau region, which presumably defines a APTES monolayer coverage, further increase in initial silane concentration in solution results in increased absorption. The subsequent adsorption points most likely to a multilayer APTES coverage, where some molecules continue to adsorb on the already adsorbed ones as a consequence of the strong interactions among themselves.

Let us now consider the plateau value for APTES adsorbed from ethanol suspensions (32.75  $\mu\text{mol}$  APTES/g cement or 0.72% APTES to cement by weight) and further analyse it. Initially we assumed that this value stands for complete silane monolayer coverage of cement. Considering the value reported by Vrancken et al [102] giving information on the area covered by a single APTES molecule, we can easily calculate the area covered by the entire amount of APTES found to be adsorbed on the plateau region.

For one gram of cement we can write:

$$S_{\text{coverage}} = \frac{m_{\text{APTES}}}{M_{\text{APTES}}} S_{\text{APTES}}^0 N_a \quad (5-1)$$

Where:

$m_{\text{APTES}}$  is the amount of adsorbed APTES

$M_{\text{APTES}}$  is APTES molecular weight

$S_{\text{APTES}}^0$  is the surface covered by one molecule of APTES, reported  $50\text{\AA}^2$

$N_a$  is Avogadro's number

Thus, for one gram of cement, the calculated surface occupied by the amount of APTES on the plateau is:

Silane modified cement obtained by liquid phase deposition and excess solvent removal

$$S_{plateau\ coverage\_ethanol} = \frac{0.0072}{221} \cdot 50 \cdot 10^{-20} \cdot 6.023 \cdot 10^{23} \quad (5-2)$$

$$S_{plateau\ coverage\_ethanol} = 9.86 \text{ m}^2 \quad (5-3)$$

If we now compare this value to the surface of one gram of cement (specific surface considered 1 m<sup>2</sup>/g) a nearly ten times difference is observed. This means that the amount of APTES adsorbed on the plateau corresponds to a ten times higher surface than available. Thus, for APTES adsorbed from ethanol suspensions ten layer coverage for the plateau region is most likely. This implies that the initial monolayer coverage assumption must be discarded.

To gain more insights on this multi layer coverage observed for the plateau region, transmission electron microscopy (TEM) combined with EDS investigations have been carried at the interface adsorbate - adsorbent. As already mentioned, for convenience reasons investigations have only been performed on tricalcium silicate-APTES. However, these situations are comparable, since APTES adsorbs similarly on tricalcium silicate as on cement as it will be later discusses.

Figure 5-4 shows a badly dispersed APTES adsorbed at the surface of tricalcium silicate. The darkest region represents the inorganic substrate to which APTES is attached. APTES is detected as a variably thick and irregular cover consisting in clustered species. APTES presence was identified through EDXS analysis. The spectrogram illustrating its presence is given in Annex II.

Silane modified cement obtained by liquid phase deposition and excess solvent removal

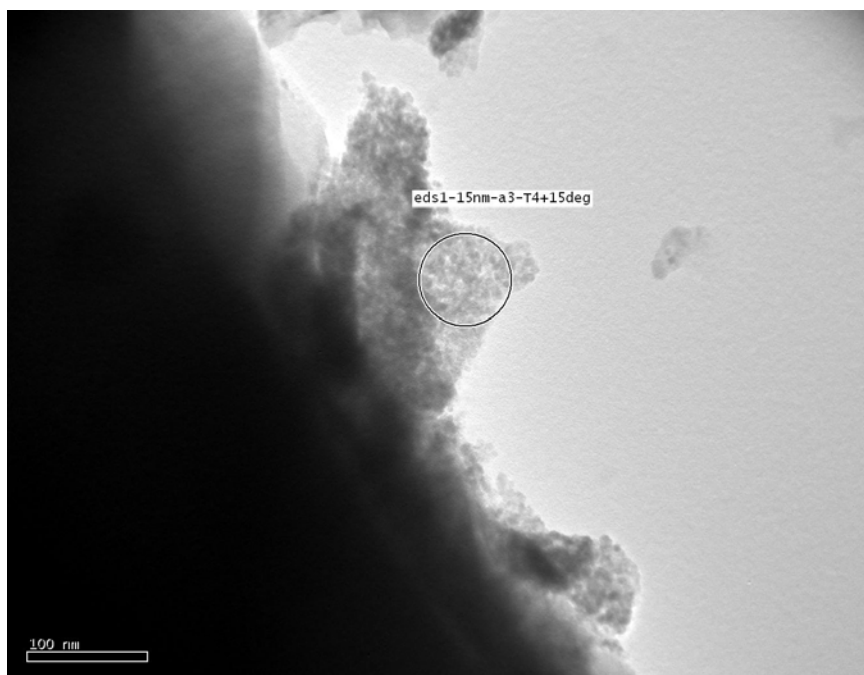


*Figure 5-4. TEM micrographs of APTES adsorbed to tricalcium silicate. The darker region defines the inorganic substrate (tricalcium silicate), while the clusters exemplify APTES's presence.*

The most important information that this micrograph brings is that APTES is not uniformly distributed over the surface. One clearly distinguishes on the one hand silicate surfaces completely lacking in silane coverage, while on the other hand there are areas covered with silane agglomerated into more or less thick formations. The data provides a reasonable explanation for plateau region values observed on the adsorption profiles.

#### **5.2.2.2 Effect of solvent**

##### **Nature of solvent**

A second series of adsorption experiments have been performed from a different organic solvent at similar solvent to cement ratio and at similar initial concentrations of silanes to cement. These experiments aimed to investigate whether the nature of the solvent can influence the adsorption behaviour of silane onto cement. We have chosen toluene as second dispersive media. This choice has been made because of its anhydrous nature. Nevertheless, there are differences reported in literature regarding

Silane modified cement obtained by liquid phase deposition and excess solvent removal

the adsorption behaviour of silanes versus a substrate from toluene and ethanol used as vehicle media[103]. Because of their different nature (ethanol- protic solvent and toluene- aprotic solvent) they were evidenced to promote different types of surface bonding. It is suggested that toluene leads mainly to covalent bonding between silanes and the adsorbate while ethanol promotes hydrogen bonding and thus a lot of silanes are physisorbed.

The adsorption profile of APTES on cement from toluene is given in Figure 5-5. The results are plotted in terms of the adsorbed fraction versus the excess measured in solution and compare it to the data obtained for adsorption from ethanol suspensions.

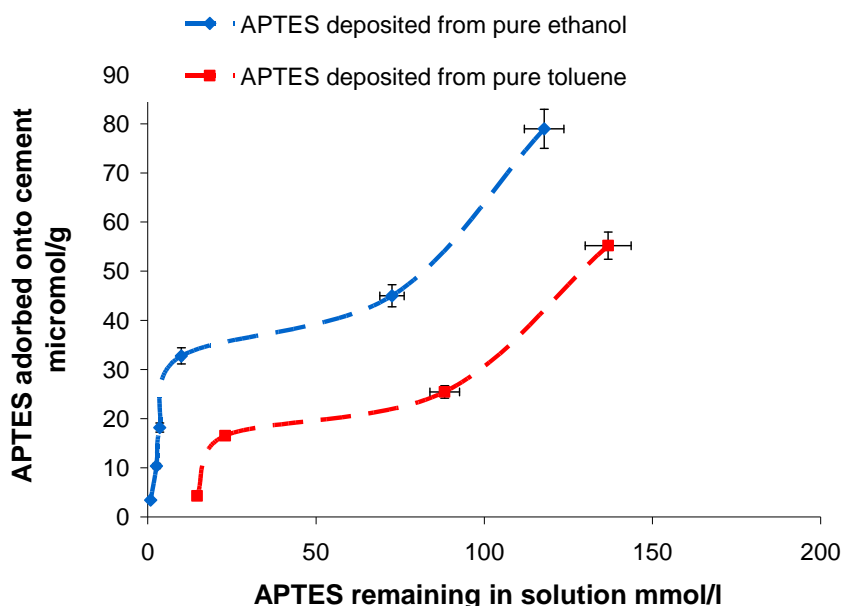


Figure 5-5. Adsorption data for APTES on cement from ethanol suspensions (upper curve) and toluene suspensions (lower one).

An overall similar adsorption path is identified, regardless of the solvent used. The initial linear domain is in both cases followed by a plateau region above which, a second linear increase of adsorbed fraction versus solution concentration is observed. Moreover, the slopes of both linear domains are similar.

However, an important difference arises from this comparison. As the graph shows lower amounts of adsorbed APTES are always observed when toluene is used as vehicle media. To better interpret and compare the data from Figure 5-5, a

Silane modified cement obtained by liquid phase deposition and excess solvent removal

recalculation can be performed to express the surface coverage of APTES adsorbed from toluene using equation 5-1. Let's consider the plateau region in case of adsorption carried out in toluene for one gram of cement. According to equation (5-1) we can write:

$$S_{\text{plateau coverage\_toluene}} = \frac{0.0036}{221} \cdot 50 \cdot 10^{-20} \cdot 6.023 \cdot 10^{23} = 4.95 \text{ m}^2 \quad (5-4)$$

Comparing this value to the surface available in one gram of cement powder ( $1 \text{ m}^2/\text{g}$ ) a factor five is obtained. Consider now the previously calculated value for plateau surface coverage in the case of ethanol ( $9.86 \text{ m}^2$ ) and compare it to our calculated value in the case of toluene. The result is half. This implies that at plateau region APTES surface covered from toluene is two times smaller than in the case of experiments carried out in ethanol, but far from being a monolayer.

The differences observed through out the whole concentrations range investigated are very likely to originate in the different characters of the two organic solvents. The results obtained above seem to match the trend highlighted by Vrancken [103] that both physisorption and covalent bonding take place from organic solvents, but that ethanol favours mainly hydrogen bonding due to its protic nature. Despite the fact that there would be less physisorption in toluene, there is still much more silane adsorbed than required for a monolayer coverage.

### **Solvent to cement ratio**

So far we have seen that the adsorption behaviour of silane onto cement depends on its dosage with respect to cement and on the nature of the solvent used as vehicle media. In what follows we investigate the possible variations arising in adsorption behaviour when variable solvent to cement ratios are used. The study has been performed using ethanol as dispersion media, APTES as adsorbate and cement as adsorbent. The liquid (ethanol) to solid (cement) ratio ranged from 1.37 to 9.5 and a constant concentration of 1% APTES to cement by weight was used in all cases. The

Silane modified cement obtained by liquid phase deposition and excess solvent removal

results displaying the amount of APTES adsorbed onto cement versus the solid to liquid ratio are shown in Figure 5-6.

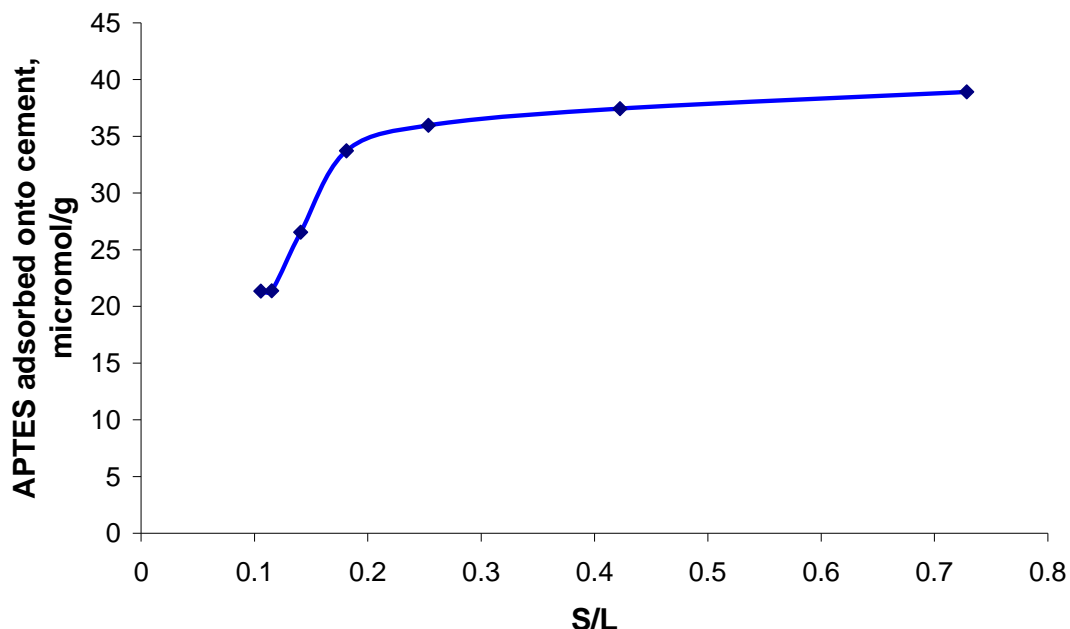


Figure 5-6. Effect of solid (cement) to liquid (solvent) ratio on the adsorption of APTES. 1% APTES to cement by weight was used in all cases.

Two different zones can be easily distinguished. First a linear increase, as the solid content in the system increases, the APTES adsorption increases linearly up to a value of approximately 33  $\mu\text{mol/g}$ . Above this value, no significant variation in the adsorption of APTES is noticed despite the fact that the solid content in the system is constantly increasing.

This means that the adsorption of APTES onto cement is strongly dependent on the quantity of the liquid available in the system. The quantity of liquid (solvent) considered as dispersion media should be kept within certain limits to allow a good dispersion of the adsorbent. When the liquid content in the system is reduced dispersion is affected and APTES tends to self agglomerate. This is confirmed by adsorbed fractions (in the case of concentrated suspension) ranking in the same range as to the ones corresponding to the plateau region in the graph given in Figure 5-3, where an excess of silane was found to be adsorbed.

### 5.2.2.3 Effect of silane nature

Figure 5-7 shows the adsorption curves obtained for all three silanes from ethanol suspensions on cement. Each curve corresponds to a different silane.

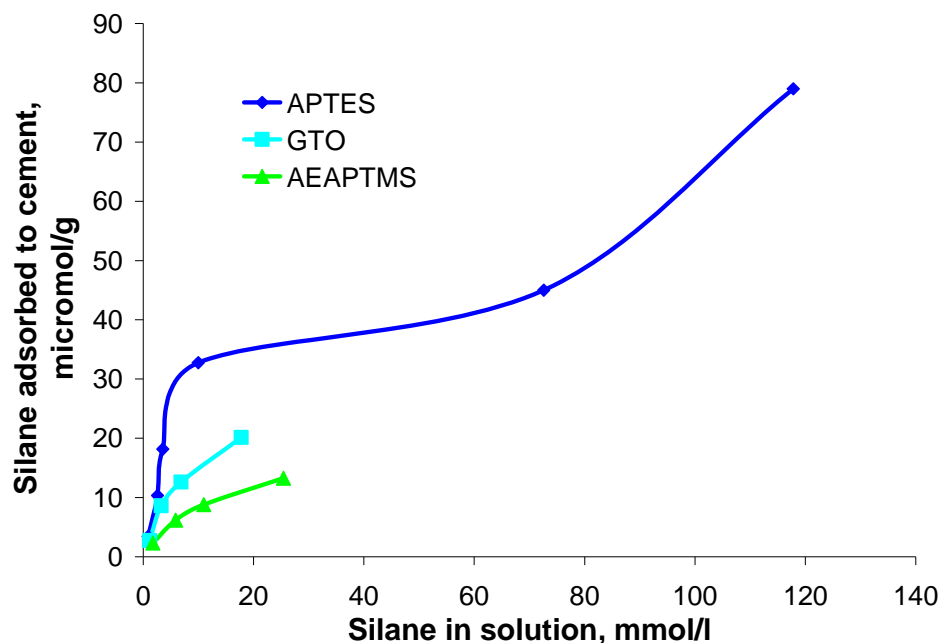


Figure 5-7. Adsorption data for APTES, GTO and AEAPTMS to cement from ethanol suspensions.

The results indicate that all three silanes investigated adsorb onto cement, but their adsorption levels are different. Initially, APTES adsorbed strongly evidenced by the sharp initial rise of the adsorption curve. In contrast, GTO and particularly AEAPTMS show lower levels of adsorption indicated by smaller slopes. This suggests weaker adsorbate-adsorbent interactions.

Further increasing the APTES dosage in the initial solution one does not see any change in the adsorbed amount up to a certain dosage when the adsorption increases by increasing the initial silane fraction. This case has been previously discussed.



Silane modified cement obtained by liquid phase deposition and excess solvent removal

In the case of GTO and AEAPTMS investigations aiming at characterising the adsorption behaviour when increasing the dosage in the initial solution were rather limited. Experimental evidence to be presented suggests that this was of no further interest (for practical applications), because even the low dosages adsorbed were found to have a very negative effect on cement hydration (Section 5.3.2.1). However, these results raised a question regarding the nature of the interactions with substrate. It is surprising how silane agents displaying low adsorption levels have the strongest influence on cement hydration. A hypothesis to be considered at this time is that the nature of the interactions with substrate is different. Further experimental investigation and discussion will be present in Section 5.3.2.1.

#### 5.2.2.4 Effect of adsorbate

Table 5-1 reports the results obtained from adsorption of silanes to cement and to tricalcium silicate from ethanol. A limited number of experiments have been carried out in toluene.

*Table 5-1. Effect of substrate on the adsorption of silanes from ethanol and toluene suspensions.*

Silane	Initial silane/solid wt %	Adsorbed silane/cement wt %	Adsorbed silane/ tricalcium silicate wt %
From ethanol			
APTES	1	0.72	0.72
GTO	0.5	0.3	0.3
AEAPTMS	0.5	0.19	0.18
From toluene			
APTES	1	0.36	0.33

The general trend observed, is that silanes adsorb in similar proportions on cement and on tricalcium silicate, regardless of their nature or of the solvent used as

Silane modified cement obtained by liquid phase deposition and excess solvent removal

dispersive media. It must be noted that both substrates used as adsorbates had nearly the same specific surfaces (Blaine).

Based on the documented silicate content in cement (approximately 80 % by weight) we can calculate the dosage of silane to silicates provided that all silanes are adsorbed on the silicates as initially assumed. Table 5-2 reports the results of these calculations and compares them to the experimental data collected from adsorption of silane to tricalcium silicate previously reported in Table 5-1.

*Table 5-2. Adsorption of silanes from ethanol and toluene suspensions to silicate phases. Comparison between the calculated dosages as resulted from experiments carried out for cement to measured fractions from experiments carried out for tricalcium silicate.*

Silane	Adsorbed silane/silicates % wt (calculated)	Adsorbed silane/ tricalcium silicate % wt (measured)
From ethanol		
APTES	0.87	0.72
GTO	0.37	0.3
AEAPTMS	0.23	0.18
From toluene		
APTES	0.45	0.33

These results indicate clearly higher adsorption levels of silanes for cement compared to tricalcium silicate. Hence, the conclusion to be drawn from these experiments is that silanes are probably not exclusively grafted on silicate phases in cement as initially assumed. Further experimental evidence will be presented within this Chapter supporting this statement.

Silane modified cement obtained by liquid phase deposition and excess solvent removal

### 5.2.3 Conclusions on adsorption

The adsorption of three different silanes from ethanol and toluene on cement has been investigated. The adsorbed fraction has been calculated as the difference between the initial dosage and the excess that remained in solution.

It was found that for a given silane agent (APTES) and a given solvent the adsorption depends on its dosage. A step-like evolution displaying a plateau region has been reported regardless of the solvent used. However, the adsorbed amounts were always higher in the case of ethanol than toluene. The effect was related to their different nature. The calculated surface coverage for plateau region corresponds to ten and five layers depending on whether experiments have been carried out in ethanol or toluene. However, TEM images showed that the silanes are not homogeneously spread onto the surface.

In addition, the adsorption was found to be strongly dependant on the nature of the silane agent. From experiments carried out in ethanol it was found that silanes adsorb in the following order:

APTES >GTO>AEAPTMS (5-5)

Furthermore, it appears that silanes are not entirely adsorbed on silicate phases (in cement). This was inferred based on the comparison of adsorbed amounts on cement and on tricalcium silicate.

## 5.3 Characterization of modified products

The aim of the work presented in this section is to characterise the modified cement system prepared according the procedure described above. The investigations will focus on evaluating the hydration kinetics and the viscoelastic properties of cement paste.

The first part outlines the techniques used to follow the evolution of the modified cement in terms of heat development and of rheological properties. A brief overlook

Silane modified cement obtained by liquid phase deposition and excess solvent removal

will be taken at each method's principle, experimental set-up and operational conditions.

This is followed by the results section where the most important findings will be highlighted and discussed.

### **5.3.1 Techniques used for investigating the properties**

#### **5.3.1.1 Techniques used for investigating the hydration kinetics**

Calorimetry is one technique which will be used extensively to follow hydration evolution. In addition to isothermal calorimetry which has been presented and discussed in Chapter 4, several results collected in semi-adiabatic mode will be presented. Therefore a brief characterisation of the technique will be given below.

##### **Semi-adiabatic calorimetry**

This method has been used alternatively for monitoring the hydration kinetics. The main difference and the advantage of using it, compared to isothermal measurements, is that it accounts for changes in reactivity of cement with changing temperature and therefore it reflects the conditions in the real structure where temperature changes continuously[104].

The semi-adiabatic calorimeter is essentially made up of thermocouple and a chamber which is a vessel filled with an insulating material to slow down the rate of heat loss (Figure 5-8).

Silane modified cement obtained by liquid phase deposition and excess solvent removal

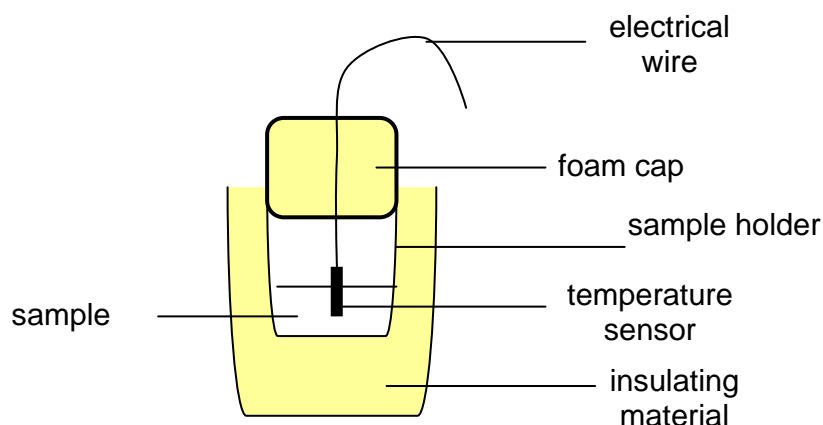


*Figure 5-8. Schematic representation of a semi -adiabatic calorimeter cell: insulated vessel containing the sample under measurement and the temperature sensor.*

26.92 g of cement modified by liquid transfer of silane (subsequent of solvent and excess silane removal) and 8.08 ml water were mixed in a two step sequence (1 min at low speed - 300 rpm followed by 2 min at high speed mixing – 1500 rpm), using a Heidolph mixer. 15 ml of cement paste (approximately 31.07 g paste, w/c =0.3) were collected from each mixed paste batch and were transferred to the measuring cell immediately after mixing. Measurements were performed on cement pastes with and without admixture. Only APTES modified cement was used. The silane to cement concentrations varied between 0.1-7%.

Temperature difference measurements were recorded between the sample and the reference. Hard cement paste was used as reference material and was placed in a similar insulated vessel as the one containing the sample under investigation. The entire experimental set-up was placed into a climate controlled room where temperature was kept at  $22 \pm 2$  °C.

## **Electrical conductivity**

### **A. General considerations**

Electrical conductivity is a quite simple and efficient method used to follow up the hydration kinetics compared to isothermal calorimetry. This is because it allows investigating the nucleation and growth of cement hydrates through the evolution of

Silane modified cement obtained by liquid phase deposition and excess solvent removal

the concentration of the main ions in solution. Diluted solutions (L/S=250) are considered because ions have higher mobility and changes are more easily detected compared to concentrated solutions, like pastes for example (L/S=0.3). Water and lime saturated solutions are regularly used as dissolution media. The latter is preferred when there is the need to simulate the conditions from paste interstitial solution.

Consider now one mol of tricalcium silicate suspended in water. Initially, its surface hydroxylates fast and then it dissolves and releases calcium, silicate and hydroxyl ions in solution. The solution's electrical conductivity is given by the expression:

$$\sigma = [Ca^{2+}] \lambda_{Ca^{2+}} + [OH^{-}] \lambda_{OH^{-}} + [H_2SiO_4^{2-}] \lambda_{H_2SiO_4^{2-}} + [H_3SiO_4^{-}] \lambda_{H_3SiO_4^{-}} + [CaOH^{+}] \lambda_{CaOH^{+}} \quad (5-6)$$

Where:

$\sigma$  is the electrical conductivity

$\lambda_x$  is the activity of the species x

Because of low level concentrations in silicate ions compared to calcium and hydroxyl their contribution can be neglected. Similarly, the one coming from  $CaOH^{+}$  ions can be discarded because of low species mobility. Thus, the electrical conductivity of the liquid phase can be rewritten as:

$$\sigma = [Ca^{2+}] (\lambda_{Ca^{2+}} + 2\lambda_{OH^{-}}) \quad (5-7)$$

This indicates that the solutions' electrical conductivity is directly proportional to the calcium ions concentration in solution. This provides information on the hydration advancement. As cement is mainly made up by silicate phases (approximately 80 %), following the evolution of electrical conductivity over time gives information on the cement hydration advancement.

Silane modified cement obtained by liquid phase deposition and excess solvent removal

Figure 5-9 shows a typical example of an electrical conductivity curve evolution over time for cement in diluted suspensions ( $L/S=250$ ). Lime saturated solution has been considered as dissolution media.

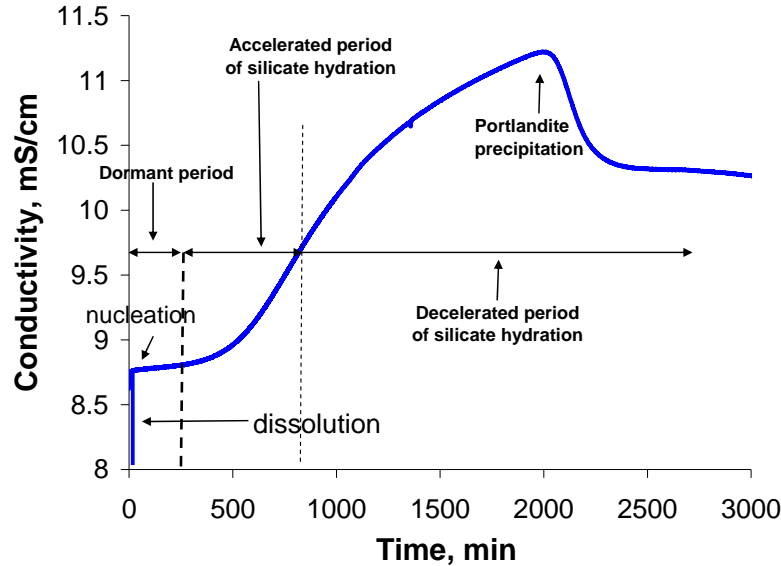


Figure 5-9. Evolution of electrical conductivity over time for cement in diluted suspensions ( $L/S=250$ ). Lime saturated solution [ $Ca^{2+}$ ]=22 mmol/L) was chosen as dissolution media .

Immediately after cement enters in contact with the dissolution media, ions are released in solution. As a result, the electrical conductivity curve displays a sharp increase. After several minutes, the rate of dissolution decreases and hydrates nucleate. This leads to a flattening of the curve. Then, nuclei start to grow and the raise in conductivity curve marks the start of the acceleration period for cement hydration. Simultaneously, cement dissolution continues and more calcium ions are released into the solution. C-S-H growth changes from free to diffusion controlled and a change in the curves' slope marks the deceleration period. The excess of calcium, not consumed by C-S-H precipitation accumulates in solution. Ultimately, Portlandite precipitates as the solution reaches its maximum supersaturation degree. The phenomenon is associated with a sharp decrease of the curve over time.

Silane modified cement obtained by liquid phase deposition and excess solvent removal

It must be noted that, for experiments carried out in water the curve significantly shifts downwards. In addition, portlandite precipitation may appear after longer periods of time or may never occur depending on the experimental conditions. An increase in L/S ratio results in longer times before Portlandite precipitates.

## B. Experimental set-up

All measurements were performed in diluted suspensions ( $L/S=250$ ) in a temperature controlled cell [105]. The experimental set-up consisted in a 20°C thermoregulated cell constantly connected to nitrogen flow to avoid solution carbonation, an electrode, a conductimeter and a computer assisted device for data recording. The electrode was calibrated in KCl solution tempered at 23° C, previously to each measurement.

0.8 g of cement powder were introduced into the measuring cell containing 200 ml of liquid and mixed with a magnetic stirrer. Both water and lime saturated solutions (22mmol/L) were considered as dissolution media. Saturated lime solutions were obtained by mixing freshly decarbonated lime with water. For the latter case, a second electrode calibration was carried out in lime solution. A schematic illustration of the measuring cell is presented in Figure 5-10.

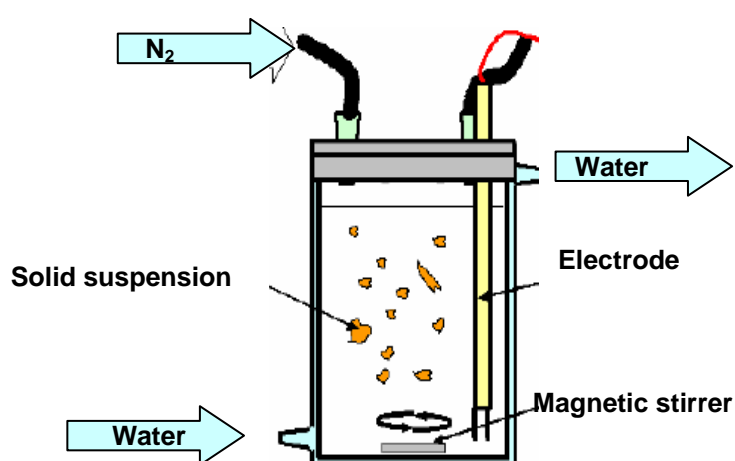


Figure 5-10. Schematic illustration of a thermostated cell used in electrical conductivity measurements (reproduced from [105]).



Silane modified cement obtained by liquid phase deposition and excess solvent removal

### **ICP-AES spectrometry**

This method is highly effective for studying how hydration kinetics of cement is affected by organic admixtures. This is because it offers the possibility to detect changes in the dissolution process at the very early stages of hydration.

An Inductively Coupled Plasma-Atomic Emission Spectroscopy (ICP – AES) Vista Pro spectrometer from Varian was used to monitor the evolution of several ions concentration over the first 30 minutes of reaction. A 200 ml cell containing the suspension under investigation (dissolution media –water or lime - and the cement powder with and without silanes) was connected directly to the spectrometer.

Experiments were carried out at liquid to solid ratios of 250 and 50 000. The cell was equipped with a filter (0.1  $\mu\text{m}$ ) to prevent solid particles from going into the analysing chamber. The solution was constantly stirred and was pumped towards the analysing chamber, where small quantities of liquid were frequently qualitatively dosed. The remaining parts were redirected back into the cell. The overall liquid consumption over the timescale of the experiment is rather small and thus does not lead to significant errors.

#### **5.3.1.2 Techniques used to investigate viscoelastic properties**

##### **Basics of rheology**

Rheology is ‘the science that studies the deformation and flow of matter’ (Eugene Cook Bingham), which means that it is concerned with relationships between stress, strain, rate of strain and time [106]. Restrictively, it deals with relations between force and deformation.

For a better understanding of the outlined results it is useful to first start by looking at some fundamental concepts and several types of materials responses when subjected to stress or strain.

Silane modified cement obtained by liquid phase deposition and excess solvent removal

Concerning flow, let us imagine two parallel planes from a liquid of equal areas  $A$ , separated by a distance  $dx$  and moving in the same direction, but at different velocities  $v_1$  and  $v_2$  (Figure 5-11).

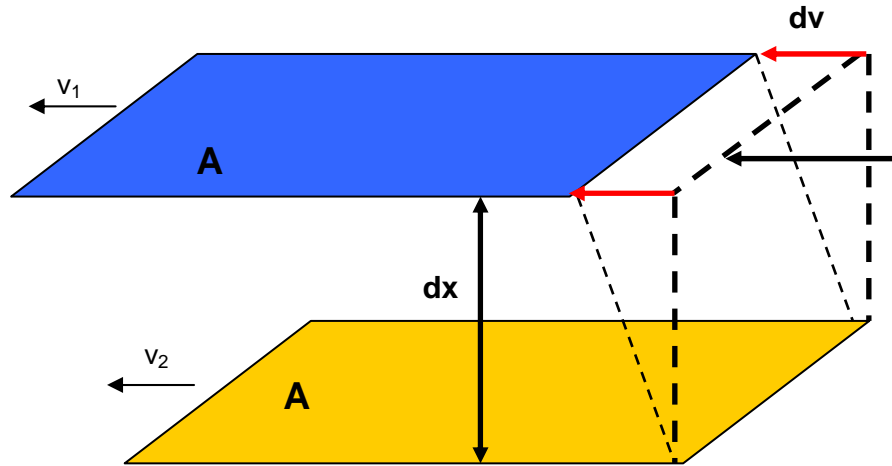


Figure 5-11. Schematic representation of two parallel planes of equal areas  $A$ , moving parallel to each other but at different velocities.

The adjacent movement of the layers is called **shear** and is a measure of the force required to cause this movement. Newton assumed that the force required to maintain constant the difference in speed ( $dv$ ) was proportional to the velocity gradient ( $dv/dx$ ). The mathematical expression for this scenario is:

$$\frac{F}{A} = \eta \frac{dv}{dx} \quad (5-8)$$

The term  $\frac{F}{A}$  indicates the force per unit area required to produce the shear action. It is known as the **shear stress**,  $\tau$  and defines the case when the force is distributed parallel to the surface, unlike normal stress which refers to the situation when the force is normal to the surface.

The deformation induced in the material by the shear stress is called **shear strain** and it is defined by the following equation:

Silane modified cement obtained by liquid phase deposition and excess solvent removal

$$\gamma = \frac{dv}{dx} \quad (5-9)$$

The ratio of shear stress to shear strain gives the shear modulus, which describes the tendency of an object to shear (deform in shape at constant volume) when acted upon is:

$$G = \frac{\tau}{\gamma} \quad (5-10)$$

Depending on the materials response to stress we can distinguish between elastic, Newtonian and non-Newtonian behaviour.

### **Elastic Hooken behaviour**

The simplest case, the **elastic behaviour** defines the capacity of a material (solid body) to completely recover once the load is removed. The material obeys Hook's law described by equation ( 5-11), which shows that the deformation is proportional to the load applied, or stated more generally, the strain is proportional to the stress [106]. Equation (5-10) becomes:

$$\tau = G\gamma \quad (5-11)$$

Where:

G is the elastic modulus, a constant of proportionality in this case.

### **Newtonian behaviour**

A fluid for which the shear stress is linearly proportional to the rate of shear is said to have a **Newtonian behaviour**. The viscosity does not dependent on the rate of shear. Newton's law describes this type of ideal viscous fluid equation (5-12):

Silane modified cement obtained by liquid phase deposition and excess solvent removal

$$\tau = \eta \dot{\gamma} \quad (5-12)$$

### **Non-Newtonian behaviour**

Non-Newtonian fluids do not have a well defined viscosity. It depends both on the shear rate at which it is measured and on the ‘shear history’.

Several mathematical formulas have been developed to characterize the flow behaviour of such materials lying in between the extreme classical Hooke solid and the Newtonian viscous liquid, all indicating the existence of a yield stress. It is known that when subjected to load, materials can exhibit elastic behaviour (solid-like), viscous behaviour (liquid-like) or a combined behaviour termed visco-elasticity. The minimum stress applied to a material marking the transition solid-like to liquid like behaviour is called yield stress.

Most popular equations that have been used to describe this situation are the Bingham model [107], Casson [108], and Herschel-Buckley (sometimes called generalized Bingham) models [108] :

$$\tau = \tau_0 + \mu_B \dot{\gamma} \quad \text{Bingham} \quad (5-13)$$

$$\sqrt{\tau} = \sqrt{\tau_0} + \sqrt{\mu_C \dot{\gamma}} \quad \text{Casson} \quad (5-14)$$

$$\tau = \tau_0 + \mu_{H-B} \dot{\gamma}^n \quad \text{Herschel-Buckley} \quad (5-15)$$

Where

$\tau_0$  is the yield stress,

$\mu_B, \mu_C, \mu_{H-B}$  are the intrinsic (plastic) viscosities.

Silane modified cement obtained by liquid phase deposition and excess solvent removal

### **Rheology of viscoelastic fluids – cement based systems**

Cement paste is one eloquent example of materials that at low shear rates exhibit solid- like behaviour, whereas at high shear rates liquid-like behaviour.

Low amplitude oscillatory shear have been reported by Schultz [109] to be a suitable method of studying the rheological behaviour of viscoelastic materials such as concentrated dispersions of solid in liquid. Cement based-systems were reported to have rather a very limited linear viscoelastic domain (region where the material is able to recover elastically and the paste behaves as a solid)[109, 110]. In what follows we refer to this linear viscoelastic domain as LVD. At larger amplitudes a structural breakdown takes place and the paste behaves like-liquid. In terms of deformation, the LVD is limited by a critical strain beyond which the structure is destroyed.

The critical strain for cement pastes reported by Schultz [109] was approximately  $10^{-4}$ . Results in the same range of magnitude were confirmed by Nachbaur [110]. Zukoski [111] associated the small critical strain with the nature of the forces existing between particles, which in the case of cement pastes are strong interparticle attractions.

When a sinusoidal oscillatory strain at low amplitude and constant frequency [109], is applied to a material the resulted shear stress (sinusoidal as well and  $\delta$  phase shifted), provides information on its viscoelastic behaviour. This is characterized by the complex number, named complex modulus given by the equation (5-16):

$$G^* = \frac{\tau}{\gamma} \quad (5-16)$$

Where:

$$\tau = \tau_0 \cos(\omega t + \delta) \quad (5-17)$$

$$\gamma = \gamma_0 \cos(\omega t) \quad (5-18)$$

Silane modified cement obtained by liquid phase deposition and excess solvent removal

Where:

$\omega$  is the angular speed,

t is time,

$\gamma_0$  is the maximum strain amplitude

$\delta$  is the out-of-phase angle between stress and strain

The complex modulus defines the total energy required to deform the material and sums up the storage modulus and the loss modulus as follow:

$$G^* = G' + iG'' \quad (5-19)$$

Where  $G'$  is the storage modulus or the elastic component, reflecting the ability of the material to elastically store energy.  $G''$  is the loss modulus which is proportional to the amount of energy lost to viscous dissipation.

Consequently, if:

$G'' = 0$ , the material is an elastic Hooken solid ( $G^* = G'$ )

$G' = 0$ , the material is a viscous Newtonian liquid ( $G^* = G''$ )

However, most real fluids exhibit an intermediate behaviour (both  $G' \neq 0$  and  $G'' \neq 0$ )  
As a result, when  $G' \gg G''$  the material exhibits a solid-like behaviour, whereas  $G'' \gg G'$  defines a liquid-like behaviour.

A representative example is given in Figure 5-12. For cement pastes the transition liquid-like to solid-like behaviour occurs in very short period of time subsequent to mixing. Initially, the fresh cement paste exhibits a liquid-like behaviour, illustrated by higher viscous modulus values ( $G''$ ). In less than 2 minutes, the storage modulus increases rapidly and overtakes the loss modulus, pointing to a material that acts solid-like.

Silane modified cement obtained by liquid phase deposition and excess solvent removal

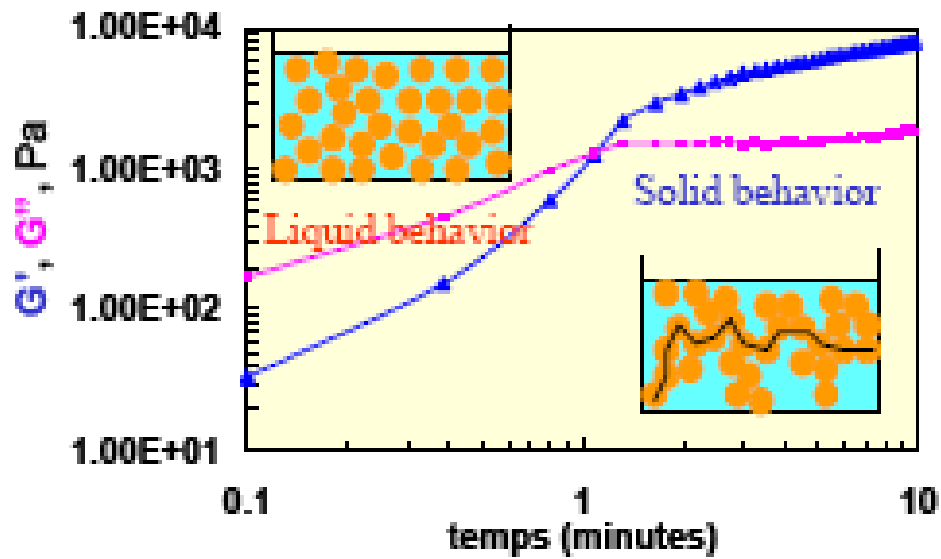


Figure 5-12. Evolution versus time of the viscoelastic properties of cement paste by viscoelastimetry (reproduced from [112]).

Because of the objective of the present study only the results concerning the evolution of the storage modulus are presented and discussed for both neat and silane modified cement pastes.

## Rheological measurements

### A. Rheometer

The apparatus used in this study was a computer-controlled shear strain ARES rheometer from Rheometric Scientific.

The data were collected in dynamic mode (oscillatory) using parallel plate geometry, with a narrow gap (2mm) so that a uniform velocity gradient can be assumed over the separation gap. The surface of the plates has also been serrated (100  $\mu\text{m}$  rugosity) in

Silane modified cement obtained by liquid phase deposition and excess solvent removal

order to avoid wall slippage[113] which is a current source of errors in rheology measurements.

The specimen under testing was a freshly mixed paste, w/c 0.25, prepared according to the procedure described for calorimetry (Section 4.2.1.5), except for having extended the mixing time to 60 seconds to assure complete sample homogeneity. The specimen was hand transferred with a spatula into the measuring position resulting in a disk with a diameter of 6 mm and a thickness of 2 mm. In order to avoid drying of the specimen, water was placed around the specimen creating a water-saturated medium and a bell shaped cover was positioned over the entire measuring area creating an enclosed chamber. Specimen temperature was controlled and maintained at 25 °C by water bath.

A schematic representation of the section containing the specimen under investigation is given in Figure 5-13.

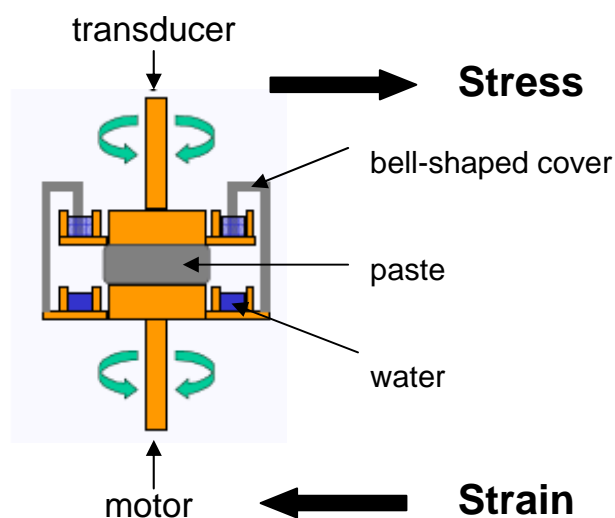


*Figure 5-13. Schematic representation of the parallel plate geometry used in this study and its operational principle: the bottom plate submits the sample to a strain (angular displacement) with the result that the top one tends also to turn because of the viscous drag exerted by the sample. The torque to prevent it from turning is measured and converted into stress.*



## **B. Tests performed in oscillatory mode**

As mentioned above, oscillatory mode is a suitable technique for rheological investigations of cement based systems provided that the amplitude is kept in the low range. In addition, this technique is particularly interesting for our study since it allows us to evaluate possible differences in rheological behaviour of silane modified cement pastes with respect to the neat cement paste. The testing protocol included two types of tests namely a strain sweep test and a time sweep test.

First, the strain sweep was performed to determine the LVD for each sample. It consists in submitting the sample under measurement to increased strain amplitude while keeping the frequency constant. Strain amplitudes from  $10^{-6}$  to  $10^{-1}$  and constant frequency amplitudes of 1Hz were investigated. The end of the LVD is characterized by a critical strain which was determined for each sample.

Below the critical strain the moduli are independent of the strain applied and the structure is able to recover elastically. The material behaves as a solid and the measurement does not disturb the material's microstructure. Above the critical strain the particles are not able to recover elastically, the structure loses its integrity and as a consequence the moduli decay as a function of the strain applied. [109].

Second, in order to monitor the consolidation of the structure, time sweep tests were performed. They consist in submitting the specimen to a constant strain ( $10^{-4}$ ) and to a constant frequency (1Hz). It is important to notice that the chosen strain value is inferior to the critical strain value previously determined to avoid damaging the microstructure.

It must be noted that immediately after pastes' positioning in the measuring spot and before starting one of the tests described above, all specimens were pre-sheared for one minute at high frequencies (10 Hz) and high amplitude strain (0.1) outside of the linear viscoelastic domain. This aimed at breaking-down the flocculated structures

Silane modified cement obtained by liquid phase deposition and excess solvent removal

that are formed in cement pastes in less than 2 minutes after mixing is stopped [112]. Nevertheless, it was a way to ensure similar initial conditions for all measurements.

### **C. Simultaneous calorimetric and rheological measurements**

Rheological properties of cement pastes are complex. On the one hand because the suspension is flocculated and on the other hand because the time dependent chemical reactions alter the liquid phase composition, particle volume fraction and interparticle forces [111].

Simultaneous measurements of hydration rate and rheology on cement paste [114] carried out by Banfill pointed out that additional information on the interactions between chemical changes and rheological behaviour in cement pastes can be gained. Furthermore, attempts to correlate the cement pastes' consolidation phenomenon and their rheological behaviour under the influence of chemical admixtures present in the system have been previously reported [115]. For this reason, this type of investigation was chosen for this study.

In order to do so, we started from the same batch of paste and divided it into two parts: the first was placed into the rheometer while the second was placed into the isothermal calorimeter at almost identical times. Both measurements were carried out at 25°C. This investigation is particularly interesting for this study since it allows, not only to follow in parallel the advancement of reaction and the building up of the structure, but it provides insights on how the silanes change the rheological behaviour and how this may or may not be related to chemical changes taking place.

## **5.3.2 Results**

This section presents detailed experimental evidence on how cement properties are affected by the presence of various silanes adsorbed from different solvents. The study will investigate the changes in hydration kinetics and rheological properties of the modified cements.

Silane modified cement obtained by liquid phase deposition and excess solvent removal

#### **5.3.2.1 Effect of silanes on the hydration kinetics of cement paste**

In this section we present a detailed study of several parameters found to influence the hydration kinetics of silane modified cements prepared subsequently to a liquid phase deposition method followed by solvent removal that contained the unadsorbed silane fraction. In what follows, we will focus our attention on answering and discussing the questions below:

- how does the dosage of silane employed affect the hydration of cement?
- what is the effect of the nature of the solvent used as vehicle media on cement hydration provided that similar silane adsorbed dosages are used?
- what is the effect of the nature of the silane on the cement hydration for equal silane addition levels?
- could the overall retarding effect observed on cement hydration be considered cumulative and result from a direct summing up of effects observed on individual cement phase?

#### **Effect of dosage**

The influence of different adsorbed dosages of silane on cement hydration is given in Figure 5-14. We have chosen to concentrate our study on APTES deposited from ethanol and we have monitored the heat evolution curves for 1.75%, 1% and 0.72% APTES modified cements. Reference cement paste heat flow has been recorded for comparison.

Silane modified cement obtained by liquid phase deposition and excess solvent removal

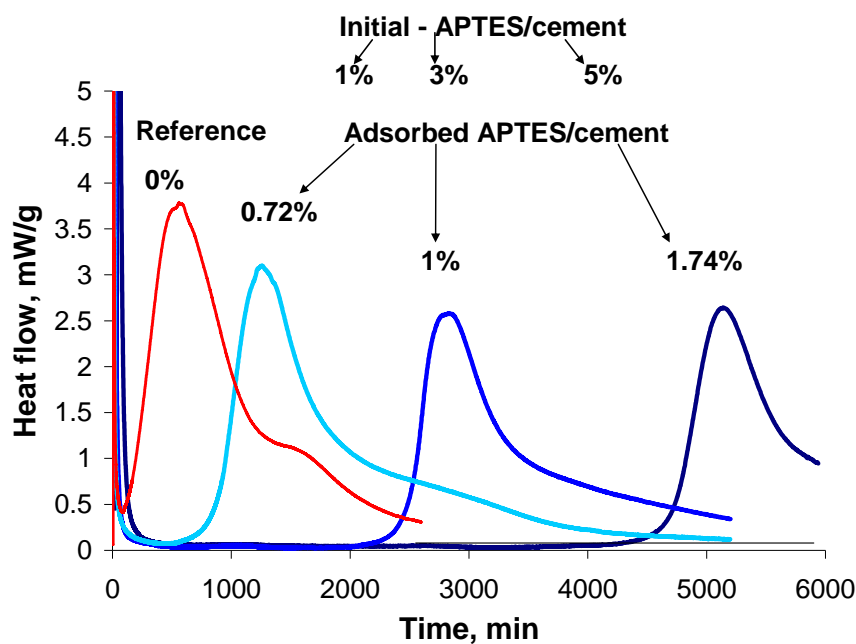


Figure 5-14. Heat evolution curves for different APTES modified cement pastes prepared with a constant  $w/c=0.3$ . APTES was deposited from ethanol. Percentage of silane by weight of cement.

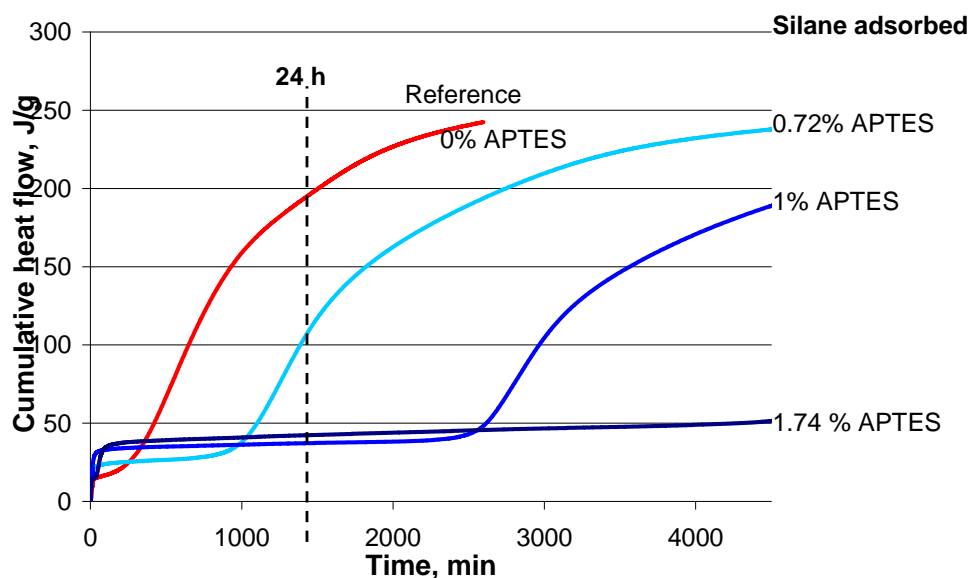


Figure 5-15. Total heat flow curves for different APTES modified cement pastes prepared with a  $w/c$  of 0.3. APTES was deposited from ethanol. Percentage of silane by weight of cement.

Silane modified cement obtained by liquid phase deposition and excess solvent removal

As expected, APTES was found to significantly affect the cement hydration compared to plain paste. The silane does not change the typical profile of the curve, but it has a strong retarding effect. The retardation mainly affects the hydration of the alite phase, illustrated by the right shifting of the main heat peak. Results clearly indicate that an increased dosage of the adsorbed silane extended the induction period from 100 min (plain cement paste) up to 825 min (0.72% APTES) and up to 4715 min (1.74% APTES). Although the maximum rate of heat output wasn't much affected, the total heat release after 24 h of hydration has been reduced by 45% for 0.72% APTES cement paste and by 81% for 1.74% APTES cement paste compared to reference (Figure 5-15). This is because all silane modified cement pastes, showed higher amounts of initial heat release than plain paste. Most probably, the effect is linked to the presence of the silane agent which interfered with the hydration of aluminates and sulphate phases, as it is known that the initial heat release originates in thermal effects associated to these phases.

Similar evolution trends have been found for APTES modified cement pastes, with silane deposited from toluene suspensions. Increased addition levels of APTES lead to stronger retardation of cement hydration and ultimately to a reduced rate of hydration. The results are presented in Annex III.

### **Effect of solvent nature**

So far, we have seen that increased addition levels of adsorbed APTES retards systematically the hydration of cement, regardless of the solvent used as vehicle media. However, the effects appear to be solvent nature dependent. This is illustrated in Figure 5-16, which sums up the previously reported results. The effect on hydration has been evaluated with respect to the length of the induction period. This was derived from calorimetric curves and was calculated as described in Section 4.2.1.5.

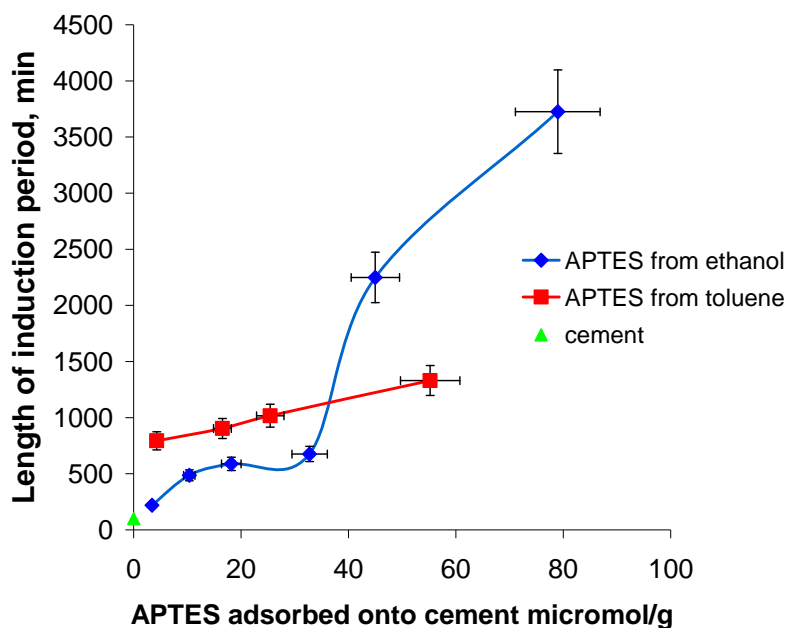


Figure 5-16. Effect of solvent nature used as vehicle media on the hydration of APTES modified cement pastes. Similar concentrations of silane induce different retardation levels on cement hydration.

Using toluene as dispersive media, a clear linear dependency between the fraction of APTES adsorbed to cement and its corresponding retardation levels has been found. Increasing additions of silane lead to a direct proportional increase in retardation of cement hydration. It must be noted that even low dosages (3 to 10  $\mu\text{mol/g}$ ) have a significant retarding effect compared to plain cement paste.

For cements containing APTES deposited from ethanol, the retardation is strongly dependent on the adsorbed silane fractions. The overall evolution indicates a step-like correlation. For low APTES dosages, in the range of 3 to 10  $\mu\text{mol/g}$ , increasing the dosage results in a direct proportional increase of the induction period. In this case, the retardation levels are kept in acceptable limits. This is followed by a plateau region, marked by similar retardation levels obtained upon increasing the concentration of APTES. The end of the plateau occurs for a concentration of APTES/cement of 32  $\mu\text{mol/g}$ . Above this, the curve shows a sharp increase. As a result, the induction periods increase substantially with increasing the silane to cement

Silane modified cement obtained by liquid phase deposition and excess solvent removal

ratio. This results in completely unacceptable induction periods (3725 min for 80  $\mu\text{mol/g}$  of APTES to cement).

Taken together, these results indicate that **similar dosages of APTES induce different retardation levels** on cement hydration depending on the solvent nature used as vehicle media.

In what follows, we report that **different dosages of APTES lead to similar retardation** levels depending on the solvent. The situation is illustrated in Figure 5-17.

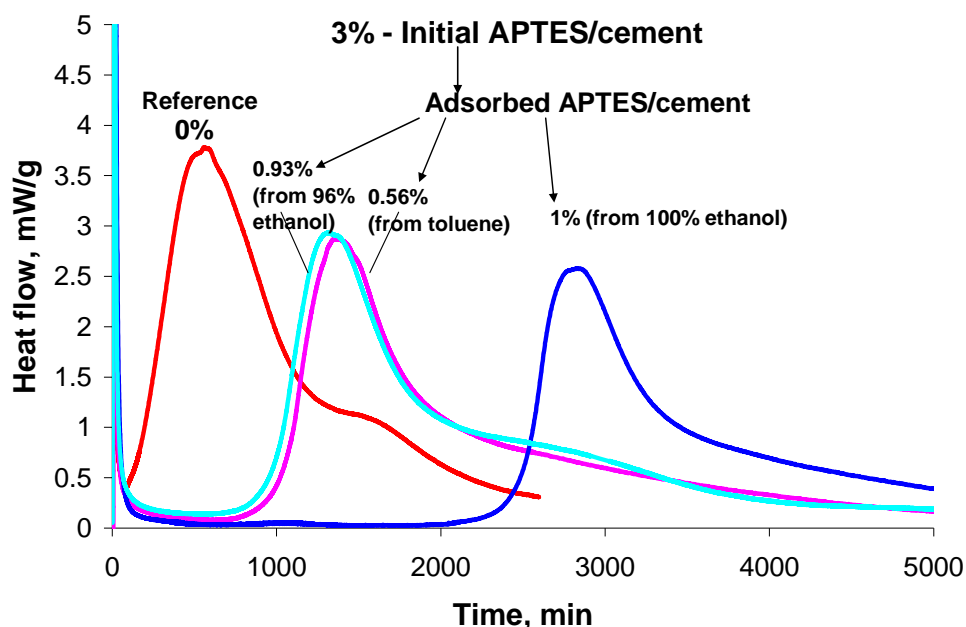


Figure 5-17. Heat evolution curves for APTES modified cement pastes prepared with a constant  $w/c = 0.3$ . APTES was deposited from 100 % ethanol, 100 % toluene and 96 % ethanol. Different dosages of APTES lead to similar retardation levels depending on the solvent's nature used as dispersive media. Percentage of silane by weight of cement.

Comparing the heat evolution curves (Figure 5-17) for APTES modified cements, with silanes deposited from different solvents, we observe nearly similar levels of retardation in cement hydration for different fractions of adsorbed silanes (100%

Silane modified cement obtained by liquid phase deposition and excess solvent removal

toluene and 96% ethanol). Moreover, the values for the maximum rate of heat release are equal. However, after 48 h of hydration, the total heat output was found to be higher for modified pastes having the silane deposited from ethanol (96%) than from toluene, due to the differences in the very early stages of hydration.

Such behaviours are the direct result of dissimilar solvent nature used for adsorption. As discussed, literature reports toluene being successfully used for silane adsorption, leading to chemical bonding between the adsorbate and the adsorbent [99]. On the contrary, it is generally accepted that ethanol promotes hydrogen bonding with the adsorbent and in between the adsorbate molecules. In addition, presence of water traces is reported to have a pivotal role in enhancing physisorption of adsorbate molecules. Indeed, higher adsorption of silane molecules by up to 66% has been found in the case of ethanol 96% compared to toluene.

The fact that nearly equal retarding effects have been observed for different adsorbed fractions implies that there are differences in conformations of adsorbed layers. It seems there is an equal number of covalently bonding sites occupied on adsorbent for both cases. This results in similar retardation levels. In addition, there is a supplementary fraction of physisorbed silane molecules for the case of APTES adsorbed from ethanol 96% connect to the already bonded ones and most probably agglomerate into a non defined shape (lump) that does not affect the hydration kinetics. This idea is presented schematically in Figure 5-18.



## Silane modified cement obtained by liquid phase deposition and excess solvent removal

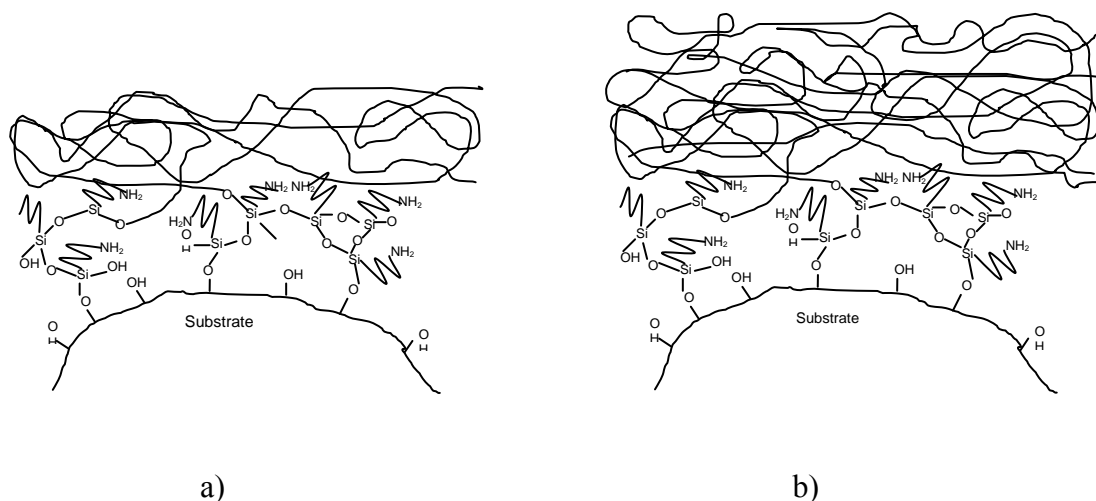


*Figure 5-18. Schematic representation of hypothetical configuration of APTES adsorbed to cement from toluene (a) and ethanol 96% (b). It is suggested that in both cases equal number of covalent bonding to substrate occurs leading to similar retardation levels, despite the fact that different APTES to cement ratios were found to be adsorbed.*

The fact that adsorption from a protic solvent (ethanol) leads highly locally agglomerated species arranged into multilayer has been experimentally confirmed by the TEM investigation presented in Section 5.2.2.1.

Furthermore, after 48 h of hydration, the cumulative heat flow curves indicate higher amounts of heat output for APTES modified cement, with silane deposited from ethanol (96%) than from toluene (Figure 5-19).

Silane modified cement obtained by liquid phase deposition and excess solvent removal

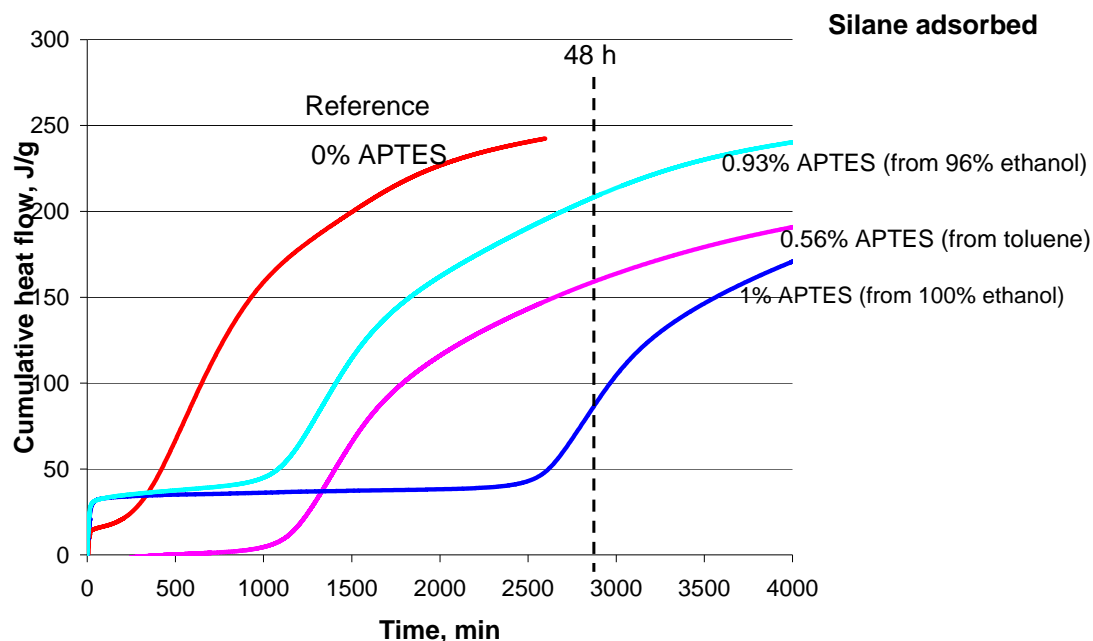


Figure 5-19. Total heat flow curves for different APTES modified cement pastes prepared with a constant  $w/c=0.3$ . Different APTES to cement concentrations lead to similar retardation levels depending on the solvent's nature. However, the overall values for heat release are different depending on the solvent's nature. Percentage of silane by weight of cement.

As it can be observed the differences stem in the initial heat release at very early ages of hydration. It is known that primary contribution to the initial heat release is attributed to aluminates. This means that silane agents affect aluminates reactivity. On one hand, when adsorbed from ethanol either pure or with water traces, there is an increase of heat generated, whereas adsorbed from toluene silanes reduce the amounts of heat generated by the aluminates hydration.

Having seen that APTES always causes retardation of cement hydration, we wish now to know whether the silanes are the entirely responsible for this outcome or additional contributions brought by other factors (such as the solvent used as vehicle media or the ethanol generated during the hydrolysis of silanes) may partially contribute to the observed retardation. In what follows the next two topics will be discussed.

Silane modified cement obtained by liquid phase deposition and excess solvent removal

### Is the solvent used as dispersion media retarding the hydration of cement?

To verify the fact that the retardation issues observed stem exclusively in the addition of silane to cement and are not connected to the solvent used for deposition (even though the solvent had been evaporated after surface functionalisation), the next investigations were considered. Cement powder was separately mixed with i) ethanol and ii) toluene following similar procedures as the ones employed when silanes have been adsorbed to cement, except for the fact that no silane was added. After the solid substrate (cement) has been mixed with the solvents, it was separated by centrifugation, collected and oven cured to evaporate the remaining solvent which could not have been removed in the centrifugation step. After cooling, the samples were hydrated and the heat flow curves were recorded. In Figure 5-20 we report the data collected from the above mentioned measurements and we compared them to the heat flow recorded for cement hydrated in standard conditions, which was not subject to any previous treatments.

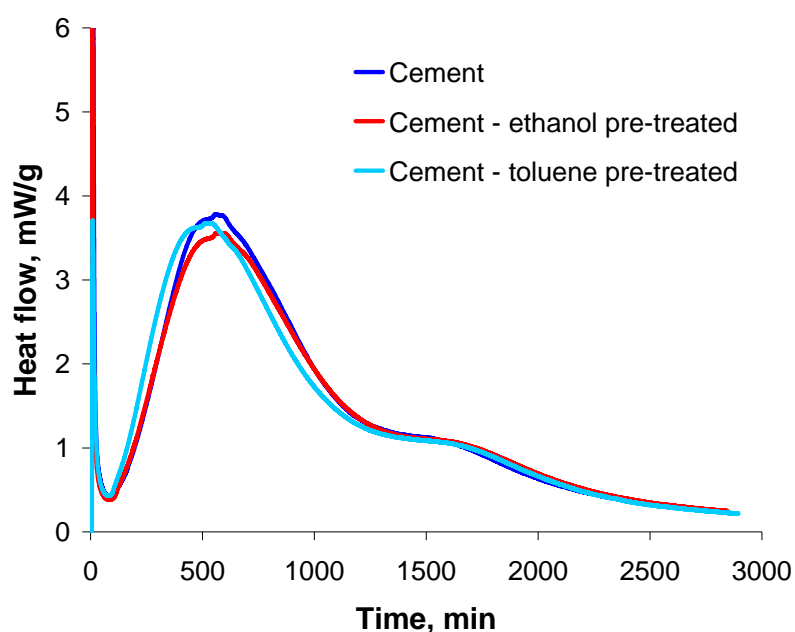


Figure 5-20. Heat evolution curves for plain cement, ethanol pre-treated cement and toluene pre-treated cement prepared with a constant w/c of 0.3. Initially, the solvents were removed by centrifugation. Additional oven curing was applied for entire solvent removal.

The data clearly show that cement pastes prepared from cements which had been subjected to solvent treatment prior to hydration, give similar heat flow curves to cement paste prepared in standard condition. Therefore, it can be concluded that the solvent used as vehicle media does not have any contribution to the changes observed in silane modified cements hydration kinetics.

**Could the ethanol released during the hydrolysis of silane be responsible and/or contributing to the retardation of cement hydration?**

Van der Voort [116] states that the grafting of trialkoxysilane onto inorganic surfaces can never undergo a tridentated form due to steric hindrances. As a result, there are always hydrolysable alkoxy groups that remain unattached to the surface. For our particular case study, it may happen that when water is added to the modified cement powder, the unattached groups undergo hydrolysis, releasing ethanol. The presence of this by-product could be responsible and/or contributing to the changes in kinetics observed for the silane modified cement pastes.

The topic regarding the presence of ethanol, as a by-product of the hydrolysis of aminosilanes molecules, that might be an important source of inhibition on the cement set, has been brought up previously by Svegl et al [84]. They showed that it was not possible to experimentally prove any influence of ethanol on the setting process of cement. However, the assessment of set was done using Vicat techniques, which are known to be oversimplified in interpreting this phenomenon. Therefore, this hypothesis needs further investigation and is discussed below.

A convenient way to answer the above stated question is to calorimetrically investigate how cement hydration is affected by adding similar amounts of ethanol as the ones estimated to be released during hydrolysis of silanes. We chose several concentrations of APTES by weight of cement from 0.1% to 5% and we calculated the amount of ethanol theoretically considered to be generated from a total hydrolysis reaction. Thus, ethanol to cement concentrations were found to be ranging from 0% to 3.12% while ethanol to water concentrations were found ranging from 0% to 10.4% (wt). The experiments have been carried out by adding the corresponding amounts of

Silane modified cement obtained by liquid phase deposition and excess solvent removal

ethanol to water before beginning mixing the liquid to cement powder. The cement pastes have been prepared with a constant w/c of 0.3 and the heat flow curves were recorded using a semi-adiabatic calorimeter. The results are given Figure 5-21.

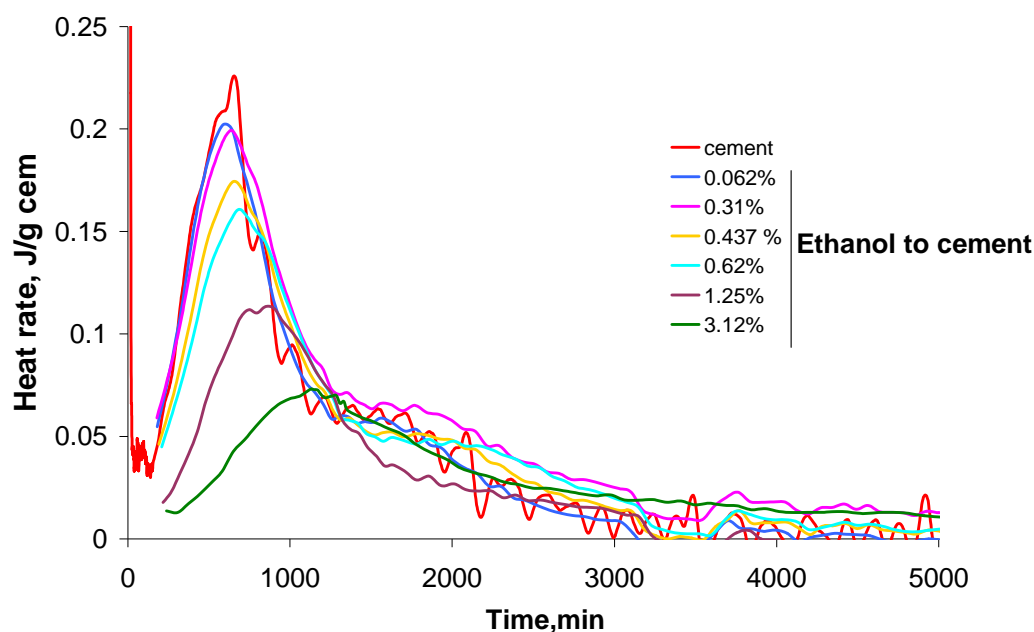


Figure 5-21. Effect of ethanol on hydration of cement. The ethanol was added to water before beginning of mixing.

The results indicate that increasing additions of ethanol lead to a decreased rate of heat outputs during the accelerating period. Consequently, the maximum of the main heat peak release is right shifted. In addition, a decrease in the maximum rate of heat output by up to 75% for the highest ethanol addition level was observed compared to the plain paste.

Also, it must be noted that the presence of ethanol induced bleeding in all specimens. The undesired effect became significant for higher addition levels of ethanol.

To answer to the question addressed above (Could the ethanol released during the hydrolysis of silane be responsible and/or contributing to the retardation of cement hydration?), we plotted the time corresponding to the maximum rate of heat release from the calorimetric curves against ethanol concentration with respect to cement for

Silane modified cement obtained by liquid phase deposition and excess solvent removal

(i) cement hydration recorded in the case of direct ethanol addition and (ii) for APTES modified cement (assuming that ethanol is generated from APTES hydrolysis). The results are given in Figure 5-22.

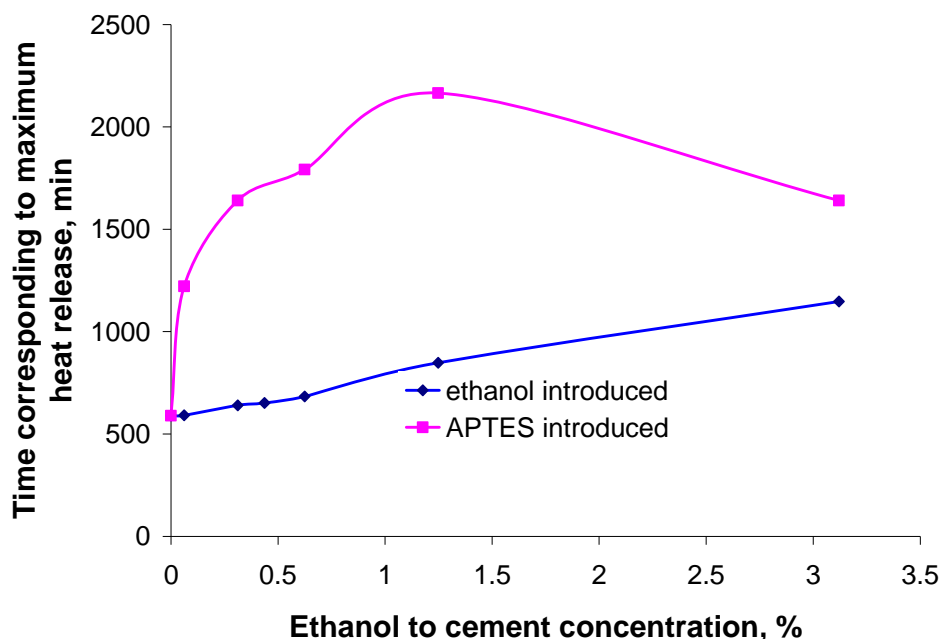


Figure 5-22. Effect of direct addition of ethanol (lower curve) and of the quantity of ethanol assumed to be released from the hydrolysis of APTES (upper curve) on the cement hydration.

Data clearly show that ethanol has indeed a contribution to the retarding effects observed on cement hydration. However, the effect is rather insignificant, in particular for low ethanol dosages.

## Effect of silane nature

### A. Individually silane modified cement

We recall that the adsorption of silanes to cement from a liquid phase is a process depending on the silane agent nature. We found that starting from equal initial dosages of silane to cement the adsorbed fractions are different. The following series has been found to describe their affinity for the substrate:

The data concerning the adsorption behaviour has been presented and discussed in Section 5.2.2.3.

Now, we want to evaluate the effect of silane nature on cement hydration. This assumes comparing the heat evolution over time for modified cement pastes with equal adsorbed silane to cement concentrations. To achieve this, heat flow data has been recorded for various concentrations of APTES, GTO and AEAPTMS modified cement pastes. From the calorimetric curves the extent of the induction period was determined, as described in Section 4.5.2.1., and plotted against the adsorbed silane dosage. The results are reported in Figure 5-23.

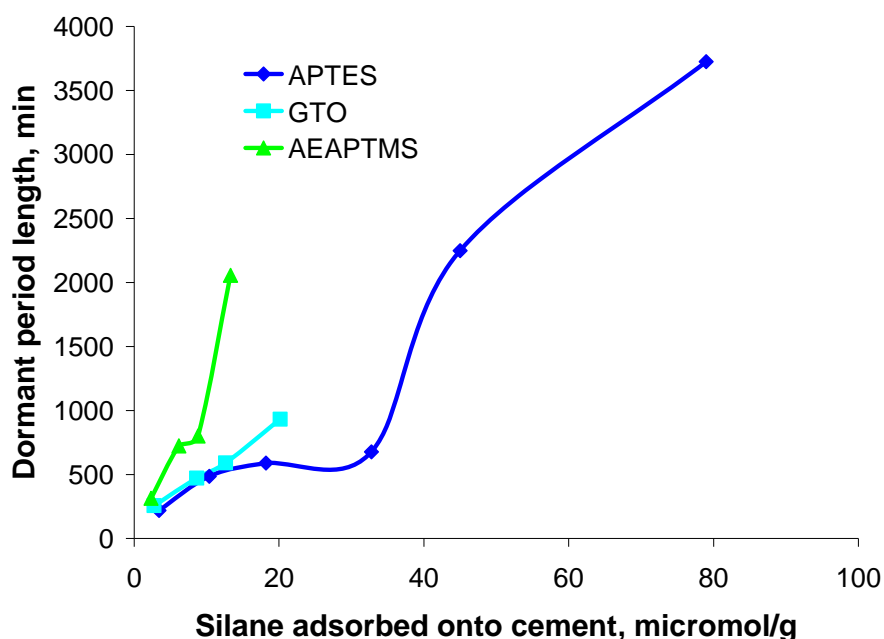


Figure 5-23. Effect of silane nature on the hydration kinetics of cement. The induction period was determined graphically, as described in Section 5-23.

For equal concentrations of adsorbed silane to cement, AEAPTMS has the strongest effect on hydration indicated by the longest induction periods. In the case of low addition levels, GTO and APTES give similar retardation of cement hydration. Above

Silane modified cement obtained by liquid phase deposition and excess solvent removal

a certain concentration (12  $\mu\text{mol/g}$ ), the effect on cement hydration becomes dependent on their nature.

In addition, APTES gives a step-like dependency of retardation versus dosage, displaying a plateau region up to concentrations of 32  $\mu\text{mol/g}$ . This is followed by a sharp increase of the slope indicating that small adsorbed amounts induce significant retardation levels. On the other hand, GTO's impact on cement hydration shows a well defined linear correlation retardation-dosage, upon increasing the latter.

Results obtained highlight that the nature of silane is key factor in the hydration process. For equal adsorbed silane to cement ratios, the impact on cement hydration can be qualitatively described by the following series:

$$\text{APTES} < \text{GTO} < \text{AEAPTMS} \quad (5-21)$$

It must be noted that the series above is the reverse order pattern describing silanes affinity for the substrate. This observation is extremely surprising. Moreover, it raises questions on how silane agents displaying low substrate affinity have actually the strongest influence on hydration. A reasonable answer to be given is that different retarding effects account for different interactions to the substrate. The strongest retarding effect observed in the case of AEAPTMS is most probably due to stronger AEAPTMS – cement interactions than GTO- or APTMS-cement interactions. These stronger interactions are assumed to be related to a higher extent of covalent bonding to the substrate. Given the fact that all silanes have been adsorbed from experiments using in ethanol, physical interactions are very likely to be found as well for all cases. But it seems that the latter prevails in the case of APTES since the retarding effect on cement hydration is the smallest.

Literature frequently reports retarding effects on cement hydration brought by organic admixtures. Also different mechanisms have been proposed for explaining this [117, 118]. So far, we could not evidence nor conclude which is the mechanism that explains the retardation on cement hydration when using silanes. However, a small number of experimental investigations have been carried out to assess whether silanes limit the dissolution of anhydrous phases or prevent nucleation and growth processes



Silane modified cement obtained by liquid phase deposition and excess solvent removal

of hydrate assemblages. These investigations will be later presented and discussed in this work.

### **B. Effects of blends of individually modified cements**

Up to now, we have seen that regardless of their dosage or of their nature, individually, silanes always induce a retarding effect on cement hydration.

As explained, the final purpose of this work is to improve the mechanical properties by creating chemical bonds among different silane functionalized cements (provided that reactively compatible silanes modified cements are mixed). Because the hydration kinetics is known to have significant consequences on the development of the mechanical properties of the system, in what follows, we look at how blends of individually modified cements affect the heat development in cement pastes.

We chose to investigate the effects on cement hydration for the following blends:

- a) GTO modified cement + AEAPTMS modified cement (Figure 5-24)
- b) GTO modified cement + APTES modified cement (Figure 5-25)

Silane modified cement obtained by liquid phase deposition and excess solvent removal

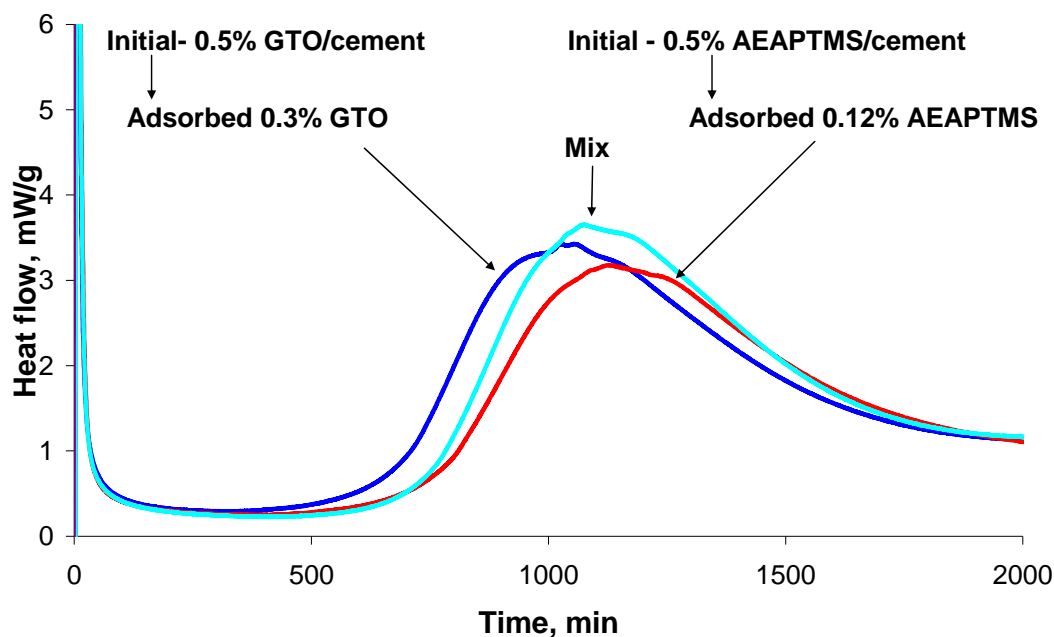


Figure 5-24. Heat evolution curves for GTO modified cement paste, AEAPTMS modified cement paste and their 1:1 by weight blend. All samples were prepared with a constant  $w/c = 0.3$ . Percentage of silane by weight of cement.

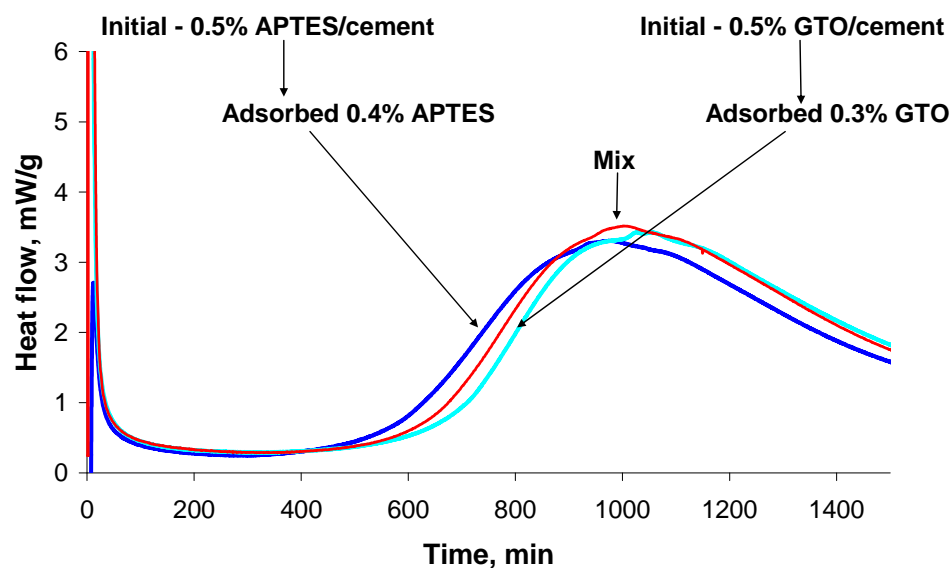


Figure 5-25. Heat evolution curves for GTO modified cement paste, APTES modified cement paste and their mix 1:1 by weight. All samples were prepared with a constant  $w/c$  of 0.3. Percentage of silane by weight of cement.

Generally, in terms of the retarding effect on cement hydration, the systems containing the mix of individually silane modified cements position themselves in between the individual components. This behaviour appears to be surprising, since both silanes act as individual retarders on cement hydration. Moreover, blends give a small increase of maximum rate of heat output, during the acceleration period, with respect to both its constituents. Additionally, a decreased rate of heat output during the onset of the accelerating period of the mix with respect to the first constituent is always noticed. This is probably due to that fact that the hydrates growth process goes slower with respect to the first constituent and faster with respect to the second one. The effects observed are more pronounced for the case of blended AEAPTMS modified cement and GTO modified cement.

In terms of total heat release, blended systems show dissimilarities. In the case of blended GTO & AEAPTMS modified cement, the total heat output has intermediary values with respect to its constituents, once the induction period is over. On the contrary, blended GTO modified cement and APTES modified cement reach the highest degree of hydration throughout the entire time scale of the experiment compared to both individually silane modified cements. These are illustrated in Figure 5-26 and Figure 5-27.

Silane modified cement obtained by liquid phase deposition and excess solvent removal

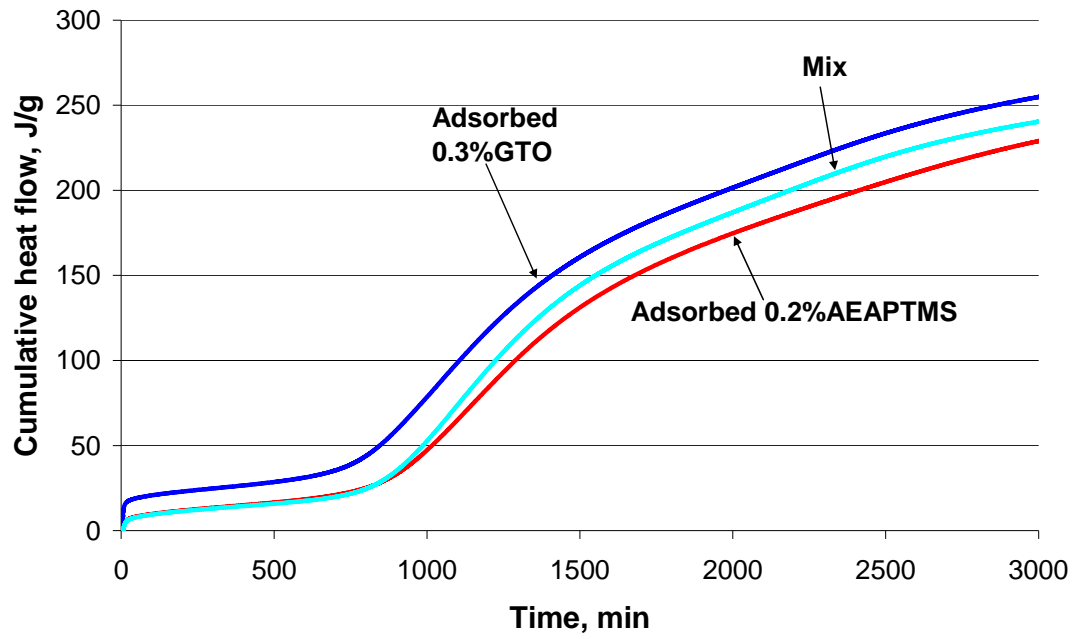


Figure 5-26. Total heat flow curves for GTO modified cement paste, AEAPTMS modified cement paste and their mix 1:1 by weight. Percentage of silane by weight of cement.

Silane modified cement obtained by liquid phase deposition and excess solvent removal

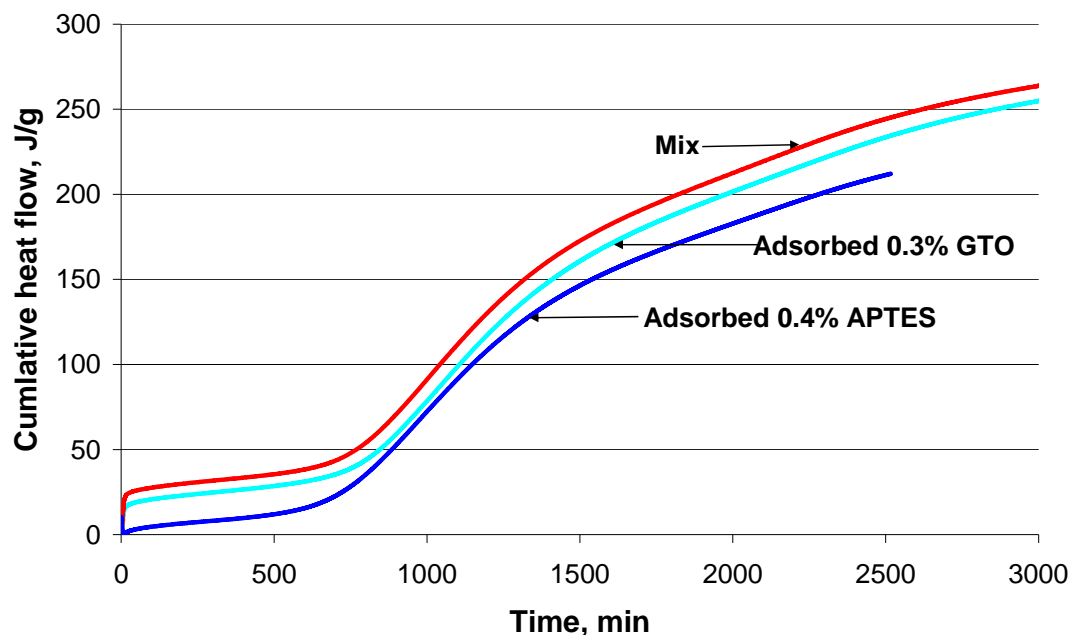


Figure 5-27. Total heat flow curves for GTO modified cement paste, AEAPTMS modified cement paste and their mix 1:1 by weight. Percentage of silane by weight of cement.

### Effect of substrate

We have previously seen that silanes retard the cement hydration. The retardation appears to mainly affect the hydration of the silicate phase, as shown by the right shifting of the main hydration peak. In what follows, we would like to see if the overall retarding effect observed on cement hydration can be considered cumulative and resulting from a direct sum up of effects observed on individual cement phases.

To properly asses such task we have recorded the heat flow curves for silane modified tricalcium silicate pastes and compared them to plain tricalcium silicate paste. The results for APTES modified tricalcium silicate and plain tricalcium silicate pastes are given in Figure 5-28. From the calorimetric curves the time corresponding to the onset of the acceleration period was calculated and compared to the one measured for the case of APTES modified cement. Figure 5-29 reports the heat flow curves for APTES modified cement.

Silane modified cement obtained by liquid phase deposition and excess solvent removal

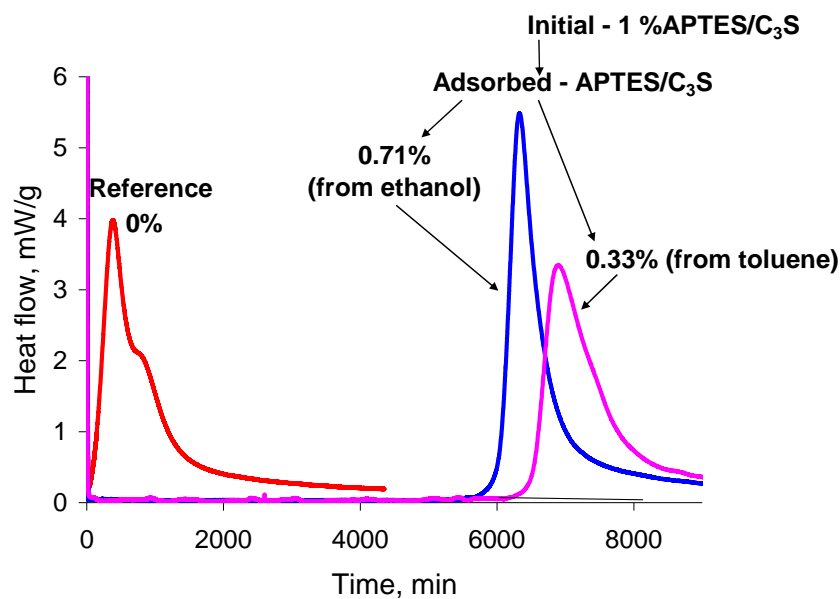


Figure 5-28. Heat evolution curves for tricalcium silicate and APTES modified tricalcium silicate. Percentage of silane by weight of cement.

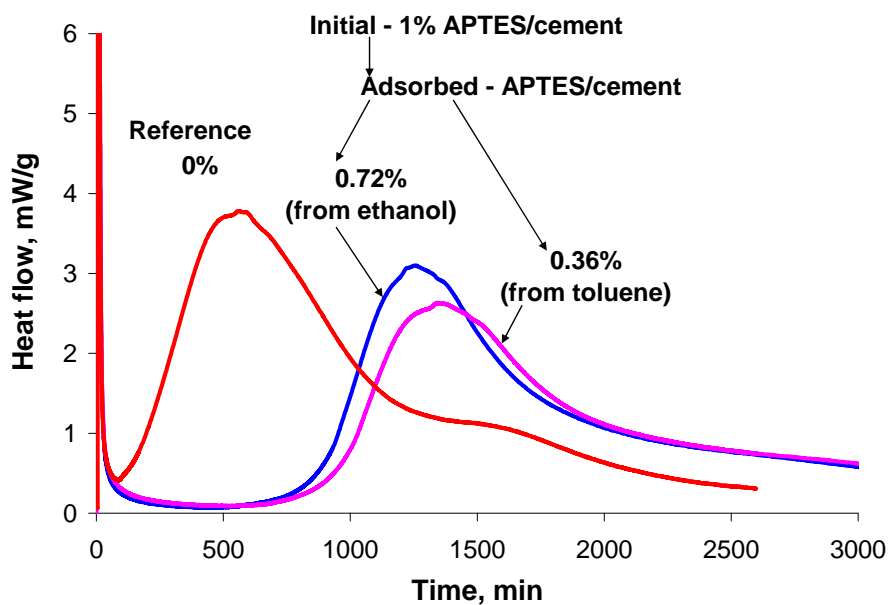


Figure 5-29. Heat evolution curves for cement and APTES modified cement. Percentage of silane by weight of cement.

Silane modified cement obtained by liquid phase deposition and excess solvent removal

Several aspects must be considered before interpreting the results.

First, the cement used in this study contains nearly 80% silicate by weight (59.7%  $C_3S$  and 21.3%  $C_2S$ ). Second, the APTES adsorbed amounts are nearly equal for both adsorbents. Therefore, the ratio of APTES/silicate is greater for the case of cement. This can be summed up in what follows:

1 g cement → 0.8 g silicate phase .....	0.0072 g APTES adsorbed
1 g pure silicate.....	0.0071 g APTES adsorbed

If we now compare the results given in Figure 5.28 and Figure 5.29 certain observations can be made:

On the one hand, in the presence of APTES on cement the onset of the acceleration period starts after 860 min for ethanol deposited APTES and after 920 min for toluene deposited APTES when compared to plain cement paste. On the other hand, in the presence of equal amount of APTES on tricalcium silicate, significantly longer induction periods were found. The onset of the acceleration period is registered after 5900 min for ethanol deposited APTES and after 6450 min for toluene deposited APTES. The results indicate huge discrepancies. We initially assumed that the entire APTES is deposited on the silicate phase. Therefore, we expected stronger retarding effects on cement than on tricalcium silicate, given the higher APTES to silicate ratio in the former case. This is in accordance with our previous findings from the adsorption measurements where experimental evidence first questioned the assumption of silanes being entirely grafted on silicates (Section 5.2.2.4.).

Furthermore, differences are noticed in the maximum rate of heat output. In the case of cement, the maximum of main heat peak is reduced by 16.48% for ethanol deposited APTES and by 29% for toluene deposited APTES compared to reference. For the case of tricalcium silicate, there is an increase by 37.75% in the maximum rate of heat output for the ethanol deposited APTES and a decrease by 15% for toluene deposited APTES compared to reference. These differences could not have been explained so far.

Silane modified cement obtained by liquid phase deposition and excess solvent removal

Equally, the heat flow curves registered for AEAPTMS and GTO deposited onto tricalciumsilicate indicated similar unexpected differences in evolution compared to AEAPTMS and GTO deposited onto cement. The results are given in Annex III.

The implication of these results is that, when deposited on cement, silanes are not entirely grafted on the silicate phase as we initially assumed. However, it appears that a fraction of silane is indeed deposited on the silicate phase from cement. This is proved by that fact that silanes always induce a retarding effect on cement hydration. The extent to which silanes are grafted on the silicate phase in cement could not be quantified so far.

To summarize, the heat development measurements showed that, modified cements and modified tricalcium silicates carrying nearly similar amounts of adsorbate (silanes), behave very differently. Decreasing silane/silicate ratio has been found to extend the induction period by 6.5 up to 7 times depending on the solvent used for deposition, contrary to our expectations. These results imply that silanes are only partially grafted to silicate phases in cement as one always observes a retarding effect on cement hydration. However, further investigations are needed in order to assess the mechanism responsible for the retarding effects. These will be discussed in more detail in later within this chapter.

### **Effects of the silanization methodology**

So far, we have found that silanes adsorbed on cement from an organic solvent retard hydration. Similar effects on cement hydration have been reported when dry blending the constituents (Chapter 4). However, the silanization methodology appears to have a strong influence on the magnitude of the retarding effect. This is discussed in what follows.

When the isothermal calorimetry curves of APTES modified cement pastes with equal silane dosages, from dry blending of constituents and absorbed from liquid phase with solvent excess removal, are compared, both cement pastes show nearly equal dormant periods (slightly shorter for silane modified by dry blending) (Figure 5-30). In



Silane modified cement obtained by liquid phase deposition and excess solvent removal

addition, there is always a higher initial heat release for silane modified cement pastes compared to neat pastes. This strongly argues in favour of silanes aluminates and/or gypsum interactions. However, more work is required in order to fully understand this effect.

In terms of total heat release, the dry blending seems to have less negative influences. This might originate from the fact dry blended silanes disperse worse than in suspension. Because by dry blending silanes tend to cake up and do not reach the same surface coverage as for liquid phase adsorption, the influence on cement hydration is smaller.

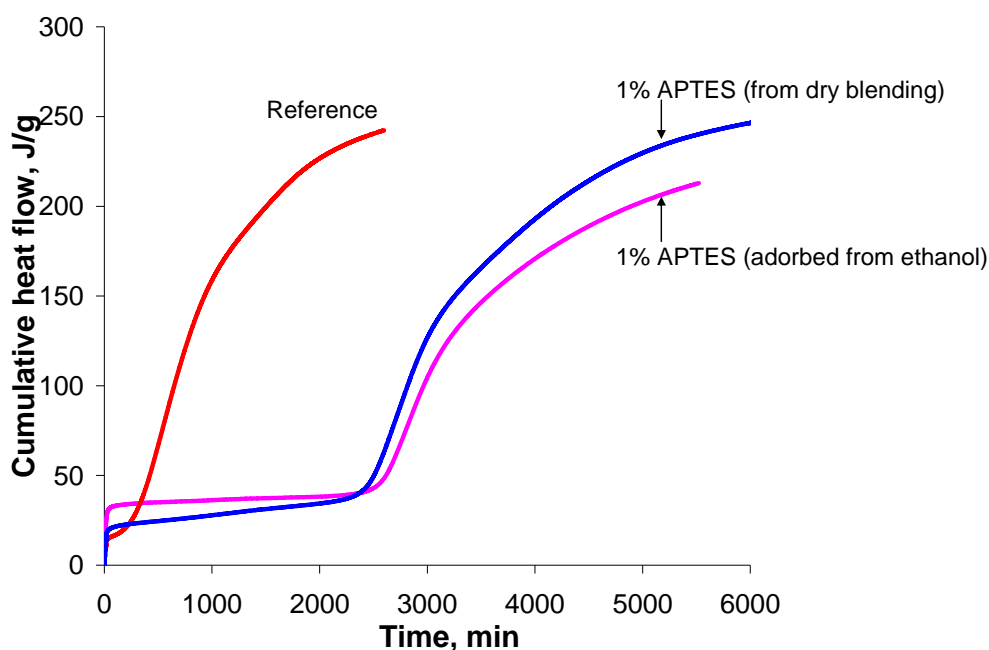


Figure 5-30. Effect of different methodology used for silanization on cement hydration kinetics. Percentage of silane by weight of cement.

Further increasing the dosage of APTES to cement (from 1 to 10 %) does not change the length of the dormant period for modified cement obtained by dry blending, but reduces considerably the rate of silicate hydration (Figure 4.16 b). On the other hand, only a slight increase in the dosage of APTES (from 1 to 1.74%) for modified cements by silane adsorbed from ethanol, doubles the length of the dormant period and does not significantly affect the maximum heat rate release (Figure 5.17). As expected, silanes adsorbed from solvent modify the cement matrix more uniformly as

Silane modified cement obtained by liquid phase deposition and excess solvent removal

compared to the dry blending case. So, there is a higher silane surface coverage with a significantly smaller silane dosage attained when a liquid is used. This affects clearly the number of nucleation sites that are poisoned and thus the onset of acceleration period is shifted to much longer times. As the dormant period comes to an end, the hydrates growth is not much affected. On the contrary, for the dry blending, hydrates growth is substantially similar to the reference, but slightly diminished for the ethanol deposition case. The differences found suggest once more that hydration kinetics is strongly dependent on the silanization methodology.

For the other two silanes considered we do not have enough experimental data for an absolute comparison. Modifying cement by dry blending required a minimum silane dosage of 1 % by weight of cement to reach roughly good naked-eye mix homogeneity. When adsorbed on cement GTO and AEAPTMS give very low adsorbed fractions (maximum 0.3% for AEAPTMS and 0.4% GTO). Thus, an absolute comparison is not possible because the concentration ranges do not overlap. However, huge differences in hydration kinetics are observed between the two cases upon increasing the dosage of silane to cement.

In the case of GTO (Figure 5-31 a), a high increase of dosage results in substantial retardation and reduced silicate hydration when the silane and cement are dry blended. In contrast, when silanization is obtained by adsorption from ethanol, progressively increasing the dosage leads to simply increasing the dormant period without much affecting the silicate hydration (Figure 5-31 b). However, in the latter case the dosages are quite low. But surprisingly, quasi equal retardation levels are observed for higher dosages of cement modified by dry blending (1% GTO) compared to cement modified subsequently to adsorption from solvent (0.4% GTO). This means that both fractions affect the nucleation process in a similar degree, implying that there is an equal number of strong silane to cement interaction in both cases. Most probably this is the chemically bonded fraction. The difference represents silane moieties crosslinked to the chemically adsorbed ones. This reinforces the idea that silanes dry blended to cement tend to concentrate in localized clumps. Adsorption from solvent appears to provide a more homogeneous surface coverage.

## Silane modified cement obtained by liquid phase deposition and excess solvent removal

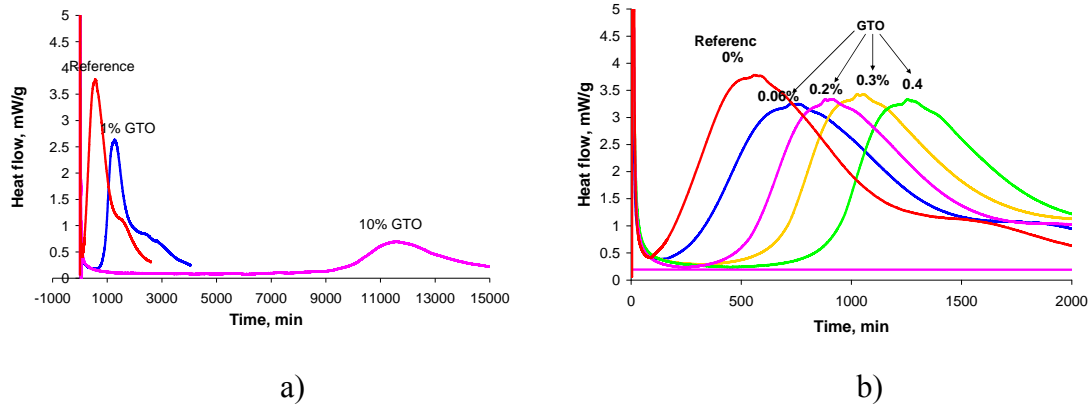


Figure 5-31. GTO dosage effect on the hydration kinetics; (a) silanization obtained by dry blending of constituents (b) silanization obtained from ethanol adsorption.

Similarly, increased dosages of AEAPTMS induce great differences on the hydration kinetics related to the silanization method (Figure 5-32).

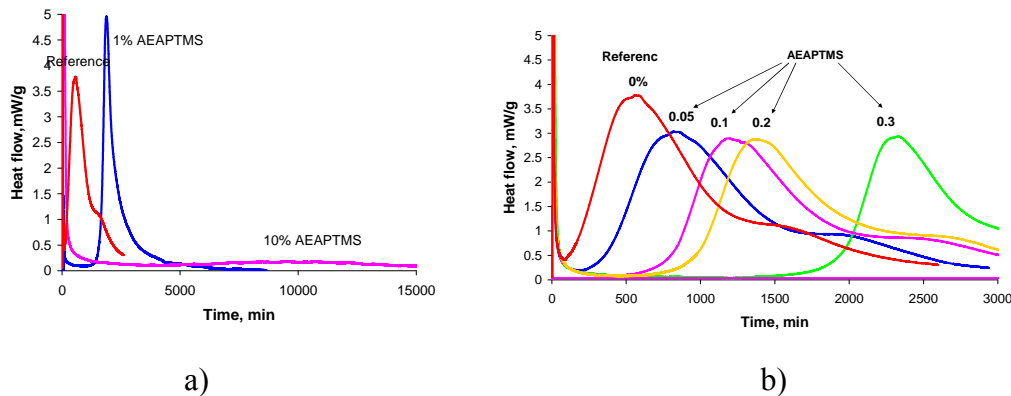


Figure 5-32. AEAPTMS dosage effect on the hydration kinetics; (a) silanization obtained by dry blending of constituents (b) silanization obtained from ethanol adsorption.

The effects observed upon dry blending are in contrast totally with the ones observed for previous silanes and also with the ones observed for modified cement from solvent adsorption. Dry blending favours equal retardation levels for higher silane dosage compared to solvent adsorption (1% AEAPTMS dry blended & 0.3% AEAPTMS adsorbed from ethanol). However, the rate of the maximum heat release is significantly lower for the latter and also the shape of the peak differs very much.

Silane modified cement obtained by liquid phase deposition and excess solvent removal

Generally, AEAPTMS silanization from solvent adsorption does not appear to affect much the broadening of the main heat peak release, whereas dry blending leads to either sharper or much broader peaks depending on the dosage. This clearly points out to the fact that adsorption from solvent modifies the substrate more uniformly.

In conclusion, the results indicate that the presence of silanes strongly affects cement hydration kinetics but effects associated to the nature and dosage of silanes and are strongly dependent on the silanization methodology.

### **Investigations on the retarding mechanism**

After having seen that silanes induce a retarding effect on cement hydration, mainly affecting the alite phase, we will focus next on obtaining more data in explaining this effect. By following the evolution over time of several ion concentrations we can obtain information on how the presence of silanes affects the dissolution, nucleation and growth processes of cement hydrates.

Two experimental techniques namely, ICP-AES and electrical conductivity have been employed in monitoring the evolution of calcium and silicon ions in diluted solutions of silane modified cements. The data have been always compared to results obtained for neat cement, since it is known that organic admixtures may act as inhibitors or catalysers on the dissolution process. Experiments have been carried out both in water and in lime saturated solutions.

Results of measurements performed in pure water, at  $L/S = 50\ 000$  for cement with and without silane are presented in Figure 5-33 and Figure 5-34. The evolution of calcium and silicon ions concentration during the first 30 minutes of hydration indicate similar dissolution rates for cement and ethanol deposited APTES cement. On the other hand, APTES modified cement from toluene seems to lead to higher dissolution rates. So far, we can clearly infer that silanes do not act as inhibitors on the dissolution processes of anhydrous phases. However, we cannot conclude whether the higher dissolution rates observed in the case of toluene adsorbed APTES

Silane modified cement obtained by liquid phase deposition and excess solvent removal

are related to silane dosage or to the nature of the solvent used during the adsorption experiments.

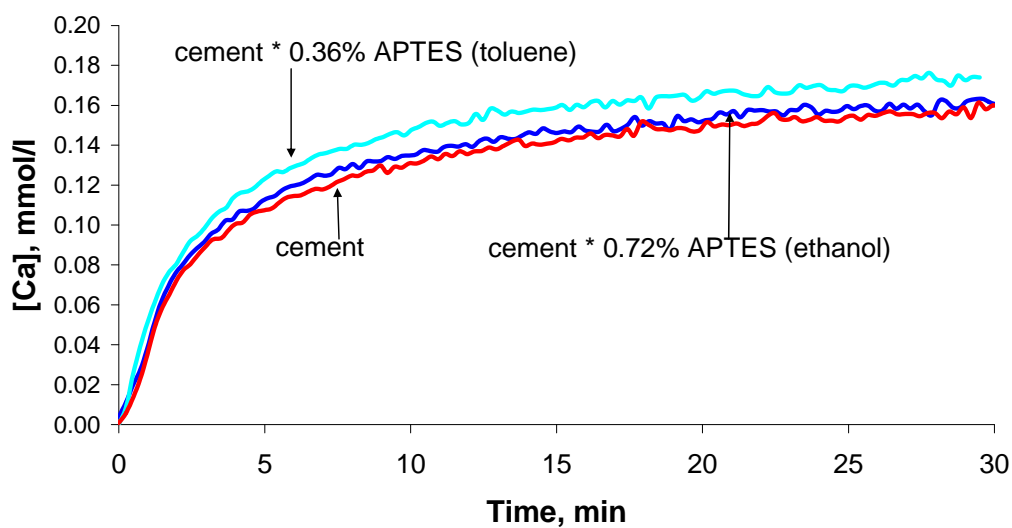


Figure 5-33. Evolution of calcium ions concentration during the first 30 minutes of hydration for cement and APTES modified cement, in pure water,  $L/S = 50\ 000$ .

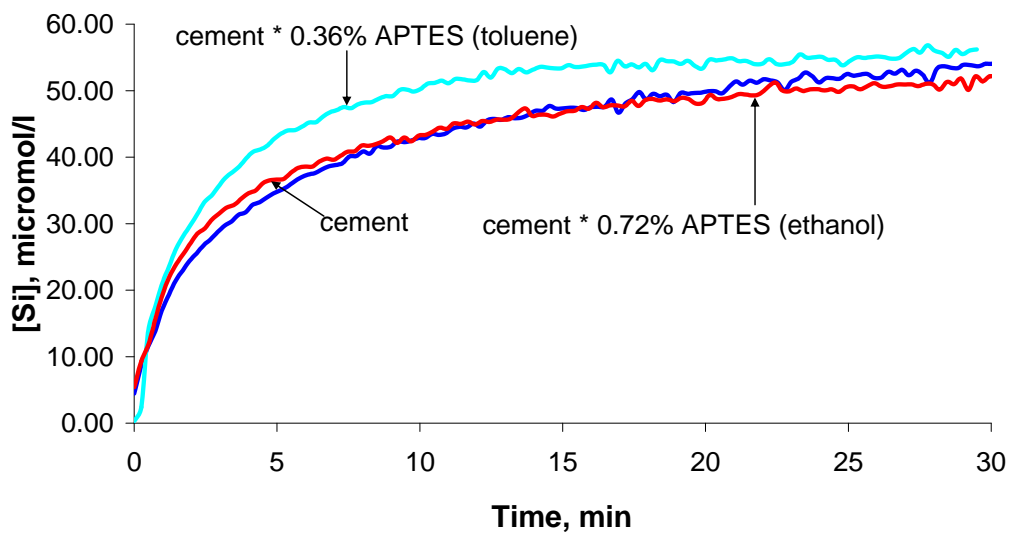


Figure 5-34. Evolution of silicon ions concentration during the first 30 minutes of hydration for cement and APTES modified cement, in pure water,  $L/S = 50\ 000$ .

Silane modified cement obtained by liquid phase deposition and excess solvent removal

Also results from experiments carried out in lime saturated solution indicated that silanes do not block the dissolution processes of anhydrous phases. The results are reported in Annex III.

Next, we decreased the L/S ratio to 250 in order to acquire data on the nucleation process. Similarly experiments have been carried out in water and lime saturated solution. Monitoring the evolution of ions concentration over time has been done using electrical conductivity.

The results from a first experiments carried out in water are presented in Figure 5-35.

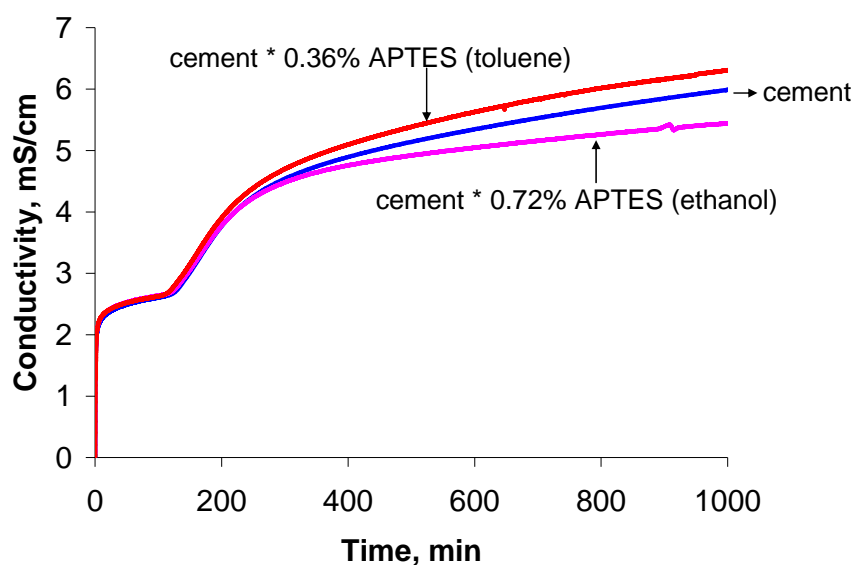


Figure 5-35. Evolution over time of the electrical conductivity during the hydration of cement and APTES modified cement in pure water,  $L/S=250$ .

During the first minutes, all of the conductivity-time curves show perfect overlapping. The pure dissolution processes end for similar conductivities values for all three cements investigated. This indicates that APTES does not affect the dissolution processes of anhydrous phases. This confirms our previous conclusion from the above reported experiments focused on the study of the dissolution process. The length of

Silane modified cement obtained by liquid phase deposition and excess solvent removal

the plateau within the first 100 min of reaction (induction period) is equal for all cements investigated. That means that equal numbers of nuclei are formed in all three cases and ultimately that APTES does not induce any changes in the nucleation process of the hydrates in excess of water.

As the induction period comes to the end, the growth of the hydrates is a bit slowed down for the plain cement compared to modified ones. APTES deposited from toluene seems to favour further growth of hydrates as the conductivity curve raises up first marking the onset of the acceleration period. This clearly shows that APTES does not influence the nuclei growth process in excess of water.

A second set of measurements investigating the effect of silanes on the nucleation process has been carried out in lime saturated solutions ( $[Ca]=22$  mmol/l) at similar L/S as previous set of measurements (250). The results are shown in Figure 5-36. The reason for having chosen lime saturated solutions as dissolution media is because it replicates very well the conditions found in pastes.

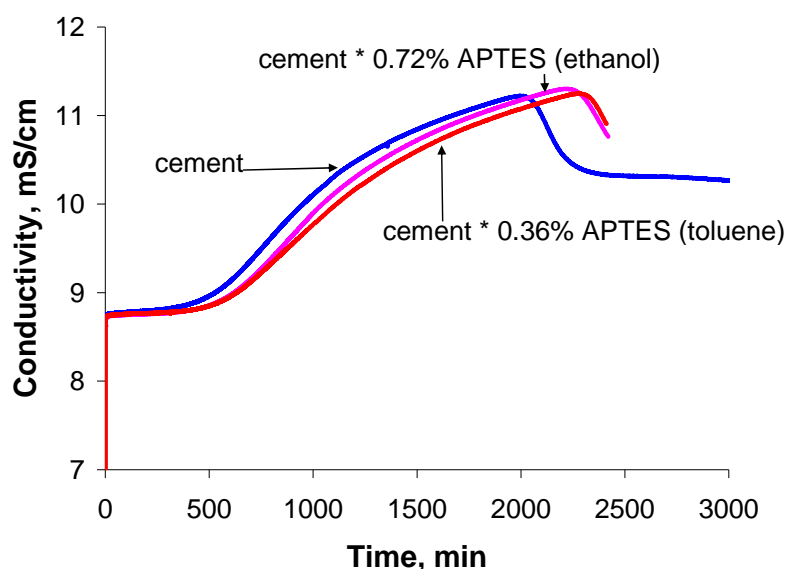


Figure 5-36. Evolution over time of the electrical conductivity during the hydration of cement and APTES modified cement in lime saturated solution,  $L/S=250$ .

Silane modified cement obtained by liquid phase deposition and excess solvent removal

Initially, all the three curves overlap indicating similar dissolution processes for all three samples considered. This is in agreement to what we have been previously reported.

Then, all three samples display a conductivity plateau. The length of the plateau is visibly shorter for neat cement compared to modified cements. As a result, the conductivity-time curve for neat cement rises up first marking the onset of acceleration period. This implies that APTES (regardless of which solvent has been used for adsorption) has a retarding effect on the growth of nuclei in lime saturated solutions.

On one hand these results differ clearly to what has been found for experiments carried out in water. On the other hand they are closer to what is commonly observed for experiments carried out in paste (concentrated suspensions) where a retarding effect has been constantly observed. The situation can be explained as follows.

Suppose a given number of nuclei 'n' are formed at the end of the dissolution process for experiments carried out in excess of water. Similar number 'n' of nuclei can be assumed to be formed for cement with and without APTES since all curves displayed perfect overlapping.

Consider now the experiments carried out in lime saturated solutions. Compared to previous case there is smaller number of nuclei 'm' ( $m < n$ ) formed at the end of the dissolution process for all three cements investigated.

In addition it must be remembered that similar dosages of APTES have been used in both water and lime experiments.

The fact that there has been a retarding effect observed on the growth of nuclei in lime solution is the direct result of smaller number of nuclei formed initially which are poisoned by APTES and thus their growth postponed. In the case of experiments carried out in pure water, there is larger number of nuclei generated initially and the poisoning effect is not noticeable. As a result, there has been no retardation on the growth process.



Silane modified cement obtained by liquid phase deposition and excess solvent removal

What these investigations clearly showed is that APTES does not block the dissolution and nucleation process of anhydrous phases. However, the hydrates growth appears to be affected by the presence of APTES when the liquid phase is a lime saturated solution rather than pure water.

### **5.3.2.2 Conclusions**

Considering the results obtained using several techniques, significant changes in hydration kinetics have been observed on the silane modified cements compared to neat cement.

The first conclusion to be drawn is that silanes retard the hydration of cement. An increased silane dosage results in increased induction periods, regardless of the nature of silane and of the solvent. The retarding effect isn't attributed to the solvent used for adsorption, but for a given silane the retardation has been found to be dependent on the nature of the solvent. Among the two solvents investigated, ethanol appears to give acceptable retardation levels, particularly for low APTES dosages.

Based on the adsorption data and the calorimetric measurements it has been found that equal dosages of silanes induce different effects on cement hydration. This emphasises the importance of silane nature on cement hydration. Also, the results indicated the strongest retarding effects for silanes displaying the lower affinity.

A further conclusion is that silanes are not entirely grafted on the silicates as initially presumed to be. This has been inferred after comparing the data collected from modified cement and modified tricalcium silicate with equal dosages of silane to solid.

Finally, we have looked at the cause of the retarding effects by closely analysing the dissolution, nucleation and hydrates growth processes. Here we have found that the dissolution and nucleation processes are not affected by the presence of silanes. However, it appears that hydrates growth is limited by the poisoning effect exerted on the initial number of nuclei in presence of lime saturated solution. This leads to longer induction periods always observed in the case of modified cement pastes.

Silane modified cement obtained by liquid phase deposition and excess solvent removal

### **5.3.2.3 Effect of silanes on the viscoelastic properties of cement paste at early age**

As pointed out earlier in Chapter 2, from a chemical standpoint the main cause associated with the cement's low tendency to deform before fracture is the cohesive nature of its network based on short range cohesive forces between C-S-H particles [111]. Mechanically, this is reflected in a short elastic limit of the material, which rheologically accounts for a critical strain of approximately  $10^{-4}$  [109, 110].

The aim of the work described in this section is to try to identify the effect of silanes on the viscoelastic properties of cement pastes and in particular to determine if their presence can modify the short range interparticle forces which was the initial goal of this project.

This will be done by using dynamic mode rheology measurements which should provide suitable evidence for changes in the interaction forces between particles. Furthermore, we compare rheological and calorimetric data, as hydration is known to influence the rheological performances of the cement systems.

#### **Individually silane modified cement**

##### **A. Linear viscoelastic domain (LVD)**

Figure 5-37 shows the evolution of the storage modulus as a function of the strain applied for cement pastes with and without silanes. All pastes have been prepared with constant  $w/c=0.25$  and all silanes have been prior adsorbed from ethanol suspensions.

Silane modified cement obtained by liquid phase deposition and excess solvent removal

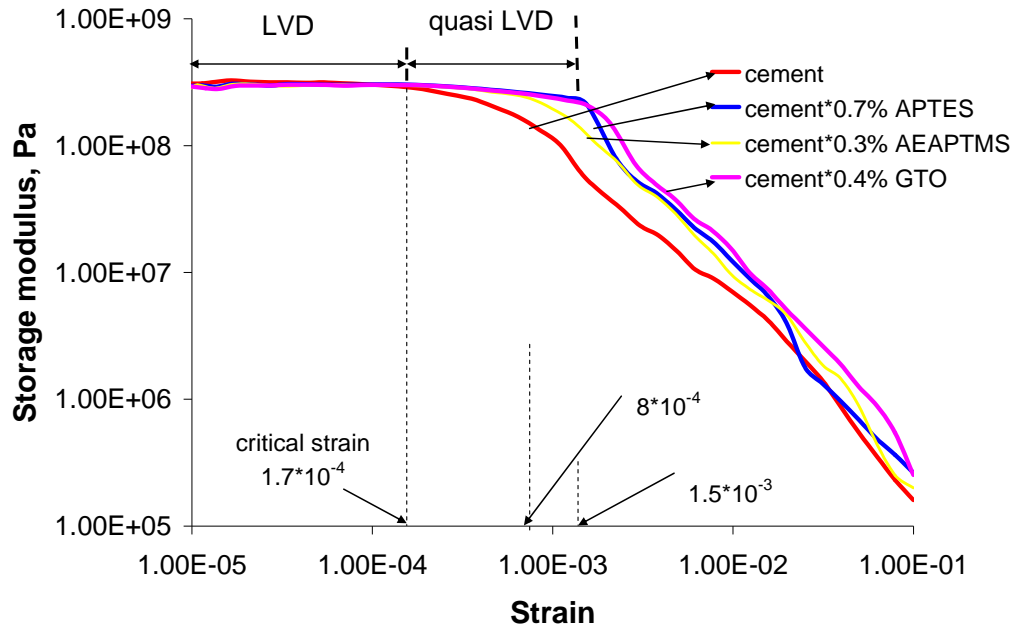


Figure 5-37. Evolution of the storage modulus as a function of the strain applied for plain and silane-containing cement pastes prepared with constant  $w/c = 0.25$ . For convenience, all measurements have been performed for equal storage modulus values of  $3 \cdot 10^8$  Pa. All silanes have been adsorbed from ethanol and the results are reported in percentage of silane by weight of cement.

### A.1. Neat cement paste

The neat cement paste displays initially a plateau region, where the storage modulus is independent of the strain amplitude indicating that the material behaves elastically. The end of the plateau domain (LVD) is attained for a strain in the range of  $10^{-4}$  attesting the small elastic limit, previously reported by Schultz [109] and Nachbaur [110]. Above this critical strain, the particles are separated, they move away from each other and the structure is destroyed. The transition is marked by a sharp fall-off in modulus, approximately four decades, over a large range of increasing strains.

Silane modified cement obtained by liquid phase deposition and excess solvent removal

## **A.2. Silane modified cement pastes**

All silane modified samples exhibit similar behaviour over the strain ranges investigated. Moreover, it seems that the critical deformations are reached for strains in the same range ( $10^{-4}$ ) as for the neat cement paste. However, silanes appear to have a strong effect on the viscoelastic properties by extending the LVD with a quasi linear region above the critical strain. This quasi-linear domain extends up to  $8 \cdot 10^{-4}$  for AEAPTMS modified paste and up to  $15 \cdot 10^{-4}$  for APTES and GTO modified ones. Further strain increase results in a complete structural breakdown marked by the steep decrease in moduli.

It must be noted that the measurements were performed at equal storage modulus values for all specimens ( $3 \cdot 10^8$  Pa), for easy comparison. As a result, when the strain sweep tests have been performed the samples under testing had different age and possibly hydration degrees, as will be later pointed out. This is not a problem since the critical strain remains constant from 10 min after mixing to after setting. Similar values for strain at rupture are also observed on an aged concrete, about ( $10^{-4}$ ) [110]. In our experiments, we did not detect any major variations for the critical strain of plain cement pastes surpassing  $10^{-4}$ , therefore considerations regarding the time when strain sweeps were performed are of little importance.

## **Discussion**

The results reported above indicate significant improvement in the modified cements' capacity to sustain load. Despite that the critical strain has been found to be in the same range as for neat cement paste, the presence of the silanes extended the LVD by 8 up to 15 times with a quasi-linear domain. For these cases, above the critical strain the structure appears not to be completely destroyed as there is no steep decrease of the moduli (as for the neat cement). Most probably this increase is attributed to the formation of a multi-dimensional siloxane bonds based network inside the cement paste. This can be explained as follows. As silanes are less likely to undergo a tridentate adsorption on cement [116] there are always ungrafted alkoxy or silanol groups, which can easily hydrolyse and co-polymerize, when water is added for cement hydration. As a consequence, a highly cross-linked network of siloxane bonds

Silane modified cement obtained by liquid phase deposition and excess solvent removal

is generated within the cement paste, which is responsible for the 8 up to 15 times increase in materials capacity to withstand loads above the critical deformation.

Such interconnected systems based on siloxane bonds created among aminosilanes are frequently reported in literature. Various investigations carried out on silica gel modified with aminosilanes [119] evidenced by IR spectroscopy and NMR siloxane bonds formation between the ungrafted alkoxy groups. However, in the case of cement it was not possible to prove the formation of this type of bonding. This is because the low silane dosages employed and the complex chemical nature of cement.

Increase in the critical strain as a consequence of the polymer (cellulose ethers) addition in the cement systems has been reported by Betioli et al.[115]. The author explained the formation of a three dimensional gel structure resulting in higher viscosity of the aqueous phase. Ultimately, the gel has been assumed to bridge the cement particles creating a structure that withstands higher critical deformations than neat cement paste.

Also, Nicoleau [105] showed that considerable critical deformation can be obtained in cement pastes with additions of latex (polyacrylamide) during the first minutes of hydration, but the effect is lost rapidly. The increase has been correlated to structure's dynamic behaviour under load. This means that by applying a certain strain a local structural breakdown indeed takes place, but that results automatically in creating several other contact points between latex particles. The effect is lost rapidly as the paste turns rigid. Hence, the increase is related to some additional short range forces created by increasing the number of contact points in presence of the latex particles.

As for our case, we can conclude that the increase observed for all silane modified cement pastes can be correlated directly to the long range interaction forces brought by the siloxane bonds formed within the cement paste.

Silane modified cement obtained by liquid phase deposition and excess solvent removal

## **B. Structure stiffening.**

The building up of the structure has been monitored by applying time sweep tests. The measurements have been performed according to the description given in Section 5.3.4.1. and taking into consideration the limitation imposed by the critical strain determined previously. It must be remembered that the structure consolidation measurements have to be performed by applying a constant strain lower than the critical one. Thus, we can non-destructively monitor the paste evolution over time.

In addition, heat development measurements have been recorded in parallel for reasons previously explained in Section 5.3.4.1.

### **B.1. Neat cement paste**

Figure 5-38 shows the continuous development of the storage modulus of a plain cement paste with  $w/c = 0.25$  during the first 800 min of hydration. The storage modulus is plotted against the total heat output of the reaction recorded by isothermal calorimetry, measured on a sample coming from the same batch of paste as used for rheological tests.

Silane modified cement obtained by liquid phase deposition and excess solvent removal

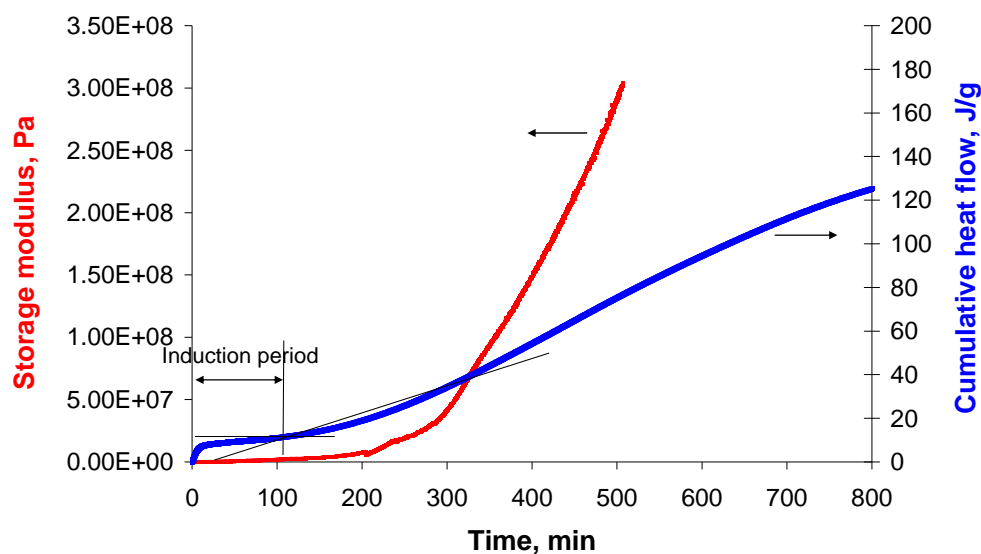


Figure 5-38. Evolution of storage modulus and evolution of total heat output for plain cement paste with  $w/c=0.25$  during the first 800 min of hydration. Measurements have been performed under constant strain of  $10^{-5}$  and constant frequency of 1 rad/s.

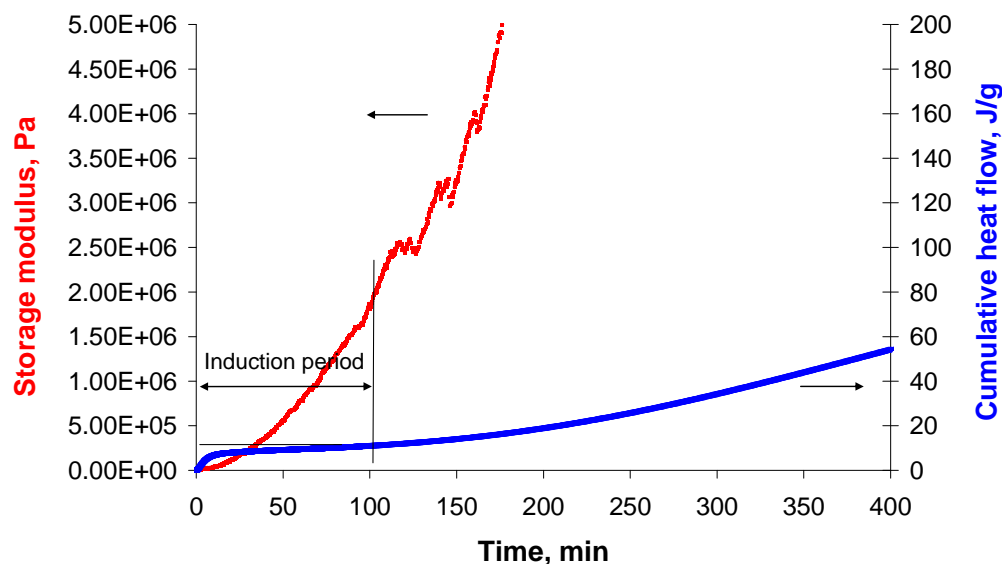


Figure 5-39. Evolution of storage modulus and evolution of total heat output for plain cement paste with  $w/c=0.25$  during the first 400 min of hydration (enlarged from Figure 5-38). This is in line to what has been previously reported.

Silane modified cement obtained by liquid phase deposition and excess solvent removal

The storage modulus shows an exponential-like evolution. During the first 100 min of hydration, it increases with time from an initial value of  $4 \cdot 10^3$  Pa to above  $1.8 \cdot 10^6$  Pa, timescale corresponding to the induction period on the calorimetric flow curve. The beginning of the evolution is detailed in Figure 5-39. After 200 min, there is a steep increase in the evolution of the storage modulus as the acceleration period starts. The curve shows an ordinate axis oriented concavity. In parallel, significant heat output is indicated by the calorimetric curve. After 500 min the storage modulus reaches  $3 \cdot 10^8$  Pa. In all tests to follow, this value will be imposed and we will refer to it as MIM (maximum imposed modulus).

## **B.2. Silane modified cement pastes**

Figure 5-40 reports the consolidation of silane modified cement pastes parallel to the systems' total heat release over time. Similar nature and dosage of the silanes were used as for the strain sweep tests reported above.



Silane modified cement obtained by liquid phase deposition and excess solvent removal

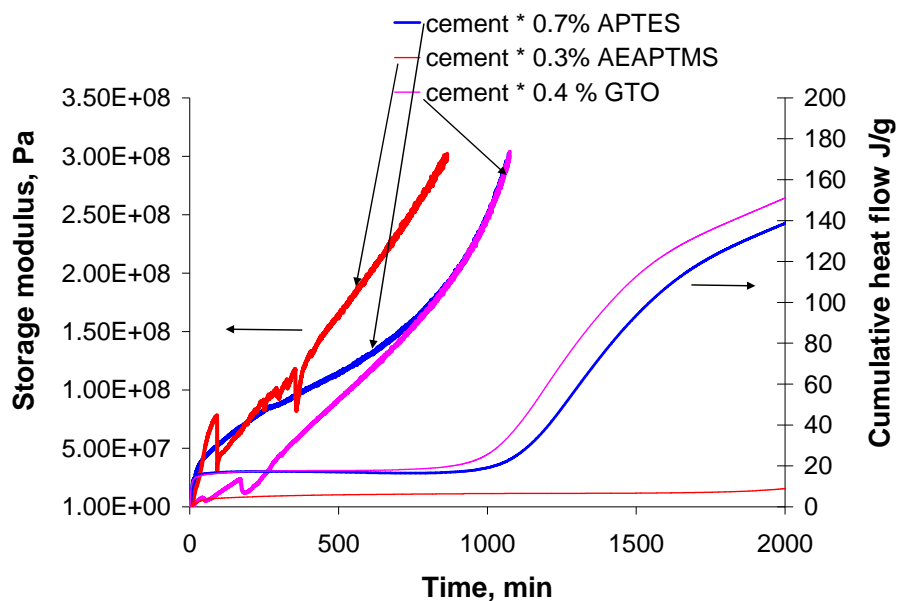


Figure 5-40. Storage modulus and cumulative heat flow for silane modified cement pastes with  $w/c=0.25$  during the first 2000 min. Measurements have been performed under constant strain of  $10^{-5}$  and constant frequency of 1 rad/s. All silanes have been adsorbed from ethanol and the results are reported in percentage of silane by weight of cement.

Silane modified cement obtained by liquid phase deposition and excess solvent removal

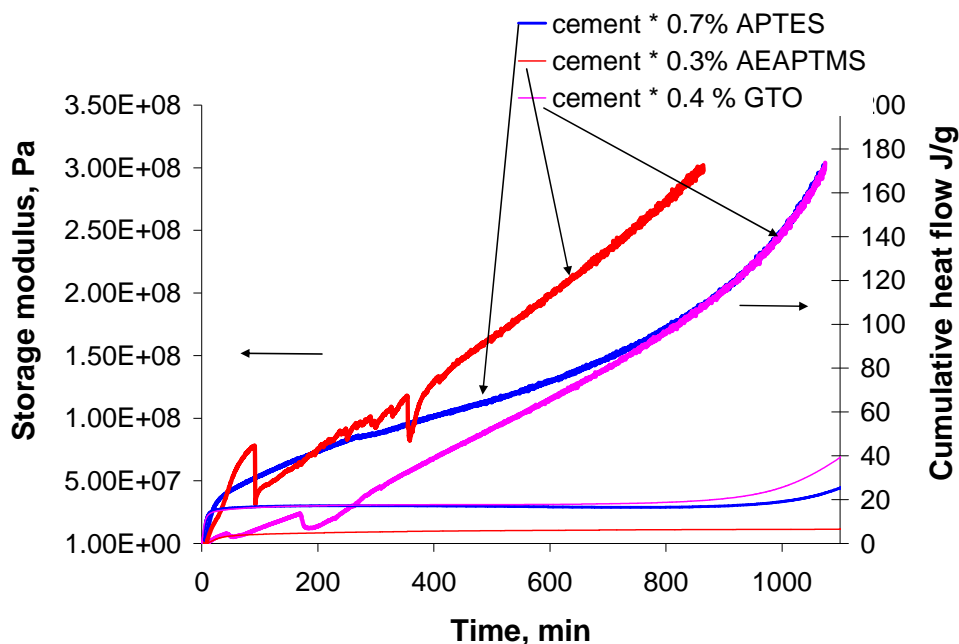


Figure 5-41. Storage modulus and cumulative heat flow for silane modified cement pastes with  $w/c=0.25$  during the first 1100 min (enlarged from Figure 5-40). All silanes have been adsorbed from ethanol and the results are reported in percentage of silane by weight of cement.

All silane modified cement pastes display significant differences in evolution, for both the storage modulus and the heat release over time, compared to the plain cement paste.

The first observation is that, during the first 100 min, all modified cement pastes consolidate significantly. The storage modulus increases greatly from initial values in the range of  $10^3$  to  $10^7$  at about 100 min ( $1.2 \cdot 10^7$  for GTO modified paste, to  $5.3 \cdot 10^7$  for APTES modified paste and to  $7.8 \cdot 10^7$  for AEAPTMS modified pastes). Practically, this results in a stiffening of the pastes. The period corresponds to the induction period for all modified cement specimens.

This is followed by a continuous development of the storage modulus for all silane modified cement pastes that goes along with absolutely no changes in the amount of heat output, since the hydration reaction is still in the induction period, as indicated by the calorimetric curves. Unlike the plain cement paste, the curves displaying the

Silane modified cement obtained by liquid phase deposition and excess solvent removal

evolution of the storage modulus over time exhibit an abscissa oriented concavity for aminosilanes modified pastes. GTO gives a rather linear dependency.

Finally, MIM is first attained after 865 min by the AEAPTMS containing cement paste. No changes in the heat release of the system have been measured as the hydration reaction remains in the induction period. Cement paste containing APTES and GTO attain the MIM after 1075 min. The moment corresponds to the onset of acceleration period.

An inflexion point in the curve describing the APTES systems consolidation must be noticed around 500 min, as the curvature changes from concave to convex with respect to the abscissa. AEAPTMS induces a rather linear dependency of storage modulus over the entire investigated time scale, while GTO evolution turns from linear to convex toward the x axis after 500 min.

## **Discussion**

The results clearly indicate that the presence of silanes in cement affect significantly its stiffening behaviour over time. The differences will be analyzed and discussed below.

Several studies have already addresses the topic dealing with cement paste stiffening over time by correlating it to the time dependent changes associated with the hydration reaction [22, 110, 114, 120].

For plain cement paste, the initial rise of the modulus is the result of the coagulation phenomenon. At this stage the systems consolidation can be explained based on the facts outlined in Chapter 2. We recall that particle interactions result from surface forces between charged particles in electrolytic solution. Upon water addition, the surfaces of cement grains enter a protonation-dissolution process. As a result the aqueous phase becomes quickly an electrolyte with high ionic strength [22, 120]. This case can be reduced conditions of high surface charge densities and multivalent ions. Thus, the coagulation phenomenon can be explained based on the attractive electrostatic forces between particles with the same charges brought by ion-ion

Silane modified cement obtained by liquid phase deposition and excess solvent removal

correlation forces. The attractive contribution overcomes the entropic repulsion and thus the particles attract each other. At this stage, the attractive interparticle forces are reversible [120]. The hydration reaction is in the induction period, so no contribution from hydration products can be considered. Nevertheless, it is important to notice that the hydration of aluminates is equally important to the first increase in modulus [21].

Silane modified cement pastes, particularly aminosilanes, show a much steeper initial increase of storage modulus, reaching approximately ten times higher values than plain cement paste does during the same period of time (Figure 5-39). This leads to early paste stiffening. Further discussion concerning the origin of this phenomenon will be given after having presented additional experimental evidence to support our arguments.

The second increase in modulus for the plain cement paste corresponds calorimetrically to the acceleration period of cement hydration. As hydrates grow the number of contact points between particles increases due to the increase in specific surface area. Furthermore, the reversible character of the connections among particles turns gradually to be irreversible [120] causing the system to rigidify. Surprisingly, the modified cement pastes show further consolidation while the hydration reaction remains entirely in the induction period. Most probably, this can be explained by the fact that silanes develop a wide spread network inside the cement paste, increasing the overall number of contact points between particles (explaining the increasing values for the storage modulus), although the number of contact points between cement particles is minimum (explaining the lack of strength). Similar findings have been reported by Nicoleau [105] on latex modified cement pastes. **This indicates that hydration reaction is a necessary condition for developing good mechanical strength, but on the other hand is not sufficient, at least for early strengths, as it will be later pointed out.**

Silane modified cement obtained by liquid phase deposition and excess solvent removal

### **Silane modified tricalciumsilicate**

So far, we have seen that the presence of silanes in cement pastes has a strong influence on how the material behaves above the critical strain. This phenomenon seems to be the result of a network based on multiple siloxane bonds formed inside the cement pastes. Furthermore there is a steep increase in the early development of storage modulus for silane modified cement pastes compared to neat cement paste.

In order to clarify what exactly causes these changes, we performed similar experiments on tricalciumsilicate (gypsum & tricalciumaluminate free system) and on modified tricalciumsilicate system. We have chosen to focus our study on APTES modified tricalcium silicate. The results are presented below.

#### **A. Linear viscoelastic domain (LVD)**

Figure 5-42 shows the evolution of storage modulus as a function of the strain applied for plain tricalciumsilicate ( $w/c=0.3$ ) and APTES modified tricalciumsilicate paste ( $w/c=0.25$ ).

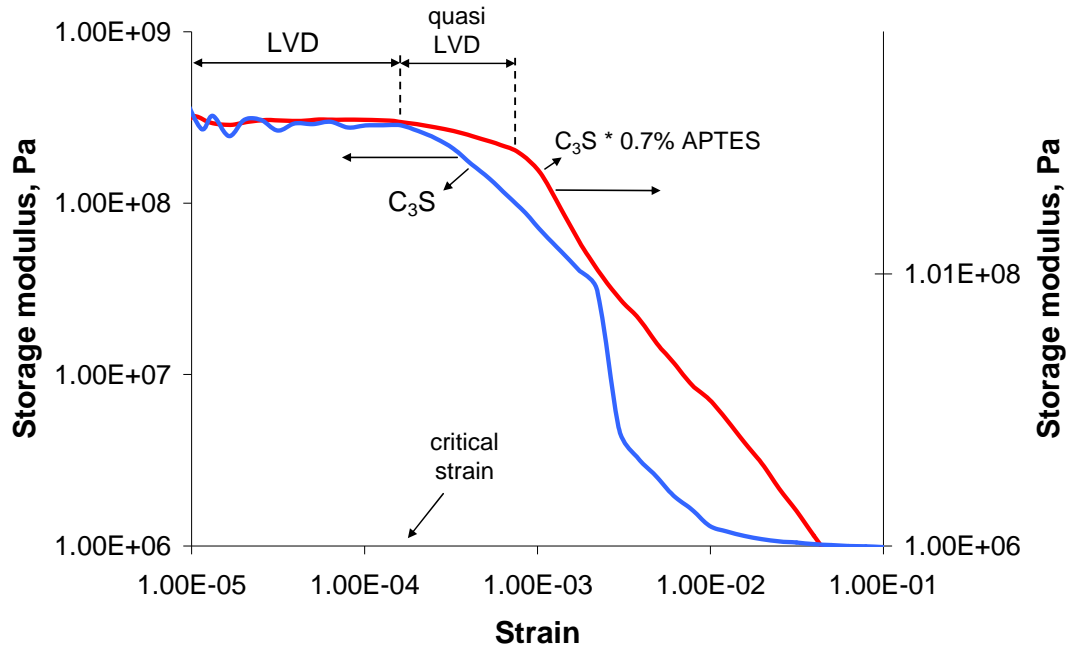


Figure 5-42. Strain sweep tests for plain tricalciumsilicate ( $w/c = 0.3$ ) and APTES-containing tricalciumsilicate pastes ( $w/c = 0.25$ ). The measurements were performed for storage modulus in the same range of values ( $10^8$  Pa). APTES has been adsorbed from ethanol and the results are reported in percentage by weight of cement

For neat tricalciumsilicate, the initial plateau region (LVD), ends for strain in the range of  $10^{-4}$ . This is in line with the results reported by Nachbaur [110]. Further increase in strain results in fast decay in storage modulus.

For APTES modified tricalciumsilicate paste, the LVD ends for critical strains within the same range as for neat tricalciumsilicate paste. However, above the critical strain the material behaviour is clearly different compared to neat paste. The drop off in the modulus is visibly slower thus an additional quasi LVD can be taken into account up to strains in the range of  $10^{-3}$ . This means that the presence of silanes influenced the material's flowing behaviour after the structure is destroyed. This is in line with the results we reported previously for APTES modified cement pastes.

Therefore, we can infer that the change in flow above the critical deformation is due to the cross-linked network based on siloxane bonds formed within the pastes after water addition. The newly created siloxane bonds seem to act like long range

Silane modified cement obtained by liquid phase deposition and excess solvent removal

interactions, which enables the silane-cement system to deform elastically up to higher deformations than neat system.

## B. Structure stiffening

The evolution of the structure for neat and APTES modified tricalciumsilicate pastes are reported in Figure 5-43. A magnification on the first 1500 min of hydration is given in Figure 5-44. APTES/tricalciumsilicate ratio employed was equal to APTES/cement ratio from previous experiments reported. Equally, APTES has been adsorbed from ethanol.

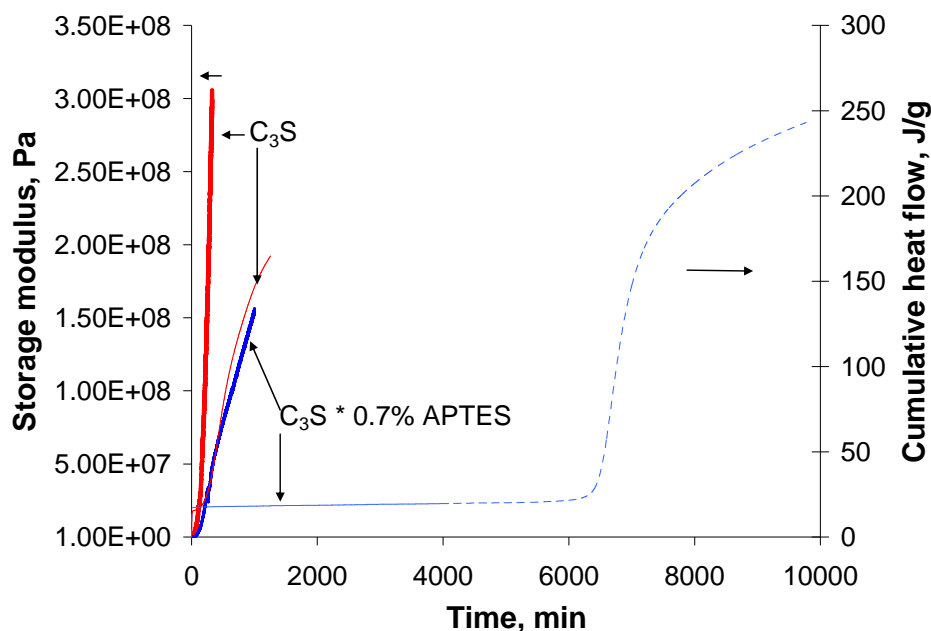


Figure 5-43. Evolution of storage modulus and cumulative heat flow for tricalcium silicate ( $w/c=0.3$ ) and APTES modified tricalciumsilicate pastes ( $w/c=0.25$ ). Measurements have been performed under constant strain of  $10^{-5}$  and constant frequency of 1 rad/s.

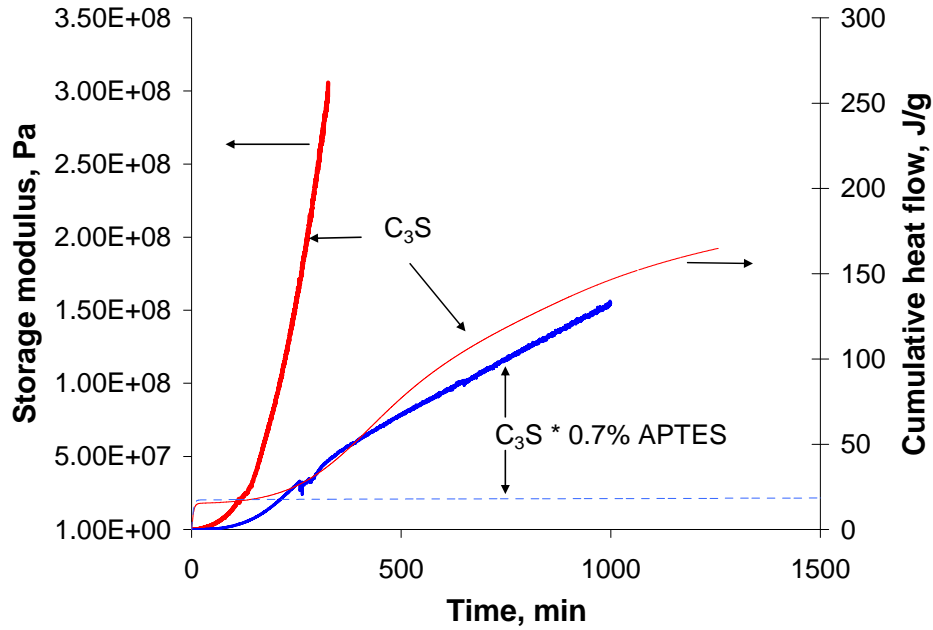


Figure 5-44. Evolution storage modulus and cumulative heat flow for tricalcium silicate ( $w/c=0.3$ ) and APTES modified tricalcium silicate pastes ( $w/c=0.25$ ), during the first 1500 min (enlarged from Figure 5-43).

The differences observed between the two systems are highlighted and discussed below.

### B.1. Neat tricalciumsilicate paste

On the one hand, the neat tricalcium silicate paste shows an initial exponential-like stiffening during the first 65 minutes of hydration from initial value of  $6 \cdot 10^3$  to  $5.6 \cdot 10^6$ . With respect to the heat release, this interval corresponds to the induction period, as indicated by the calorimetric curve. Therefore, the increase in modulus is the direct result of the coagulation phenomenon, which takes place due to attractive forces between particles [121]. The second increase in modulus from values in the range of  $10^6$  to values in the range of  $10^8$  is attributed to the onset of the acceleration period. This is the direct effect of the hydrates formed on the surface of the grains, which become bridging elements at their contact zones, turning the coagulated



Silane modified cement obtained by liquid phase deposition and excess solvent removal

structure rigid [120]. The results are in perfect agreement with the previous studies [110].

## **B.2. APTES modified tricalcium silicate**

On the other hand, during the same initial period of time, APTES modified tricalcium silicate paste develops a less well interconnected network. The value measured for the storage modulus, after 65 min, is ten times lower ( $7.6 \cdot 10^5$ ) compared to plain paste. With respect to the heat output, this period of time falls in the induction period. As a consequence, the lower consolidation degree for APTES modified tricalciumsilicate paste can be explained by lower number of interconnected sites. This is due to the dispersion induced by APTES, which on the one hand prevents particles to connect by modifying the interparticle forces and on the other hand retards the hydration reaction.

Overall, APTES tricalciumsilicate paste shows a quasi-linear structure consolidation over the time scale of the investigations, which falls entirely within induction period as indicated by the heat flow curve. As a result, the stiffening of the paste is explained by an overall increase in number of contact points established among the additive, and not the hydrates.

Similar trends in evolution of paste consolidation have been found for APTES deposited from toluene. Results are given in Annex IV.

So far, we can conclude that APTES delays the consolidation in tricalciumsilicate pastes. This is very important information for our understanding on what causes the premature stiffening in silane modified cement systems. In what follows, we discuss the implication of our finding.

## **Discussion**

Figure 5-45 illustrates a comparative study between neat & APTES modified cement and neat & APTES modified tricalciumsilicate. Constant APTES/solid ratio was considered in both cases.

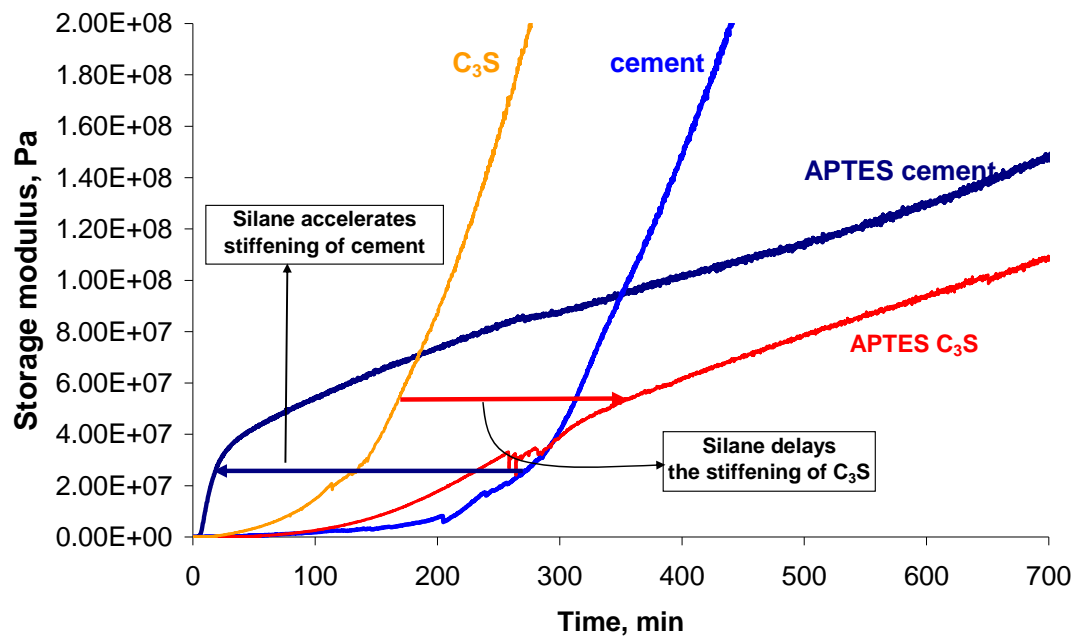


Figure 5-45. Consolidation of structure over time for neat & APTES modified cement pastes and neat & APTES modified tricalciumsilicate at constant APTES/solid ratio.

The first observation visible from Figure 5-45 is that APTES delays the consolidation in modified tricalcium silicate paste compared to neat pastes. The hydration reaction falls in the dormant period for the modified tricalciumsilicate throughout the entire timescale of the experiment.

The second observation to be made from Figure 5-45 is that a steep initial increase of the storage modulus is clearly visible on APTES modified cement paste compared to the neat cement paste. Practically, this results in premature stiffening of the paste under investigation. Heat development measurements presented above indicated that both reactions fall in the induction period. However, it must be remembered that all silane modified cement pastes, showed higher amounts of initial heat release than plain paste (as discussed on Section 5.3.2.1). It is known that primary contribution to the initial amounts of heat released due to aluminates. This means that the presence of silane in cement interfered with the reactivity of the aluminates resulting in higher amounts of heat generated. As a result, the paste shows premature stiffening confirmed by the sharp increase in observed in system stiffness.

Another factor which should be taken into consideration concerns certain aspects connected to the preparation of the modified substrates. After preparing the silanes modified substrates, we found that gypsum separated as distinct phase in the new modified solid substrate. To overcome this inconveniency, after solvent removal and heat treatment, the modified substrates have been dry homogenized as reported in Section 5.1.2. However, we are not completely convinced that this homogenisation was absolutely efficient. Thus, unequal distribution of gypsum among the rest of the phases might have also contributed to that sharp initial increase of modulus during the initial period as aluminates reacted faster than normally.

The conclusion to be drawn after having highlighted several differences observed for cement and tricalcium silicate with and without silanes is that when adsorbed on cement, silanes lead to changes in the reactivity of the aluminates and/or of the gypsum.

In addition, it must be noted that later evolution of the structure stiffening over time shows similar slopes for both silane modified systems. This suggests similar stiffening processes ongoing in both cases. The reason for this behaviour is almost certainly due to the development of the previously reported cross-linked networked based on Si-O-Si bonds for both silane modified pastes. Indeed, this is confirmed by similar changes observed in the flow behaviour above the critical deformation for the modified systems compared to the neat systems. Hence, we can infer that the increase in materials capacity to withstand loads above the critical strain is directly associated to the presence of the siloxane based network formed within the paste. However, further work is needed in order to clearly understand the mechanism leading to this change in behaviour.

### **Blends of individually silane modified cement**

Up to now, we have seen that, taken individually, each silane modified cement paste exhibits differences compared to neat pastes. The primary change has been the increase in material's capacity to withstand load above the critical deformation. This

Silane modified cement obtained by liquid phase deposition and excess solvent removal

effect has been related to the presence of a network based on siloxane bonds formed within the cement paste.

The question that is being raised now concerns the possibility of further increasing the LVD for blends of individually silane modified cements. This could be achieved via supplementary chemical bonding assumed to take place between reactively compatible end functions from the different silane species. This section outlines a series of tests carried out to investigate this topic. For this purpose, we chose to analyse:

- a) GTO modified cement + AEAPTMS modified cement
- b) GTO modified cement + APTES modified cement

a) GTO modified cement + AEAPTMS modified cement

**A. Linear viscoelastic domain (LVD)**

The effect of blending cements prepared with different silanes on the evolution of the storage modulus as a function of the strain applied is examined by comparing to pastes containing cement treated with a single silane. Results are given in Figure 5-46. The mix consisted in equal amounts by weight of GTO modified cement and AEAPTMS modified cement

Silane modified cement obtained by liquid phase deposition and excess solvent removal

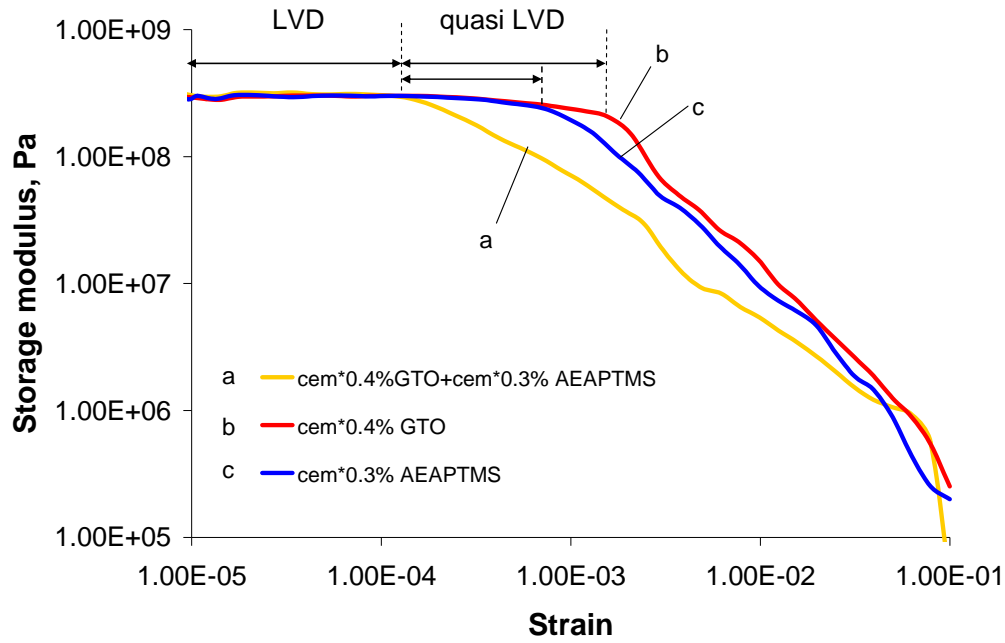


Figure 5-46. Evolution of the storage modulus as a function of the strain applied for individual and blended silane modified cement pastes prepared with constant  $w/c = 0.25$ . The measurements have been performed for equal storage modulus values ( $3 \cdot 10^8$  Pa). Percentage of silane by weight of cement.

Surprisingly, the results indicate that the end of the LVD for blend modified cement paste lies exactly in the same range of strains as for each constituent of the mix ( $10^{-4}$ ). Moreover, above the critical deformation there is a steep decrease in storage modulus over a wide range of strains, contrary to what we have been expecting. As a result, the curve does not display any additional quasi linear zone as the individually silane pastes do. So far it seems that taken individually each silane modified paste behaves better in terms of capacity to deform under strains than their mix.

The same investigation has been performed on several other blended silane modified cement pastes containing various silane dosages. The results are shown in Figure 5-47.

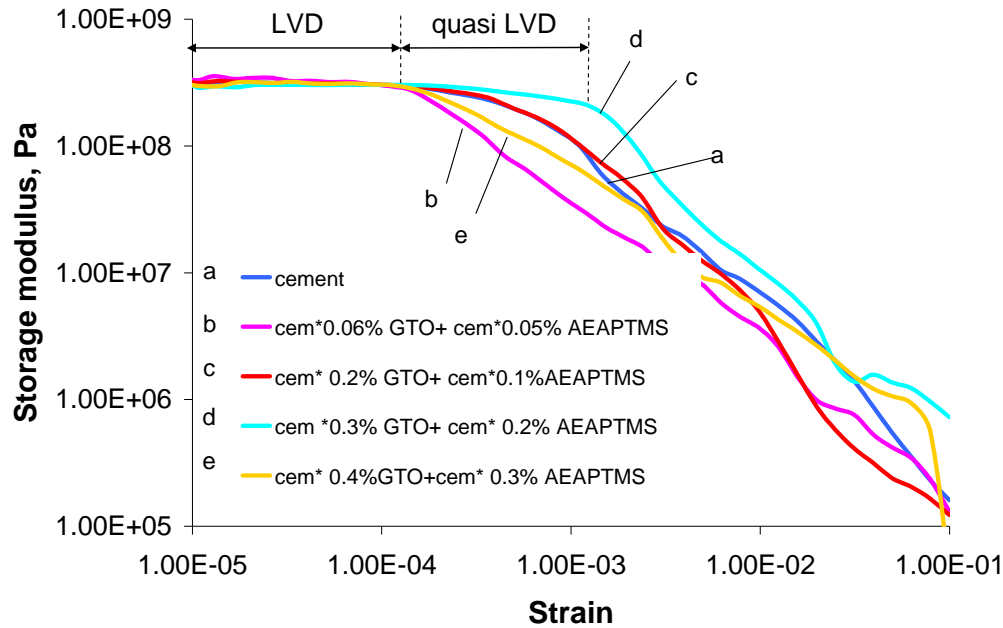


Figure 5-47. Evolution of the storage modulus as a function of the strain applied for blended silane modified cement pastes prepared with constant  $w/c = 0.25$ . The measurements have been performed for equal storage modulus values ( $3 \cdot 10^8$  Pa). Percentage of silane by weight of cement.

It is immediately noticeable that the all blended silane modified pastes display similar LVD. However, there are some other observations that can be made concerning how the dosage employed affects the behaviour of blended systems above the critical deformation.

The foremost observation is that there is an optimum silane dosage for which blends show a quasi linear zone in addition to the LVD. This has been found for the case of blended 0.3% GTO cement and 0.2% AEAPTMS cement. This increase could be either coming from amine-epoxy chemical bonding, cross linked network based on siloxane bonds or could be the cumulative effect of both bonding types. Because further increasing the silane concentrations (above the optimum) does not lead to additional improvements, but on the contrary eliminates the positive effect, we conclude that there is most probably no amine-epoxy chemical bonding taking place. This case has already been discussed above (0.4% GTO and 0.3% AEAPTMS). Moreover, the maximum increase is of about ten times, which is similar to what we

Silane modified cement obtained by liquid phase deposition and excess solvent removal

have reported for individual silane modified pastes. Therefore it is reasonable to assume that the increase in the material's capacity to sustain load above the critical deformation is due to the multiple siloxane bonds formed within the paste.

Blends of modified pastes with dosages below the optimum, do not show any additional extension in the LVD. There is always a sharper drop-off in the moduli with strains above the critical one. However, it must be noted that depending on the silanes addition levels, the fall-off from the modulus plateau differs significantly. Some blends display similar modulus decay as the neat cement paste, while others shows a much sharper decay. This indicates that the material behaviour is strongly dependent on the dosages employed and that there is no additional amine-epoxy bonding taking place in blended systems.

All these features show that mixing individually silane modified cement does not necessarily result in positive effects on the blended system. These findings contrast with our initial expectations that amine-epoxy chemical bonding could form upon mixing of two modified cements and could lead to further increase of the LVD.

This approach has been unsuccessful, but results clearly indicate that individually or blended (for certain dosages) silane modified cement pastes lead to a change in the materials behaviour to deform after the critical strain has been surpassed. The change is associated to the highly cross linked network build within the paste and is based on siloxane bonds.

## **B. Structure stiffening**

Figure 5-48 illustrates the development of storage moduli for blend silane of modified cements compared to its constituents. The blend has been prepared by mixing equal parts from 0.3% GTO modified cement and 0.2% AEAPTMS modified cement.

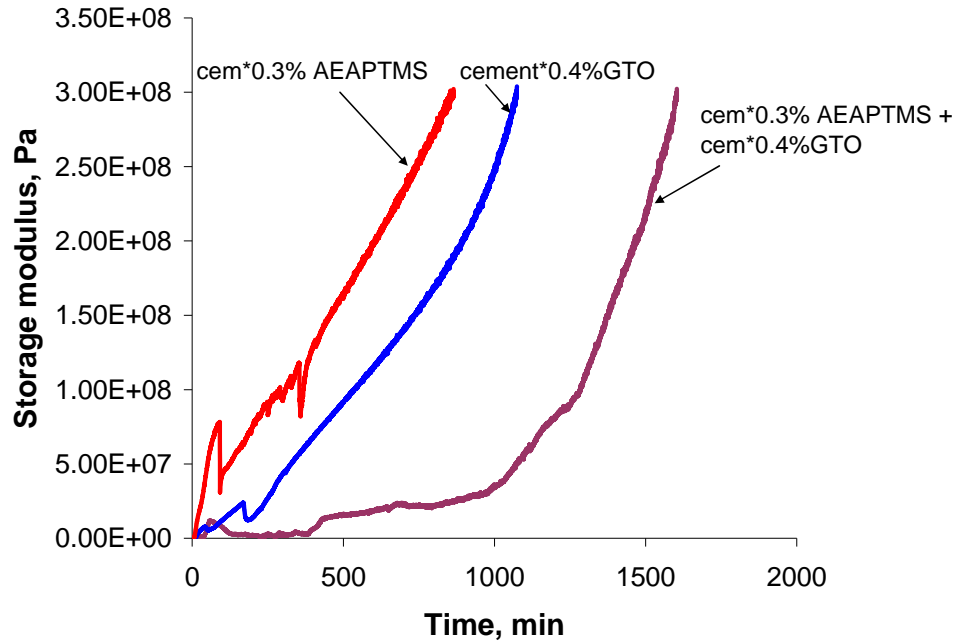


Figure 5-48. Evolution of storage modulus blended and individually silane modified cement pastes prepared with  $w/c=0.25$ . Measurements have been performed under constant strain of  $10^{-5}$  and constant frequency of 1 rad/s. Percentage of silane by weight of cement. Percentage of silane by weight of cement.

The results concerning the structure consolidation over time for individually silane modified cement pastes have been discussed above. It must be remembered that all individually silane modified pastes show a rapid structure stiffening initially evidenced by the steep increase in the moduli (visible in Figure 5-41). This was correlated with the interactions silane aluminates and/or gypsum content.

Remarkably, the data acquired for blended system does not show the same time evolution (Figure 5-48). On the contrary, it appears that the structure needs considerable longer time to stiffen. To illustrate this we can compare the time at which the pastes develop a given modulus. Consider this value to be  $10^8$  Pa. In the case of individually silane modified cements this occurs after 290 min (AEAPTMS) and 540 min (GTO), respectively. Similar modulus values are reached for the blended system after 1290 min.



Silane modified cement obtained by liquid phase deposition and excess solvent removal

In addition, it must be noted that there is no contribution on the structure consolidation coming from the silicates as the period of time corresponds entirely to the induction period for all samples investigated. Experimental evidence to prove this has been presented above for individual silane modified paste (Section 5.3.2.3 B2). For the blended system the results are presented in Annex IV.

Hence, the conclusion that can be drawn from these experiments is that by blending silane modified cements one does not observe similar changes as for individual constituents.

To further investigate this, we have considered several blends containing different silane dosages and monitored the structure consolidation. The results are shown in Figure 5-49.

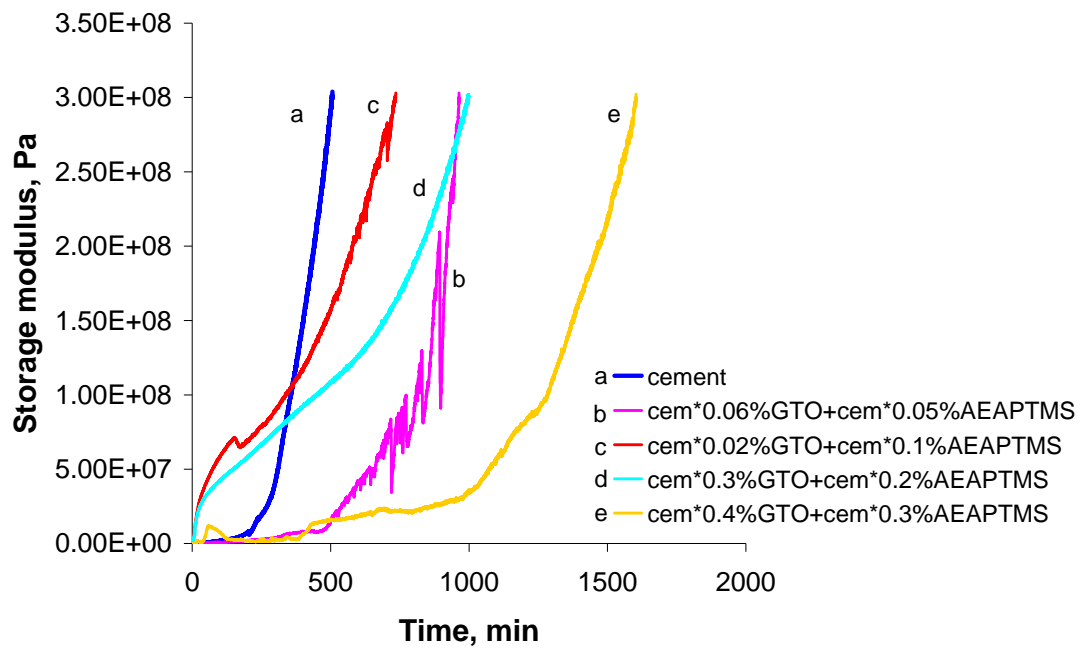


Figure 5-49. Evolution of storage modulus for blended silane modified cement pastes prepared with  $w/c=0.25$ . Measurements have been performed under constant strain of  $10^{-5}$  and constant frequency of 1 rad/s. Percentage of silane by weight of cement.

These data indicate that the structure consolidation for blended silane modified cements is strongly affected by the dosage of silane in individual mixes. For some

Silane modified cement obtained by liquid phase deposition and excess solvent removal

cases, blended pastes display similar evolution in structure consolidation as seen on individually silane modified pastes with a steep early increase. This has been explained and evidenced by the fact that silanes affect the reactivity of the aluminates. (for individual silane modified pastes). It is reasonable to assume that similar causes lead to the effects observed in blended systems.

Further increasing or decreasing the silane dosage results in significantly longer times for structures to reach similar moduli values. So far, this could not be clearly explained, but the variation seems to follow a similar tendency as previously reported for the LVD.

#### b) GTO modified cement + APTES modified cement

A second set of experiments has been carried out for blended cement system consisting in equal amounts of GTO modified cement and APTES modified cement. The concentrations of silane to cement analysed ranged from 0.3% to 0.06% for GTO and from 0.4% to 0.07% for APTES.

Equally, the results did not show any improvement in the LVD for any of the concentrations investigated. Some minor changes have been observed in the materials capacity to withstand load above the critical strain. In addition, paste stiffening for blends consisting in GTO modified cement and APTES modified cement has been found to evolve similarly to what has been observed in the case of other blended cement systems investigated. The data are reported in Annex IV.

### **Conclusions**

It has been shown within this section that viscoelastic properties of cement pastes are strongly affected by the presence of the adsorbed silane agents.

Taken individually, it has been found that all silanes induce changes on how cement paste stiffen their structure over time by affecting the reactivity of the aluminates. This results in very steep increases for moduli corresponding to silane modified

Silane modified cement obtained by liquid phase deposition and excess solvent removal

cement pastes at very early ages. This has been inferred after comparing the results with similar experiments carried out on aluminates free system (tricalcium silicate). The fact that silanes affected the aluminates reactivity has been also confirmed by monitoring the heat evolution curves which showed higher initial heat release for silane modified cement pastes compared to neat cement pastes. Further stiffening of the structure in the case of silane modified paste is the direct result of the overall increase in number of contact points due to the presence of silane agents.

No contribution from the hydrates can be considered contrary to the case of neat cement paste that consolidates significantly after the onset of the acceleration period. These observations have been confirmed by the calorimetric measurements.

A significant improvement in pastes ability to withstand loads has been observed. Despite the fact that all silane modified systems display similar limits for the LVD as neat paste does, there is a substantial difference on how silane pastes deform above the critical strain compared to neat pastes. An additional quasi linear zone has been found to extend the LVD and thus the pastes' ability to sustain load increases significantly. This originates in the highly cross-linked networked hypothesised to form within the cement paste as a result of silanes polymerisation.

The experiments carried out on blended silane modified systems expecting to further increase the LVD by creating chemical bonding between the end groups of individually silanes (amine and epoxy) failed. Similar LVD has been detected for all blends. Furthermore, it has been shown that blended systems do not display similar improved behaviour under load despite the fact that both constituents show the improvement. However, it appears that the dosage of silane is a key factor because in some cases blended silane modified pastes showed an additional quasi linear zone for strains higher than the critical one.

## **6 Silane modified cement obtained by liquid phase deposition with solvent evaporation**



As already discussed and stressed, grafting silane to anhydrous cement by dry blending of constituents proves to be rather inefficient. There are two main limitations. First, the lack of knowledge in what happens to the silane once it contacts the cement powder. Second, it affects badly the mechanical properties. This is due to the fact that a homogenous silane to cement mix requires relatively high silane addition levels. This results in strong delays of cement hydration and overall reduced degree of hydration.

A much more successful approach was to use of organic solvents as dispersion media, for adsorbing silanes onto anhydrous cement. This optimized technique provided the means for a systematic study of the adsorption process by analyzing the residual admixture from the supernatant. Nevertheless, it enabled a better characterisation of the modified substrates. It was found that a certain dosage of silane to cement leads to significantly improvements in the viscoelastic properties at early age, while keeping the retarding phenomenon within acceptable limits.

Next, we are interested to examine whether the improvement in viscoelastic properties detected on rheological measurements can be measured at a macroscopic scale. It was fast becoming clear that large quantities of silane modified cements were needed. By liquid phase technique this was practically not achievable. The average silane modified cement batch size was less than 5 grams. In addition, the preparation procedure was both time and energy consuming and it required a certain number of consecutive steps to be followed.

For these reasons, we developed a complementary liquid phase technique, referred to as ‘one pot’, to overcome the inconveniences brought by the latter. On one hand it provided means of producing large quantities of modified cements for our macroscopical mechanical tests, while on the other hand it simplified the preparation procedure.

In this section, we first present the different approach used to modify cement by silane. Then, the study focuses on analysing several properties of the modified cements: hydration, rheological and mechanical properties. Semi-adiabatic

calorimetry has been used to investigate the evolution of the paste over time in parallel to penetration tests. Three point bending tests have been used to evaluate the macro scale changes in mechanical properties of the modified systems. Scanning electron microscopy (SEM) and X-ray diffraction (XRD) was employed as complementary techniques for gaining additional information on the changes induced by the presence of silanes.

All the measurements presented in this section have been carried out in collaboration with Sika Technology during the visit to their laboratories in Zurich, except for XRD –Rietveld which was performed at EPFL (Lausanne, Switzerland).

## **6.1 Methodology**

### **6.1.1 In principle**

The powder to be modified is mixed with a diluted solution of a silane in a solvent. The solvent is chosen in such a way as to be inert to both the adsorbate and the adsorbent. After a given time, considered sufficient for silane to diffuse to the cement surface the solvent is removed by heating based on the different boiling points between itself and the one of the surface modifier. Once this had been achieved, the modified substrate is further dried for complete solvent removal and silane to cement additional fixation.

### **6.1.2 In practice**

For these experiments only ethanol and APTES were considered as vehicle media and as surface modifier, respectively. 200 g of cement were dispersed into 100 ml ethanol. Silane concentrations ranged from 0.1% to 7% by weight of cement. After 30 min homogenisation at room temperature in the evaporation flask from a rotary evaporator (R-II Buchi, Switzerland) the operation mode was switched on (bath temperature - 60°C, vacuum pressure - 300 mbar, evaporation flask spinning level - 5). Both glass and plastic evaporation flasks were used. However, due to severe adhesion of silane to the glass flask further preparations were carried out exclusively in the plastic evaporation flask. After the major part of the solvent has been removed, the modified

cement has been additionally oven cured at 80°C for 1 hour. Weight loss of the dry modified substrate was checked after that period of time and was measured to be less than 0.1%. The modified anhydrous cement powder was stored in sealed plastic containers until it was tested.

## **6.2 Characterization of modified products**

### **6.2.1 Techniques used for investigating the properties**

#### **6.2.1.1 Semi-adiabatic calorimetry**

Hydration was monitored using semi-adiabatic calorimetry. The principle, the experimental set-up and operational mode has been described in Chapter 5. The measurements were used to monitor the heat evolution in parallel to other investigation techniques. Thus, they mainly provided a better understanding and interpreting of data collected by other techniques. No direct comparison with the results collected from isothermal calorimetry is possible, because of several differences in sample mixing protocols, sample size, and testing conditions (semi-adiabatic versus isothermal). However, similar retarding tendencies on cement hydration have been observed.

#### **6.2.1.2 Penetrometry**

Penetration tests using penetrometers have been carried out to investigate rheological properties.

A penetrometer consists of a measuring cell which is filled with the paste under investigation and a needle which is driven into the sample at a constant speed, 1  $\mu\text{m}/\text{min}$  in our case. Initially, the needle is hand submerged into the sample. The measurement is initiated once the cell holder drives the cell upwards, causing the needle to penetrate the sample. The force on the needle is recorded over time. The needle keeps on penetrating the sample because the stress generated is higher than the yield stress and the material flows. As soon as the stress generated in the sample is



lower than the yield stress, the flow stops and so does the penetration of the needle [122].

Adjustments regarding sample size have been made from the standard norm D34441-79 and D15558-84 for the purpose of this study. Sample cell holder was reduced to a cylinder 40 mm height and 40 mm in diameter. Needle's tip shape used was conical and connected through a cylinder with the upper cylindrical region.

The cement-water mixtures were prepared according the procedure described for the semi-adiabatic measurements.

Penetration tests have been carried out simultaneously to semi-adiabatic calorimetric measurements for the cement pastes with and without silane for the reasons previously explained (Section 5.3.1.2). APTES dosages considered ranged between 0.1% -2% by weight of cement.

#### **6.2.1.3 Three point bending test**

These strength investigations have been performed in the laboratory of Sika Technology and were different from the previously described mechanical tests carried out in the laboratory of ZAG Ljubljana.

The experimental program included testing two sets of cement pastes, prepared at constant w/c ratios of 0.3, with and without admixture. Because the interest was in investigating the mechanical performances of the modified cement that displayed previously improved elastic performances only 0.7% APTES silane modified cement was tested.

The preparation of specimens for mechanical tests took place at room temperature. The mixing procedure was similar to the one described above for the already described tests. The fresh cement pastes were cast in 10 x 10 x 80 mm moulds and sealed in plastic bags. The samples were demoulded when their strength allowed it to,

Silane modified cement obtained by liquid phase deposition with solvent evaporation

but not prior to 24 h after casting. After demoulding, specimens have been sealed cured until tested.

Only measurements of flexural strength were performed using a three point bending technique. All measurements were performed at loading rates of 0.5N/s. The strength value was the average of three tested specimens.

#### **6.2.1.4 Scanning electron microscopy (SEM)**

Microstructure of cement pastes has been qualitatively investigated using a Hitach S3400N scanning electron microscope (SEM) equipped with an Ametek EDAX energy dispersive X-ray analyser (EDX).

Cement paste specimens with (0.5%APTES) and without admixtures have been prepared according to the protocol described for the penetration tests. The specimens were placed in vessels and heat development was followed by semi-adiabatic calorimetry. At equivalent hydration degrees (assessed by equal amounts of heat release) hydration was quenched by solvent (ethanol) replacement. After a week of storage in the solvent, the samples were dried at 80°C and SEM/EDX analysis was performed on freshly fractures pieces after sputtering with about 10 nm platinum (Bal–Tec SCD 005 Sputter Coater).

SEM imaging was performed by environmental secondary electron detection (ESED) at 80 Pa. Micrographs were taken at 15 keV acceleration voltage. EDX was performed under high vacuum conditions. Only qualitatively EDX investigations were performed.

#### **6.2.1.5 X-Ray diffraction (XRD)**

Cement samples prepared previously for SEM imaging were ground by hand. XRD-Rietveld investigations have been carried out for phase quantification. Measurements have been performed in the laboratory of EPFL (Switzerland) with a PANalytical X’Pert Pro MPD diffractometer using configuration employing CuK $\alpha$  radiation

Silane modified cement obtained by liquid phase deposition with solvent evaporation

( $\lambda=1.54 \text{ \AA}$ ). Data have been collected over a Bragg angle range of  $6-70^\circ (2\theta)$ , using 3830 steps at an angular step size of  $0.0167^\circ$  at a counting time per step of 57.15 s.

Quantification was done by Rietveld analysis with software X'Pert High Score Plus. The amorphous content was calculated using rutile as external standard.

## **6.2.2 Results and discussion**

### **6.2.2.1 Method validation**

A first set of experiments has been performed to make sure that the much simplified substrate modification we consider was suitable to produce silane modified cement displaying similar characteristics to the ones obtained by removing the solvent excess. Therefore we performed the following test. We prepared two modified cement systems by (1) adding a set amount of silane (0.7% APTES by weight of cement) and evaporating the solvent and by (2) adding a higher amount of silane (1% APTES by weight of cement) and removing the solvent containing the unabsorbed fraction. It must be noted that the dosages of silane have been chosen in such a way as to allow comparisons between similar modified cements. The fact that an initial dosage of 1% APTES (by weight of cement) leads to 0.7% adsorbed APTES (by weight of cement) has been shown in Chapter 5.

After drying, semi-adiabatic calorimetric measurements have been carried out for both modified cements. Experimental evidence presented in Figure 6-1 proves that there is no visible difference in the temperature evolution over time for the two pastes. This implies that the technique described above can be efficiently used in preparing silane modified cements.

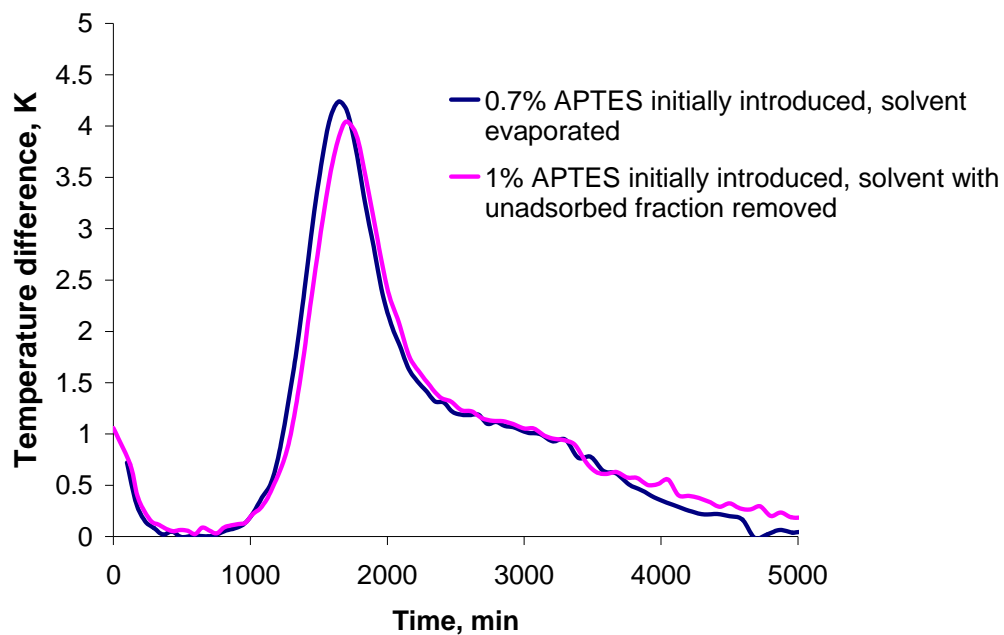


*Figure 6-1. Time dependant temperature curves for two silane modified cement pastes. The good signal superposition indicates that ‘one pot’ approach can be successfully used for surface modification. Percentage of silane by weight of cement.*

#### **6.2.2.2 Simultaneous hydration rate and rheology measurements**

Penetration techniques have been used simultaneous to semi adiabatic calorimetric measurements to characterise the rheological changes associated with hydration for cement pastes with and without APTES. The test results are summarised in Figure 6-2.

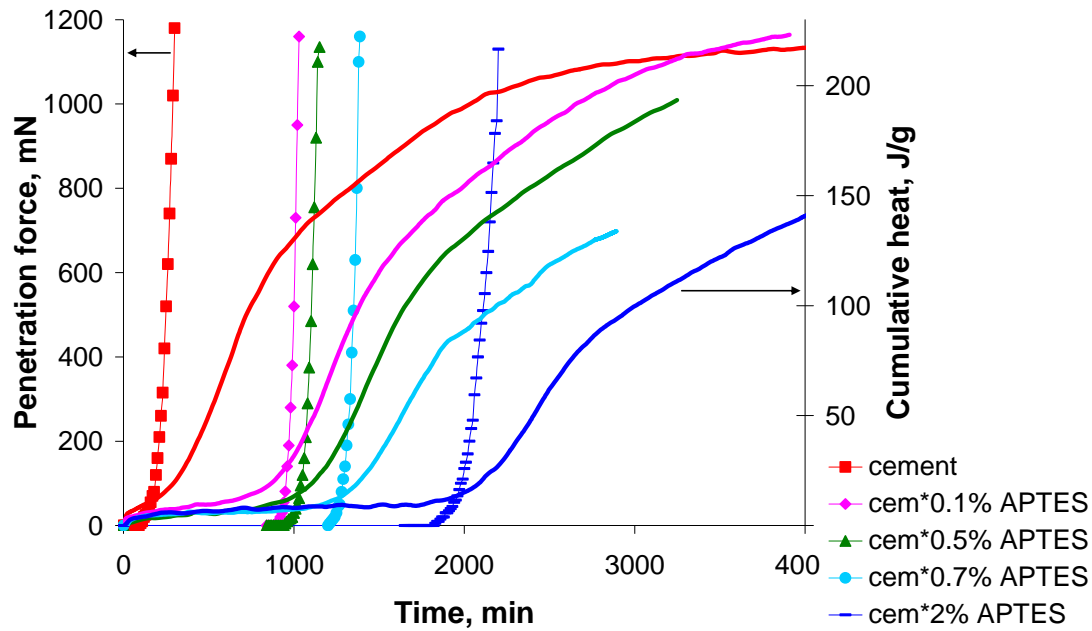


Figure 6-2. Needle penetration and cumulative heat release as a function of time for cement pastes with and without APTES. Percentage of silane by weight of cement.

All samples show similar behaviour. During the time when the rate of heat flow is low, none of the flow curves indicate any measurable force on the needle. The material flows and the needle keeps on penetrating until the stress generated becomes lower than yield stress. This happens as the induction periods come to an end, indicated by the increase in the heat output. As a result the penetration force starts increasing slowly. This is followed by an abrupt increase over a narrow timescale that goes along with a progressive increase in heat flow as the reaction enters in the acceleration period. This substantial increase corresponds to the setting.

We recall that the penetration force is proportional to the yield stress of the material for very low penetration velocities and it also scales up with shear modulus.

The reason for the increase in the penetration force can be explained by the fact that the material develops a certain resistance to flow. This due to the increased number of interparticle bonds developed in pastes as hydration advances. Yield stress is known to be particularly sensitive to hydration [123]. In our experiments, during the dormant period there was no change in the penetration force and thus in the yield stress. An

increase in the heat flow results in increase in penetration force and consequently in the yield stress.

The conclusion that can be drawn from this experiment is that a certain degree of hydration is needed in order to develop some measurable force in the needle. This seems to correlate well with the onset of the acceleration period for all samples investigated.

An interesting comparison could be made between the results obtained by low amplitude oscillatory measurements and penetration tests investigating the rheological behaviour of silane modified cement pastes. This is illustrated in Figure 6-3. To help visualize the influence of admixture on cement paste behaviour simultaneous heat development measurements have been carried out for both cases. Also, it must be noted that similar dosage of silane to cement has been considered in both cases and both modified substrates have been obtained from liquid phase adsorption.

For oscillatory shear tests, results give directly the evolution of the storage modulus versus time. For penetration tests, results provide information on the evolution of the penetration force versus time. Given the fact that the critical strain in cement pastes is constant during hydration, the force measured by penetrometers should generally scale with the shear modulus, although it is really a yield stress measurement [122]. The yield stress of the tested material is calculated by dividing the measured force by the surface of the penetrating tip. Assuming the needle has a conical tip connected to a cylindrical part, we have:

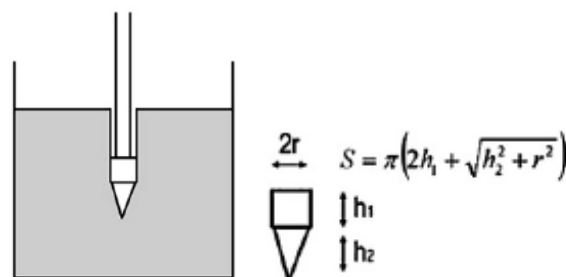


Figure 6-3. Schematic illustration of penetrometer needle geometry (reproduced from [122]).

$$\tau_0 = \frac{F}{\pi r \sqrt{r^2 + h_2^2} + 2\pi r h_1} \quad (6-1)$$

Where:

$\tau_0$  is the yield stress

$F$  is the penetration force

$R$  is the cylinder radius

$h_1$  and  $h_2$  are respectively the heights of the cylindrical and conical section.

Further, the modulus can be calculated using equation (6-2):

$$G = \frac{\tau_0}{\gamma_c} \quad (6-2)$$

Where:

$G$  is the storage modulus

$\gamma_c$  is the critical strain for cement

Comparative results of rheological measurements performed are displayed in Figure 6-4.

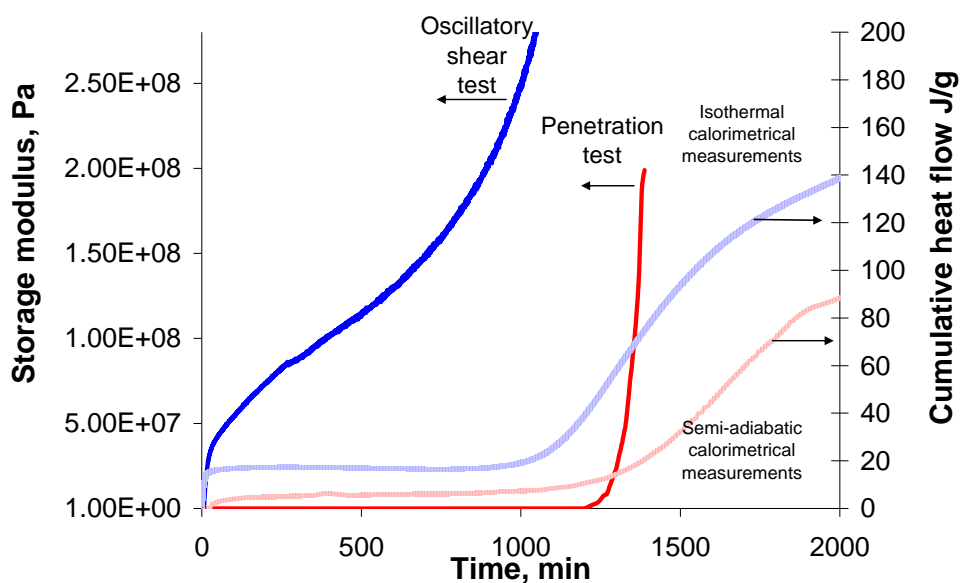


Figure 6-4. Storage modulus and cumulative heat flow for 0.7% APTES modified cement pastes measured by low amplitude oscillatory shear test and isothermal calorimetry versus penetration tests and semi-adiabatic calorimetry.

When oscillatory tests have been used, a sharp increase in modulus, suggestive of early paste stiffening has been observed since the cement hydration falls in the induction period. In the other investigation there is no structural consolidation of paste prior to the onset of the acceleration period.

The differences observed can be explained as follows. The measurements performed in oscillatory mode consist in submitting the sample to strains characterized by very low amplitudes. Moreover, the strains are kept below the critical one to avoid structural breakdown. Thus, non-destructive testing conditions are met. In the case of penetration tests, the stress applied in the sample is higher than the yield stress and the paste flows until the generated stress becomes lower than the yield stress. In addition, the penetration is constant and at very low speeds ( $1\mu\text{m/s}$ ) suggesting a quasi static flow. This suggests quite obviously that the material is in a different regime compared to previous case and therefore it shows a completely different behaviour. Thus, comparing the changes observed does not provide any further relevant information concerning the rheological behaviour of silane modified cement pastes.



### 6.2.2.3 Three point bending tests

Three point bending tests were performed on cement pastes with and without admixture for equivalent hydration degrees. The modified silane cement system chosen for strength tests was 0.7% APTES modified cement for reasons described previously in the experimental section. The times considered for specimens to have reached similar hydration degrees (assessed by equal amounts of heat release) have been previously determined by calorimetric measurements. The comparative cumulative heat flow curves indicating when strength measurements have been performed are shown below.

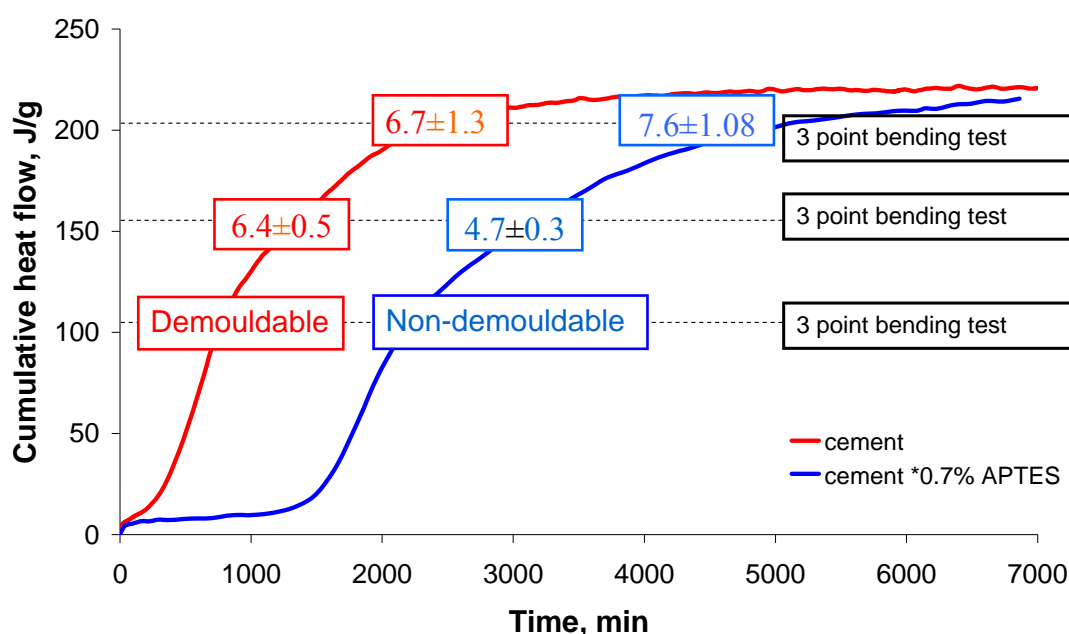


Figure 6-5. Comparison between heat flow curves obtained for cement and 0.7% APTES modified cement. The dashed lines indicate that strength tests have been carried out for equivalent amounts of heat release. The values on the curves represent the flexural strength test values measured.

The bending strength tests results for cement pastes with and without APTES over the time scale investigated are presented Figure 6-6.

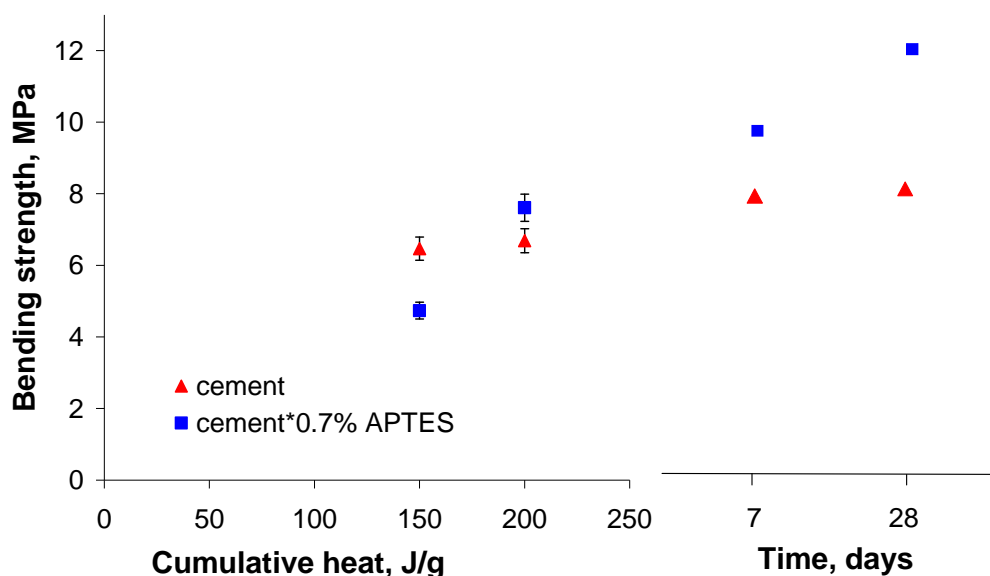


Figure 6-6. Comparison between bending strength values for cement pastes with and without admixture prepared with constant  $w/c = 0.3$ . Percentage of APTES by weight of cement.

It must be noted that for early age, strength values have been plotted against the total heat output, while for 7 days onwards the strength values have been plotted against hydration time. The reason for presenting the results in such manner results from the difficulty in collecting long time heat output values using semi-adiabatic calorimetric measurements.

As a first attempt, mechanical strength testing turned out to be unsuccessful, because the silane modified paste specimens did not show enough strength to allow demoulding, despite the heat release recorded.

Moving to higher amounts of heat outputs, all strength tests planned have been successfully carried out. Initially, silane modified cement pastes showed lower bending strength values compared to neat paste. As curing time increased, contribution of APTES started to be significant. The bending strength for all silane modified pastes gradually increased, while the plain cement pastes showed levelling off. At 28 days the improvement in strength for silane modified cement specimens was of 35% compared to plain cement paste.

In addition, C-S-H precipitation must occur on the surface of the anhydrous phases for strength to develop. On the contrary, if the precipitation takes place in the pore solution, specimens do not develop good strength despite the fact they show significant hydration advancement. The latter situation could apply to our case. At early age the modified silane specimens show strength loss compared to plain cement paste. On the heat evolution curve this corresponds to the post-accelerating period. Hence, it could be assumed that C-S-H precipitated in the pore solution and not on the surface of the grains. In this hypothesis, the effect was certainly connected to the presence of APTES in the system.

These observations seem to match with general trend highlighted in the literature that organic admixtures which affect the early hydration processes alter the phase composition and the microstructure of cement pastes [124, 125].

However, the problematic reduced intercrystallite cohesion in silane modified paste for early age seems to disappear fast. From the second sets of strength measurements onward the modified cement specimens showed constant strength gain and moreover all the values measured overpassed the ones for plain cement paste. This suggests that the cross-linked network created at early age remains stable with increasing the curing time. This is a surprising result because this type of bonding is reported not to be stable at high pH, which is undoubtedly the case here. A modification in the sample microstructure and/or degree might however also be the explanation for this difference in strength at later ages.

#### **6.2.2.4 SEM**

In order to gain more and fast insights on the microstructural evolution during early hydration, qualitative ESEM investigations have been carried out on cement pastes with and without APTES for specimens displaying similar amounts of heat outputs. Figure 6-7 shows the heat output dependence on time and the specimen's age when microstructural investigations have been carried out.

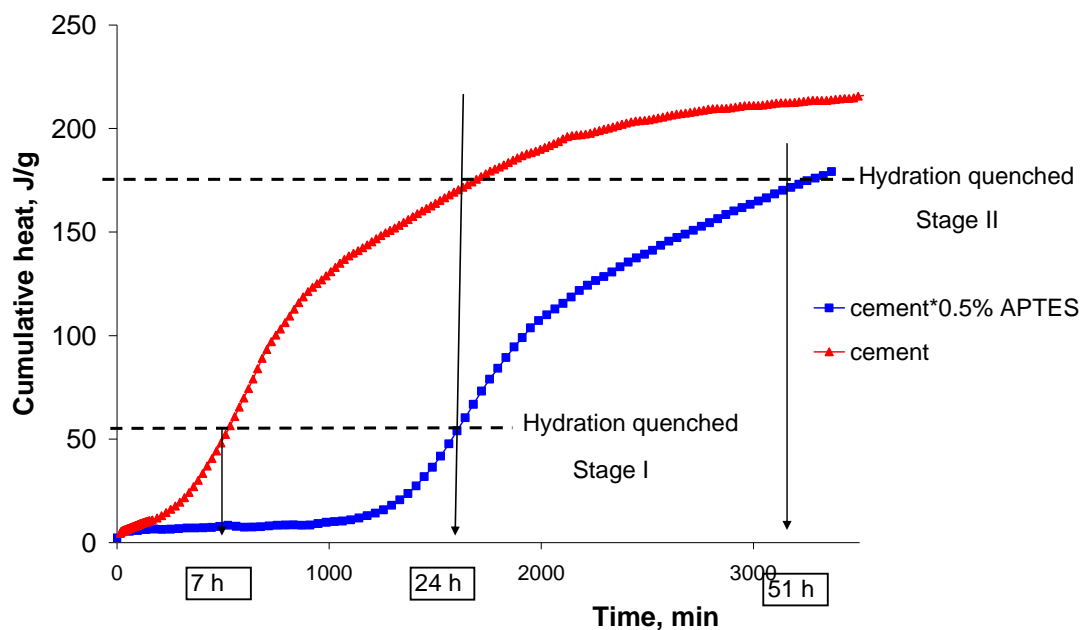
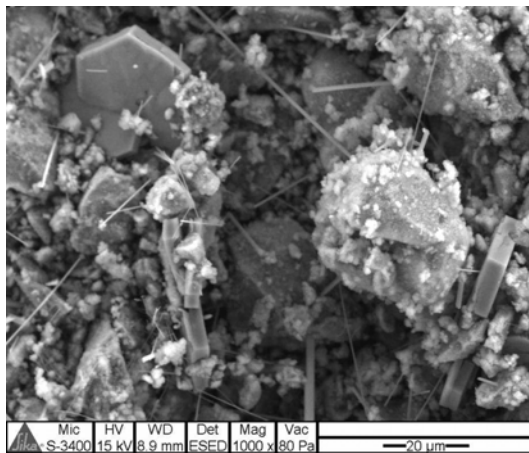


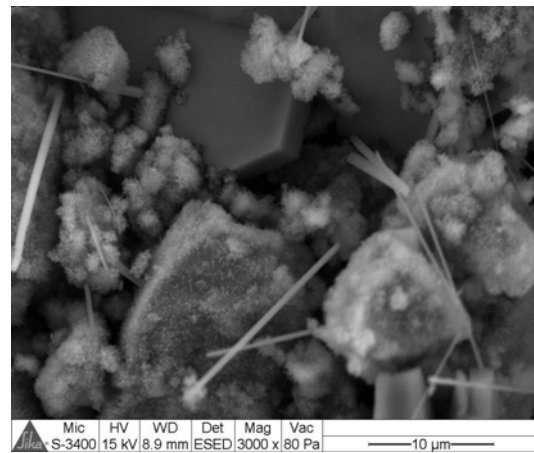
Figure 6-7. Evolution over time of the heat outputs obtained for plain and 0.5% APTES modified cement pastes. ESEM investigations have been carried out on samples displaying similar amount of heat outs as indicated by the dashed lines.

ESEM pictures of cement pastes with and without APTES at equal stages of heat release are shown in Figure 6-8 (Stage I) and Figure 6-9 (Stage II).

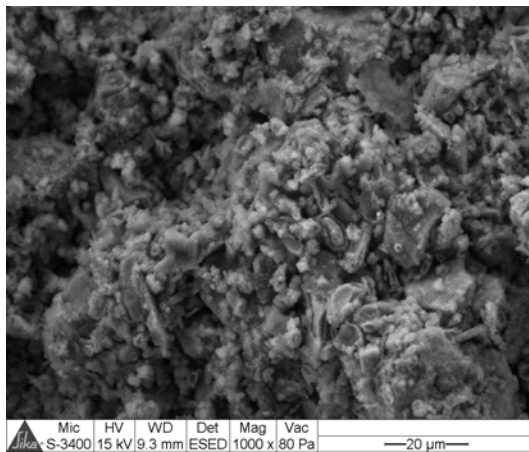
## Stage I



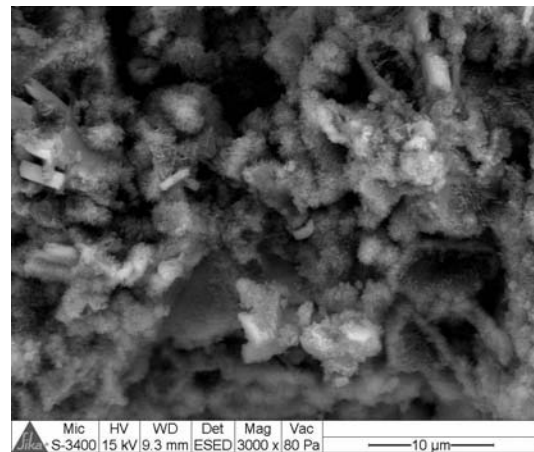
a) Cement paste hydrated 7h



b) Cement paste hydrated 7h  
(enlarged image of a)



c) 0.5% APTES cement paste hydrated 24 h



d) 0.5% APTES cement paste 24 h  
(enlarged image of c)

*Figure 6-8. ESEM images of cement paste and 0.5%APTES cement pastes. The samples imaged displayed similar amount of heat outputs.*

## Stage II

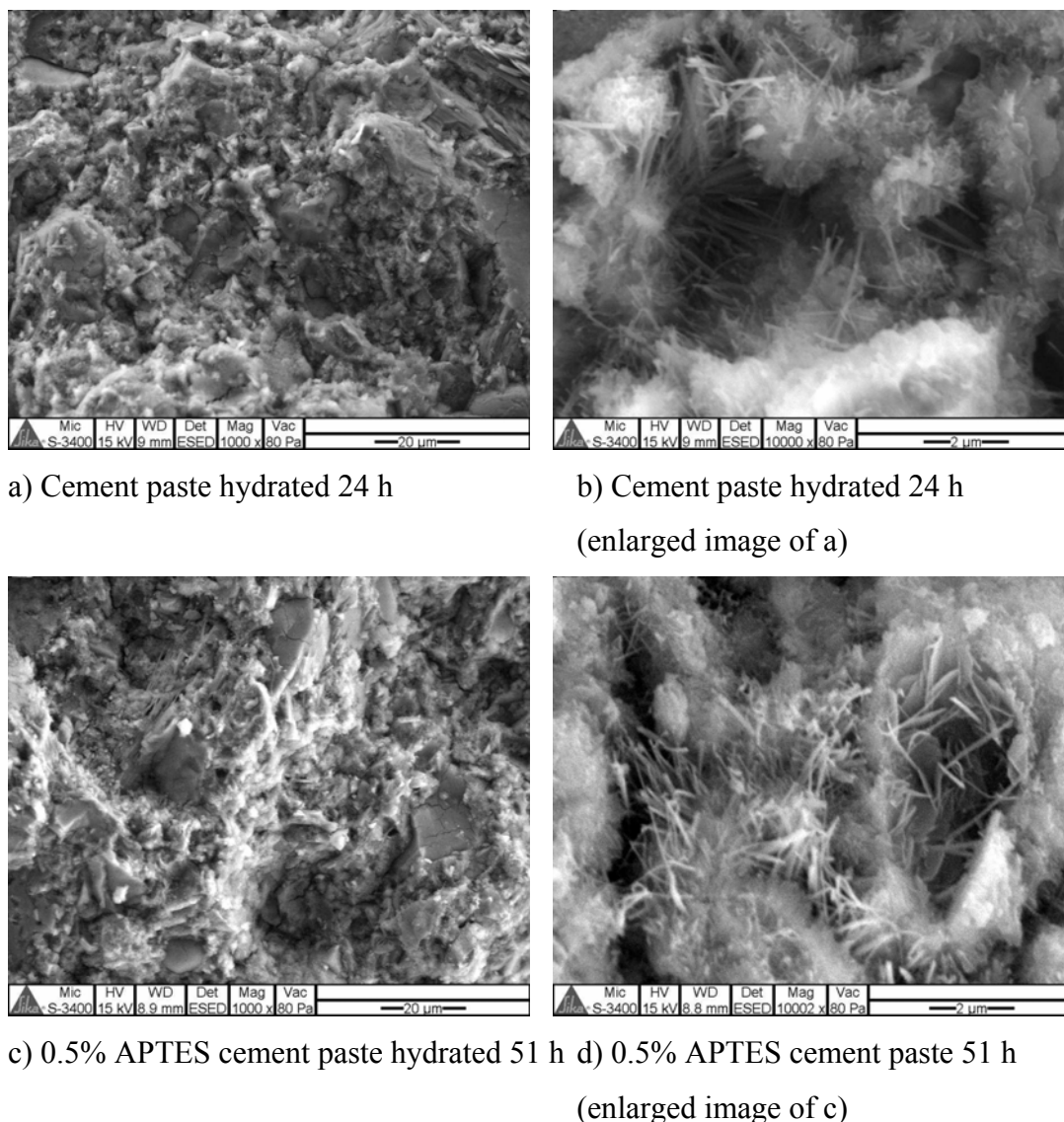


*Figure 6-9. ESEM images of cement paste and 0.5%APTES cement pastes. The samples imaged displayed similar amount of heat outputs.*

In the first set of investigations (Stage I) carried out on cement paste specimens with and without APTES significant morphological differences were observed. On the one hand plain cement paste showed frequent dense bundles of long and thin syngenite and well defined large hexagonal plates of portlandite (as proven by the EDX spectra). On the other hand, for the same heat output, APTES modified sample displayed a more densely packed structure with abundant C-S-H formation and short thick prismatic syngenite crystals encountered randomly. Surprisingly, at this stage none of the micrographs indicated the existence of ettringite, which is usually reported to be easily visible within this time scale.

Despite the clear differences in microstructure seen on the first stage of equal heat release, there appears to be no difference between the neat and the modified cement pastes them in terms of morphology at later ages (Stage II). For low magnification levels both specimens revealed images characteristic for forced ruptured brittle materials with compact C-S-H packing. For high magnification levels ettringite is observed in both cases.

The fact that clearly visible changes were initially observed, mainly the lack of visible portlandite in the modified specimen raised a questions regarding its existence in specimen at the time the measurements were performed versus its undetectably via this method because its shape changed. Therefore, the following experiments focused on answering this question. Quantitative XRD-Rietveld analysis was used to quantify all crystalline and amorphous phases. The results are presented and discussed below.

#### **6.2.2.5 XRD-Rietveld**

The results from XRD-Rietveld analysis for both paste with and without silane and for both ages are summarised in Table 6-1.

Table 6-1. Phase composition of cement paste with and without APTES from XRD-Rietveld analysis

Phase	Hydration Stage I		Hydration Stage II	
	7h	24 h	24 h	51 h
	Neat	0.5%APTES	Neat	0.5%APTES
Phase	%wt	%wt	%wt	%wt
C <sub>3</sub> S	46.9	37.7	25.7	22.9
C <sub>2</sub> S	14.1	14.5	14.9	16.2
C <sub>4</sub> AF	10.4	11.2	9.6	10.1
C <sub>3</sub> A, cubic	1.1	0.7	0.7	0.0
C <sub>3</sub> A, orthorhombic	0.0	0.9	1.0	1.1
Gypsum	0.0	0.0	0.0	0.0
Hemihydrate	0.0	0.0	0.0	0.0
Anhydrite	0.0	0.0	0.0	0.0
Portlandite	3.1	8.1	12.8	15.7
Calcite	0.0	0.0	0.0	0.0
Ettringite	3.5	2.6	6.4	3.8
Amorphous content	20.8	24.2	28.8	30.1
Rwp (from Rietveld)	7.2	6.3	6.9	7.0

The results indicate that at first stage, there was less anhydrous silicate phases left in the modified sample as compared to the plain paste. However, differences were not that huge. As a result, the C-S-H content calculated for the modified paste is slightly higher, but in the same range compared to neat paste. This correlates well with denser structure observed by ESEM investigation.

Furthermore, in both cementitious pastes portlandite was detected. Moreover, in the modified paste the amount found is significantly higher compared to plain paste. This is in accordance with the general trend displayed by the other XRD quantified phases. Nevertheless, it answers the question raised previously regarding the lack of portlandite found on a naked-eye investigation of ESEM micrographs. Thus, results of



XRD-Rietveld confirmed that portlandite is found in the modified pastes at the first stage investigated. Moreover, it was found in substantially higher amounts than in the neat paste. The fact that it was not observed on ESEM pictures means that it crystallized in other shapes than the most commonly observed large hexagonal plates.

In addition, XRD–Rietveld analysis showed that after the first hydration stage considered, ettringite was present in both types of cement pastes and no gypsum or other calcium sulfate phases were any longer detectable. Slightly higher ettringite content was found in the neat paste compared to modified one. This is agreement with a higher consumption of  $C_3A$  measured for neat cement paste.

Also, it must be noted that no syngenite was detected by XRD–Rietveld analysis, despite its abundance observed on ESEM pictures. Furthermore, no ettringite has been identified by SEM investigations, whereas XRD–Rietveld measurements clearly indicate its presence and moreover quantifies its amount.

At the second stage, there was less variation between the various phases formed within the pastes investigated. Values measured for anhydrous phases remained very close for the pastes with and without admixtures. Similarly, the amorphous content calculated gave nearly equal values. The amount of Portlandite is again higher in the modified paste but difference is much reduced from the previous case. As for ettringite content, the neat paste showed higher values compared to modified paste. At this time, the increase in ettringite content is clearly visible compared to the former case.

### **6.3 Conclusions**

It has been shown within this chapter that methodological improvements allowed preparing larger quantities of silane modified cements. In addition, the modified cement systems have been characterised in terms of mechanical and rheological properties. Furthermore, a quick attempt to investigate the microstructure development and phase assemblages at early aged has been attempted.

The foremost conclusion to be considered from the results of the experiments carried out within this chapter is that a given concentration of silane leads to improved mechanical performances for silane modified cement pastes at later ages. A constant gain in flexural strength has been observed from 3 days onwards ultimately resulting in improved bending strength of up to 35 % at 28 days compared to neat cement paste. However, at early ages (less than 3 days) results indicated lower strength values and problematic demoulding at 24 h.

These effects have been tentatively attributed to the presence of a three dimensional network based on siloxane bonds generated by the cross-linking of ungrafted silane alkoxy groups which hydrolyse after water contacts the cement powder. It seems that the network interferes with early age hydration, but as curing time extends it reinforces the structure and contributes to superior strength values when compared to neat pastes.

Early age ESEM investigations have revealed differences in terms of morphological aspects between sample with and without silane. ESEM observations concluded that no portlandite formation is visible in the silane modified specimens. This fact was proven to be nonsense as XRD-Rietveld analysis revealed the presence of even higher amounts of Portlandite in the modified specimens measured for equal amounts of heat outputs in samples with and without silane.

The ESEM and XRD-Rietveld investigations did not clarify why there is a lack of strength at early ages for the modified specimens. However, direct comparisons to the mechanical tests results are not entirely relevant because of the minor differences in silane to cement ratios used. Further experiments and more detailed microstructural investigations would be needed to fully explain the reason for the increased strength as a change in hydration degree cannot be ruled out at this stage.

According to the penetration methods used within this chapter all samples show similar rheological behaviour. Most probably this is because the method employed is not sensitive enough to detect changes occurring, before the onset of the acceleration period as seen previously when using low amplitude oscillatory techniques (Chapter 5).



## **7 Conclusions and perspectives**



## 7.1 General overview

The aim of this work has been to increase the mechanical performances of cementitious materials, in particular their flexibility which will additionally result in increased durability.

Despite the fact that concrete structures are traditionally believed to be durable, practice shows that this is not always the case. The economic magnitude of maintenance and repairs is astonishing (sometimes surpassing the costs of a new construction [3]). This happens mainly because concrete is a brittle fracturing material. This means that as soon as the peak stress level is exceeded there is an immediate loss of load-bearing capacity which ultimately leads to failure[126]. However, even before complete failure occurs, structures develop cracks and micro-cracks that make it more prone to early deterioration because they allow supplementary penetration of hazardous species (permeability is known to be the key factor responsible for aggressive ions ingress).

Commonly adopted solutions to maximize mechanical performances are generally targeting an optimized packing of constituents in the concrete mix. This is achieved by lowering the w/c ratio, or by using fillers, superplasticizers and fibres. This brings significant overall improvement to the flexural strengths and toughness, but it does not change the nature of cohesion in cement paste which is the key ingredient that glues the components together. It is agreed that the cohesion of cement paste occurs through the formation of a network of nanoparticles of a C-S-H [40]. AFM studies and numerical simulations showed that cohesion in C-S-H comes from physical surface forces and very short ranged ionic-covalent forces [6]. Modifying these forces could in principle modify the cohesion and result in drastic improvement of mechanical properties.

This novel approach has been investigated in this thesis. The strategy adopted here was to introduce long range chemical bonds between cement hydrates. This has been done by hybridizing cement with organofunctional alkoxysilanes prior to hydration.

## Conclusions and perspectives

The possibility of creating hybrid trialkoxysilane – calcium silicate hydrate materials have already been reported via sol-gel synthesis [127, 128].  $^{29}\text{Si}$  NMR evidenced the C-S-H structure for hybrid materials with partial replacement of silicon tetraedra with silane silicon. Moreover, silane grafted polymers have been confirmed to covalently bond to C-S-H [129]. Thus we have strong reasons to believe that new cement based materials displaying improved performances can be produced at macroscale as well.

Two methods of hybridizing cement with organofunctional silanes have been reported within this work. In the first part, hybridizing has been performed by direct dry blending of constituents. The study was focused on evaluating the macroscopical changes in cement pastes related to the presence of silanes. Because the results did not show any improvement and moreover there was loss in properties, it became clear that another approach is needed.

The second path developed aimed for a better understanding of the cement – silanes interactions. Therefore, silanes were adsorbed from an organic solvent and after equilibrium has been reached the excess of solvent with the unabsorbed silane fraction has been removed. A complementary technique, based on adsorbing a well defined dosage of silane from a solvent followed by evaporating the latter, has been developed for producing larger quantities of silane modified cement. The characterisation of silane modified substrates focused on investigating the changes in hydration kinetics and in rheological behaviour compared to neat cement pastes. In addition, mechanical measurements pointed out the increased flexural strength for silane hybridized cement compared to neat samples.

The most important findings, achievements and failures will be summarised in this chapter together with some suggestions for future work.

## **7.2 Conclusions on the silane modified cements obtained by dry blending of constituents**

The direct dry blending of constituents has been the simplest and the easiest way of preparing silane modified cements. The method has been commonly reported to be employed for treatment of fillers with silane agents and therefore employed. The hypothesis considered here was that upon mixing silanes chemically connect to the silicates, thus hybridizing cement prior to hydration.

Standard physico-mechanical tests have been performed to evaluate the macroscopic changes in properties of the modified systems. In addition heat development measurements have been used to better understand the changes observed.

It was found that all silanes induce a dispersive effect on cement pastes and mortars indicated by reduced water demands for pastes to reach standard consistency and improved flow table spreads. This is most probably due the carbonic chain carrying the organic function moiety. The dispersive effect was found to scale up with the dosage of silane and with the nature of silane agents. AEAPTMS and GTO give always better fluidifying effects compared to APTES. This originates in the nature of the bonding to substrate. It is believed that AEAPTMS and GTO are more likely to chemically bond to cement, whereas APTES has significant additional physical substrate interactions. This implies also that the nature of the dispersive capacity is different and depending on the nature of the bonding to the substrate. A clear distinction was not possible, but it is assumed that steric repulsive effects are dominant in preventing cement particles to agglomerate for APTES modified pastes, while AEAPTMS and GTO pastes display mainly repulsion originating in the electrical double layer forces.

Mechanical measurements pointed out the loss in performances for silane modified cement pastes and mortars compared to neat pastes and mortars. All measured values were lower than the ones for reference. This was because silanes significantly retard cement hydration by extending the induction period and drastically reducing the degree of hydration, mainly of alite. This has been indicated by the heat development



curves. In addition, it was found that an increased silane dosage results in longer induction periods and decreased rates of heat release. Furthermore, calorimetric measurements evidenced that all time Vicat set-time tests estimated unrealistically the setting times for silane modified systems. This implies that silane modified pastes stiffen prior to set.

It has turned out that simple dry blending of alkoxysilanes with cement at room temperature is not successful in preparing modified cement systems that display improved mechanical performances. The reason is probably because the dosages employed were too high. The disadvantage in moving to lower silane dosages is the obvious loss in homogeneity of the mix, because tiny proportions of silanes would tend to concentrate in localized lumps rather than optimum covering the substrate surface. Consequently, it became clear that a different approach is needed in order to effectively disperse lower amounts of silanes through anhydrous cement particles.

### **7.3 Conclusions on the silane modified cements obtained by liquid phase adsorption of silanes to cement**

Modifying cement with silane agents from liquid phase has been a successful way of preparing hybrid organo-mineral compounds never reported in literature for the case of cementitious materials. However, the method is extensively employed for tailoring silica particles with silane agents used in differing areas of science, engineering and medicine.

The main idea was to effectively disperse low amounts of silanes through cement particles prior to its hydration without altering its reactivity. This has been achieved using organic solvents (ethanol and toluene) inert to both adsorbate and adsorbent.

In a first step a detailed study on the adsorption process of silanes towards cement substrate has been successfully performed by quantifying the silane fractions consumed and remaining in solution. The adsorption data have been correlated with the experimental results collected from the calorimetric and rheological investigations carried out on the modified substrates. In a second step cement grains were modified with the desired silane fraction added as a dilute solution of silane in

## Conclusions and perspectives

ethanol. The solvent was later removed by evaporation. The development of this complementary liquid phase adsorption methodology was necessary in order to produce large quantities for mechanical tests.

Results indicated that silanes retard cement hydration. Ethanol was the most effective solvent for silane adsorption, keeping retardation of silane modified pastes within acceptable levels; toluene favoured higher retardation of silane modified pastes, in particular at low dosages. Thus, the work focused accordingly in adsorbing silanes from ethanol. Also, it has been found that for AEAPTMS and GTO there are always lower absorbed fractions compared to APTES. Surprisingly, the effects on cement hydration indicated significantly stronger retarding effects associated to AEAPTMS and GTO compared to APTES for similar adsorbed dosages. This has been interpreted in terms of nature of interactions with the substrate. We assume that AEAPTMS and GTO is predominantly chemically bond to cement, while APTES appears to be mainly physically adsorbed to cement.

In terms of surface coverage, for APTES, it has been calculated that the adsorbed fractions corresponding to plateau region are far too high for monolayer-level coverage. In fact five up to ten layers were found whether adsorption had been carried out in toluene or ethanol. However, TEM investigations evidenced that silanes agglomerate randomly in lumps, rather than uniformly covering the surface. Moreover, parallel investigations on carried out on  $C_3S$  and cement proved that silanes are not entirely adsorbed on silicates as initially assumed.

The fact has been confirmed by rheological measurements which pointed out that there is substantial stiffening of the structure in the very early ages, reflected as a stiffening effect. Higher initial heat releases have also been observed for silane modified cement pastes compared to neat paste. This strongly suggests that silanes affect the reactivity of aluminates as well. Besides this inconvenient stiffening effect, the presence of individual silane agents in cement increases the pastes ability to withstand loads above the critical deformation. This has been related with the hypothesised cross-linked siloxane network build within the cement pastes and is reflected in an additional quasi linear zone extending the LVD. This is an extremely

valuable finding, because the chemical stability of APTES functionalized materials is reported to be limited to neutral or slightly alkaline media.

Another major achievement was the continuous increase in bending strength over time for silane modified cements compared to neat cement. At 28 days silanes modified cement displayed higher bending strength by 35% compared to neat paste. This increase was assigned to the presence of siloxane based network which develops within the cement paste and surprisingly is long-term stable. However, samples demoulding at 24 h turned out to be rather problematic indicating reduced paste cohesion.

Blended systems of individually silane modified cement have been investigated also but to a rather limited extent. So far, results suggest that there is no chemical reaction occurring between the end groups of individually silane modified cements which would bring additional benefits, mainly in terms of longer LVD.

## 7.4 Perspectives

It has been shown that silanes retard the hydration of cement, mainly of silicates by extending the length of the dormant period and by reducing the rate of maximum heat release. This resulted in reduced degree of hydration. Direct evidence has been presented concerning the fact that silanes do not affect the dissolution neither the nucleation process of hydrates, but they seem to limit their growth. This subject must be looked into more thoroughly because overcoming the retardation could bring major benefits in the future use of silane modified cements.

Nevertheless, our investigations clearly reflected the fact that silanes are not entirely adsorbed on silicates. They affect also the reactivity of the aluminates leading to premature stiffening of pastes that correlates well with higher initial amounts of heat release in case of modified pastes compared to neat. Further investigations on silane modified  $C_3A$  are needed in order to clearly assess how silanes affect its reactivity.

## Conclusions and perspectives

This should help understand and surpass, if possible, cement paste inconvenient early age stiffening.

Another important aspect to be further investigated is the increase in the paste ability to deform quasi elastically once the structure has been broken down and how this capacity is related to the dosage of silane agents on individual silane modified cement pastes and on blended systems. Our experiments indicated that above the critical deformation, individually silane modified cement pastes display significant changes in terms of flow behaviour compared to neat pastes. Surprisingly, upon blending the effect is lost. However, blending low level additions of individually silane modified cements reverses the effect. More work would be helpful in order to correlate these effects. The next stage will have to be probably mechanical tests on blended silane modified cements after the above mentioned issued have been solved.

Although the strength tests showed continuous improvement in properties, there was a problematic early age specimens demoulding that raised questions on what might cause the temporarily reduced paste cohesion. What would be helpful are additional strength tests on cement pastes containing ethanol added as admixture in similar amounts as the ones supposed to be released as by product of silane hydrolysis. This should clearly evidence whether ethanol is preventing early paste rigidification or not.

On long term perspectives, alternative blending of silane modified cement with reactively compatible silane functionalized nanosilica would be worth looking into. Because of its high surface area functionalized nanosilica particles should increase the probability of end groups to contact and react. This should contribute substantially to increasing the cohesion in cement paste by chemically bonding the hydrates. Ultimately this should results in significant increased strength and better durability.



## References



## References

1. Maxwell-Cook, P., *Editor's Comment*, in *World Cement*, 2009, p. 5.
2. Scrivener, K.L. and R.J. Kirkpatrick, *Innovation in use and research on cementitious material*, Cement and Concrete Research, 2008, **38**(2), p. 128-136.
3. Bentur, A., Mindess, S., Katz, A., *Future of concrete: Vision and Challenges*, in *Anna Maria Workshop*, 2004.
4. Richard, P., Cheyrezy, M., *Reactive powder concrete with high ductility and 200-800MPa compressive strenght*, ACI 1994, **144**, p. 507-518.
5. Geiker, M., *Basic mechanisms. NANOCEM RTN, 3rd training course.*, 2007, Madrid, Spain.
6. Pellenq R.J.-M, L.N., van Damme H., *Engineering the bonding in CSH: The ionic covalent framework*, Cement and Concrete Research, 2008, **38**, p. 159-174.
7. Pellenq, R.J.-M., *Sur l'origine de la cohésion du ciment*, L'actualité Chimique, 2004, **273**, p. 12-22.
8. Van Damme, H., R. Pellenq, and A. Delville, *La physique des liaisons entre hydrates et les moyens d'agir au niveau moléculaire.*, Revue française de génie civil, 1998, **2**(7), p. 767-779.
9. Jonsson, B., et al., *Controlling the Cohesion of Cement Paste*, Langmuir, 2005, **21**(20), p. 9211-9221.
10. Plassard, C., et al., *Nanoscale Experimental Investigation of Particle Interactions at the Origin of the Cohesion of Cement*, Langmuir, 2005, **21**(16), p. 7263-7270.
11. Pellenq, R.J.-M., Gmira, A., van Damme, H. *The nature of cohesion forces in hardened cement-based materials: the view from the nanoscale* in *12th ICCG*, 2007, Canada.
12. Nonat, A., *Cohesion of cement paste at nanoscale*, in *NANOCEM MCRTN 3rd training course.*, 2008, Prague, Czech Republic.
13. Itul, A., Nonat, A., Flatt, R. J., Svegli, . *The effects of silane on the hydration of cements*, Les annals de chimie et physique, 2008, **33**, p. 283-290.
14. Taylor, H.F.W., *Cement chemistry*, 1997, Academic press, 475.



## References

15. Young, J.F., Gartner, E. M., Damidot, D. A., Jawed, I., *Hydration of Portland cement in Second edition of "Structure and performance of Cements"* 2000.
16. Jolicoeur, C. and M.-A. Simard, *Chemical admixture-cement interactions: phenomenology and physico-chemical concepts.*, Cement & Concrete Composites, 1998, **20**, p. 87-101.
17. Struble, L. and G.K. Sun, *Viscosity of Portland cement paste as a function of concentration*, "Advn Cem Bas Mat, 1995; 2:62-69", 1995.
18. Scrivener, K.L., *Introduction:General concepts. NANOCEM MCRTN. 1st training course*, 2006, Aalborg, Denmark.
19. Aitcin, P.C., *Binders for durable and sustainable concrete*, 2006.
20. Powers, T.C., *Structure and physical properties of hardened Portland cement paste*, Journal of american ceramic society, 1958, **41**(1), p. 1-6.
21. H.F.W.Taylor, *Cement chemistry*, 2ème édition, Edition Thomas Telford - Londres, 1997.
22. Jiang S.P., M.J.C., Nonat A., *Studies on mechanism and physico chemical parameters at the origin of the cement setting. II Physico -chemical parameters determining the coagulation process*, cement and Concrete Research, 1996, **26**, p. 491-500.
23. Rueb, C.J. and C.F. Zukoski. *Interparticle attractions and the mechanical properties of colloidal gels*, in *Materials Research Society Symposium Proceeding*, 1992, Pittsburg.
24. Hansen, T.C., *Physical structure of hardened cement paste. A classical approach*, Materiaux et Constructions, **19**(114), p. 423-436.
25. Feldman, R.F. and P.J. Sereda, *A New model for hydrated Portland cement and its practical implications*, Engineering Journal, 1970, **August/September** p. 53-59.
26. Jennings, H.M., *A model for the microstructure of calcium silicate hydrate in cement paste*, Cement and Concrete Research, 2000, **30**(1), p. 101-116.
27. Richardson, I.G., *The nature of C-S-H in hardened cements*, Cement and Concrete Research, 1999, **29**(8), p. 1131-1147.
28. Pellenq R.J.-M, G.A., van Damme H. *The nature of cohesion forces in hardened cement-based materials: the view from the nanoscale in 12th ICCG*, 2007, Canada.

## References

29. Richardson, I.G., *The calcium silicate hydrates*, Cement and Concrete Research, 2008, **38**(2), p. 137-158.
30. Cong, X. and R.J. Kirkpatrick, *<sup>29</sup>Si MAS NMR study of the structure of calcium silicate hydrate*, Advanced Cement Based Materials, 1996, **3**(3-4), p. 144-156.
31. Van Damme, H., *Colloidal chemo-mechanics of cement hydrates and smectite clays : cohesion vs. swelling*, Encyclopedia of Surface and Colloid Science, 2002, p. 1087-1103.
32. Delville, A. and P. Laszlo, *The origin of the swelling of clays by water*, Langmuir, 1990, **6**(7), p. 1289-1294.
33. Hamid, S.A., *The cristal structure of the 11A natural tobermorite  $Ca_{2.25}[Si_3O_{7.5}(OH)_{1.5}] \cdot 1 H_2O$* , Zeitschrift für Kristallographie, 1981, **154**, p. 189.
34. Soroka, I. and P.J. Sereda, *The structure of cement-stone and the use of compacts as structural models*, Proc. 5th Int. Sym. on the chemistry of cement, Tokyo 1968. Part III, Properties of cement, 1968, p. 67-73.
35. Relis, M. and I. Soroka, *Compressive strength of low-porosity hydrated Portland cement*, J. Amer. Ceram. Soc., 1980, **63**, p. 690-694.
36. Verwey, E.J.W. and J.T.G. Overbeek, *Theory of the stability of lyophobic colloids*, 1948, Amsterdam, Elsevier.
37. Nonat, A., *Cohesion of cement paste at nanoscale*. In NANOCEM MCRTN 4th training course, 2008, Prague, Czech Republic.
38. Israelachvili, J., *Intermolecular & Surface Forces, 2nd Edition*, 1992, San Diego, Academic Press, Harcourt Brace & Company.
39. Wernersson, E., *Theoretical investigations of the role of the ion-ion correlations and ion-specific interactions in electrical double layers*, in Department of Chemistry, 2009, University of Gothenburg.
40. Jonsson, B., Wennerstrom, H., Nonat, A., Cabane, B., *Onset of Cohesion in Cement Paste*, Langmuir, 2004, **20**(16), p. 6702-6709.
41. Guldbrand, L., Jonsson, B., Wennerstrom, H., Linse, P., *Electrical double layer forces. A Monte Carlo study*, Journal of Physical Chemistry. 80(5) 2221-2228 (1984), 1984.

## References

42. Pellenq, R.J.-M., Crespin, M., Lequeux, N., Menager, C., Costalin, L., Delville, A., Caillol, J.-M., Van Damme, H. *A (NTV) Monte-carlo study of the stability of charged interfaces application to cement and clay minerals.*, in *Second Rilem Workshop on Hydration and Setting : "Why does cement set ?"* 1997, Dijon, Rilem Editions.
43. Delville, A. and R.J.-M. Pellenq, *Electrostatic Attraction and/or Repulsion Between Charged Colloids: A (NVT) Monte-Carlo Study*, Molecular Simulation, 2000, **24**(1), p. 1 - 24.
44. Jonsson, B. and H. Wennerstrom, *When ion-ion correlations are important in charged colloidal systems*, in *Theoretical Chemistry and Physical Chemistry I*, 2002, Lund University, Lund, Sweden, p. 35.
45. Lesko, S., Lesniewska, E., Nonat, A., Mutin, J.-C., Goudonnet, J.-P., *Investigation by atomic force microscopy of forces at the origin of cement cohesion*, Ultramicroscopy, 2001, **86**(1-2), p. 11-21.
46. Jonsson, B., et al., *Onset of Cohesion in Cement Paste*, Langmuir, 2004, **20**(16), p. 6702-6709.
47. Goyal, S., *Silanes: chemistry and applications*, The journal of Indian Prosthodontic Society, 2006, **6**(1), p. 14-18.
48. Corning, D., *A guide to silane solutions*.
49. Plueddemann, E., *Silane coupling agents*, ed. P. press, 1991, NY.
50. DiBenedetto, A.T., *Tailoring of interfaces in glass fiber reinforced polymer composites: a review*, Materials Science and Engineering A, 2001, **302**(1), p. 74-82.
51. van Ooij, W.J., Zhu D., Stacy, M., Seth, A., Mugada, T., Gandhi, J., Puomi, P., *Corrosion Protection Properties of Organofunctional Silanes—An Overview*, Tsinghua Science and technology, 2005, **10**(6), p. 639-664.
52. Geniosil, *Organofunctional silanes- molecular bridges forge stable bonds*.
53. Stermann, S. and J.G. Marsden, *SILANE COUPLING AGENTS*, Industrial & Engineering Chemistry, 1966, **58**(3), p. 33-37.
54. Miller, D.J. and H. Ishida, *Identification of covalent bonds between substituted silanes and inorganic surfaces*, in *Chemically modified surfaces. Silanes surfaces and interfaces.*, Donald E. Leyden.
55. Luan, Z., Fournier, J. A., Wooten, J. B., Miser, D. E., *Preparation and characterization of (3-aminopropyl)triethoxysilane-modified mesoporous*

## References

- SBA-15 silica molecular sieves*, Microporous and Mesoporous Materials, 2005, **83**(1-3), p. 150-158.
56. Liu, X.M., J.L. Thomason, and J. F.R., *Differential of silane adsorption onto model E-glass surfaces from mixed solutions of amino and glycidyl silanes*, in *Silanes and other coupling agents*, Ed.K.L.Mittal, 2007.
57. Kallury, K., P. Macdonald, and M. Thompson, *Effect of surface water and base catalysis on the silanization of silica by aminopropyl alkoxysilanes studied by X-ray Photoelectron Spectroscopy and <sup>13</sup>C Cross-Polarisation/Magic Angle Spinning Nuclear Magnetic Resonance*, Langmuir, 1994, **10**, p. 492-499.
58. Caravajal, G.S., D.E. Leyden, and G.E. Maciel, *Solid-state NMR studies of aminopropylsilane modified silica*, in *Chemically modified surfaces*, D.E. Leyden, 1986, Taylor & Francis, Inc.
59. Shimizu, I., Okabayashi, H., Taga, K., Yoshino, A., Nishio, E., O'Connor, C. J., *Raman scattering study of the interaction of 3-aminopropyltriethoxy silane on silica gel. Time-dependent conformational change of aminopropylsilyl segments*, Vibrational Spectroscopy, 1997, **14**(1), p. 125-132.
60. McGovern, M.E., K.M.R. Kallury, and M. Thompson, *Role of Solvent on the Silanization of Glass with Octadecyltrichlorosilane*, Langmuir, 1994, **10**(10), p. 3607-3614.
61. Golub, A.A., A.I. Zubenko, and B.V. Zhmud, *[gamma]-APTES Modified Silica Gels: The Structure of the Surface Layer*, Journal of Colloid and Interface Science, 1996, **179**(2), p. 482-487.
62. Ogasawara, T., Yonehara, H., Okabayashi, H., O'Connor, C. J., *Raman scattering study of [gamma] polyaminopropylsiloxane' aggregates and conformational change of aminopropylsilyl segments*, Colloids and Surfaces A: Physicochemical and Engineering Aspects, 2000, **168**(2), p. 147-158.
63. Simon, A., Cohen-Bouhacina, T., Porté, M. C., Aimé, J. P., Baquey, C., *Study of Two Grafting Methods for Obtaining a 3-Aminopropyltriethoxysilane Monolayer on Silica Surface*, Journal of Colloid and Interface Science, 2002, **251**(2), p. 278-283.
64. Miller, A.C. and J.C. Berg, *Effect of silane coupling agent adsorbate structure on adhesion performance with a polymeric matrix*, Composites Part A: Applied Science and Manufacturing, 2003, **34**(4), p. 327-332.

## References

65. Slomkowski, S., Miska, B., Chehimi, M.M., Delamar, M., Cabet-Deliry, E., Majoral, J.-P., Caminade, A.-M., *Inorganic-organic systems with tailored properties controlled on molecular, macromolecular and microscopical level*, Reactive and functional polymers, 1999, **41**, p. 45-57.
66. Schleifstein, R., *Coated microparticles, plastic compositions and methods*, 2002, Innovative Concepts Unlimited, LLC, USA.
67. Xiameter, *A Guide to Silane Solutions.Mineral and Filler Treatment*, D. Corning.
68. Yang, R., Liu, Y., Wang, K., Yu, J., *Characterization of surface interaction of inorganic fillers with silane coupling agents*, Journal of Analytical and Applied Pyrolysis, 2003, **70**(2), p. 413-425.
69. Bruce, I.J. and T. Sen, *Surface Modification of Magnetic Nanoparticles with Alkoxysilanes and Their Application in Magnetic Bioseparations*, Langmuir, 2005, **21**(15), p. 7029-7035.
70. Zucchi, F., Grassi, V., Frignani, A., Trabanelli, G., *Inhibition of copper corrosion by silane coatings*, Corrosion Science, 2004, **46**(11), p. 2853-2865.
71. Wu, D., J. Liu, and Y. Wang, *Enhancing indium tin oxide (ITO) thin film adhesiveness using the coupling agent silane*, Applied Surface Science, **256**(9), p. 2934-2938.
72. <http://www.specialchem4polymers.com/tc/silane-crosslinking-agents/index.aspx?id=mechanism>. SpecialChem web page, Series, SpecialChem web page, [cited].
73. Toutanji, H.A., El-Korchi, T., *The influence of silica fume on the compressive strength of cement paste and mortar*, Cement and Concrete Research, 1995, **25**(7), p. 1591-1602.
74. Xu, Y., Chung, D.D.L., *Cement of high specific heat and high thermal conductivity, obtained by using silane and silica fume as admixtures*, Cement and Concrete Research, 2000, **30**, p. 1175-1178.
75. Xu, Y., Chung, D.D.L., *Improving the workability and strength of silica fume concrete by using silane-treated silica fume*, Cement and Concrete Research, 1999, **29**, p. 451-453.
76. Yunsheng Xu, C.D.D.L., *Improving silica fume cement by using silane*, Cement and Concrete Research, 2000, **30**, p. 1305-1311.

## References

77. Jingyao Cao, C.D.D.L., *Improving the dispersion of steel fibers in cement mortar by the addition of silane*, Cement and Concrete Research, 2001, **31**, p. 309-311.
78. Yunsheng Xu, C.D.D.L., *Reducing the drying shrinkage of cement paste by admixture surface treatments*, Cement and Concrete Research, 2000, **30**, p. 241-245.
79. Yunsheng Xu, C.D.D.L., *Silane-treated carbon fiber for reinforcing cement*, Carbon, 2001, **39**, p. 1995-2001.
80. Yunsheng Xu, C.D.D.L., *Increasing the specific heat of cement paste by admixture surface treatments*, Cement and Concrete Research, 1999, **29**, p. 1117-1121.
81. Chemielewska B, C.L., Sustersic J., Zajc A., *The influence of silane coupling agents on the polymer mortar*, Cement and Concrete Research, 2006, **28**, p. 803-810.
82. Svegl F., S.-S.J. *Concrete nad mortars witht the addition of mineral fillers and coupling agents*, in *Eurofillers 03*, 2003, Alicante ( Spain)
83. Svegl F., S.-S.J., Linkon M., Skrlep L., Kalcher K., . *Preparation and characterization of polymer modified mortars with the addition of copling agents*, in *International Congress on Polymers in Concrete*, 2004, Berlin, Germany.
84. Svegl F., S.-S.J., *The influence of aminosilanes on macroscopic properties of cement paste*, Cement and Concrete Research, 2008, **38**, p. 945-954.
85. Standardisation, E.C.f., *European standard EN 196-3. Methods of testing cement - Part 3: Determination of setting time and soundness*, 2005.
86. Gartner, E.M., et al., *Hydration of portland cement*, p. 57-113.
87. Jiang, S.P., Mutin, J.C., Nonat, A. *Effect of melment superplasticizer on C3S hydration: from suspension to paste.*, in *3rd Beijing International Symposium on Cement and Concrete.*, 1993.
88. K.C. Vrancken, P.v.d.V., K. Possemiers, P. Grobet and E.F. Vansant., *Chemically Modified Surfaces*, 1994, The Royal Society of Chemistry, Cambridge, UK (1994), p. 46.
89. Yamada, K., Tomoo Takahashi, Shunsuke Hanehara and Makoto Matsuhisa et al., *Effects of the chemical structure on the properties of polycarboxylate-type superplasticizer*, Cement and Concrete Research, 2000, **30**(2), p. 197-207.

## References

90. Li, C.-Z., et al., *Effects of polyethylene oxide chains on the performance of polycarboxylate-type water-reducers*, Cement and Concrete Research, 2005, **35**(5), p. 867-873.
91. Sant, G., C.F. Ferraris, and J. Weiss, *Rheological properties of cement pastes: A discussion of structure formation and mechanical property development*, Cement and Concrete Research, 2008, **38**(11), p. 1286-1296.
92. Howarter, J.A. and J.P. Youngblood, *Optimization of Silica Silanization by 3-Aminopropyltriethoxysilane*, Langmuir, 2006, **22**(26), p. 11142-11147.
93. Xu, Z., Q. Liu, and J.A. Finch, *Silanation and stability of 3-aminopropyl triethoxy silane on nanosized superparamagnetic particles: I. Direct silanation*, Applied Surface Science, 1997, **120**(3-4), p. 269-278.
94. Blitz, J.P., R.S.S. Murthy, and D.E. Leyden, *Studies of silylation of Cab-O-Sil with methoxymethylsilanes by diffuse reflectance FTIR spectroscopy*, Journal of Colloid and Interface Science, 1988, **121**(1), p. 63-69.
95. Blitz, J.P., R.S. Shreedhara Murthy, and D.E. Leyden, *The role of amine structure on catalytic activity for silylation reactions with Cab-O-Sil*, Journal of Colloid and Interface Science, 1988, **126**(2), p. 387-392.
96. Morrall, S.W. and D.E. Leyden, *Modification of siliceous surfaces with alkoxysilanes from a nonaqueous solvent in Chemically modified surfaces* D.E. Leyden, 1986, Taylor & Francis, Inc.
97. Brzoska, J.B., I.B. Azouz, and F. Rondelez, *Silanization of Solid Substrates: A step toward reproducibility*, Langmuir, 1994, **10**, p. 4367-4373.
98. Caravajal, G.S., et al., *Structural characterization of (3-aminopropyl)triethoxysilane-modified silicas by silicon-29 and carbon-13 nuclear magnetic resonance*, Analytical Chemistry, 1988, **60**, p. 1776-1786.
99. Caravajal, G.S., et al., *Structural characterization of (3-aminopropyl)triethoxysilane-modified silicas by silicon-29 and carbon-13 nuclear magnetic resonance*, Analytical Chemistry, 2002, **60**(17), p. 1776-1786.
100. Kelly, D.J. and D.E. Leyden, *Thermodynamic and kinetic investigation of the protonation of silica-immobilized 3-aminopropylsilane*, Journal of Colloid and Interface Science, 1991, **147**(1), p. 213-224.
101. Murthy, R.S.S. and D.E. Leyden, *Quantitative determination of (3-aminopropyl)triethoxysilane on silica gel surface using diffuse reflectance*

## References

- infrared Fourier transform spectrometry*, Analytical Chemistry, 1986, **58**(6), p. 1228-1233.
102. Vrancken, K.C., et al., *Surface and structural properties of silica gel in the modification with gama-aminopropyltriethoxysilane*, Journal of Colloid and Interface Science, 1995, **174**, p. 86-91.
  103. Vrancken, K.C., et al., *Surface modification of silica gels with aminoorganosilanes*, Colloids and Surfaces A: Physicochemical and Engineering Aspects, 1995, **98**(3), p. 235-241.
  104. TCEI: *Adiabatic and semi-adiabatic calorimetry to determine the temperature increase in concrete due to hydration heat of the cement*, Materials and Structures, 1997, **30**(8), p. 451-464.
  105. Nicoleau, L., *Interactions physico-chimiques entre le latex et les phases minérales constituant le ciment au cours de l'hydratation*, Thèse de Doctorat, Université de Bourgogne, 2004.
  106. Tattersall G.H., B.P.F.G., *The rheology of fresh concrete*, 1983.
  107. E.C., B., *Fluidity and Plasticity*, 1922, New York, McGrawHill.
  108. Barnes, H.A., *The yield stress--a review or  $[\pi][\alpha][\nu][\tau][\alpha][\rho][\varphi][\iota]$ --everything flows?*, Journal of Non-Newtonian Fluid Mechanics, 1999, **81**(1-2), p. 133-178.
  109. Schultz, M.A. and L.J. Struble, *Use of oscillatory shear to study flow behaviour of fresh cement paste*, Cement Concrete Research, 1993, **23**(2), p. 273-282.
  110. Nachbaur, L., et al., *Dynamic mode rheology of cement and tricalcium silicate pastes from mixing to setting*, Cement and Concrete Research, 2001, **31**(2), p. 183-192.
  111. Zukoski, C.F. and L.J. Struble, *Rheology of Cementitious systems*, MRS bulletin, 1993, p. 39-42.
  112. Nonat, A., *Modelling hydration and setting of cement*, Ceramika/Ceramics, 2005, **92**.
  113. Tattersall, G.H. and P.F.G. Banfill *The rheology of fresh concrete*, 1983, Pitman Advanced Publishing Program, 356.
  114. Banfill, P.F.G. *Simultaneous measurements of hydration rate and rheology on cement pastes.*, in *Dijon*, 1991, 1st Int Workshop on hydration and setting.



## References

115. Betioli, A.M., et al., *Effect of HMEC on the consolidation of cement pastes: Isothermal calorimetry versus oscillatory rheometry*, Cement and Concrete Research, 2009, **39**(5), p. 440-445.
116. Van Der Voort, P. and E.F. Vansant, *Modification of the silica surface with aminosilanes*, Polish Journal of Chemistry, 1997, **71**, p. 550-567.
117. Mollah, M., et al., *A review of cement-superplasticizer intereactions and their models*, Advance Cement Research 2000, **12**(4), p. 153-61.
118. Winnefeld, F., et al., *Effects of the molecular architecture of comb-shaped superplasticizers on their performance in cementitious systems*, Cement and Concrete Composites, 2007, **29**(4), p. 251-262.
119. Bayer, T., et al., Macromol. Chem. Phys, 1999, (200), p. 852-857.
120. Jiang S.P., M.J.C., Nonat A., *Studies on mechanism and physico-chemical parameters at the origin of the cement setting.I The fundamental processes involved during the cement setting*, Cement and Concrete Research, 1995, **25**, p. 779-789.
121. Nonat, A., et al., *Physico-chemical parameters determining hydration and particle interactions during the setting of silicate cements*, Solid state ionics, 1997, **101-103**, p. 923-930.
122. Lootens, D., et al., *Yield stress during setting of cement pastes from penetration tests*, Cement and Concrete Research, 2009, **39**(5), p. 401-408.
123. Struble, L.J. and W.-G. Lei, *Rheological changes associated with setting of cement paste*, Advanced Cement Based Materials, 1995, **2**(6), p. 224-230.
124. Roessler, C., et al., *Influence of Hydration on the fluidity of normal Portland Cement pastes*, Cement and Concrete Research.
125. Jolicoeur, C., Simard, M.-A., *Chemical admixture-cement interactions: Phenomenology and physico-chemical concepts*, Cement and Concrete Composites, 1998, **20**(2-3), p. 87-101.
126. Kotsovos, M., *Concrete. A brittle fracturing material*, Materials and Structures, 1984, **17**(2), p. 107-115.
127. Minet J., A.S., Bresson B., Franceshini A., van Damme H., *Organic calcium silicate hydrate hybrids: a new approach to cement based nanocomposited*, Journal of Materials Chemistry, 2006, **16**, p. 1379-1383.

## References

128. Minet J., A.S., Bresson B., Sanchez C., *New Layered Calcium Organosilicate Hybrids with Covalently Linked Organic Functionalities* Chemistry of Materials, 2004, **16**, p. 3955-3962.
129. Franceschini A., A.S., Bresson B., Van Damme H., Lequeux N. *Cement silylated polymers nanocomposites*, in *International Congress on the Chemistry of Cement*, 2007, Canada.



## **Annexes**



## Annex I Glossary

The simplified writing used within this work, is given below:

### Chemical abbreviations

C = CaO

S = SiO<sub>2</sub>

H = H<sub>2</sub>O

A = Al<sub>2</sub>O<sub>3</sub>

F = Fe<sub>2</sub>O<sub>3</sub>

C<sub>3</sub>S - 3CaO·SiO<sub>2</sub>

Tricalcium silicate

C<sub>2</sub>S - 2CaO·SiO<sub>2</sub>

Dicalcium silicate

C<sub>3</sub>A - 3CaO·Al<sub>2</sub>O<sub>3</sub>

Tricalcium aluminate

C<sub>4</sub>AF - 4CaO·Al<sub>2</sub>O<sub>3</sub>·Fe<sub>2</sub>O<sub>3</sub>

Ferrite

CH - Ca(OH)<sub>2</sub>

Calcium hydroxide/ Portlandite

C-S-H - CaO·SiO<sub>2</sub>·H<sub>2</sub>O

Calcium silicate hydrates

C-A-H - CaO·Al<sub>2</sub>O<sub>3</sub>·H<sub>2</sub>O

Calcium aluminate hydrates

### Other notations

w/c    Water to cement ratio

L/S    Liquid to solid ratio

wt%    Weight percent

LVD    Linear viscoelastic domain

MIM    Maximum imposed modulus

### Abbreviations for techniques used or referred to

ESED	Environmental Secondary Electron Detection
EDS or	
EDX	Energy Dispersive X-Ray Spectroscopy
FTIR	Fourier transform infrared spectroscopy
ICP – AES	Inductively Coupled Plasma-Atomic Emission Spectroscopy
NMR	Nuclear Magnetic Resonance
SEM	Scanning Electron Microscopy
TEM	Transmission Electron Microscopy
XPS	X-Ray Photoelectron Spectroscopy
XRD	X-Ray Diffraction
XRF	X-Ray Fluorescence

## Annex II Patterns from TEM/EDS and SEM/EDS investigations

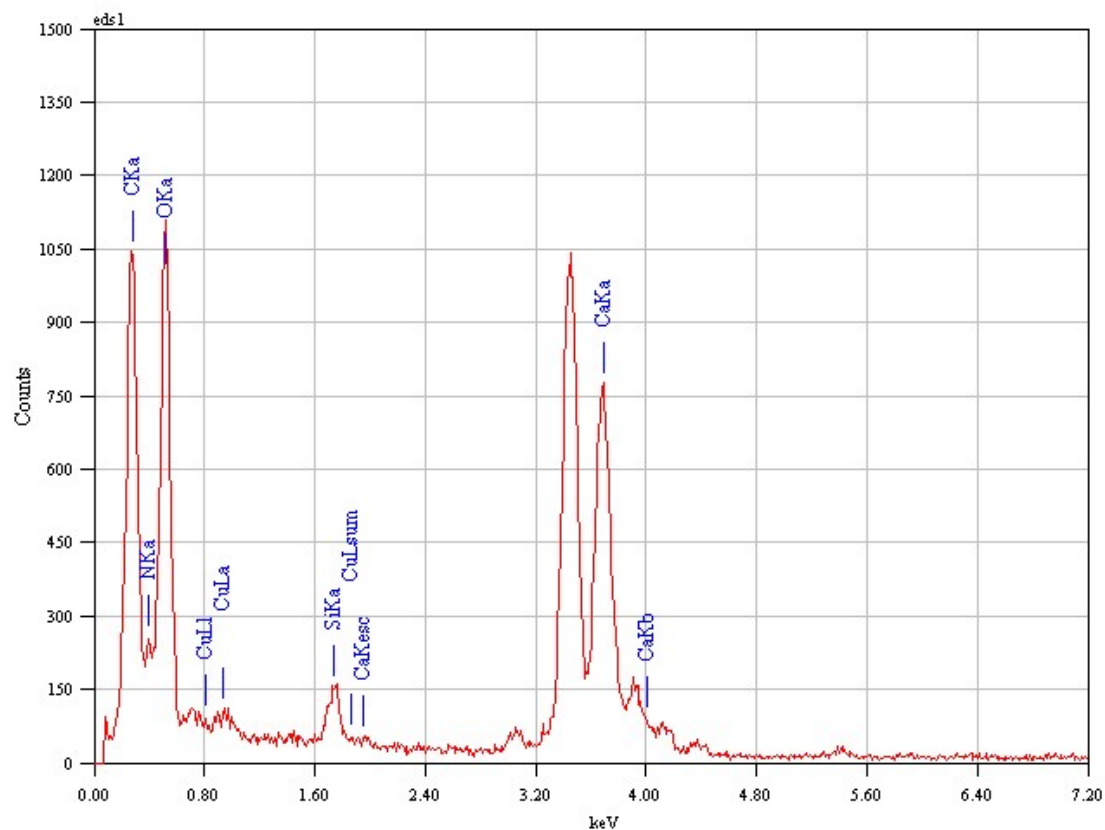


Figure II-1. Spectrogram from TEM EDS analysis evidencing nitrogen and thus confirming the presence of APTES on the surface of tricalciumsilicate.

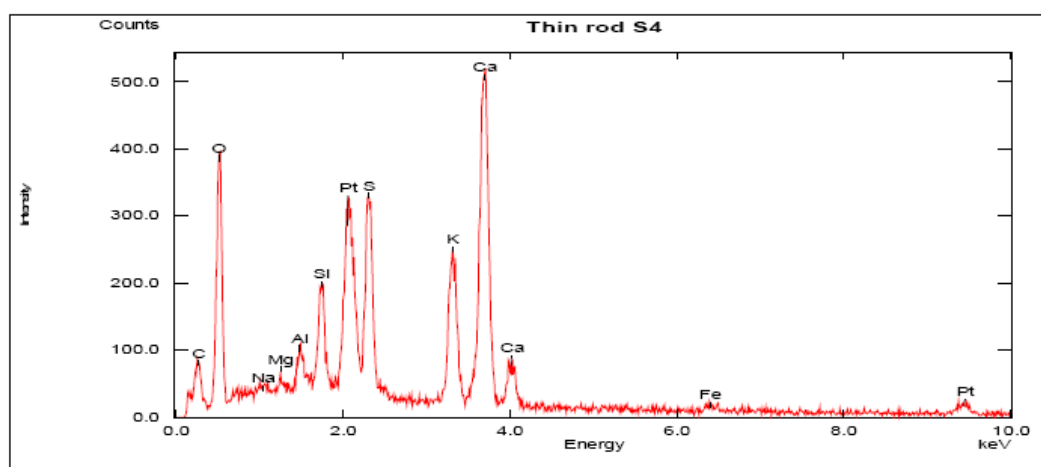
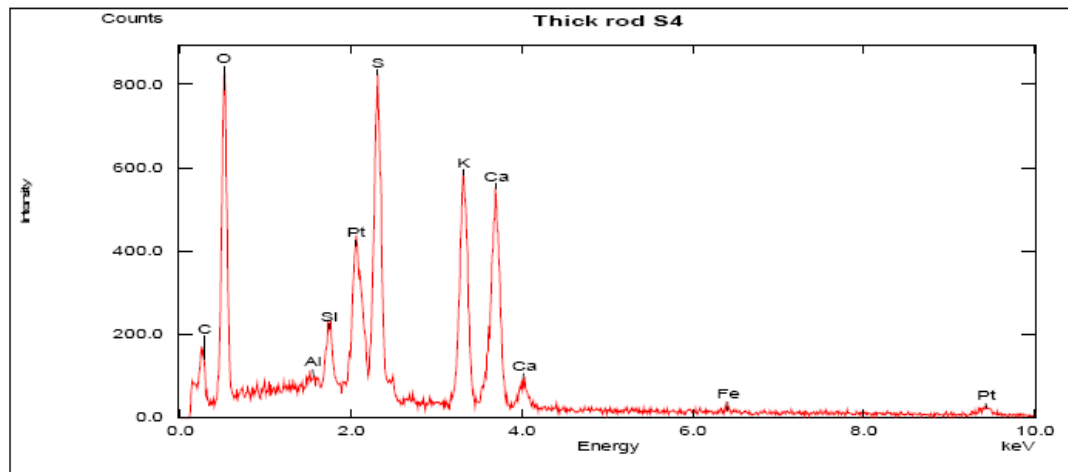


Figure II-2. Spectrogram from SEM EDX investigations indicating the presence of syngenite in neat cement pastes after 7h of hydration.





*Figure II-3. Spectrogram from SEM EDX investigations indicating the presence of syngenite in APTES modified cement pastes after 24h of hydration.*

### Annex III Data from investigations on the hydration kinetics of silane modified cement and tricalciumsilicate modified cement

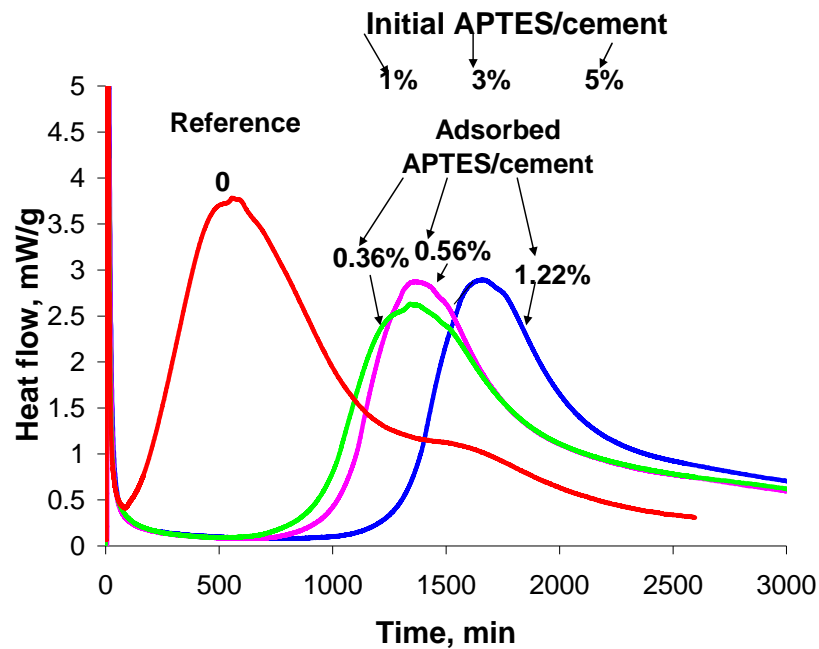


Figure III-1. Heat evolution curves for different APTES modified cement pastes prepared with constant  $w/c=0.3$ . APTES was adsorbed from toluene and the percentages are reported by weight of cement.

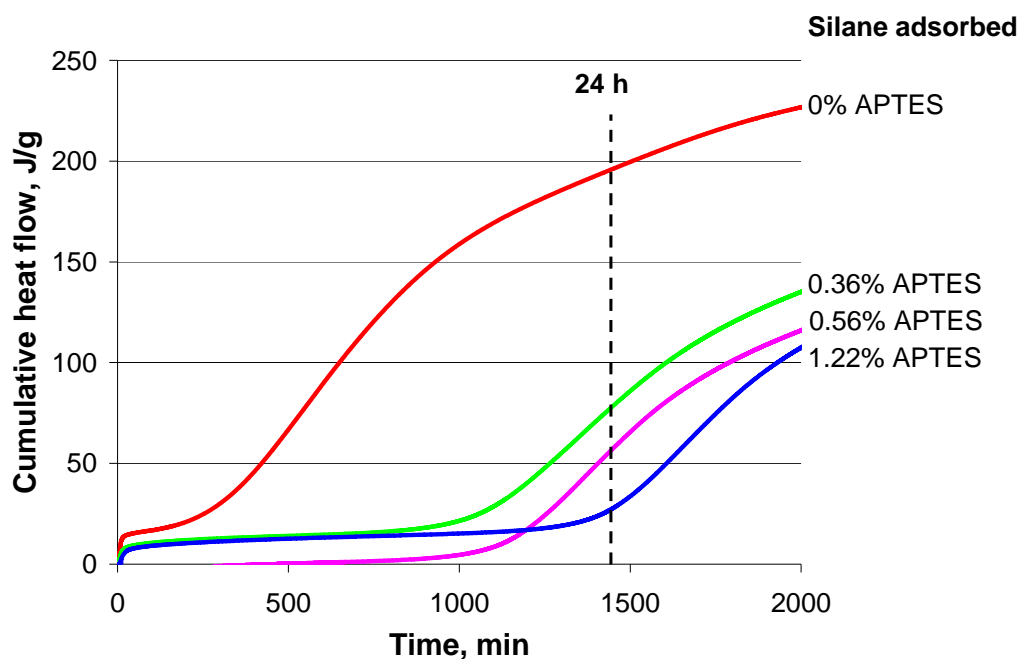


Figure III-2. Total heat flow curves for different APTES modified cement pastes prepared with constant  $w/c = 0.3$ . APTES was adsorbed from toluene and the percentages are reported by weight of cement.

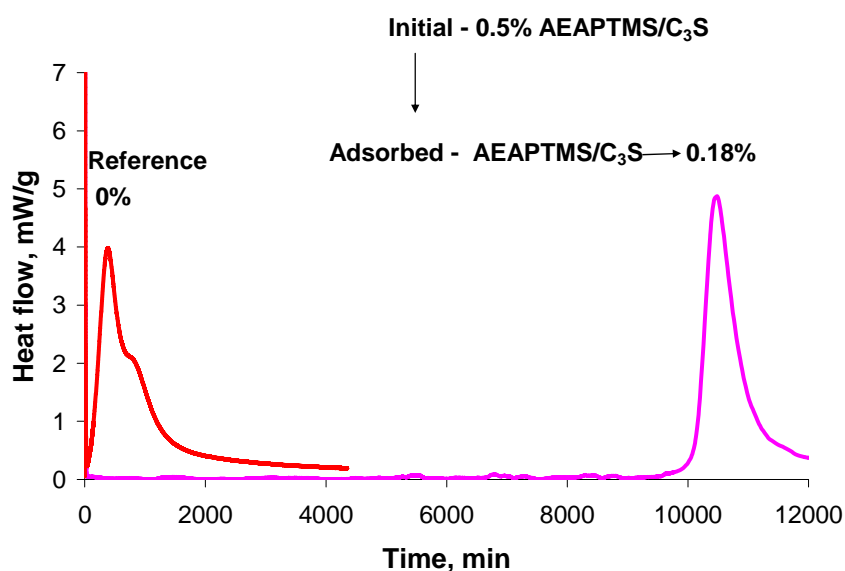


Figure III-3. Heat evolution curves for tricalciumsilicate and AEAPTMS tricalcium silicate pastes prepared with constant  $w/c=0.3$ . AEAPTMS was adsorbed from ethanol and its dosage is reported in percentage by weight of tricalciumsilicate.

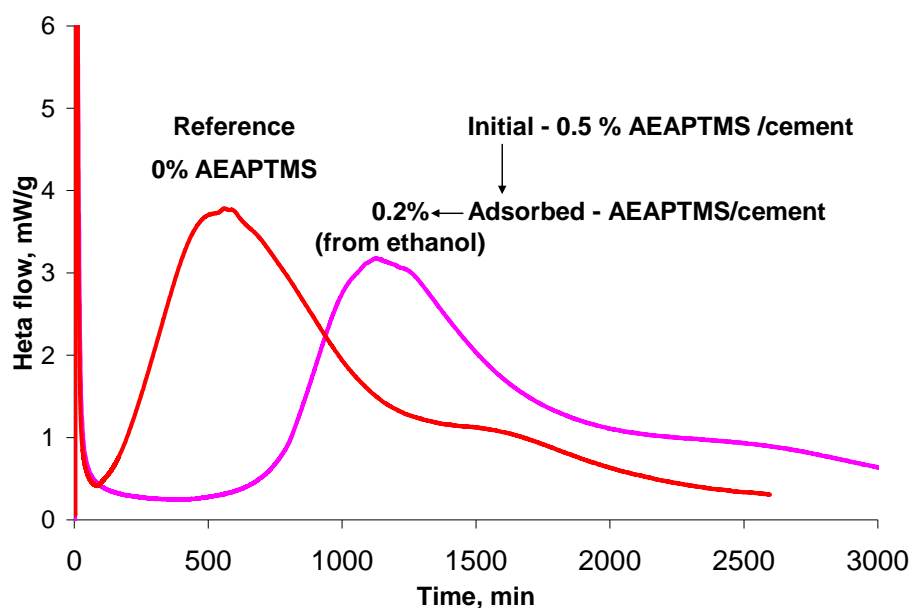


Figure III-4. Heat evolution curves for cement and AEAPTMS cement pastes prepared with constant  $w/c=0.3$ . AEAPTMS was adsorbed from ethanol and its dosage is reported in percentage by weight of cement.

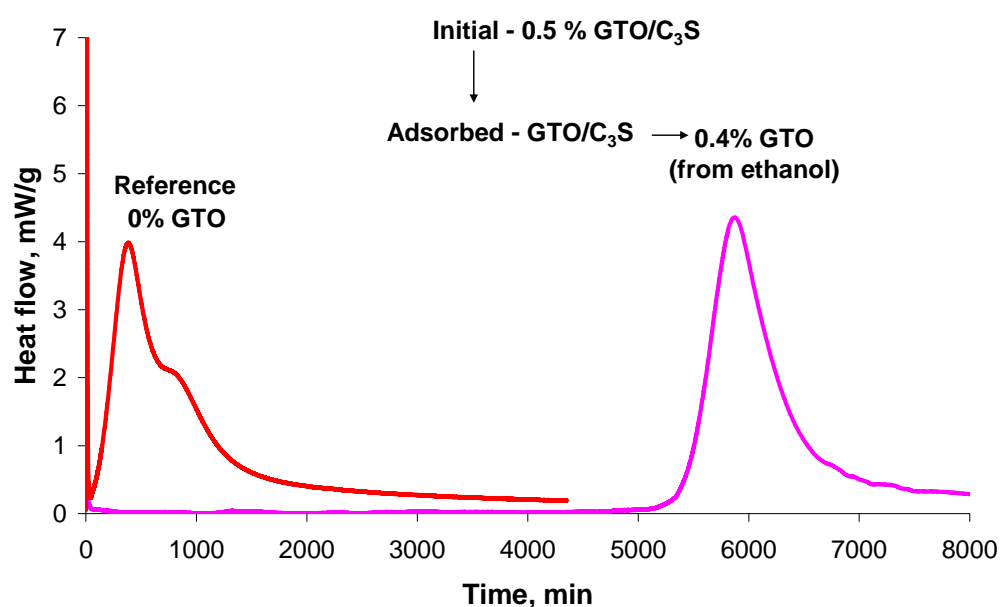


Figure III-5. Heat evolution curves for tricalciumsilicate and GTO tricalciumsilicate pastes prepared with constant  $w/c=0.3$ . GTO was adsorbed from ethanol and its dosage is reported in percentage by weight of tricalciumsilicate.

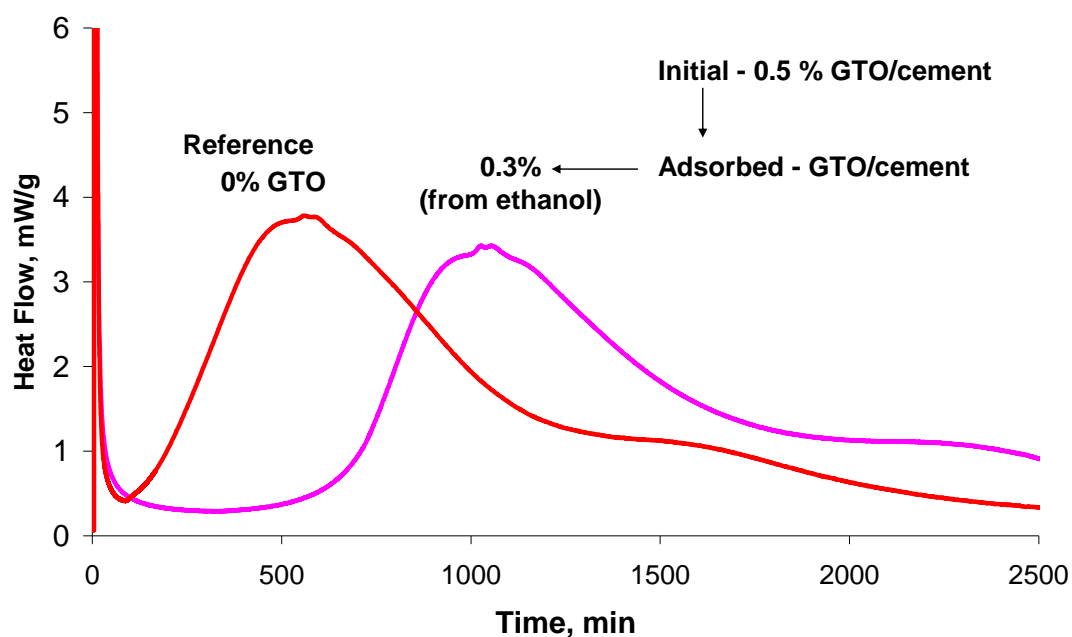


Figure III-6. Heat evolution curves for cement and GTO cement pastes prepared with constant  $w/c=0.3$ . GTO was adsorbed from ethanol and its dosage is reported in percentage by weight of cement.

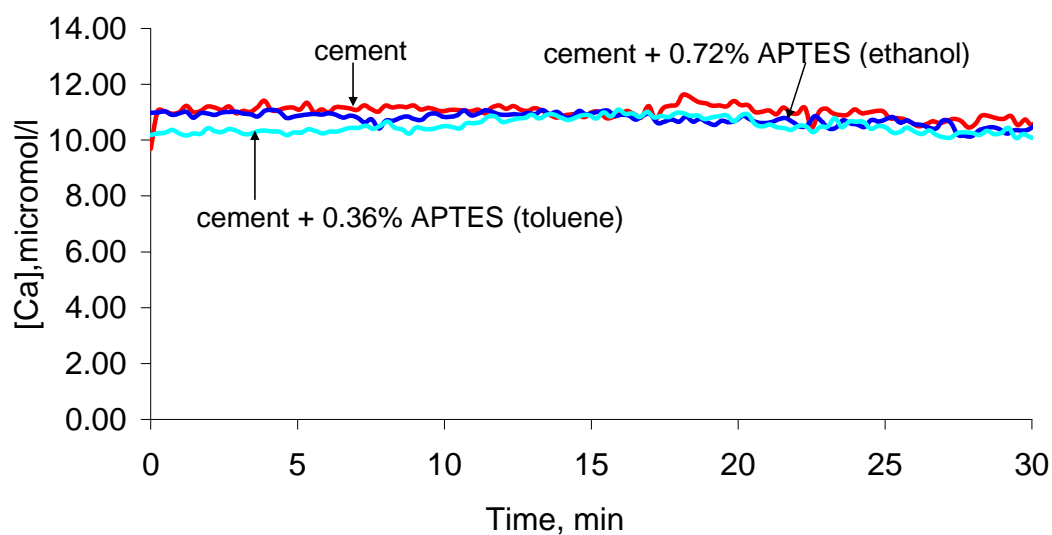


Figure III-7. Evolution of calcium ions concentrations during the first 30 minutes of hydration for cement and APTES modified cement, in lime ( $[Ca]=22 \text{ mmol/l}$ ),  $L/S=50\ 000$ . Percentage of silane by weight of cement.

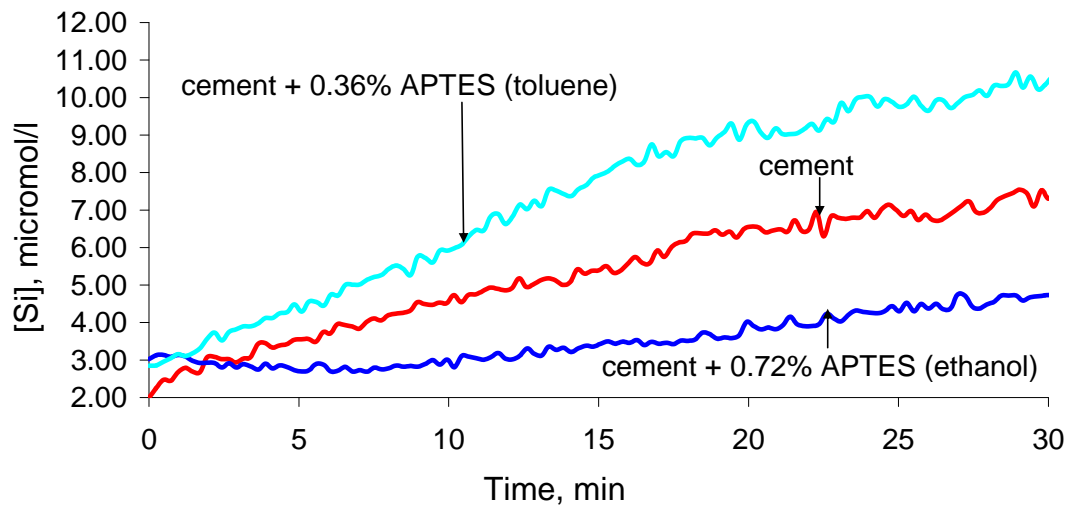


Figure III-8. Evolution of silicon ions concentrations during the first 30 minutes of hydration for cement and APTES modified cement, in lime ( $[Ca]=22$  mmol/l),  $L/S=50\ 000$ . Percentage of silane by weight of cement.



## Annex IV Data from investigations on viscoelastic properties of silane modified cements and silane modified tricalcium silicates.

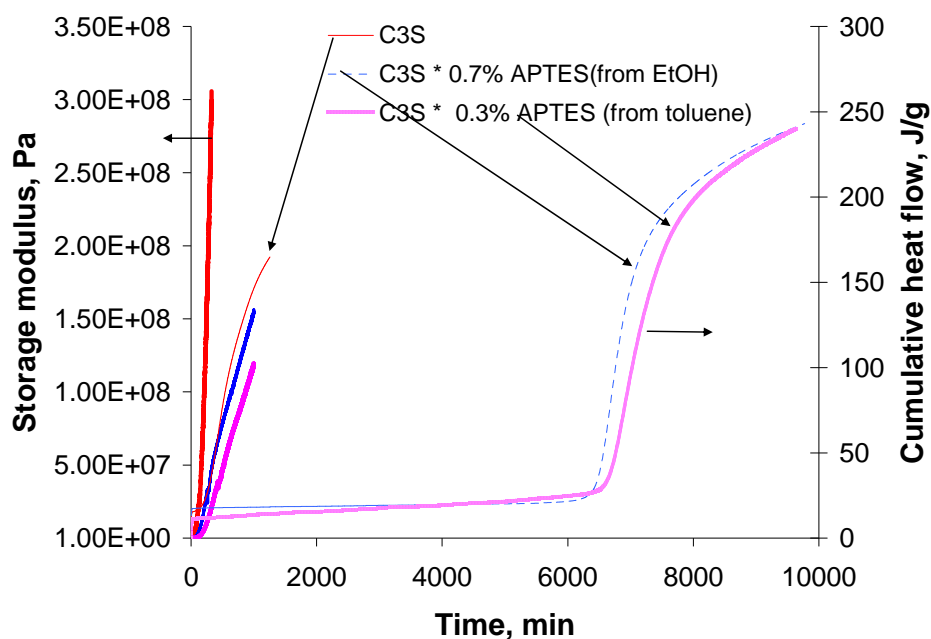


Figure IV-1. Evolution of storage modulus and cumulative heat flow for tricalcium silicate ( $w/c=0.3$ ) and APTES modified tricalciumsilicate pastes ( $w/c=0.25$ ). Measurements have been performed under constant strain of  $10^{-5}$  and constant frequency of 1 rad/s. The silanes concentrations are reported as percentage by weight of cement.



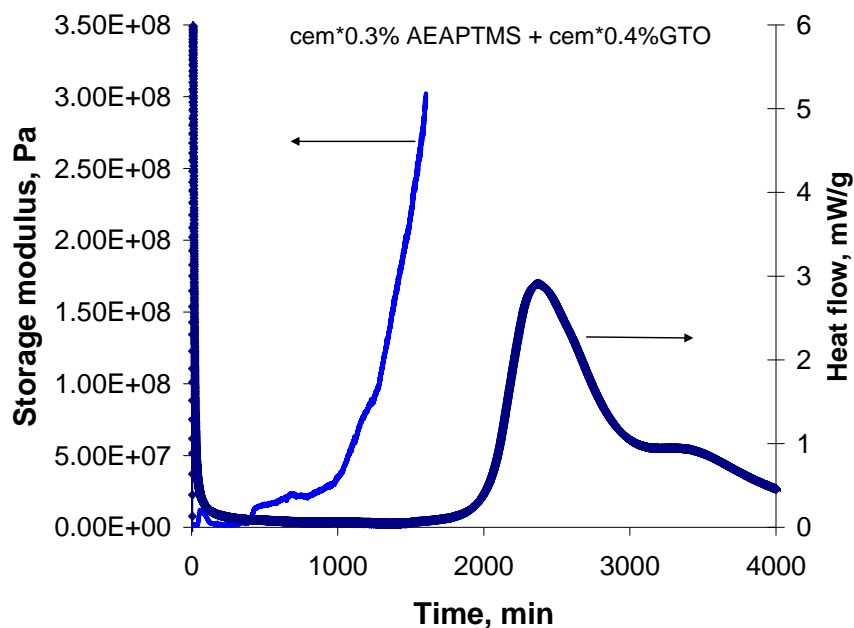


Figure IV-2. Evolution of storage modulus and heat flow for equi-masic blends of silane modified cements ( $w/c=0.25$ ). Rheological measurements have been performed under constant strain of  $10^{-5}$  and constant frequency of 1 rad/s. Silanes have been adsorbed from ethanol and the results are reported in percentage by weight of cement.

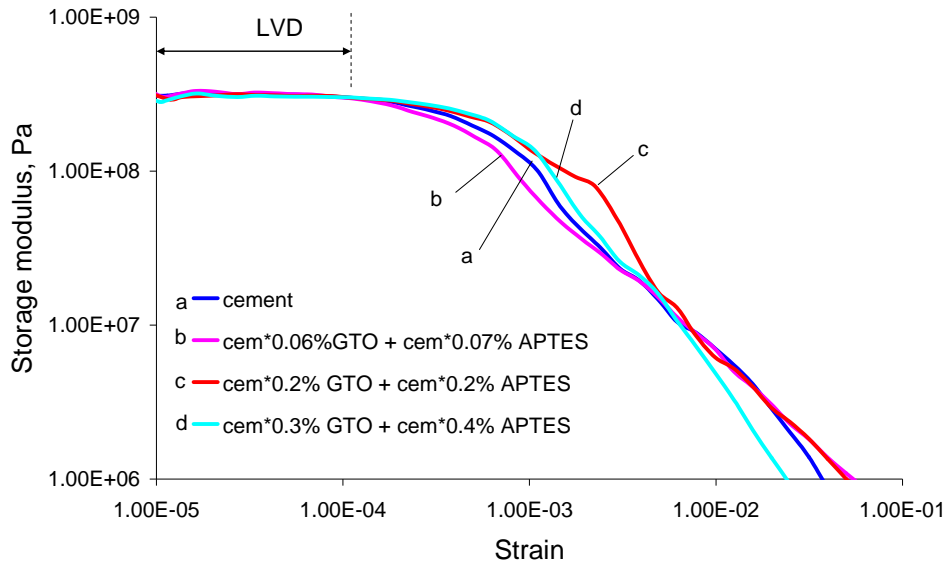


Figure IV-3. Evolution of the storage modulus as a function of the strain applied for blended silane modified cement pastes prepared with constant  $w/c = 0.25$ . The measurements have been performed for equal storage modulus values ( $3 \cdot 10^8$  Pa). All silanes have been adsorbed from ethanol and the results are reported in percentage by weight of cement.

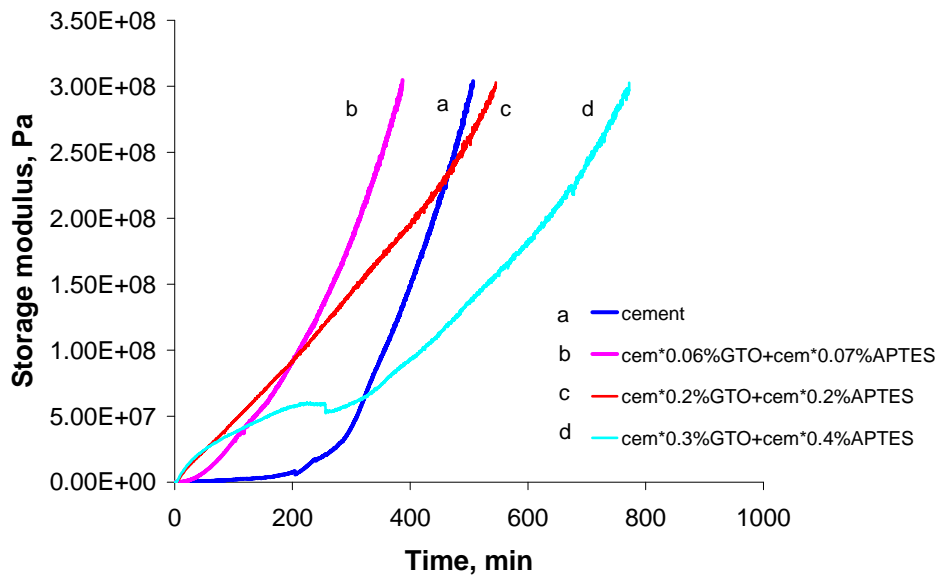


Figure IV-4. Evolution of storage modulus for blended silane modified cement pastes prepared with  $w/c=0.25$ . Measurements have been performed under constant strain of  $10^{-5}$  and constant frequency of 1 rad/s. All silanes have been adsorbed from ethanol and the results are reported in percentage by weight of cement.